COLEGIO DE POSTGRADUADOS

INSTITUCIÓN DE ENSEÑANZA E INVESTIGACIÓN EN CIENCIAS AGRÍCOLAS

CAMPUS MONTECILLO

POSTGRADO DE EDAFOLOGÍA

INTERACTION OF $CoFe_2O_4$ NANOPARTICLES FOR WHEAT AND BEAN FORTIFICATION

YAZMÍN STEFANI PEREA VÉLEZ

T E S I S
PRESENTADA COMO REQUISITO PARCIAL
PARA OBTENER EL GRADO DE:

DOCTORA EN CIENCIAS

MONTECILLO, TEXCOCO, ESTADO DE MÉXICO, MÉXICO

2023

COLEGIO DE POSTGRADUADOS

INSTITUCIÓN DE ENSEÑANZA E INVESTIGACIÓN EN CIENCIAS AGRÍCOLAS

La presente tesis titulada: **Interaction of $CoFe_2O_4$ nanoparticles for wheat and bean fortification** realizada por el (la) estudiante: **Yazmín Stefani Perea Vélez** bajo la dirección del Consejo Particular indicado, ha sido aprobada por el mismo y aceptada como requisito parcial para obtener el grado de:

DOCTORA EN CIENCIAS
EDAFOLOGÍA

CONSEJO PARTICULAR

CONSEJERO (A)

Ph.D. Ma. del Carmen A. González Chávez

CO-DIRECTOR (A)

Ph.D. Jaco Vangronsveld

ASESOR (A)

Ph.D. Rogelio Carrillo González

ASESOR (A)

Dr. Jaime López Luna

ASESOR (A)

Ph.D. Carolina Sénes Guerrero

ASESOR (A)

Dra. Vinisa Saynes Santillán

Montecillo, Texcoco, Estado de México, México, febrero de 2023

INTERACTION OF $CoFe_2O_4$ NANOPARTICLES FOR WHEAT AND BEAN FORTIFICATION

Yazmín Stefani Perea Vélez, D.C.
Colegio de Postgraduados, 2023

ABSTRACT

This research was inspired by the existing need to transform our current food production system into one that is more sustainable, and the growing concern to produce food with better nutritional quality. In this regard, I explored the use of citrate-coated cobalt ferrite nanoparticles ($CoFe_2O_4$ NPs) as an alternative Fe fertilizer for the agronomic fortification of wheat and beans. This thesis comprises four chapters. In the first section, the context of agricultural nanotechnology (focusing on the use of metal NPs) and the various issues to consider in the design of nanofertilizers are presented. The variables that influence the NP-plant-microorganism-soil interaction and the different ways in which nanotechnology is applied in agriculture and soil remediation are also discussed. Chapter two discusses the characterization of $CoFe_2O_4$ NPs and their dissolution model based on the effect of soil solution and artificial root exudates (ARE), which are relevant for determining the dosage and application form. I found that the NPs are almost insoluble in the soil solution. However, they can also be used as a source of controlled release of Fe and Co through the action of artificial root exudation. The model of NPs dissolution by the effect of ARE on Co was a pseudo-second-order model, and Fe followed the Korsmeyer-Peppas model. Meanwhile, NPs were applied in three different forms: soil and foliar (Chapter 2), and seed priming (Chapter 3). In the wheat experiment, soil application of NPs at 68 mg Fe kg^{-1} increased grain by 1.37 and 0.26 times above the target biofortification concentration (60 mg kg^{-1}) of the lines inefficient in grain Zn storage and inefficient in P uptake, respectively. Likewise, soil fertilization with NPs significantly reduced grain phytic acid concentration compared to fertilization with Fe-EDTA, and foliar application of NPs. Surprisingly, the nano-priming treatment at 10 and 40 mg NPs L^{-1} increased the Zn concentration in beans by 5% -27% compared to the control treatment seeds. Seeds from plants of the treatment with 10 mg NPs L^{-1} had the lowest phytic acid:Zn molar ratio. Although bean yield was not improved, nano-priming may be an alternative to improve bean quality without the addition of an external nutrient source. These results are encouraging for the nano-enabled biofortification of wheat and bean; however, the cost may be a key concern for its widespread application and business investment. The calculated cost of nano-priming of bean seeds ranged from 121 to 143 USD per ha when using NPs suspension concentrations from 10 to 40 mg NPs L^{-1}. Meanwhile, the estimated cost for soil fertilization of wheat (98-145 mg NPs kg^{-1}), ranged from 44,283 to 65,523 USD per ha, and 1,553 USD for foliar fertilization per ha. Finally, the indirect benefits of nano-enabled biofortification should be considered in the cost-benefit analysis, such as the burden costs of micronutrient deficiencies in the population, the Scope 2 emissions, or the potential low inputs.

Keywords: Environmental innovative technology, nano-fertilizers, nano-agricultural technology, seed priming, nano-priming.

INTERACCIÓN DE NANOPARTÍCULAS DE $CoFe_2O_4$ PARA LA FORTIFICACIÓN DE TRIGO Y FRIJOL

Yazmín Stefani Perea Vélez, D.C.
Colegio de Postgraduados, 2023

RESUMEN

Esta investigación se realizó por necesidad de transformar nuestro actual sistema de producción de alimentos en uno más sustentable; y que permita producir alimentos con mayor valor nutricional. En este sentido, exploré el uso de nanopartículas (NPs) de cobalto-ferrita recubiertas de citrato ($CoFe_2O_4$ NPs) como fertilizante alternativo para la fortificación agronómica de Fe de trigo y frijol. El trabajo se divide en cuatro capítulos. A través del primer capítulo, el lector descubrirá el contexto de la nanotecnología agrícola (con énfasis en el uso de NPs metálicas) y los aspectos a tomar en cuenta para el diseño de nano fertilizantes, así como las variables que influyen en la interacción entre NP-planta-microorganismo-suelo, formas de aplicar la nanotecnología en la agricultura y la remediación de suelos. En el Capítulo 2 se presenta la caracterización de las NPs de $CoFe_2O_4$ y su modelo de disolución por efecto de la solución del suelo y exudados radicales artificiales (ERA). Identifiqué que las NPs son insolubles en la solución del suelo, pero tanto Fe como Co se liberan por la acción de los ERA. El modelo de disolución de las NPs por efecto de los ERA con base a Co y Fe fue de pseudo-segundo orden y de Korsmeyer-Peppas, respectivamente. En los Capítulos 3 (experimento con trigo) y 4 (experimento con frijol) se presentan los resultados de la aplicación de NPs con propósito de biofortificación. Las NPs se aplicaron en tres formas: al suelo, y foliares (Capítulo 3) y a través de seed priming (o nano-priming; Capítulo 4). En trigo, la fertilización al suelo con 68 mg Fe kg^{-1} como NPs incrementó la concentración de Fe en grano 1.37 y 0.26 veces por arriba de la concentración objetivo de biofortificación (60 mg kg^{-1}). A demás se redujo significativamente la concentración de ácido fítico del grano en comparación con la fertilización con Fe-EDTA y foliar de NPs. Sorprendentemente, el nano-priming en frijol (10 y 40 mg L^{-1}) aumentó de 5% a 27% la concentración de Zn en grano con respecto a la de los granos del testigo. La relación molar ácido fítico:Zn más baja (3:1) se observó en las semillas de las plantas procedentes de semillas con nano-priming a 10 mg L^{-1}. A pesar de que el nano-priming no aumentó el rendimiento económico del frijol, éste puede ser una herramienta para aumentar el contenido mineral del grano sin necesidad de añadir una fuente externa de nutrientes. Estos resultados son prometedores, sin embargo, el costo de la tecnología es clave para su uso extendido e inversión comercial. Para el nano-priming, el costo osciló de 121 a 143 USD por ha de cultivo de frijol y usando una suspensión de NPs de 10 a 40 mg L^{-1}. Para la biofortificación del trigo, el costo por ha de fertilización al suelo (98-145 mg kg^{-1}) osciló de 44,283 a 65,523 USD y 1.553 USD para la fertilización foliar. Por último, al analizar el costo-beneficio de los nanofertilizantes en la biofortificación se recomienda considerar los beneficios indirectos, como el costo indirecto de las deficiencias de micronutrientes en la población, o las emisiones de alcance 2.

Palabras clave: Tecnología medioambiental innovadora, nano-fertilizantes, tecnología nanoagrícola, seed priming, nano-priming

ACKNOWLEDGMENTS

I would like to thank the Consejo Nacional de Ciencia y Tecnología (CONACyT) for funding my doctoral studies. I am also thankful to the Colegio de Postgraduados campus Montecillo, Edaphology Specialty for the support provided through my doctoral studies.

I would like to express my sincere gratitude to my supervisor Dra. Ma. Del Carmen A. González Chávez for trusting me and letting me participate in her research group. I also thank her for her support, motivation, and teachings. Her mentorship has inspired me to become a better scientist. Besides my advisor, I would like to thank the rest of my advisory committee: Dr. Rogelio Carrillo Gónzález, Dr. Jaco Vangronsveld, Dr. Jaime López Luna, Dra. Vinisa Saynes Santillán, and Dra. Carolina Senes Guerrero for their comments, questions, and suggestions that improved the quality of this research and encouraged my curiosity to think outside the box. Undoubtedly, behind this work and my formation as a scientist, there is an exceptional group of professors who have motivated me.

I would like to thank Dr. Daniel Tapia Maruri for his help with the microscopic analysis and, above all, for his human warmth and for making me feel at home in his laboratory. I would also like to thank Dr. Serafin Izquierdo and Dr. Iván Monasterio for kindly providing the seed material. Cecilia Garcia Osorio for her help with the gas chromatography analysis; Biol. Simón for his help with cutting the leaf samples and fixing the samples; M.C. Jorge Valdez for his help with photographing my seed samples; Dr. Juan José Almaraz Suaréz for his support and advice with the nitrogenase activity analysis; Dr. Ignacio Maldonado for letting me discover and learn a little bit about mycorrhizal fungi through the short research stage in his laboratory; and Dr. Daniel Padilla Chacón for this help with the sugar and free amino acids analysis.

I thank my laboratory partners: Jesús Eulises Corona, Nancy Flores, Adrian Barajas, Abraham, Uriel, Abigail Díaz, and Berenice for their help when I asked for it during the experimental phase of my project. I also thank them for their human warmth, and for the time spent together outside the laboratory which helped me a lot in balancing

my personal and professional life. I also thank my colleagues Dario Flores, José Luis Salinas, Eliud Serrano Flores, Carlos, Juan Vargas, Bernardo Galeote, and Luis Cisneros for their support whenever I asked for it.

I would also like to express my deep gratitude to my mom Clara Vélez 😭, my brothers Christian and Jordi, and my nephews Héctor and Sami for supporting me throughout my doctorate studies. Family, thank you for encouraging me to pursue my dreams, and for being a source of inspiration. I would like to thank Máté 😭 for his support in technical aspects (economic analysis of the use of nanoparticles), and for listening to me talk about nanotechnology all the time. Szívem, köszönök minden segítséget and for joining me in this adventure 😊. Finally, I would like to thank myself for never giving up, even when it seemed hard to finish my doctoral studies. Stefani, thank you for this amazing adventure…

Up and atom!

DEDICATION

To my lovely mother and brothers

A mi mamá y hermanos

CONTENT

LIST OF TABLES

LIST OF FIGURES

GENERAL INTRODUCTION

Our current global food system is facing tough and unprecedented challenges in the age of climate change (Agrawal et al. 2022). For instance, it can be made more eco-friendly (Maqbool et al., 2020) while producing good-quality nourishing food. In addition, the COVID-19 pandemic has highlighted the fragilities in our agri-food system and the inequalities in our societies, driving an increase in food insecurity (FAO et al. 2022) and concern for nutritional security.

Nutritional security goes beyond food security because it aims to ensure that everyone has access to nutrients from all food groups (proteins, carbohydrates, fiber, vitamins, and minerals) (FAO et al. 2020). Moreover, it means people have consistent access, availability, and affordability of food that promotes well-being, prevents diseases, and if needed, treats diseases, particularly among the vulnerable population (lower income, rural, and remote populations)(USDA 2022). However, access to a healthy and diversified diet at a lower cost is unaffordable for almost 3.1 billion people (FAO et al. 2022). On the other hand, between 2019 and 2020, the world's undernourished population increased from 8.4% to 10% (FAO 2021), while Fe deficiency is the cause of 12.5% of anemia cases worldwide (Warner and Kamran 2021). The situation is even more alarming in the regions of Africa, Latin America, and the Caribbean, where the percentage of undernourishment increased from 18% to 21%, and from 7% to 9%, respectively (FAO 2021).

Multiple factors play a role in achieving nutritional security, such as food production, input supply, storage, distribution, processing, consumption, retail, marketing, sustainability, governance, economics, and cultural identities (Ingram 2020; Pandohee et al. 2023). This research focused on the production of nutritional crops for nutritional security (with emphasis on Fe). Wheat and beans are among the most widely consumed cereals and legumes worldwide. Wheat is the staple food for 35% of the world's population (Cakmak and Kutman 2018), whereas beans provide 65% of the total protein consumed by African, Latin American, and Caribbean populations (Petry et al. 2015). The production of Fe-biofortified staple crops is a short-term and cost-effective approach to improve the nutrition of the population of rural and marginalized areas without modifying

their consumption patterns (Velu et al. 2014; Knijnenburg et al. 2018; Ramírez-Jaspeado et al. 2020). Agronomic fortification is the application of fertilizers to increase the mineral content in edible plant parts and is one of the ways to produce Fe-biofortified cereals and legumes (de Valença et al. 2017). Recently, decreasing seed concentration of anti-nutritional factors is also part of the objectives for crop seed biofortification (Cominelli et al. 2020). However, producing Fe-biofortified cereals and legumes is a challenge compared with other micronutrients like Zn or Se (Knijnenburg et al. 2018; Blanco-Rojo and Vaquero 2019), because both cereals and legumes contain high concentrations of substances considered antinutrients such as phytic acid and polyphenols (Murphy et al. 2008; Glahn and Noh 2021). Phytic acid is a strong chelator of cations such as Fe, Zn, Mg, and Ca. In wheat, 80% of phytic acid is stored in the aleurone and brand (where most of the Fe seed is stored) in cereals, while in legume seeds, such as common bean, more than 95% of the phytic acid is accumulated in the cotyledons (Sparvoli and Cominelli 2015). In addition, Fe plant uptake through the roots and its translocation throughout the plant are highly regulated by complex genetic and homeostasis mechanisms (Connorton et al. 2017).

To improve Fe uptake and its translocation from the site of application to the edible parts, inorganic Fe salts or chelates have been used. However, contradictory results have also been reported (Malhotra et al. 2020). In this scenario, NPs containing Fe is an alternative to achieve Fe seed biofortification (Sundaria et al. 2019). In wheat, foliar fertilization with Fe oxide NPs improved yield and grain protein, carbohydrate, and amino acid content in grains (Armin and Asgharipour 2011; Bakhtiari et al. 2015; Wang et al. 2019a).

Seed priming is an innovative, user-friendly, and eco-friendly approach to seed biofortification that triggers Fe acquisition and accumulation in grains (Sundaria et al. 2019; do Espirito Santo Pereira et al. 2021). Sundaria et al. (2019) assessed the biofortification of two wheat genotypes (low and high Fe grain storage capacity) through seed priming (25-60 mg L^{-1}). Treatment with 25 mg L^{-1} significantly increased the Fe concentration in grains by 26.8% in the low-Fe storage genotype and by 45.7% in the high-Fe storage genotype. In this context, this research aimed to explore the use of

citrate-coated $CoFe_2O_4$ NPs for Fe fortification of wheat and bean. I hypothesized that NPs could be a feasible approach to enhance the nutritional quality of wheat and bean compared to current methods.

Thus, this dissertation explores different issues that need to be considered for nano-enabled biofortification. First, a review of the current situation of the application of nanotechnology in agriculture is presented (Chapter 1). This chapter aimed to understand the different aspects that must be considered for the design of nano-fertilizers, variables that influence the NP-plant-microorganism-soil interaction, and the different forms of applying nanotechnology in agriculture and soil remediation. Secondly, I determined the dissolution rate of NPs as a function of pH and time in the soil solution, and the effect of artificial root exudates (Chapter 2). This information is part of the NPs characterization that is key information to understanding the interactions of NPs with plants, to designing doses and forms of application. Thirdly, I assessed the Fe biofortification of three contrasting wheat lines (Zn-efficient, Zn-inefficient grain storage, and P-uptake inefficient) through NPs application to soil or by foliar spray (Chapter 3). The effect of NPs fertilization was also compared with one of the conventional Fe fertilizers used. Fourthly, in common bean crops, I explored Fe biofortification through seed priming as an innovative strategy (Chapter 4). The effects of nano-priming were evaluated through the life cycle of the bean (germination, pre-flowering, and maturity plant stage). Finally, the economic evaluation of the use of NPs for the biofortification of wheat and bean was calculated, to know their feasibility.

LITERATURE REVIEW

Interaction metal nanoparticles-plant-microorganisms in agriculture and soil remediation[1]

Abstract

Design products or technologies that incorporate metal nanoparticles (NPs) in agriculture need to be safe for consumers, soil microorganisms, and environment-friendly. This review analyzes advances in metal NPs application in crop production and soil remediation: two major challenges that are constraining world sustainability and food security. The use of NPs in agriculture is also explored as a tool to improve plant productivity, control phytopathogens, and viruses; monitor the quality and health of plants and soil, and seed-priming. Concerning soil remediation, this review focuses on potentially toxic element pollution when NPs may be used as an assisted phytoremediation alternative, be combined with electrokinetic remediation, or for acid mining drainage remediation, as well as their role in photocatalysis. Besides, it addresses the pathways of interaction with soil properties, plants, and soil microorganisms, which are relevant factors influencing NPs fate and behavior in soil and their functions. Finally, this review aims to explore the common purposes and challenges of nanotechnology in agriculture and remediation, which may be the basis for new technologies.

Keywords: Environmental innovative technology, environmental and agricultural issues, Nanoagrochemicals, Nano-enabled agriculture, Nanoremediation, Rhizosphere.

---

[1] This is an Accepted Manuscript of an article published in the *Journal of Nanoparticle Research* online [03 September 2021] available online: https://link.springer.com/article/10.1007/s11051-021-05269-3

Resumen

Los productos o tecnologías que incorporan nanopartículas (NPs) metálicas y que están destinados a usarse en la agricultura deben ser seguros para los consumidores, los microorganismos del suelo y respetuosos con el medio ambiente. En esta revisión se analizan los avances en la aplicación de las NPs metálicas en la producción de cultivos y en la remediación de suelos: dos grandes retos que están limitando la sostenibilidad y la seguridad alimentaria en el mundo. También se explora el uso de las NPs en la agricultura como herramienta para mejorar la productividad de las plantas, herramienta para el control de fitopatógenos y virus; herramienta para monitorear la calidad y la salud de las plantas y el suelo, y el cebado de semillas. En lo que respecta a la remediación del suelo, esta revisión se centra en la contaminación por elementos potencialmente tóxicos, el uso de NPs como alternativa de fitorremediación asistida, la combinación de NPs con la remediación electrocinética o para la remediación del drenaje minero ácido, así como su papel en la fotocatálisis. Además, se abordan las vías de interacción con las propiedades del suelo, las plantas y los microorganismos del suelo, que son factores relevantes que influyen en el destino y el comportamiento de las NPs en el suelo y en sus funciones. Por último, esta revisión pretende explorar los propósitos y retos comunes de la nanotecnología en la agricultura y la remediación; que pueden ser la base de nuevas tecnologías.

Palabras clave: Tecnología ambiental innovadora, desafíos ambientales y agrícolas, Nanoagroquímicos, Agricultura con nanopartículas, Nanoremediación, Rizosfera.

Introduction

Fifty years ago, Richard Feynman suggested manipulating matter on an atomic scale by building machines at the nanoscale level allowing arrange atoms (Toumey 2009). Afterward, what seemed to be science fiction became reality originating in nanoscience —the science of objects of size smaller than 100 nm— and nanotechnology the design, synthesis, and use of nanomaterials (NMs) (Whitesides 2005).

NMs are materials with any external dimension or with surface or internal structures at the nanoscale (Santos et al. 2015). Some examples of synthesized NMs are nanoparticles (NPs), nanolayers, nanofibers, nanotubes, and quantum dots (Whitesides 2005). Matter of nanoscale has different properties than the same material at the macroscale size, for example, a high relative surface area, greater chemical reactivity, and optical, electrical, and magnetic behavior (Ma et al., 2010; Raliya et al., 2018). Nowadays, NMs are mainly used in electronic, automobile, energy, chemical, health, cosmetic, and textile industries (Bundschuh et al., 2018; Sabourin and Ayande, 2015) due to their properties. According to the nanotechnology products database (https://product.statnano.com/), more than 9,000 products claim to contain NMs (StatNano 2018). Figure 1 shows the distribution of NMs used in different branch industries, and Figure 2 shows the subdivisions of products for agronomic and environmental purposes.

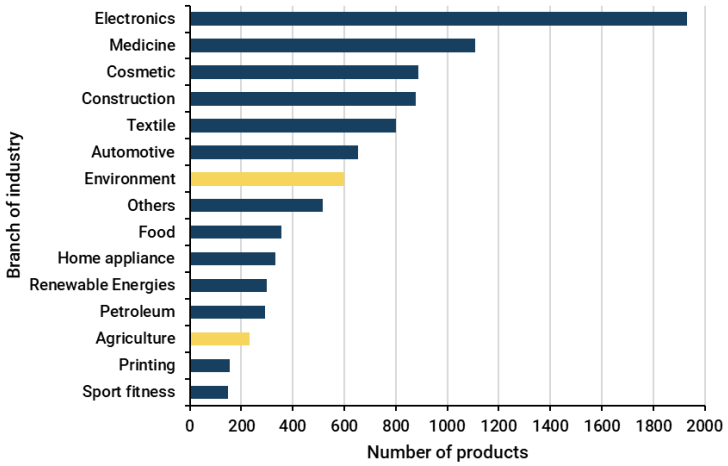

Figure 1. Distribution of nanomaterials currently used in different industry branches according to the nanotechnology products database (StatNano 2018).

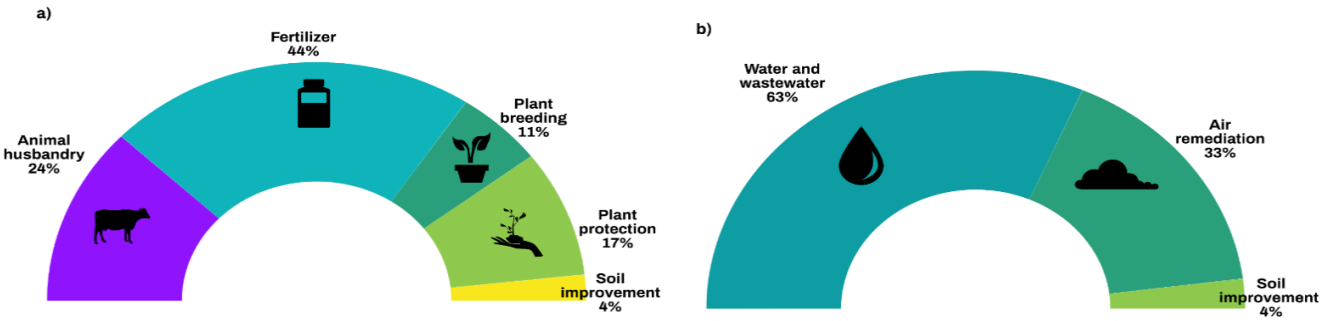

Figure 2. Subdivisions of products for a) agronomic and b) environmental purposes according to the nanotechnology products database (StatNano 2018).

When comparing the number of commercialized products in the agronomic and environmental sectors with other industrial branches, it results that nanotechnology is an emergent activity, on a large-scale application in these sectors (Belal and El-Ramady, 2016; V. D. Rajput et al., 2018). Moreover, the current market value in the agri-food sector was projected to increase to 160 billion dollars by 2020 because of the incorporation of nanotechnology in food production, processing, and packaging (Sabourin and Ayande, 2015). The global nano-pesticide market size is forecasted to grow at a compound annual growth rate of 14.6% from 2020 to 2027 (Bratovcic et al. 2021). The global market value for remediation using nanotechnology in 2010 was estimated to be 6 billion dollars (Bardos et al. 2018), and increase to $41.8 trillion by 2020, with a 10.2% average annual growth rate from 2015 to 2020 (Corsi et al. 2018). Besides the financial advantages, nanotechnology offers technological and environmental benefits in both sectors, agriculture, and remediation, which are circumstantially linked (Figure 3). On the one hand, the use of nano-agrochemicals in agriculture can increase crop yield with fewer amounts of substances applied, reduce the volume of spread chemicals, increase the capacity of plants to absorb nutrients, and minimize nutrient losses (Prasad et al. 2017), consequently, reduce soil and water pollution. P.e. foliar-sprayed of nano-Fe (0.25 g L^{-1}) on cowpea plants (*Vigna unguiculata*) increased the yield by 63% and 41% compared to plants treated with bulk $FeSO_4$ at 0.25 and 0.5 g L^{-1}, respectively (Delfani et al. 2014a). The application of nano-pesticides (including fungicides, bactericides, acaricides, nematicides, insecticides, herbicides, rodenticides, etc.) can also augment the efficiency of pest control with lower concentrations. On the other hand, a common world concern

has been excessive and no reasonable use of agrochemicals such as fertilizers and pesticides for crop production. This uncontrolled use has propitiated soil, sediments, and water contamination; has negatively influenced organisms across the food chain. Therefore developing remediation alternatives to control contamination is a priority (Kumar et al. 2019; Singh and Kumar 2020). Nano-agrochemicals may be suitable in soil remediation; nano-remediation can reduce the reaction times compared to *in situ* conventional remediation techniques (Grieger et al. 2015), and be up to 80% cheaper (Corsi et al. 2018).

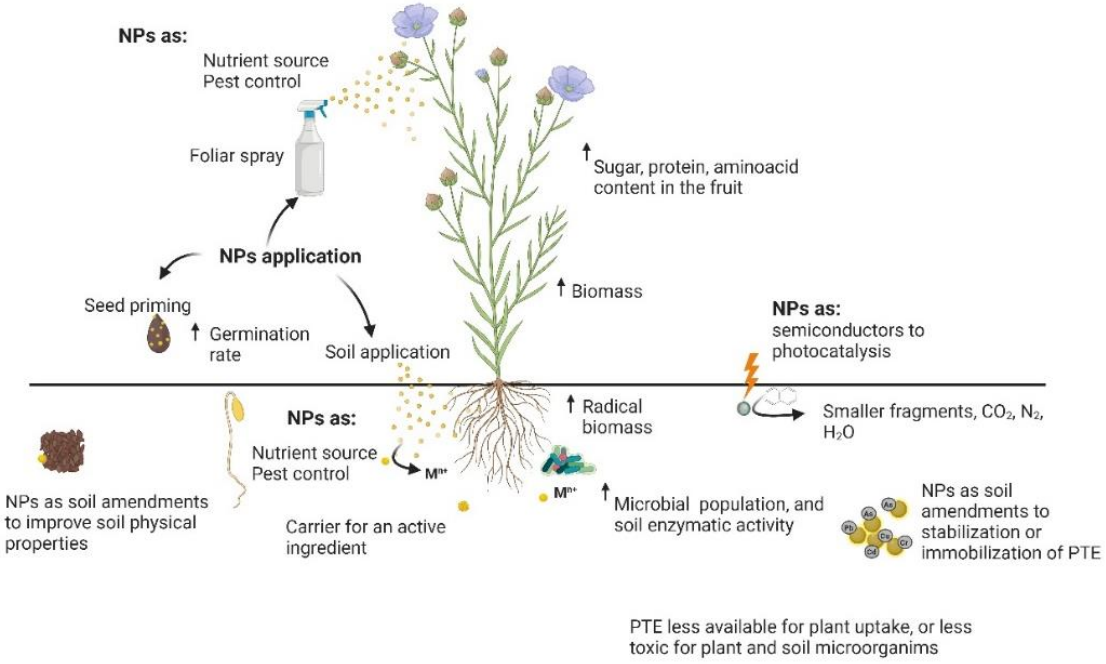

Figure 3. Common applications of NPs in agriculture and soil remediation.

Even though NMs offer several benefits to food production and soil remediation, there remain gaps in knowledge to be studied that can be decisive in to sooner and safer transfer of laboratory results on a large-scale application. The study of the interaction between nano-sizer materials and soil microorganisms is in the emerging stage. Microorganisms have crucial functions in biogeochemical cycles such as turnover of organic matter, the architecture of soil formation, plant nutrition, and health. Moreover, they are strongly involved in the decomposition of xenobiotics, control of contamination, and soil remediation (Schloter et al. 2018). Especially, beneficial soil microorganisms are being recognized to play a paramount role in plant productivity and soil health and they

build an intricate bond between plants and soil. In plants, beneficial soil microorganisms improve nutrient uptake and enhance plant tolerance to different biotic or abiotic stresses (drought, heat, acidity, alkalinity, salinity, pathogens, and contaminants). In soils, microorganisms participate in the aggregate formation, organic matter degradation, carbon sequestration, remediation, etc. (Jacoby et al. 2017). The use of NMs in agriculture and remediation compulsory requires analyzing their interaction with plants, soil, and beneficial microorganism, which has rarely been taken into account, therefore, it is addressed in this review. In the same way, unexplored effects of NMs on seed priming, soil quality, and environmental abiotic stresses such as salinity and drought need more attention. It is expected that arguments exposed here, may contribute to propitiate sustainable agricultural production systems under environmentally friendly conditions, as the use of NPs without negative affectation of activity of beneficial soil microorganisms is highly desirable. Similarly, the interaction between NMs and soil microorganisms needs to be documented, including the fate of NMs after application, the residual effects, and the environmental and biological factors that affect their toxicity. These are some of the key points to predict the ecotoxicology of metal-based NMs and to formulate safe and wide public accepted technologies.

Nanotechnology and NMs in agriculture

Agriculture is a sector that has a duality, on the one hand, it supplies food, and raw materials to produce consumer goods. That is to say, the agri-food industry can provide bioactive compounds (phenols, peptides, carotenoids, etc.) to produce drugs and cosmetics, fibers to the textile industry, lignocellulosic materials, and vegetable oils to produce ethanol and biodiesel (Boehlje and Broring, 2011), and because of that Zulfiqar et al. (2019) pointed out to agriculture as an economic sector that involves a “worldwide multitrillion dollars industry”. Regarding its role in the economy, agriculture is one of the main sources of direct employment and income, e.g., in 2010 it was estimated that 2.6 billion people around the world depended on agriculture for their livelihoods (Alston and Pardey, 2014), and in 2018 the agriculture accounted 4% of global gross domestic product (GDP). Even, in some developing countries, it accounted for more than 25% of their GDP (The World Bank 2021). On the other hand, intensive agriculture has a negative

environmental cost that ironically also endangers agriculture itself. For instance, agriculture is responsible for 15% of the total emission of methane and nitrous oxide, they both are greenhouse gases involved in global warming (Park et al. 2012; Malhi et al. 2021). Moreover, the immoderate use of agrochemicals (due to the low efficiency of some fertilizers) causes soil chemical contamination and low crop yields in the long term (Kothari and Wani 2018).

The global annual crop production (more than three billion tons) requires approximately 187 million tons of fertilizers and 4 million tons of pesticides (Usman et al. 2020). However, up to 75% of fertilizers applied to soil can be lost due to volatilization, leaching, or the runoff process (Trenkel 2013; Dimkpa et al. 2020). The range of losses from the soil is 40% -70% of N, 80% -90% of P, and 50% -90 % of K (Pitambara et al. 2019). This is also applicable to pesticides, where 90% of pesticides may escape during the application step (Ghormade et al. 2011; Kumar et al. 2019). So, annually 140 million tons of fertilizers and 3.6 million tons of pesticides are lost. This inefficient use makes agrochemicals harmful to the environment and human beings.

Therefore, the efficient use of agrochemicals and the conservation of soil quality are two of the main challenges in agriculture. They both affect food production, the economy, and environmental quality. In this regard, nanotechnology is an emerging alternative that may revolutionize agriculture because of its diverse application (which will be discussed in more detail in the following section) as fertilizers, pesticides, plant growth promoters, seed treatments, opportune detection of plant diseases, monitoring soil and water quality, identification and detection of the toxic agrochemical, and soil and water remediation (Acharya and Pal 2020; do Espirito Santo Pereira et al. 2021; Prerna et al. 2021). Singh et al. (2021) referred to the application of nanotechnology to agriculture production as phytonanotechnology. While Acharya and Pal (2020) mentioned the use of nanotechnology in agriculture in three specific areas: precision farming (by the application of nanosensors), crop productivity, and crop improvement (by the application of nanoagrochemicals). Furthermore, these authors discussed several qualities of NMs useful to agriculture: compact size, easy way to carry and handling, long-term storage, high effectiveness, and when used rationally, not toxic. Thus, these nanometric materials

may be a favorite selection for farmers over conventional agrochemicals. Moreover, these may improve the efficiency of agricultural inputs, and achieve sustainable agroecosystems at a lesser cost, energy, and waste production.

Nanoagrochemicals can improve the efficiency of applications while reducing the loss of both nutrients and pesticides through the smart delivery and controlled release of an active ingredient (Seleiman et al. 2021). In this regard, tailored delivery systems can be designed based on the release time or environmental conditions (humidity, heat, light, pH, enzyme, redox state, and magnetic release) (Huang et al. 2018; Grillo et al. 2021). It will depend on the NMs' properties and their interaction with the surrounding media. Moreover, nanoformulations may function in relation to not only time-control or spatial-target release, but also self or remote-regulation delivery to guarantee effective targeting (Kumar et al. 2019). In the case of fertilizers with high solubility and fixation in the soil, such as urea or iron, slow-release is desirable to avoid losses. Kottegoda et al. (2017) evaluated the slow release of N from urea-hydroxyapatite nanocomposites (6:1) in water. They found that the N release rate was approximately 12 times slower compared to pure urea. The urea released 99% of the nitrogen content in 5.3 min, whereas the nanocomposite released 86% of the nitrogen after 1.06 h. In this case, urea-hydroxyapatite nanocomposites may be an option to increase the efficiency of N application and reduce the N volatilization as N_2O emissions. In contrast, when the effectiveness of a fertilizer mainly depends on the solubility of the nutrient source, nano-sized materials can improve their dissolution, because, in theory, the solubility of solids depends on the excess surface energy, which is correlated with the specific surface area and the particle size (Milani et al. 2012; Avramescu et al. 2017). To avoid undesirable effects or losses by the fast solubility of a NM, their release pattern can be improved through surface modification (by the addition of coating materials or nanoencapsulation) or by NMs coated onto granular macronutrient fertilizers (Milani et al. 2012). From this point of view, Milani et al. (2012) synthesized urea and monoammonium phosphate-coated ZnO NPs, which had a higher fast dissolution degree and Zn solubility than bulk ZnO.

In the case of nano-pesticides, the slow release may minimize crops' demand for pesticides (then, reduction of residues and environmental pollution), and achieve more effective, safe pesticide usage (Huang et al. 2018). Also, the controlled and slow release of an active ingredient is advantageous to treat specific pests or insects for a longer duration without harm to non-specific targets (Nehra et al. 2021). The use of nano-pesticides is in the early stage of development with safe environmental applications (Kumar et al. 2019). Gradually, the kinds of pesticide presentations are increasing, new provisions are available: nanosuspensions, nanoemulsions, nanocapsules, nanospheres, nanogels, nanoliposomes, micelles, clay-based nanoformulations, and their function is the result of the physical and chemical properties at the nanoscale level (Table 1).

Table 1. Types of nano-agrochemical formulations and their functions.

Type of formulation	Function
Nanoemulsions, microemulsions of an active ingredient	Increase solubility in water of hydrophobic cargo, increase the absorption efficiency
Nanocatalyst-active ingredient conjugated in microcapsules	Rapid separation of the active ingredient in soil or plant
Nanocapsules with a conjugated catalyst with the active ingredient	Protection against premature degradation
Nanocapsules and nanospheres	Controlled release, guided delivery, and protection against premature degradation, as carriers
Nanodispersions and nanosuspensions	Increase toxicity of an active ingredient in the target organism at low doses
Nanocrystals	Improve the bioavailability of water-insoluble compounds, and drug adhesiveness to surface cell membranes, enhance particle stability in suspension, and as a carrier
Dendrimers	Improve delivery, carriers for the active ingredient
Metal-nanoparticles and nano-clays	Active substance as NPs

Modified from Kookana et al. (2014)

In synthesis, it is expected to maximize the crop yield with the minimum amount of fertilizers and pesticides, and to reduce the accumulation of organic and inorganic compounds in soils, as well as a decrement greenhouse gas emissions (Kah et al. 2018; Raliya et al. 2018) by using nano-agrochemicals. It is expected that the action of external factors that cause the loss of agrochemicals will be reduced due to the properties of nano-formulations (Qureshi et al. 2018). Recently, the use of NPs as a tool for the fortification of plants was suggested (Elemike et al. 2019). In consequence, the use of nano-

agrochemicals will improve crop yields, and the nutrient value of crops, and may reduce the costs of production (Pestovsky and Martínez-Antonio 2017).

Nano-fertilizers

Nano-fertilizers are NMs or nano-enabled bulk materials used to improve plant nutrition (Raliya et al. 2018). Moreover, they have been mentioned as next-generation fertilizers (Palchoudhury et al. 2018) that may help us to guarantee the world's food security (Usman et al. 2020), improve the nutritional value of food through Fe and Zn agronomic fortification (ZnO, Fe_3O_4) (Elemike et al. 2019), keep balanced nutrition to ameliorate biotic and abiotic stresses (Zulfiqar et al. 2019; Cai et al. 2020), reduce the ecological footprint due to less amount of agrochemical used and low nutrient losses (Lal 2020). Regarding agricultural management, nano-fertilizers offer some advantages: reduced transportation and application costs; the soil is not overloaded with salts; nutrient-delivered control may be synchronized to soil nutrient status, plant growth stage, and environmental conditions by using nanosensors (Zulfiqar et al. 2019; Cai et al. 2020).

Nano-fertilizers, currently available in the market, are usually reformulations of active ingredients that already have a registration (Table 2, Figure 2). There are several examples of nano-fertilizers containing the macro (N, P, K) or micronutrients (Cu, Fe, Mn, Mo, and Zn); however, some metal NPs such as Al, Zn, Ti, Ce, Cu, Ni, Ag, ZnO, AgO, MgO, TiO_2 and magnetic NPs as Fe_3O_4, Fe_2O_3, already used in the industry, also have versatile effects (Table 2) with potential use in agriculture (Rastogi et al. 2017). Also, carbon nanotubes and other NMs like urea and monoamonniun phosphate-coated ZnO NPs, Fe-pyrite, and nanocomposites of humic substances with Fe_2O_3 have shown their action also as fertilizers (Lin et al. 2009; Mastronardi et al. 2015).

Table 2. Some nano-agrochemicals are currently available in the market.

Product name	Composition	Formulation	Function	Properties	Use mode	Concentration	Country	Manufacturer	Reference
NanoK™	K_2O	Nanocapsule	Fertilizer	Crop yield enhancement, K delivery	Foliar spray	21%	USA	Aqua-Yield Hub	Aqua-Yield® (2021)
NanoZn™	Zn	Nanocapsule	Fertilizer	Plant growth regulation and Zn delivery	Foliar spray	9%	USA	Aqua-Yield Hub	
NovaLand-Nano	NPs of microelements p.e. Mn, Cu, Fe, Zn, Mo, N	NPs	Fertilizer	Plant nutrition			Taiwan	Land Green and Technology Co	Land Green and Technology Co (2020)
Nano Zinc (chelated)	Zn	NPs	Fertilizer	Plant growth regulation	Foliar spray	12%	India	Alert Biotech	Alert Biotech (n.d.)
Nano Bor	B	NPs	Fertilizer	Plant growth	Foliar spray	20%	India	Alert Biotech	
Nano Cu	Cu NPs, adjuvants, and chelating materials	NPs	Pesticide	Fungicide and bactericide properties		10%	Egypt	Bio-Nano Technology	Bio Nano (2021)
Agro 2400	AgNPs, citric acid, trisodium citrate, polymerized organic compounds, and water	NPs	Pesticide	Permanent disinfection, disease prevention, extra crop growth	Soil and foliar application	2400 mg L^{-1}	Turkey	Silvertech Kimya Sanayi ve Ticared Ltd	Silvertech Kimya Sanayi ve Ticaret Ltd.(n.d.)
Agro 2475	AgNPs, CuNPs, citric acid, trisodium	NPs	Fertilizer and pesticide	Fungi control, and plant nutrition		2400, 7500 mg L^{-1}	Turkey	Silvertech Kimya Sanayi ve Ticared Ltd	

Product name	Composition	Formulation	Function	Properties	Use mode	Concentration	Country	Manufacturer	Reference
Agro 2490	citrate, polymerized organic compounds, and citrate AgNPs, CuNPs, nano chitosan, citric acid, polymerized organic compounds, and water	NPs	Fertilizer and pesticide	Fungi control, and plant nutrition	Soil and foliar application	2400, 7500, 1500 mg L^{-1}	Turkey	Silvertech Kimya Sanayi ve Ticared Ltd	
Argovit™	AgNPs	NPs	Pesticide	Huanglongbing disease	Trunk injection	2 – 300 mg	Mexico		Stephano-Hornedo et al. (2020)

NPs=Nanoparticles

One main advantage of nano-fertilizers over bulk materials is boosting the crop yield (Kottegoda et al. 2017) even by applying lower amounts of the suggested nutrient dose. For example, P-nano-fertilizers in *Glycine max* produced a 32% more growth rate and 20% higher seed yield compared to plants treated with bulk P fertilizer (Liu and Lal 2014). In field experiments, the yield of rice after the application of urea-hydroxyapatite composites at 50% of the suggested dose (50 kg of N ha^{-1}) was 7.9 tons ha^{-1} while applying 100 kg of N ha^{-1} as bulk urea, the yield was 7.3 tons ha^{-1}, and the nutrient absorption efficiency was 48% and 18% for urea-hydroxyapatite composites and pure urea, respectively (Kottegoda et al. 2017).

Micronutrient deficiencies in plants can result in a significant reduction of their yield attributes (Rahi et al. 2021) because micronutrients are essential to proper functioning in several processes such as plant growth regulation, chlorophyll formation, seed production, and regulation of enzyme systems. Moreover, there are important crops sensitive to micronutrient deficiency. In this regard, NPs also fix micronutrient deficiencies and increase crop yield. For instance, foliar application of Fe_3O_4- NPs was efficient to increase plant growth and improve Fe uptake in the order leaves>stem>roots in plants of *Nicotiana benthamiana*. Magnetita-NP was an exceptional Fe supplement (Cai et al. 2020). Iron deficiencies in soils are a common problem that is difficult to fix due to the insolubility of Fe^{3+} in the soil and their quick fixation in soils after the application of iron-soluble fertilizers (Abbaspour et al. 2014). However, several types of Fe NMs as fertilizers and encapsulation methods have been tested. Khosroyar et al. (2012) used Fe-saccharate encapsulation with alginate coating and observed that the size of capsules influenced more the Fe release time than the doses inside of these, and the loading efficiency was higher than 90%. Iron released from these nano-fertilizers is a key prospective Fe plant source. Rui et al. (2016) tested Fe_2O_3 NPs (20 nm) as iron fertilizer for peanut variety Kainong 15, a highly sensitive Fe deficiency crop. They observed increased iron shoot and root concentrations when using between 10 and 1000 mg kg^{-1} and comparable concentrations to the use of EDTA (45.8 mg kg^{-1}). The authors suggested that NPs are adsorbed on sandy soil, and are slowly dissolved, so the Fe availability increases. Also, humic substances may improve Fe solubility, plant uptake, Fe translocation, and corrected Fe deficiency in cucumber plants. The use of humic

substances with nano-fertilizer was considered an ecologically safe NM (Sorkina et al. 2014).

Nano-fertilizers can also increase nutrient availability and absorption efficiency (between 18 to 29%) than traditional fertilizers (Usman et al. 2020), thus increasing the plant yield and nutrient value of some crops (Kah et al. 2018). Monreal et al. (2016) defined micronutrient use efficiency (MUE), according to soil fertility, as the quantity of added fertilizer-micronutrient that integrates into the crop (less than 5%). This term is related to transport, use, plant storage, and fate in the environment. To enhance MUE, foliar applications and the protection of conventional micronutrients are suggested; however, the information regarding these approaches is still sparse. Interestingly, NMs can be an option to improve MUE because the small size of NMs allows them to cross biological barriers and diffuses into the vascular system of plants. Furthermore, the surface chemistry of NMs can be modified by coatings to provide new properties and functionalities to carry a target nutrient in the right place (Lowry et al. 2019). Examples of protected NM-micronutrients to improve the MUE is CuO NPs carried into mesoporous aluminosilicates with 1%-10% of loading efficiency (Huo et al. 2014). Zn was nano-encapsulated on Mn carbonate-hollow core-shell with a reduction of loss of nutrients and improved rice Zn use efficiency (Yuvaraj and Subramanian 2015).

Similar to conventional fertilizers, nano-fertilizers can be applied to roots or leaves, which influences their performance on these plant organs, bioavailability, and plant uptake. Nano-fertilizers have longer and regulated nutrient release (40 to 50 days) compared to the short time availability (4 to 10 days) and less uptake efficiency (between 40% and 75%) of traditional fertilizers. For example, the concentration of Zn in leaves, fruit quality, and yield was increased by 30% (number of fruits) by foliar application of commercial Zn-NM (636 mg $tree^{-1}$) in *Punica granatum* cv. Ardestani trees (Davarpanah et al. 2016). The tomato yield increased, in field and greenhouse experiments, by foliar application of CuO and MnO NPs (1000 mg L^{-1}) due to the better micronutrient plant absorption (Elmer and White 2016). Nano-fertilizer obtained from green synthesis also have favorable results. Biosynthesized (*Rhizoctonia bataticola* TFR-6)-Zn NPs, size between 15 and 25 nm, were applied at 10 mg L^{-1} concentration at germination and 16 L

ha^{-1} two weeks later in the fields to pear millet plants (*Pennisetum americanum*). Plants treated with Zn NPs showed higher (37%) grain yield and (10%) plant Zn concentrations (Tarafdar et al. 2014).

NMs and plant diseases control

Nano-agrochemicals can be sorted as nano-fertilizers and nano-pesticides, however, some metal NPs have a dual function. Metal and metal oxides NMs have a role in plant protection, which has been tested under *in vitro* and *in vivo* experiments (Table 3). The foliar application of CuO and MnO NPs (1000 mg L^{-1}) reduced diseases caused by *Verticillium* and *Fusarium* in tomatoes and eggplants by 31% and 28%, respectively, compared to untreated plants (Elmer and White 2016). Similarly, Cu NPs were effective against *Curvularia lunata*, *Phoma destructiva*, and *Alternaria alternate*, and CuO NPs against *Saccharomyces cerevisiae* (Kanhed et al. 2014). Giannousi et al. (2013) tested diverse Cu-NPs (Cu/Cu_2O, Cu_2O, or CuO), which effectively controlled field plants of tomatoes against *Phytophthora infestans*. Foliar application at low concentrations (150-340 mg L^{-1} of active ingredient) of NPs was more effective than four commercial products (540-2240 mg L^{-1} of active ingredient). Ag NPs exhibited antimicrobial activity against *Escherichia coli* and *Aeromonas hydrophila* (Aziz et al. 2016). Several examples presented before showed that different single metal NPs are useful to control phytopathogenic microorganisms; however, more complex NMs can protect from persistent organisms. Graphene oxide-Ag NPs were useful for crop disease prevention (*Fusarium graminearum*) *in vitro* and *in vivo* experiments (Chen et al. 2016). Cu-chitosan NPs at low concentrations (0.1%) against *A. alternate*, *Macrophomina phaseolina, and Rhizoctonia solani* (Saharan et al. 2013). ZnO and nano copper-loaded silica gel with antimicrobial activity were effective against plant fungal pathogens producing citrus canker disease and damage in grapefruit trees (Young et al. 2018). In comparison to the use of the standard fungicide captan at doses between 200 to 500 µg mL^{-1}, Sidhu et al. (2017) observed stronger antifungal *in vitro* activity against *A. alternate*, *Drechslera oryzae* and *Curvularia lunata* in the range from 3 to 15 µg mL^{-1} of copper nitrate sodium sulfide (NCuS) NP aqua formulations. These authors tested naked CuS NPs and protected CuS NPs with three capping agents (polyvinyl pyrollidone, 4-aminobutyric acid,

and tri-sodium citrate); the last one having the highest antifungal activity. Additionally, these authors observed enhanced rice seed germination, shoot and root length, and vigor index of seedlings at low concentrations (7 µg mL^{-1}). These Cu-derived NPs come from natural CuS, which is non-toxic and is used for human illnesses. CuS NPs have low production costs, and their synthesis is easy; therefore, their use should be further explored in agriculture.

Shenashen et al. (2017) also used cylindrically cubic mesoporous alumina NPs to control Fusarium root in tomato plants *in vitro* and in greenhouse experiments. Nano-sized ZnO has also antibacterial activity, Graham et al. (2016) observed an inhibitory effect of ZnO NPs on *Xanthomonas citri* subsp. *citri*, the cause of citrus canker. Additionally, ZnO was an effective bactericide against *Escherichia coli* and *X. alfafae* subsp *citrumelonis* at sevenfold less concentration than commercial Cu sources. Similarly, it also was an effective fungicide against *Elsinoe fawcetti* and *Diaporthe citri*, two fungal diseases causing citrus scab and melanoses on grapefruit, respectively. A commercial product with AgNPs was highly effective in the field against the Huanglongbing (yellow dragon) disease in *Citrus aurantifolia*, a devastating agro-industrial bacterial problem. When applied by foliar sprinkling or trunk-injection, this product was 3 to 60 times and 75 to 750 fold more effective, respectively than the current antibiotic non-recommended for protection but used to control this disease (Stephano-Hornedo et al. 2020). Ag-doped TiO_2 NPs were also effective against *Fusarium solani* and *Venturia inaequalis* isolated from potato plants (Boxi et al. 2016). Foliar spray of CeO_2 NPs at 250 mg L^{-1} suppressed the symptoms of *Fusarium* disease and increased the fruit dry weight and lycopene content by 67% and 9%, respectively, compared to infested untreated plants. Plants growing in infested soil with *F. oxysporum* and treated with CeO_2 increased total sugar and Ca content by 60% and 140%, respectively, compared to plants growing in noninfested soil (Adisa et al. 2020). Satti et al. (2021) used *Moringa oleifera* leaf aqueous extract to synthesize TiO_2 NPs, which were effective at 40 mg L^{-1} against *Bipolaris sorokiniana*, a causal fungal agent of spot blotch of wheat plants. These authors observed increased water content, membrane stability, total chlorophyll concentration in fungal stressed wheat plants, higher spikes per plant, grains per spike, and 100 g grain weight number. In contrast, less soluble sugar, proline, phenolic, and flavonoid

concentrations were observed in fungal-stressed plants. These stabilized physiological plant parameters develop wheat resistance to *B. sorokiniana*. Zn NPs (225 mg L^{-1}), after 96 h of plant treatment, also control (100%) the nematode *Meloidogyne incognita* (Kaushik and Dutta 2017). Similar effects were observed by Ag NPs, produced by green synthesis with *Cladophora glomerata*, a green macroalga, to control *M. javanica* in laboratory bioassay and when inoculated into tomato plants. These NPs had a high negative impact on egg hatchability and juvenile mortality and were a potent nematicide that induced immune defense in tomato plants with significantly fewer galls number, egg males, and females per root (Ghareeb et al. 2020). Recently, Cai et al. (2020) analyzed the influence of foliar spraying of Fe_3O_4 NPs in the *Nicotiana benthamiana* plants against the *Tobacco mosaic virus* (TMV); regarded as a plant cancer and one of the most damaging plant viruses. These authors found that these NPs controlled virus spread and its proliferation due to enhanced reactive oxygen species in tobacco leaves, increased antioxidant enzymes participation against TMV (peroxidase and catalase), upregulation of salicylic acid, and expression of salicylic acid-responsive pathogenesis-related protein genes. Biogenic Ag NPs produced by *Fusarium chlamydosporum,* and *Penicillium chrysogenum* were effective to control the fungal growth of *Aspergillus flavus,* and *A. ochraceous*; and the production of their mycotoxins, such as aflatoxin and ochratoxin A, respectively. Cytotoxic effects of Ag NPs on human melanocytes were not observed. This is an important application as mycotoxin contaminates diverse crops and is toxic at low concentrations to animals and humans causing hepatocarcinogenic diseases (Khalid et al. 2021). All these examples establish the basis for the use of NMs to control plant biotic stress; they function as new weapons helping plant protection (Cai et al. 2020). Future research should comprehensively analyze the molecular mechanisms and the toxicity of these materials.

Table 3. Positive effects of metal NPs with potential use in agriculture.

NPs	Concentration	Organism	Effect	Reference
			Plant physiology	
α-Fe_2O_3	5.5x10^{-3} mg Fe L^{-1}	*Pisum sativum* *Vigna radiata* *Cicer arietinum*	The root growth increased from 88% to 366% in seedlings.	Palchoudhury et al. (2018)
$CoFe_2O_4$	0-1000 mg L^{-1}	*Solanum Lycopersicon*	The absorption of Fe and Co improved as doses increased, but Mn and Ca absorption decreased in the presence of NPs. No negative effect on plant germination and development. Root length was greater at the 1000 mg L^{-1} dose.	López-Moreno et al. (2016)
Fe_3O_4	20 mg L^{-1}	*Vigna radiate*	The germination percentage and bud growth improved.	Ren et al. (2011)
	2- 1000 mg kg^{-1}	*Arachis hypogaea*	The root length, biomass, and chlorophyll content were augmented.	Rui et al. (2016)
CuO	200 and 400 mg Cu kg^{-1}	Lettuce (var. ramosa Hort.)	The shoot biomass increased by 16% and 19%. Changes in the transpiration rate and stomatal conductance were observed.	Wang et al. (2019)
ZnO	50-1000 mg kg^{-1}	*Triticum aestivum*	Biomass (63%), grain yield (53%), and Zn concentration in grain increased in comparison with plants treated with bulk $ZnSO_4$.	Du et al. (2019a)
	800 mg kg^{-1}	*Cucumis sativus*	The concentration of sugars and gluteine in the fruit was bigger than those in the control treatment.	Zhao et al. (2014)
	1 mg kg^{-1} (foliar application)	*Cicer arietinum*	The aerial biomass, radical and root length increased by 27%, 37%, and 53% respectively, compared to the control treatment.	Mahajan et al. (2011)
	1.5 mg kg^{-1} (foliar application)		The dry weight of leaves increased.	Burman et al. (2013)
	>10 mg kg^{-1}	*Cyamopsis tetragonoloba*	Leaves and roots growth stimulated. Photosynthetic pigments, proteins soluble in leaves, rhizospheric microbial population, and enzymatic activity of acid and alkaline phosphatase increased.	Raliya and Tarafdar (2013)

NPs	Concentration	Organism	Effect	Reference
	> 1000 mg kg^{-1}	*Arachis hypogaea*	The germination, seedling vigor, stem, and root growth, as well as pod yield, were elevated compared to the control treatment and the treatment with bulk $ZnSO_4$.	Prasad et al. (2012)
	1.2 mM y 3 mM	*Solanum lycopersicum*	The germination rate, seedling vigor, the concentration of pigments, proteins, and sugar increased. The concentration of malondialdehyde and superoxide dismutase decreased.	Singh et al. (2016a)
TiO_2	2000 mg kg^{-1}	*Brassica napus*	The germination and seedling index increased, 75% and 1.6, respectively, in comparison with plants without the addition of NPs.	Mahmoodzadeh (2013)
ZnO, CuSi dispersed in a silica gel matrix	0.22 kg ha^{-1} (foliar application)	*Citrus* × *paradise*	Antimicrobial *in vitro* activity against several model phytopathogenic bacteria. Control of citrus canker for two consecutive years in the field.	Young et al. (2018)
		Plant protection application		
Ag NPs	50 and 100 mg L^{-1} (Petri dish essay)	*Xanthomonas axonopodis* pv. *Malvacearum,* and *Xanthomonas campestris* pv. *campestri*	Both concentrations showed antibacterial activity with zone diameters of 11 and 12 mm, respectively, for *X. axonopodis* pv. *Malvacearum. a*nd antibacterial activity zone diameters of 15 mm at 100 mg Ag NPs L^{-1} were observed for *X. campestris* pv. *campestris.*	Vanti et al. (2019)
ZnO	3-12 mM (Petri dish essay)	*Botrytis cinerea* and *Penicillium expansum*	Fungal growth inhibition (63% to 80%) and hyphal malformations.	He et al. (2011a)
	100 nM (Petri dish essay)	*Fusarium oxysporum*	Fungal growth inhibition.	Rispail et al. (2014)
			Soil effects	
nZVI	2-6 g kg^{-1}	-	The concentration of dissolved organic carbon and available NH_4^+ increased.	Zhou et al. (2012)
SiO_2	100 mg of Si	-	The concentration of available P increased.	Karunakaran et al. (2013)

nZVI, zero-valent iron nanoparticles

NMs in plant pest control

Several metal NMs based on Ag, CuO, MnO, ZnO, CuSi, CeO_2, and CeAc NPs are also suitable for pest control (Singh et al. 2018; Du et al. 2019; Kah et al. 2019; Singla et al. 2019; Wang et al. 2019b; Adisa et al. 2020; Sun et al. 2020). Awasthi et al. (2020) mentioned that common agricultural insect control alternatives have some constraints; such as low efficiency, high input costs, not being insect-specific, and causing environmental imbalance and negative effects on animals and humans. Therefore, NMs may provide healthy and resourceful alternatives and be environmental-friendly. Stadler et al. (2010) mentioned that nanostructured alumina is a cheap, reliable, and safe alternative to insect pest control. It was effective (95% mortality) and had quick action (3 days) against *Sitophilus oryzae* and *Rhyzopertha domina*, major insect pests in stored food supplies of wheat grains. Moreover, it was also effective in all concentrations tested (80, 125, 250, and 500 mg kg^{-1}) against *Acromyrmex lobicornis*; leaf-cutting ants affecting cacao, cassava, citrus, coffee, cotton, and corn crops (Buteler et al. 2018). Because of the strong adhesion of the nanostructured alumina to the insect's body surface, these authors suggested this NM as a particle carrier in insect control systems (insecticides, entomopathogens, or pheromones). Ag NPs have been tested for their toxicity against phytophagous mites, Pavela et al. (2017) used Ag nanocrystals synthesized with root extracts of *Saponaria officinalis* to control eggs, larvae, and adults of *Tetranychus urticae*. These authors suggested that the demonstration of no phytotoxic effects of these NPs is needed for their safe use in integrated pest management strategies. Low concentrations of CuO NPs (10 mg L^{-1}) enhanced the expression of the *Bacillus thuringiensis* (Bt) toxin protein in transgenic cotton plants; however, at higher concentrations (1000 mg L^{-1}) the expression was inhibited (Le Van et al. 2016). These authors suggested the use of CuO NPs at low concentrations as a promising technology to improve the pest resistance of transgenic insecticide crops.

As observed a diverse kind of NMs has the potential for direct crop protection as active ingredients; however, they can be also nanocarriers of formulations. In most cases, NMs such as silica NPs, carbon nanotubes, and graphene oxides are vehicles for pesticide active ingredients to deliver in a controlled and intelligent form (Grieger et al.

2015; Pérez-de-Luque 2017; Qureshi et al. 2018; Wani et al. 2019). Nanocomposites, as plasmonically active nanorods of gold with Ag core-shell, were used as carriers of nutrients in tomato plants; moreover, to deliver bioactive agents such as the auxin growth regulator 2,4-D (Nima et al. 2014). Nano-materials may also be used to protect active compounds of biopesticides from plant or microbial origin, which have a short period, and suffer degradation by UV-rays, microbial activity, or other influencing factors (Khot et al. 2012). This protection occurs by nanoencapsulation that allows controlled dissolution kinetics as well as stability and solubility of active product. The thickness of encapsulation-wall material shells, composition, and physical and chemical properties are factors to produce environmentally friendlier nanomaterials (Kumar et al. 2019). As the time of release from the nanocarrier can be modulated, the effectiveness of the biopesticide activity may be increased and prolonged for a longer time. For instance, zinc hydroxide nitrate at the nanosize scale has high compatibility with anionic pesticides and its surface functionalization is easy, which strongly influences the rate and equilibrium pesticide release (Kumar et al. 2019). Layered metal hydroxides, with magnetic and catalytic properties, offer a novel alternative as pesticide carriers (Rives et al. 2013). Kumar et al. (2019) mentioned that cyanobacteria powder may function as a carrier of nano-pesticides. The advantages of using these microorganisms are based on their cosmopolitan abundance, biocompatibility, and heterogeneous cell wall-functional groups able to load pesticides. Cyanobacteria powder and Carbopol coating functioned as avermectin-nanocarrier under stimuli-controlled delivery; which was low and slow, and the photostability to UV radiations was enhanced compared to the use of free avermectin (Yang et al. 2013).

Nanosensors in agriculture

Nanosensors are next-generation sensors with a more compact presentation than traditional sensors (Usman et al. 2020). Nanosensors help improve agricultural practices: to identify soil contaminants and residues of their transformation, to detect nutrient soil deficiency and early plant diseases, to monitor soil temperature and humidity, and other environmental stressors (Baruah and Dutta 2009). Therefore, opportune corrections may be done and consequently positive effects on crop yield, plant health, and use of inputs.

Nanosensors are long-desired tools for precision farming (Acharya and Pal 2020); which may enhance productivity in agricultural systems by maximizing output from plants whereas reducing the inputs (fertilizers, pesticides) with environmental monitoring and wise actions.

Any sensor used to bring information, combining biological and physical-chemical aspects, from nano to macroscopic scale is a nanosensor. The principle of operation of nanosensors is that they are based on the interaction of a particular characteristic of a NM with the surrounding environment at the nanoscale level (Chakraborty et al. 2021). These smart devices are small, controllable, sensitive, accurate, and reproducible (Awasthi et al. 2020). Gold NPs, silica NPs, carbon nanotubes, graphene, quantum dots, and polymer nanocomposites have been used in nanosensor production (Kwak et al. 2017). Developing simple methods to detect chemicals, indicators of organisms, or processes is a challenge due to the constraints. Organic dyes used for optical sensors may have poor photostability, easy photobleaching, small Stokes shifts, and short lifetimes. However, metal-NPs may be useful for this goal, semiconductor quantum dots, and noble metals NPs can have the advantages of biocompatibility, low toxicity, resistance to photobleaching, and stable emission (Qian et al. 2014). Aptamers, short single-stranded DNA, or RNA are useful due to their ability to specifically bind the target (Taghdisi et al. 2015). Fluorescent nanoprobes of silica NPs were used for detecting *Xanthamonas axonopdis* which causes bacterial spot disease in Solanaceae plants (Yao et al. 2009). CuO NPs and nanolayers have been tested as a gas sensors to detect *Aspergillus niger* in bread (Etefagh et al. 2013). Alternatives such as this may be useful for detecting other phytopathogens in seeds or plants of agronomical interest. These nanodevices have high sensitivity for on-site detection at low concentrations such as parts per billion (ppb). P. e. Au NPs were used for simple, rapid, reliable, real-time, and highly sensible colorimetrically detection of organophosphorus pesticides such as diazinon (at 54 ppb), iprobenfos (54 ppb), and edifenphos (28 ppb), commonly used in agricultural production and highly toxic to human health (Kim et al. 2015).

Monreal et al. (2016) defined a nanodevice as a manufactured appliance to control and manipulate biomolecular constructs and assemblies such as proteins, cellular lipid

layers, viruses, or nucleic acids. They suggested that these nanodevices may be useful to improve MUE and crop nutritional quality by controlling nano-fertilizer delivery. Some examples are the incorporation of a fluorescent protein reporter gene (egfp) in a *P. putida*-genetically modified (GM) which detected 90% Zn content in soil:water extracts of Zn-amended soils. Similar results were observed with the *Escherichia coli*-GM and the reporter gen pZNT-lux to quantification of soil bioavailable Zn concentration. Synthetic nucleic acids function for highly specific and sensitive detection of different chemical species in fluids or single living cells. These authors proposed that aptamer nanodevices may help to study metabolites in the alive cells involved in the rhizosphere and their interaction with nutrient cycling, control temporal and spatial nano-fertilizers, and identify and treat plant and soil nutrient deficiency. Therefore, a more complete understanding of *in vivo* plant-soil-microorganism systems and their influence on global crop production may be obtained.

NMs in seeds quality and protection

Seed priming is a traditional method practiced in agriculture to induce seed germination and seedling establishment that usually use water or solutions with nutrients, hormones, plant regulators, or biopolymers. Seed priming using NMs is an innovative, easy, efficient process and convenient agricultural technique mainly for micronutrient application. Research shows that seed nano-priming not only improves seed germination and synchronization, vigor, and establishment of seedlings but also has a significant influence overall lifecycle of plants (crop resistance to biotic and abiotic stresses, storage, fortification). However, time imbibition and kind of NPs should be considered as effect on plant growth and yield may change (Rahman et al. 2020). Hence, it is expected important potential for food quality and production for agricultural applications (do Espirito Santo Pereira et al. 2021). Palchoudhury et al. (2018) suggested that seed priming with NMs functions as fertilization with fewer amounts and avoids the need for soil fertilization. This represents a more environment-friendly fertilization alternative. These authors analyzed the use of low and high concentrations of two Fe NMs (Fe_2O_3 and Pt-decorated Fe_2O_3) on priming seeds of five legumes. Seedlings of green pea (*Pisum sativum*), chickpea (*Cicer arientinum*), and green gram (*Vigna radiate*) had better grow with low

concentrations ($5.54x10^{-3}$ mg Fe L^{-1}) of Fe_2O_3 NPs. The improvement growth rate of embryonic roots was also detected in these legume plants (88-366%). ZnO NPs applied to seeds of peanut (1000 mg kg^{-1}) also enhanced the germination and vigor of seedlings (Prasad et al. 2012). Nano-iron pyrite (FeS_2) was used as seed priming from diverse vegetables, spice, fodder, and oilseed crops. Yield increment of 47% in beetroot, 19% in carrot, 65% in mustard, 66% in sesame, and 217% in alfalfa (Das et al. 2016). Prerna et al. (2021) used α-Fe_2O_3 NPs on rice (*Oryza sativa*) and maize (*Zea mays*) seeds that were primed from 20 to 200 mg L^{-1}. These authors found that 25 mg L^{-1} enhanced germination and seedlings' dry matter production of both plants in comparison to conventional hydro-priming. NPs also enhanced the levels of superoxide anions and hydrogen peroxide in seeds of rice and maize, and consequently higher concentrations of antioxidant enzymes (superoxide dismutase, catalase, and malondialdehyde) were observed in seeds of both plants imbibed for 24 h in NPs solution. They also found that foliar application of these NPs improved the yield of rice and maize measured by grain weight, and length, thickness, and width of seeds. Green synthesized FeO NPs (by *Cassia occidentalis* L. flower extract) at two concentrations (20 and 40 mg L^{-1}) were the priming treatment of Pusa basmati rice seeds. At both NPs concentrations, seeds had higher germination and vigor than treatments with $FeSO_4$ and water. At lower NP concentrations, seedlings presented 50% induction of root length, dry weight and sugar, and amylase concentrations. Moreover, Fe uptake and reactive oxygen species (ROS) production also were stimulated (Afzal et al. 2021). Seed priming with metal NPs is a promising biotechnological alternative for saline conditions. Examples of Mn, Zn, and Fe NPs in pepper (*Capsicum annuum*), lupin (*Lupinus termis*), and sorghum (*Sorghum vulgare*) seeds, respectively, also showed improvement in germination, seedling and plant growth, photosynthetic pigments, phenols, organic molecules, antioxidant enzymes, and root and shoot distribution of Na (reviewed by Do Espiritu Santo Pereira et al. (2021)). The use of Cu^0 NPs (65 µm) in seed priming resulted in developed drought resistance in corn plants. Higher chlorophyll and carotenoid concentrations were observed, and the regulation of protective mechanisms as enzymes scavenging ROS and antioxidants (Van Nguyen et al. 2021). Similarly, Cu^{2+}-loaded chitosan NPs at 0.0625 mmol L^{-1} favorably

activated enzymes related to antioxidant response in corn seeds under high temperature (42 °C) and relative air humidity, near 100% (Gomes et al. 2021).

Materials at nanoscale size are also useful to protect seeds from seed-borne diseases (Acharya and Pal 2020); which may be a valuable alternative in agriculture as crop productivity depends on seed quality. Arumugam et al. (2016) observed no effect on seed germination, or the growth rate of roots and shoots when using hydrophobic silica NPs in several seeds (*Vigna ungiculata*, *V. mungo*, *V. radiate*, *Cajanus cajan*, *Macrotyloma uniflorum,* and *Cicer arietinum*). However, these authors found a protective effect of the seeds of these plants against beetle infestation (*Callosobruchus maculatus*) by significant oviposition reduction, the emergence of adults, and seed damage. The physical seed characteristics influenced the maximum surface area covered or not by NPs. These results show the use of NMs in postharvest management. Another example in this aspect is the use of plant-extract biosynthesized Ag NPs (2000 µg mL^{-1}) to effectively protect banana fruits against *Colletotrichum musae*. Jagana et al. (2017) observed 6% of disease severity in comparison to 76% in non-treated fruits.

Choudhary et al. (2019) tested Zn-coating chitosan NPs in maize seeds priming and observed increased antioxidant enzymes and lignin concentrations, which were related to increased resistance to pathogens. Similarly, low concentrations of mesoporous Si NPs loaded with cinnamon essential oil in pea (*Pisum sativum*) primed seeds increased 90,000 times the bactericide action against *P. syringae* (Bravo Cadena et al. 2018). Moreover, the effects observed in NMs-primed seed were not only on seed growth and biotic stresses but also had a positive influence on abiotic plant stress. Li et al. (2021), under Cd stress (0 and 100 mg L^{-1}), observed significant plant growth improvement and a modified metabolomics analysis in two fragrant rice varieties treated with ZnO NPs (0, 25, 50, and 100 mg L^{-1}). The concentration of Zn in seedlings increased by ZnO NPs, but seedlings had significantly fewer Cd concentrations. As seed priming using NMs is a novel agronomical tool and more benefits by their use are expected.

Other benefits of metal NPs in agricultural soils

Scarce information is available on NMs' influence on agricultural soils, especially on their physical and chemical properties (Table 3), and their use to solve other soil limitations besides soil remediation (Zhou et al. 2012). There are several soil constraints strongly influenced by global climate change which threaten sustainable agriculture by decreasing crop productivity. For example, soil salinity is a major world environmental concern influencing nearly 800 million hectares of arable land worldwide. Some authors have demonstrated that TiO_2 NPs ameliorate the negative effects of soil salinity on agricultural or medicinal crops such as broad bean (*Vicia faba*), tomato (*Solanum lycopersicum*), or Moldavian balm (*Dracocephalum moldavica*) (Khan 2016; Abdel Latef et al. 2018; Gohari et al. 2020). Abdel Latef et al. (2018) observed that the application of 0.01 % TiO_2 NPs influenced plant growth and reduced soil salinity stress in broad bean, a widely growing leguminous crop. Proline, soluble sugars, amino acid concentrations, and antioxidant enzyme activity were increased. Gohari et al. (2020) showed that 100 mg L^{-1} of TiO_2 NPs under saline conditions (50 mM NaCl) enhanced agronomic traits (plant height, fresh and dry shoot weight, leaf number, and fresh and dry leaf weight) and antioxidant enzyme (catalase, ascorbate peroxidase, superoxide dismutase, and guaiacol peroxidase), and lowered hydrogen peroxide concentration. The amounts of geranial, geraniol, and z-citral, the dominant essential oil components of the medicinal plant *D, moldavica*, used as painkiller for kidney complaints, toothache, and colds, increased by application of TiO_2 NPs in the control treatments but decreased under salinity conditions.

Nanomaterials have applications for soil improvement from geotechnical and geological engineering and design point of view. For example, low concentrations (0.2%) of multiwall carbon nanotubes and carbon nanofiber enhanced hydraulic conductivity and reduced soil cracks of clayey sand soils. Similarly, mixtures of nano-alumina positively influenced compaction, crack intensity, and particle arrangement of soils (Alsharef et al. 2016). Metallic NPs used as soil amendments may improve soil properties. Iron oxides NPs can induce changes in the physical and chemical soil properties (Mukhopadhyay 2014), bulk density, and porosity (Bayat et al. 2018; Zhang and Zhang 2020; Sun et al.

2020; Pérez-Hernández et al. 2020). The bulk density of agricultural soil, classified as Hypocalcic Cambisols, increased from 1.05 to 1.1 g cm^{-3} with the addition of Fe_3O_4 NPs at 3% (w/w). In contrast, MgO NPs at 3% (w/w) decreased soil bulk density from 1.05 to 0.97 g cm^{-3}. Moreover, Fe_3O_4 increased the tensile strength of the soil aggregates by the establishment of bonds between Fe and soil particles (Bayat et al. 2018). Interestingly, alfalfa seed priming FeS_2 treatment not only influenced plant growth and yield but also influenced the soil. This treatment resulted in plants that increased soil cover, anchorage of the soil, and consequently reduced soil erosion (Das et al. 2016). These authors suggested this approach as sustainable in a fragile ecosystem to decrease soil erosion. Zhou et al. (2012) studied the influence of different doses (2 to 6 g kg^{-1}) of three iron-based NPs such as Fe^0, Fe_3O_4, and Fe_2O_3 on pH, dissolved organic carbon (DOC), NH_4^+ and P availability, and enzymatic activities (key components of biogeochemical cycles and soil quality) in two soils. Responses were dependent on soil type and kind and doses of NPs. Fe^0 increased DOC and NH_4^+ availability but decreased P availability. Both NP, Fe_3O_4, and Fe_2O_3 lowered pH and nutrient availabilities. Summarizing, the information shows that NMs may influence soil quality; however, more research is needed to apply this knowledge in agricultural soils to improve their quality, physical and chemical properties, and sustainability.

Interaction NMs and plants

There are several examples of the beneficial impacts of metal NPs on plants (Table 3); however, undesirable effects on plants have been also described (Table 4). This intricate impact is due to the fact the effects of metal NMs on plant morphology, physiology, and biochemistry depend on several interacting factors: shape, type, and size of NPs, concentration, agglomeration, application form, kind of metal, and their properties, etc. (Batsmanova et al. 2020). Plant species (Elemike et al. 2019), environmental conditions (Morales-díaz and Ortega-ortíz), and the nature of growth media (soil, hydroponics, *in vitro* conditions, etc.) are also key elements influencing the result of this interaction (Singla et al. 2019). Although these factors are key aspects to assess the plant response, and their analysis is partial, the type, size, and concentration are the NMs features more often studied. More information is also available in less natural

experimental conditions such as laboratory tests and soilless experiments. Therefore, generalization on the interaction of NMs-plant is not possible and proper comparison from the results obtained is difficult.

On the one hand, the positive effects of metal NPs on plants may be observable at different plant stages and growth conditions (Table 3). Metal NPs can accelerate germination (Ag NPs, nZVI, ZnO, TiO_2, $nSiO_2$), stimulate aerial and radical biomass (Ag NPs, Al NPs, CeO_2, ZnO, Fe_2O_3, $CoFe_2O_4$, CuO), and increase crop yield (Fe, Co, Cu, Au NPs). In regenerated shoots of *Vanilla planifolia* obtained by a temporary immersion bioreactor system, Ag NPs stimulated shoot multiplication and elongation; however, at high concentrations, there was inhibition of these two processes (Spinoso-Castillo et al. 2017). In a greenhouse experiment, Antisari et al. (2015) evaluated the effect of CeO_2, Fe_3O_4, SnO_2, TiO_2, Ag, Co, and Ni NPs at 20 mg L^{-1} on the morphology and nutrition of tomato plants growing in soil. The authors found that plant yield and nutrient content depended on the type of NP. For instance, SnO_2 NPs reduced root biomass by 63% compared to control plants (without the addition of NPs). While Fe_3O_4 NPs increased root biomass by 153%. Palchoudhury et al. (2018) observed a positive effect on plant growth of three legumes when low iron oxide NPs concentration (5.54×10^{-3} mg L^{-1} Fe) was used; however, these authors found contrary effects at high NPs concentrations (27.7 mg L^{-1} Fe). Jahani et al. (2019) assessed the effect of different concentrations, from 0 to 4000 mg L^{-1}, of Co_3O_4 NPs foliar sprayed in *Brassica napus* L. The results showed that at concentrations of 50 and 100 mg L^{-1} stimulated plant height, biomass, and chlorophyll concentration. Doses of 250 to 4,000 mg L^{-1} increased plant height, fresh and dry weight, leaf area, but the membrane stability index decreased due to the high concentration of oxidative stress markers like peroxide, malonaldehyde, and other aldehydes. Similar results have been observed in *Calendula officinalis* L. treated with CeO_2 NPs (Jahani et al. 2018). Askary et al. (2017) applied Fe_2O_3 NPs (0 to 40 mM) to *Catharanthus roseus*, which resulted in increased plant growth variables, photosynthetic pigments, and concentration of proteins. Prerna et al. (2021) using α-Fe_2O_3 NPs found significant yield increment in wheat and corn under field conditions. Similarly, in wheat with ZnO NPs (Kah et al. 2019) and in *Arachis hypogaea* (Das et al. 2016). More examples of the positive effect of NMs in agricultural plants were presented before, in the “Nano-fertilizer” section.

Furthermore, several specific reviews have been published recently (Acharya and Pal 2020; Awasthi et al. 2020; Usman et al. 2020; do Espirito Santo Pereira et al. 2021; Singh et al. 2021).

On the other hand, metal NPs in plants can inhibit several plant processes and several factors as mentioned before may be involved (Table 4). For example, root length (Ag NPs, Al_2O_3, CuO, ZnO), leaf expansion (Ag NPs and TiO_2, ZnO), growth (Ag NPs, CuO, TiO_2, ZnO), and nutrient uptake (Ag NPs). In addition, the reduction of biomass (Ag NPs, Ag_2S, CuO, SiO_2), photosynthetic rate (CeO_2, Co_3O_4, ZnO, TiO_2), chlorophyll content (CuO, ZnO, Ag NPs), germination rate (Si, Pd, Au, Cu, Ag NPs, ZnO, CuO, Al_2O_3). High concentration of NPs may damage vacuoles (Ag NPs); induce cell wall rupture (Ag NPs, CeO_2), lipid peroxidation (ZnO, CuO, NiO, CeO_2), and increase the concentration of reactive oxygen species (CuO, ZnO, Fe_3O_4, TiO_2, CeO_2), abscisic and jasmonic acid (TiO_2). Even DNA damage (Al_2O_3), chromosomal aberrations (ZnO, NiO), and different pattern expression of some proteins involved in cell defense (Ag NPs) have been observed (Zuverza-Mena et al. 2016, 2017; Raffi and Husen 2019; Singla et al. 2019; Rasouli et al. 2020; Youssef and Elamawi 2020; Liu et al. 2020). However, the effect of NP depends on the doses and type of particle and plant species.

Table 4. Some negative effects of metal NPs on plants and soil microorganisms.

NP	Effect	NP size (nm)	Concentration (mg L^{-1} or mg $kg^{-1)}$	Medium	Organisms	Reference
			Plants			
Ag	Oxidative stress and DNA damage.	<100	Effect dose-depend (5-80)	Solution	*Allium cepa*	Panda et al. (2011)
Ag	Low biomass and chlorophyll content.	10 -15	50-5000	Solution	*Lycopersicon esculentum*	Song et al. (2013)
Ag	Low water content, the root, and shoot length were reduced by 48%, and 40% compared to without NP addition. Less concentration of Ca, Mg, B, Cu, Mn, and Zn compared to the control plants.	2	500	Solution	*Raphanus sativus*	Zuverza-Mena et al. (2016)
ZnO	Low biomass and root length.	20±5	> 1000	Hoagland nutrient solution	*Lolium perenne*	Lin and Xing (2008)
ZnO	Reduced germination rate. Root cells denoted chromosomal aberrations and alterations in the cell cycle were observed. Enzyme systems showed an altered expressed pattern.	80	100-200	Solution	*Vicia faba*	Youssef and Elamawi (2020)
Al_2O_3, TiO_2, ZnO	TiO_2 reduced the mitotic index by 60% at 0.1 mg L^{-1}. Disturbed metaphase was observed in roots treated with Al_2O_3 at 10 and 100 mg L^{-1}. Oxidative stress increased with the increasing concentration of NPs.	>50	0.1, 10 and 100	Solution	*Allium cepa*	Debnath et al. (2020)
ZnO	At low NPs concentrations higher nitrogenase activity in the four legumes tested. At 10 mg kg^{-1} negative effects were observed	16-30	1.5 - 10 mg L^{-1}	Hogland Nutrient solution	*Vigna unguiculata*, *V. radiata*, *V. aconitifolia* and	Kumar et al. (2015)

NP	Effect	NP size (nm)	Concentration (mg L^{-1} or mg kg^{-1})	Medium	Organisms	Reference
					Cyamopsis tetragonoloba	
CuO	Reduced percentage of germination, loss of viability of root cells, oxidative stress.	<50	0.080 and 0.12	Solution	*Oryza sativa*	Shaw and Hossain (2013)
ZnO	Growth inhibition, low chlorophyll content, reduction of photosynthetic rate, stomatal conductance, and intracellular CO_2.	<50	200-300	Soil	*Arabidopsis thaliana*	Wang et al. (2016b)
TiO_2, ZnO	Both NPs reduced the biomass of wheat plants. Soil protease, catalase, and peroxidase activities were inhibited.	<100	10 5	Soil	*Triticum aestivum* L.	Du et al. (2011)
			Soil microorganisms			
Carbon-coated Ag	Concentrations >0.25 mg kg^{-1} had a negative effect on several genes involved in denitrification (DN), nitrogen fixation (NF), and nitrification (N). Concentrations between 0.025 to 0.05 mg kg^{-1} of the genes involved in DN and NF were not affected, but the gene expression in N (*amoA1* and *amoC2*) was upregulated between 2 to 3 times.	35	Several concentrations according to their minimal inhibitory concentration to Ag NPs	Pure culture	*Azotobacter vinelandii* (NF) *Nitrosomonas europaea* (N) *Pseudomonas stutzeri* (DN)	Yang et al. (2013)
Ag	Inhibition of microorganisms involved in the nitrogen cycle (nitrite and ammonia-oxidizers)	27	5, 50 mg L^{-1}	Pure culture	*Nitrospira multiformis*, *Nitrosomonas europea* and *Nitrosococcus oceani*	Beddow et al. (2014)

NP	Effect	NP size (nm)	Concentration (mg L^{-1} or mg $kg^{-1)}$	Medium	Organisms	Reference
ZnO	Modified morphology of *R. leguminosarum*, diminished root nodulation, and biological nitrogen fixation		250-750 mg L^{-1}	Liquid medium	*Vicia faba/Rhizobium leguminosarum*	Huang et al. (2014)
Ag	The abundance of Acidobacteria, Actinobacteria, Cyanobacteria, Nitrospirae, and Firmicutes decreased significantly in comparison with the control treatment. Cell damage in the cell wall of *Nitrosomonas europaea* was observed.	50	50, 100	Soil	Soil microorganisms	Wang et al. (2017)
Ag	The number of nodules and spores, nitrogenase activity, rate of mycorrhizal colonization, plant dry weight, and plant height decreased in comparison to the control treatment. Delayed nodulation processes and alterations in the number of bacteroids.	5-50	0.8	Soil	*Rhizobium leguminosarum bv. viciae ASU (KF670819), Glomus aggregatum, Vicia faba*	Abd-alla et al. (2016)
ZnO	Inhibition of root elongation. Two hours after NPs exposure the activity of glucosidase was reduced. 30 d after NPs exposure the abundance of *Actinobacteria, Proteobacteria,* and *Acidobacteria* decreased by 76%, 40%, and 11%, respectively.	50	200-1000	Soil	Soil microorganisms and *Phytolacca americana*	Shi et al. (2020)
ZnO	The number of nodules and plant biomass was reduced in non-inoculated plants (AMF) and treated with NPs. While in plants inoculated with AMF, the colonization rate	18	375 and 500	Sand:Perlite (1:1)	*Trigonella foenumgraecum*, *Rhizobium melliloti*, *Glomus intraradices*	Siani et al. (2017)

NP	Effect	NP size (nm)	Concentration (mg L^{-1} or mg $kg^{-1)}$	Medium	Organisms	Reference
	decreased in comparison to control plants.					
ZnO	Plant growth and soil enzyme activity were inhibited.	30	250-500	Soil	*Sorghum bicolor* L., *Funneliformis caledonium* (*Glomus caledonium)*	Wang et al. (2018a)
ZnO	The rate of root colonization was inhibited.	30	500	Soil: Sand (3:2)	*Zea mays* L. var Zhengdan958, *Funneliformis mosseae*	Wang et al. (2018b)
ZnO	The plant growth and the rate of AMF colonization were inhibited	90	>800	Soil	*Zea mays* L. var Zhengdan958, *Glomus versiforme, Glomus caledonium,*	Wang et al. (2016a)
ZnO s-ZnO	After 90 d, the richness and alpha diversity of the bacterial community was significantly reduced compared to the control treatment.	25	500	Soil	Soil microorganisms	Chen et al. (2020)
Ag, Ti	The colonization of AMF decreased, as well as the uptake of ^{134}Cs by mycorrhizal plants.		154	Soil	*Helianthus annus, Glomus intraradices*	Dubchak et al. (2010)
CuO	Inhibitory effects on dehydrogenase and phosphatase enzyme activity.	<50	68 and 332	Biosolids-amended soil	Soil microorganisms	Samarajeewa et al. (2020)
CuO	A decreased abundance of the denitrification genes *nirS* and *narG* was observed.	28	0.63 and 63	Soil	*Triticum aestivum* cv. Cumberland and rhizospheric bacteria	Guan et al. (2020)
FeO	Glomalin content was reduced. An inhibitory effect on the plant uptake nutrients.	10	3	Sand: Perlite (1:1)	*Trifolium repens, Glomus caledonium*	Feng et al. (2013)

NP	Effect	NP size (nm)	Concentration (mg L^{-1} or mg $kg^{-1)}$	Medium	Organisms	Reference
Fe_3O_4	The decrease in bacterial abundance and AMF diversity of corn plant rhizosphere.	10	10	Soil	*Zea mays*	Cao et al. (2016)
Fe^o	Adsorption of nZVi onto outer cell membranes may affect membrane permeability or to disruption of the membrane lipid bilayer. It may increase the generation of the free radicals	320	70-700	Ultra-pure water pH adjusted at 5-5.5	*Escherichia coli*	Auffan et al. (2008)

Nano-biotechnology is an interesting research field in which some authors have analyzed the use of NMs in transgenic plants. Le Van et al. (2016) investigated the effect of CuO NPs on conventional and transgenic cotton plants. These authors observed that at low concentrations (10 mg L^{-1}), CuO NPs did not influence plant height, root length, root hairs, shoot, and root biomasses in both cotton genotypes; however, at higher concentrations (200 or 1000 mg L^{-1}) both genotypes were negatively affected. They also observed modifications in hormone (IAA and ABA) and nutrient concentrations by adding CuO NPs. The responses were dependent on NPs concentration, part of the plant (root or shoots), and cotton genotype. Li et al. (2014) concluded that transgenic cotton plants are less tolerant than conventional cotton plants to CeO_2 NPs. Shoot biomass, Zn shoot and Fe root concentrations significantly decreased at 500 and 1000 mg L^{-1} of CeO_2 NPs in Bt-transgenic cotton plants. These authors observed significantly lower Ce shoot and root concentrations in transgenic cotton plants than the conventional ones at the three Ce NPs concentrations tested (100, 500, and 2000 mg L^{-1}). Bt-transgenic cotton plants have low transportation ability due to the consumption of energy to produce the toxic protein Lepidoptera larvae species.

Interaction metal NMs and soil

The interactions between NPs and soil control the fate and behavior of NPs. Thus, these interactions and the variables involved are relevant to make sure that NMs fulfill their function. Similar to the bulk metallic compounds transport, it is recognized that soil properties affect the mobility, size, dissolution, and toxicity of metal NPs, in addition to the NPs properties (Bruemmer et al. 1986; Dimkpa and Bindraban 2018). The interactions between metal NPs and soil are complex; due to the effects on the organisms living in the site, chemical reactions, transport, and the soil variables involved in these reactions (Figure 4).

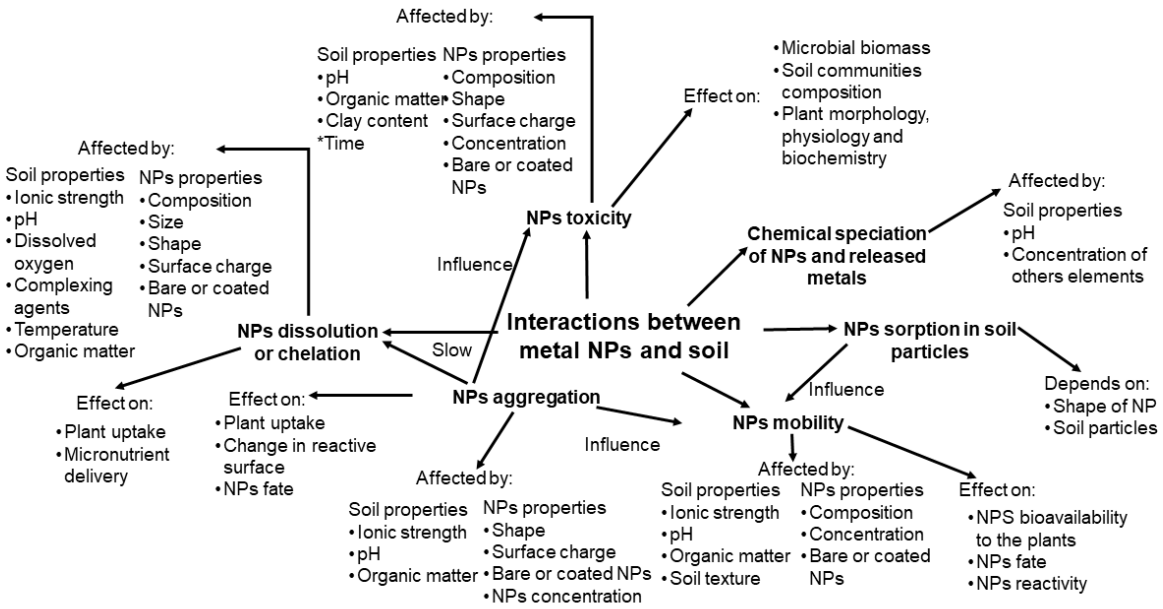

Figure 4. Main interactions between metal NPs and soil and their effects.

The mobility of NPs in soil determines their bioavailability to the plants and their fate (Singh and Kumar 2020). Some studies highlighted that ionic strength, soil humic acids, organic matter, soil texture, and pH may influence the mobility of Fe_3O_4, TiO_2, CuO, and ZnO NPs (Belal and El-Ramady 2016; Ermolin et al. 2019; Singh and Kumar 2020). Soil column experiments showed that ionic strength affects the mobility of NPs in soil and porous media (Singh and Kumar 2020). Because ionic strength affects different forces acting on NPs, like the Van der Waals, electrical double layer, and electrostatic forces, potential differences, a high ionic strength limits the mobility of NPs by promoting the agglomeration (reversible) and aggregation (irreversible) of NPs and their deposition on the surface of soil colloids (Ben-Moshe et al. 2010; Mondal et al. 2021), linking ions are relevant in these changes.

Some NPs properties influence the behavior and mobility in soil: including changes in particle aggregation or disaggregation, the surface structure, and charge. The NPs can move in porous material as individual particles, agglomerates, or micro-aggregates. As individual particles, NPs move in soils by diffusion, and mass flow, particle transport is controlled by the NPs filtration rate by the porous media (Chen 2018). In contrast, when agglomeration or aggregation occurs, NPs can be immobilized by physical straining

(Conway and Keller 2016). The physical straining means that NPs aggregates are retained in a soil pore that is smaller than them (Díaz et al. 2010). Results show that after 72 h of application of TiO_2, CeO_2, and $Cu(OH)_2$ NPs, their mobility in agricultural and grassland soils was limited to the upper 3 cm soil depth. The formation of micro-aggregates with the organic matter was the cause of the immobilization of these NPs, and the higher retention occurred in soil columns with less porous. Therefore, physical straining was the primary mechanism of retention (Conway and Keller 2016). Soil minerals can enhance or inhibit the mobility of NPs aggregates. It depends on the NPs adsorption on mobile colloids or non-mobile soil particles (Belal and El-Ramady 2016; Ermolin et al. 2019). Ermolin et al. (2019) measured the mobility of CeO_2 NPs in agricultural soil under wetting-dry cycles. The mobility of CeO_2 NPs decreased from 0.11% to 0.07% by water-stable soil aggregates formed between the NPs and soil particles. However, the authors also observed through micrographs, ensembles of CeO_2 NPs with soil minerals in the soil leachate. Soil mineralogy affects the transport of aggregates because clay minerals can serve as a carrier of NPs.

The NPs agglomeration depends on both NPs and soil properties (Singh and Kumar 2020). Some authors pointed out that NPs concentration in a liquid medium is a critical variable in the NPs agglomeration (Shrestha et al. 2020; Singh and Kumar 2020; Wang et al. 2020) because NPs-concentration determines the interparticle distance and the collision frequency between particles. If the interparticle separation is lower than the maximum repulsive potential, the agglomeration of NPs occurs. NPs remain in suspension if the interparticle gap exceeds the maximum repulsive potential (Shrestha et al. 2020). This point is relevant in the formulation of stable suspensions of nano-agrochemicals and their application.

The particle size and surface charge are other of the main NPs features that play a role in the interaction of NPs with their medium and their agglomeration or aggregation (Gatoo et al. 2014; Chen 2018; Singh and Kumar 2020). From the kinetic stability studies with NPs, it has been observed that NPs smaller than 50 nm agglomerate and form aggregates bigger than those formed by large size NPs (Ben-Moshe et al. 2010; Chen 2018). In this case, the size of agglomerates in an aqueous solution of TiO_2 NPs with a

size smaller than 100 nm and zeta potential -33.53 mV, was 190 nm. The NPs of Fe_3O_4 and CuO smaller than 50 nm and zeta potential of -8.51 and 17.13 mV formed agglomerates of 1,281 nm and 342 nm, respectively. This behavior is related to the surface charge of NPs, which determinates the type of forces (attractive or repulsive) between particles (Chen 2018; Shrestha et al. 2020). NPs size and surface charge are related to each other by a fixed background (ionic strength and pH), the magnitude of the surface charge of an NP decreases with an increase in the particle size and reaches a constant when the particle exceeds a critical value (Barisik et al. 2014). According to DLVO theory, the Van der Waals and electrical double layer interactions depend on particle diameter (Zehlike et al. 2019). Moreover, in the case of bare metal NPs and given the same solution chemistry, NPs with a high absolute value of zeta potential have a lower agglomeration tendency compared with NPs with a low absolute value of zeta potential, due to electrostatic repulsive forces between NPs are dominant at a higher absolute value of zeta potential (Chen 2018; Mondal et al. 2021).

Considering the soil solution conditions, the NPs agglomeration is also affected by the presence of organic matter, pH, and ionic strength (Kookana et al. 2014). Among environmental conditions, ionic force is the most relevant variable for NPs agglomeration (Dimkpa 2018). The ionic strength of the soil solution affects the force of the electrical double layer, which is related to the repulsive forces between particles. Then, when the ionic strength increases, the double layer is compressed, therefore, the attractive forces (Van der Waals) will be dominant and induce NPs agglomeration (Elhaj Baddar et al. 2019; Shrestha et al. 2020). High Ca^{2+} concentrations in the soil solution not only affect the ionic strength but also plays an important role in the mobility of NPs in porous media because Ca^{2+} leads to an increase in the adhesion of NPs to sediment surfaces (Degenkolb 2021). Moreover, when ions from the soil solution are adsorbed on the NP surface, the magnitude and sign of the zeta potential can change (Shrestha et al. 2020).

Dissolved organic matter (DOM) has a dual effect on NPs mobility. On the one hand, DOM can reduce NPs mobility. The mechanisms involved in the increment of NPs agglomeration are the augment of hydrophobicity, electrostatic forces between particles, or modification of the charge of the NPs surface. On the other hand, DOM can promote

the stabilization of NPs in soil solution by steric stabilization. In this case, DOM act as a coating (it will be attached to the NP surface) which influences the Van der Waal attraction forces by impending the approximation of NPs and lead to entropic repulsion by overlapping of coating molecules of different particles (Hoppe et al. 2014; Worthen et al. 2016; Degenkolb 2021). It has been observed that high molecular weight organic matter has a stronger stabilizing effect against NPs aggregation than low molecular weight organic matter (Louie et al. 2015; Degenkolb et al. 2019). The effect of DOM on NPs is relevant when the solution has higher ionic strength and the electrostatic forces play a minor role in the NPs stabilization (Degenkolb et al. 2019). However, the effect of DOM on NPs agglomeration and stabilization depends on its characteristics, concentration, ionic strength, and the type of cations present in soil solution, as well as the NPs features (Chen 2018; Zehlike et al. 2019). Ben-Moshe et al. (Ben-Moshe et al. 2010) using columns with Fe_3O_4 NPs assessed the effect of ionic strength and organic matter on NPs mobility. The NPs were introduced into the column as a suspended solution at 1000 mg L^{-1}. The authors found that increasing the ionic strength from 0.001 to 0.1 M enhanced the deposition of NPs in the porous medium. The addition of humic acids increased the stability of the NPs suspension and prevented the NPs agglomeration. The concentration of eluted NPs increased from 1.5% to 75% after the addition of humic acids from 10 to 60 mg L^{-1}. Through batch experiments with TiO_2 (particle size of 79 and 180 nm), citrate-stabilized Ag NPs (particle size of 73 and 180 nm), and soil solutions with hydrophobic and hydrophilic features from farmland and floodplain soils, Zehlike et al. (2019) found that the composition of DOM affected the size of NPs aggregates. The Ag NPs of 73 nm size formed larger agglomerates (1179 nm) in the presence of hydrophilic DOM compared to the hydrophobic one (832 nm). In contrast, the hydrophilic DOM maintained in suspension the NPs of 180 nm. Moreover, small agglomerates (192 nm) were formed compared to those formed (406 nm) in the presence of hydrophobic DOM. The authors pointed out that the stabilized effect of organic matter in Ag NPs was due to sterical hindrance rather than electrostatic stabilization because the zeta potential of NPs in soil solutions and their control (2 mM Ca^{2+} solution) was similar. In the case of TiO_2 NPs in both soil solutions, the NPs remain stabilized and formed small agglomerates, but the

stabilization of NPs in the soil solution was due to a change in their zeta potential from 0 to -25 mV.

The soil pH can regulate the surface charge of NPs, therefore the value of their zeta potential, through surface de-protonation or protonation (Wang et al. 2020). When approaching the zero charge point, the particles can agglomerate because the NPs surface is neutral (Shrestha et al. 2020). On the other hand, soil pH influences the rate at which NPs are dissolved into their constituent metal and dictates the speciation of released metals within the soil (Cartwright et al. 2020). Furthermore, the NPs dissolution rate increase as the particle size decrease in the same solution matrix (Chen 2018). In contrast, it can be slowed by the agglomeration of NPs due to a reduction in the exposed surface. Consequently, the delivery and bioavailability of a target nutrient or active ingredient are reduced (Cartwright et al. 2020). Sekine et al. (2017) analyzed the dissolution of CuO NPs in five types of soils with pH from 5 to 8. Their results showed that pH affected the NPs dissolution in the short term. After 3 d of NPs addition, a rapid dissolution occurred in acid soils, whereas the opposite effect in alkaline soils. After 5 d, the Cu released from the NPs was redistributed to the iron oxyhydroxides and soil organic matter, and Cu chemical species remained after 135 d of application.

One form to overcome the problems related to the NPs agglomeration and aggregation is through their surface functionalization. Coatings can alter the NPs surface charge, reduce the particle attraction by steric stabilization, preserve smaller agglomerates, regulate the NPs dissolution, mitigate NPs runoff into the soil, enhance the particle binding to plants and soil minerals; and provide an additional source of nutrients for plants and microorganisms (Kim et al. 2020; Shrestha et al. 2020; Cartwright et al. 2020). To avoid the agglomeration of nZVI and increase their dispersion, Xue et al. (2018) coated the nZVI with rhamnolipid. Moreover, the authors assessed changes in the Cd and Pb distribution in contaminated sediment after the application of nZVI or rhamnolipid-coated nZVI. After the application of 0.05% (w/w), rhamnolipid coated nZVI, and nZVI, the acid-soluble Cd fraction reduced by 47% and 26% after 42 d, respectively. The rhamnolipid application increased the residual fractions of Cd and Pb increased by 56% and 43% after 42 d. Besides, the urease and catalase activities were enhanced. These

authors suggested that coated nZVI contributed to the recovery of sediment metabolic function.

On the other hand, some organic coatings for NMs may have a low toxic impact on soil microorganisms due to their biocompatibility (de Oliveira Pereira et al. 2020). However, soil properties such as pH, organic matter, and clay content influence the toxicity of NPs (Raffi and Husen 2019). Simonin et al. (2015) assessed the influence of soil properties on the toxicity of TiO_2 NPs. For this purpose, the authors used six soils with three textural classes: a sandy loam, a loam, and silty clay, with high or low organic matter content (2% to 8%) and different pH (6.3 to 7.7). They evaluated two scenarios: a low concentration of NPs, 1 mg TiO_2 kg^{-1}; and a high concentration of NPs, 500 mg TiO_2 kg^{-1}. In the silty-clay soil with 8% of organic matter and treated with 500 mg TiO_2 NPs kg^{-1}, a decrease in the C mineralization over the monitored time was observed. After 90 d of NPs application, the C mineralization decreased by 16% in comparison with the control treatment. In contrast, a low concentration of TiO_2 NPs applied in loam soil with poor organic matter decreased 23% C mineralization after 7 d, but the effect seemed to be transitory over time. Similarly, in the silty-clay soil with a high organic matter content, the abundance of microbial communities decreased by 24% and 37% with doses of 1 and 500 mg kg^{-1}, respectively. The authors found a significant relationship between NPs effects, pH, and organic matter content; both factors might be related to the NPs toxicity in soil. García-Gómez et al. (García-Gómez et al. 2018) assessed the toxicity of aged ZnO NPs at 3, 20, and 225 mg kg^{-1} on *Pisum sativum* growth in acid or calcareous soil. The authors found that the concentration of ROS increased from 47% to 130% in plants grown in acid soils with doses of 3 and 20 mg kg^{-1} of NPs after 30 d exposure, compared with control plants. In contrast, no significant changes were observed in the plants from the calcareous soil regarding the control. The concentration of photosynthetic pigments decreased by 20% to 42% in the plants that grew in the acid soil after 30 d. Meanwhile, plants that grew in acid soil treated with 225 mg kg^{-1} of NPs did not survive. The authors related the toxic effects to the available Zn concentration, because, in acid soil, the available Zn fraction increased from 2 to 64 mg kg^{-1} and from 0.10 to 0.70 mg kg^{-1} in calcareous soil. The soil pH had an impact on Zn availability. Moreover, the authors

highlight that the clay content in calcareous soil was higher than in acid soil, which can contribute to the immobilization of Zn released from the NPs.

Interaction metal NMs, plants, and soil microorganisms

Exposure models suggest that NMs concentrations are higher in soil than in other systems as water or air. Therefore, the soil becomes the main sink of NMs in the environment (Bundschuh et al. 2018). Plants and microorganisms are the major co-receptors of NPs introduced to the environment by agricultural use or unintentional release (García-Gómez et al. 2018). Therefore, to lead sustainable and environmentally safe agriculture taking into account the many potential benefits of metal NMs, it is important to understand the influence of NMs applied to soil and their effect on microbial structure, diversity, and activity (Usman et al. 2020). The interaction of plant-microorganism is fundamental for agriculture as soil microbial communities keep a balanced process in the soil-plant system and provide ecosystemic services, especially the microorganisms establishing beneficial associations with plants, such as nitrogen-fixing bacteria, plant growth-promoting bacteria, and arbuscular mycorrhizal (AM) fungi (with more than 400 million years of evolution with plants), are important for efficient absorption of macro and micronutrients, plant nutrition and growth. Moreover, they are involved in carbon sequestration, effective plant protection against pests and pathogens, plant quality and productivity, plant tolerance against abiotic stresses as well as soil quality and health (Hedge and Wilson 2016; Jacoby et al. 2017; Compant et al. 2019). Soil microbial communities also participate in the degradation of soil organic matter, improvement of soil fertility through nutrient bioavailability and soil biodiversity, and bioremediation of different pollutants (Thijs et al. 2016; Jacoby et al. 2017; Mahawar and Prasanna 2018; Sánchez-López et al. 2018b). However, the deep analysis of the complex interactions between NPs and soil microorganisms (Figure 5), the methodology to identify the influence of NMs, and, the molecular and cellular mechanisms of these interactions are largely ignored (Hedge and Wilson 2016).

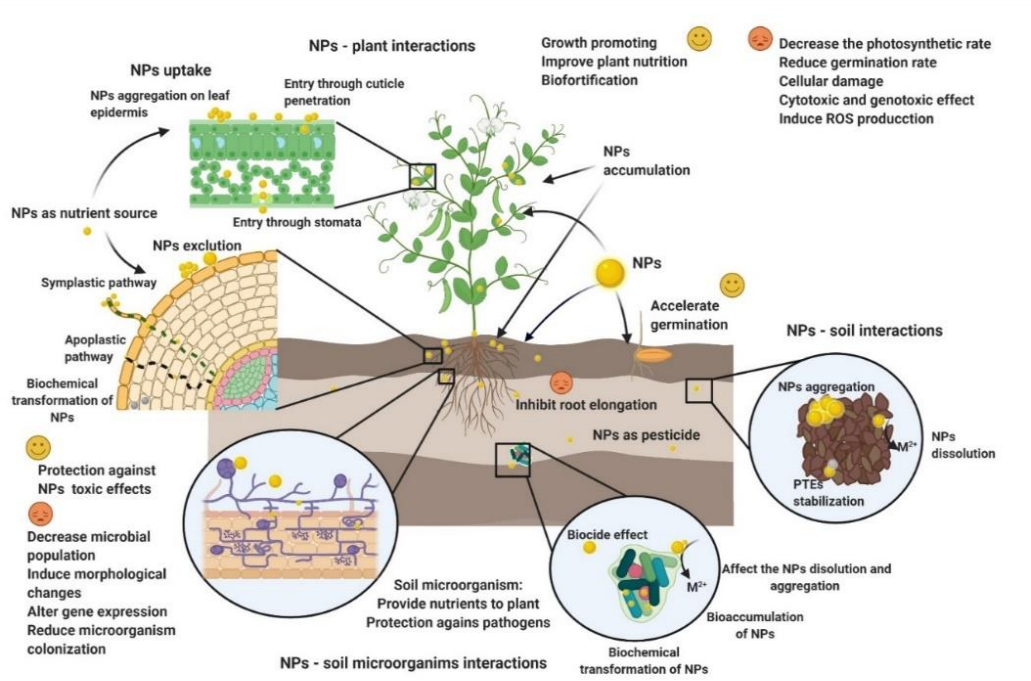

Figure 5. Interactions and effects of metallic NPs with plants and soil microorganisms.

There is an extensive toxicology analysis of metal NMs on soil microorganisms. Resumed from several authors, the negative observed effects, of metal NMs on soil microorganisms (Table 4), are antimicrobial activity (AlO_3, CuO, Ag NPs); alteration of the microbial community (TiO_2, CuO, Fe_3O_4, Cu NPs); reduction of soil enzymatic activity (CuO); soil microbial biomass (CuO, TiO_2); N-fixation (Ag NPs, WO_3); alterations in gene expression (Ag NPs); inhibition of plant growth-promoting rhizobacteria (TiO_2, AlO_3); and induction of morphological changes (TiO_2). On the other hand, positive effects of NMs on soil microorganisms (Table 5) may be observed. These are an enhancement of soil enzymatic activity (ZnO, Fe_3O_4, Fe_2O_3, CuO, ZnO); microbial population (ZnO, Ag, Fe_3O_4, and γ-Fe_2O_3); bacterial growth (Fe_3O_4, Fe_2O_3); microbial diversity and richness (Ag); AM fungal metabolites and mycorrhizal colonization (Ag, FeO); denitrification (PVP-coated Ag NP); genes involved in N cycling (CuO). The stimulating effect of NPs comes from the role of metal ions in the structure, and function of microbial enzymes (Jośko et al. 2019).

Table 5. Some positive effects of metal NPs soil microorganisms.

NP	Effect	NP size (nm)	Concentration (mg L^{-1} or mg $kg^{-1)}$	Medium	Exposure duration (d)	Reference
ZnO	Phosphatase and phytase enzyme activity increased (84%-108%)	1-7	0.025	Soil	28	Raliya et al. (2016)
Fe_3O_4, γ-Fe_2O_3	NPs stimulate the growth of *Streptomyces*, *Duganella*, and *Nocardioides* bacteria; and soil activity of invertase and urease	10 10	840, 1260	Soil	30	He et al. (2011b)
CuO, ZnO	NPs enhance the dehydrogenase activity 1 d after NPs application. Cu NPs increase the dehydrogenase activity in silt-loam soil after 90 and 730 d exposure compared to the control soil. No changes in the number of bacteria were observed after 730 d	50	10	Soil	1-730	Jośko et al. (2019)
Ag	The alpha diversity estimates of operational taxonomic unit abundance (5286 to 6077), the Chao richness (6153 to 6667), and the phylogenetic diversity (133 to 149) increased compared to control soil. The abundance of sequences of Proteobacteria increased from 44% to 62%	12	15	Soil	4	Chavan and Nadanathangam (2019)
Ag	Increment of total and easily extractable glomalin. Less Ag shoot and root content (%) in faba bean plants inoculated with *Glomus aggregatum*.	5-50	800	Autoclaved loam and sandy soil (21 w/w)	35	Abd-alla et al. (2016)
Ag	Biomass, P plant uptake, and mycorhizal colonization by *G. caledonium* were increased. Less Ag uptake and soil soluble Ag concentration in maize-mycorrhizal plants.	20	0.025	soil	20	Cao et al. (2020)
Ag	Higher root colonization by *G. caledonium* in clover plants as dose increased. AM fungi alleviate Ag NPs stress in its host plant. At high Ag concentration, extractable glomalin content	21	0.01, 0.1, 1	Sand:perlite	80	Feng et al. (2013)

NP	Effect	NP size (nm)	Concentration (mg L^{-1} or mg $kg^{-1)}$	Medium	Exposure duration (d)	Reference
	and root P uptake increased at high Ag NPs concentration.					
FeO	Increased root colonization by *G. caledonium.*	10	0.032	Sand:perlite	80	Feng et al. (2013)
CuO	The gene *nifH* was significantly more abundant than the control treatment, then the fixation capacities were increased by the addition of NPs. Also, the abundance of gene *amoA* (involved in nitrification) increased in treatments with NPs compared to the control treatment.	28	0.63 and 63	Soil	28	Guan et al. (2020)
Au:PVP, Ag:PVP	Poly(vinylpyrrolidone) stabilized Au and Ag NPs did not decrease colonization by AM fungi and *Rhizobium*.	2.6 and 3.6	1 mM	Seed priming	0.04 - 0.081 (1- 3 h)	Rahman et al. (2020)

Similar to the plant, the results of the effect of NMs on microorganisms range from biostimulation to toxicity (Juárez-Maldonado et al. 2021). Traits of NPs (nature, exposure time, concentration, type, form, and size), plant (presence or not, type, age), soil (type, chemical, and physical characteristics), microorganism (type and function), and environmental conditions (biotic stress conditions) determine the response to NMs (Kumar et al. 2015; Usman et al. 2020; Juárez-Maldonado et al. 2021). For example, numerous studies mentioning the high toxicity of NMs to soil microorganisms were conducted under pure culture media; however, extrapolation to natural environments such as soil is difficult.

Figure 5 resumes the interactions between NMs, soil microorganisms, and plants; where soils may regulate the effect of NPs on these two organisms. Complex interactions between NPs and soil surfaces are intractably involved and result in less microbial toxicity caused by NPs (as mentioned in the previous section and showed in Figure 1.4). Moll et al. (2016) observed no effect of TiO_2 NPs (10 - 1000 mg kg^{-1}) on nutrient uptake and biological nitrogen fixation on red clover inoculated plants and grown in soil. In contrast, under hydroponic conditions, TiO NPs (250, 500, and 750 mg L^{-1}) caused a delay in the root nodule development and biological nitrogen fixation in peas (Fan et al. 2014). Masrahi et al. (2014) also detected much lesser microbial toxicity of Ag^{+} and Ag NPs in soil than trials performed in pure culture media.

Concerning NPs concentrations, Juárez-Maldonado et al. (2021) and Iavicoli et al. (2018) explained that while an initial stimulus can result in a positive reaction and gene expression in microbial or plant metabolism (biostimulation), the contrary effect can occur, and cause toxicity. Therefore, response to concentration is of a biphasic or hormetic nature. This boundary between biostimulation-toxicity is variable, even for NMs with similar composition, but highly dependent on several already mentioned NMs characteristic as well as surface energy, surface charge, hydrophobicity, roughness, surface functionalization and components of the corona (organic molecules or biomolecules adsorbed to the NMs surface from the media where NM is found). High consideration of this hormetic dose-response should help for a safe application of innovative materials (Iavicoli et al. 2018). Kumar et al. (2015) observed less nitrogen

fixation in *Rhizobium* strains when Ag NPs concentration was between 0.6 to 6.6%; however, at a low concentration, no effect was found. Judy et al. (2016) did not observe the negative effect of Ag NPs (1, 10, and 100 mg kg^{-1}) on *Sinorhizobium meliloti* associated with *Medicago truncatula*. These authors emphasized that the highest Ag NPs concentration was analogous to a worst-case scenario, moreover, tested as long-term repeated soil addition with biosolids amendments.

The response of NMs to the microbial community is also dependent on the presence or not of plants and the type of soil microorganism. Ge et al. (2014) observed that plants and types of NP alter the response of NMs on soil bacterial communities. CeO_2 NPs (100 to 1000 mg kg^{-1}) did not affect soil bacterial communities in unplanted soils. However, 100 mg kg^{-1} enhanced soil bacterial communities in soil with soybean. While 500 mg kg^{-1} of ZnO increased *Rhizobium* and *Sphingomonas* communities but decreased *Enfiser*, Rhodospirillaceae, *Clostridium,* and *Azotobacter*. A higher decrement of bacterial communities was observed in unplanted than in planted soils; which indicated that soybean plants reduced the negative effects of ZnO on bacterial soil communities.

Toxicity response to NPs is also dependent on soil microbial species. The minimum inhibitory concentration of coated Ag NPs was different in three bacteria involved in the N cycle; for *Nitrosomonas europaea* (involved in nitrification) was 500 µg L^{-1}, while for *P. stutzeri* (a denitrificant-bacteria) was 4000 µg L^{-1} and for *Azotobacter vinelandii* (a nitrogen-fixing bacteria) was 12,000 µg L^{-1}. In all bacteria, ionic Ag was more toxic than Ag NPs (25, 200, and 250 µg L^{-1}, respectively). Judy et al. (2015) observed that Ag_2S NPs were less toxic to plants, AM symbiosis, and soil microbial community than polyvinylpyrrolidone (PVP) coated Ag NPs and Ag^+. However, still low concentration of Ag_2S NPs (1 mg kg^{-1}) negatively influenced the soil microbial community, but higher concentrations (100 mg kg^{-1}) did not influence the colonization by AM fungi. Differences in toxicity to metal NPs were observed in plant growth-promoting bacteria (*Bacillus thuringiensis*, *P. mosselii*, *Azotobacter chroococcum,* and *Sinorhizobium meliloti*). Concentrations up to 3000 mg L^{-1} of CuO, TiO_2, and Al_2O_3 NPs did not inhibit bacterial growth. In contrast, these bacteria were sensitive to concentrations less than 1500 mg L^{-1} of Ag and ZnO NPs (Ahmed et al. 2020). A high concentration of Ag NPs (800 µg kg^{-1})

significantly decreased the structure, nitrogen fixation, number, and dry weight of nodules produced in faba plants inoculated with *Rhizobium leguminosarum* bv. *viciae*. Therefore, root nodules showed autophagy (internal degradation of bacilli) as an Ag detoxification mechanism (Abd-alla et al. 2016).

Most of the studies related to the interaction between metal NPs and agricultural soil beneficial microorganisms show negative effects of NPs because of their antimicrobial effect (Table 4). Metal and metal oxide appears to have higher toxicity than organic NPs such as fullerenes and carbon nanotubes (Rajput et al. 2018, 2020). Michels et al. (2017) showed Ag and magnetite NPs were attached to the bacterial surface and reduced membrane permeability; however, Ag NPs were 45 folds more toxic than magnetite NPs. The EC_{50} to decrease ammonia-oxidizing bacteria for Ag NPs was 10.75 mg L^{-1} while for magnetite it was 483.01mg L^{-1}. The highest doses of Ag NPs (30 mg L^{-1}) and magnetite (1000 mg L^{-1}) decreased 90% and 71% of the nitrite production of this kind of bacteria, respectively. Ti_2O and ZnO NPs decreased microbial biomass carbon and Gram-negative bacterial community (Rashid et al. 2017).

Hedge and Wilson (2016) resumed that NMs may influence soil microbial communities through four mechanisms: (a) direct particle-cell interaction, (b) indirectly by NMs interaction with natural organic compounds, (c) interaction with recalcitrant organic pollutants and enhancing toxicity, and (d) modifying toxin or nutrients bioavailability. Similar to plants and with metal bulk-size compounds, the general toxicity mechanisms of NMs known in microorganisms are related to cellular level response: cell membrane damage, proteins denaturalization, respiratory chain alteration, oxidative damage, and genotoxicity (Ševců et al. 2011; Dinesh et al. 2012; Wang et al. 2017; Jośko et al. 2019). However, scarce information is available related to molecular mechanisms to deal NMs in soil microorganisms.

Noori et al. (2017) analyzed the impact of Ag NPs (2 and 15 nm) in concentrations 0, 12, 24, and 36 mg kg^{-1} on colonization by the AM fungus (*Rhizophagus intraradices*) on the growth and accumulation of Ag in tomato plants, and the expression of gene-related with uptake pathways (potassium channel proteins: KC; aquaporins proteins such as plasma membrane intrinsic protein: PIP and tonoplast membrane intrinsic protein:

TIP). These authors observed that mycorrhizal colonization was reduced at the higher Ag NPs concentration and that smaller-sized NPs had not only the highest impact on colonization but also on plant biomass. Moreover, mycorrhizal colonization moderates plant Ag uptake (14% less accumulation) and changes in the expression level of membrane transport proteins. The expression of KC, PIP, and TIP in mycorrhizal tomato plants was 5.8, 3.5, and 2 than in control plants (without the addition of NPs), respectively. In contrast, the expression in non-mycorrhizal plants the expression was 8, 5, and 9 times higher than in control plants. Cao et al. (2020) also observed modification of genes putatively related to Ag/Ag NPs transport in maize-mycorrhizal plants inoculated with *Glomus caledonium* (current name *Funneliformis caledonium*); which were involved in the mitigation of Ag NPs phytotoxicity. At high Ag NPs concentration (2.5 mg kg^{-1}) the expression of *Pht1;6* (related to P uptake) was higher in mycorrhizal plants, but lower in the expression of *PIP1;2*, *TIP2;1,* and *Mt2* (related to metal homeostasis and cell detoxification). Furthermore, these fungi ameliorated the negative effects of Ag NPs on the metabolic activity of other soil microorganisms enhanced soil bacterial diversity, and altered the bacterial community composition at the mycorrhizosphere/rhizosphere or corn plants.

Fajardo et al. (2014) analyzed the cellular response of *P. stutzeri* and *Bacillus cereus* to two types of NPs. These authors tested Al_2O_3 NPs (50 nm) in concentrations 1, 5, and 10 g L^{-1}, and Ag NPs (40 nm) in concentrations 0.5, 1, and 5 mg L^{-1}. These bacteria responded differently to NPs exposure. While no modification was observed in the transcriptional response of four genes involved with cellular activity in *B. cereus*, in *P. stutzeri* exposed to Al_2O_3 NPs*,* the gen related to catalase enzyme (KatB) was overexpressed, resulting in less cellular oxidative stress. Ag NPs (35 nm) did not modify the expression of denitrifying genes or nitrogen-fixing genes of *P. stutzeri* (20 µg L^{-1}) and *A. vinelandii* (25 µg L^{-1}). In *N. europaea*, up-regulation of ammonia mono-oxygenase genes at low concentrations of 2.5 µg L^{-1} (Yang et al. 2013). ZnO NPs applied at high concentrations (500 mg kg^{-1}) negatively influenced AM fungi species diversity, and altered their community composition. *Ambispora* genus was decreased, but *Paraglomus* increased (Yang et al. 2021).

Iavicoli et al. (2018) concluded that suitable assessment of NMs, *in vitro* or *in vivo* conditions, should be done in long-term experimental studies and with low-dose realistic environmental exposure scenarios; moreover, in the presence of other co-exposed substances. These authors showed hormetic dose-response in several biological models: microorganisms, algae, nematodes, plants, and superior aquatic organisms. It is also suggested that a low concentration of NPs induces a beneficial defense response in organisms (Juárez-Maldonado et al. 2021). Wheat plants exposed to TiO_2 NPs enhanced their growth when were inoculated with *Paenibacillus polymyxa*, *Alcaligenes faecalis*, *Bacillus thuringiensis,* and a mutant strain of *P. polymixa* A26Dsfp (Timmusk et al. 2018).

Wang et al. (2016b) observed that ZnO NPs did not have negative effects on maize mycorrhizal plants at 400 mg kg^{-1}; however, when NPs concentration was higher (800 mg kg^{-1}), inhibition of plant growth and mycorrhizal colonization were found. AM fungi putatively mitigate the negative effects of ZnO NPs in plants as increased growth, nutrient absorption, photosynthetic pigment concentration, and leaves SOD activity. The mycorrhizal plants also presented less ROS accumulation, Zn shoot concentrations, and DTPA-extractable Zn concentrations. Similar results have been observed by other authors (Abd-alla et al. 2016; Cao et al. 2017; Noori et al. 2017; Wang et al. 2018b) Joseph et al. (2015) used biochar rich in magnetic Fe NPs on the growth of wheat. These authors concluded that the use of biochar (100 kg ha^{-1}) increased P and N plant nutrition, mycorrhizal colonization, and soil microorganisms. This is due to high concentrations of Fe NPs within the biochar that are involved in nutrient availability due to acidic functional groups and soil organic matter decomposition, and labile organic molecules stimulating soil microorganisms.

The effect of NPs used in seed priming on soil microorganisms is a novel area demanding more efforts to avoid negative effects on soil, but more specifically on beneficial microorganisms. The effects are type, size, and concentration of NPs, and the time of imbibition among other factors. Rahman et al. (2020) observed that seed priming (1-2 h) with 1 mM Pt NPs stabilized with poly(vinylpyrrolidone) (PVP) hurt colonization by AM fungi and *Rhizobium* in *Pisum sativum* plants. After 3 h imbibition, microbial

colonization was absent. However, with Au- and Ag-PVP NPs the effect was negligent, independently of imbibition time.

Information already presented showed research on the effect of NMs on soil microorganisms, still unexplored is the interaction of NMs with microorganisms associated with other plant niches, which may influence response to next-generation fertilizers, pesticides, and other products at a nanometric scale, useful for agriculture and phytoremediation. Currently, plants are recognized as meta-organisms. This refers to plants by themselves and their associated microorganisms from roots, leaves, seeds, fruits, flowers, etc. Hence forming specific microbial-plant interactions located at the rhizosphere: phyllosphere, spermosphere, anthosphere, and carphosphere, respectively; all of them influence plant performance in agricultural and natural ecosystems (Mendes et al. 2013; Vryzas 2016; Compant et al. 2019; Jaspers et al. 2019). In consequence, in-depth research is urgent to explore the risk assessment of NMs on non-target toxicity of beneficial microbe communities from several plant niches which are key actors directing health, quality, and productivity.

Metal NPs for remediation of polluted soils with potentially toxic elements

Raj and Maiti (2020) reviewed that potential toxic elements (PTE) such as As, Cd, Cr, Pb, Ni, Zn, and Hg are recognized as the utmost hazardous and persistent elements in the environment. Several agrochemicals contain PTE in their formulations. Continued use for long periods enriches soil and water. These elements also accumulate in the tissues of organisms and increase their concentration through the food chain (biomagnification). Thus, PTE contamination is a serious concern to human health, and in the case of agricultural lands may be jeopardy for productivity and the living soil organisms. Therefore, diverse remediation alternatives have been developed to remediate contamination by PTE, and one of them is the application of nanotechnology.

Nanotechnology for soil remediation, also called nano-remediation, nano-enabled remediation, or NMs-assisted remediation, uses NMs to detect, degrade, or stabilize contaminants (Pulimi and Subramanian 2016). In the case of soils polluted with PTE, NMs are used as amendments to immobilize or stabilize PTE by some of the processes shown

in Figure 6 (Bardos et al. 2018; Souza et al. 2020). The application of NMs aims to reduce the ability of PTE to partition to water or biota, potential transport, and toxicity (O'Day and Vlassopoulos 2010), by forming less toxic chemical species. Moreover, when soil pollution is due to organic compounds, several NMs (TiO_2, ZnO, Fe_2O_3, ZnS, and CdS) are useful as semiconductors for photocatalysis. The NPs absorb light energy to break down organic molecules into smaller fragments and turn them into minerals. acids, CO_2, N_2, and H_2O (Baruah and Dutta 2009). Mourão et al. (2010) evaluated the photocatalytic potential of TiO_2 coated with $CoFe_2O_4$ NPs. These authors observed that $TiO_2/CoFe_2O_4$ nanocomposites were more effective than pure TiO_2 for atrazine degradation. The application of nanocomposites of $TiO_2/CoFe_2O_4$ can be an alternative for pesticide degradation in soil. Furthermore, the recovery and reuse of magnetic nanocomposites are possible due to their magnetic features (Zuverza-Mena et al. 2017). More recently, Mazarji et al. (2021) reviewed the use of NZVi (single or in combination with biochar), metal oxides (TiO_2, Fe_2O_3, green synthetized-potassium zinc hexacyanoferrate nanocubes or NPs, magnetite NPs modified graphite), and several carbon- and polymer-based NMs for remediation of toxic polycyclic aromatic hydrocarbons. Nehra et al. (2021) provide a comprehensive review on the management of pesticide residues in soils that can be consulted, while this paper focuses on the applications of nanotechnology for the remediation of soils polluted with PTE.

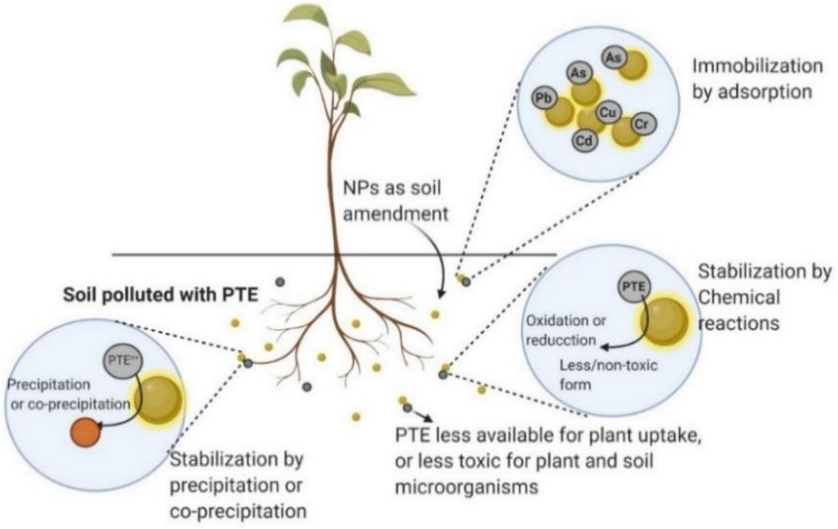

Figure 6. Pathways in which nanoparticles can assist soil remediation and phytoremediation.

The use of NMs as amendments has an advantage over bulk materials because they have a higher reactive surface and area/volume ratio than bulk materials. These properties enhance the NMs' capacity to adsorb, reduce, or oxidize PTE (Pulimi and Subramanian 2016; Bardos et al. 2018; Guerra et al. 2018). For instance, zero-valent iron (Fe^{o}) and $CoFe_2O_4$ NPs have a total specific surface area of 20-40 $m^2\ g^{-1}$ and 1,243 $m^2\ g^{-1}$, respectively. In contrast, the total specific surface area for granular Fe is <1 $m^2\ g^{-1}$. Reactivity is also from 10 to 1,000 times more in NPs of these compounds (Karn et al. 2009; Qiu et al. 2016).

Many of the NMs recommended for soil remediation (Table 6) have been adapted from technologies for water treatment, and the results were observed in sorption kinetic assays in aqueous media (Zhang et al. 2010; Zhao et al. 2016; Kefeni et al. 2017). Nevertheless, Fe NPs seem to be the best material (Kefeni et al. 2017; Caroline and Antônio 2019; Souza et al. 2020) due to their magnetic properties. This feature facilitates their recovery (Martinez-Vargas et al. 2017a; Zuverza-Mena et al. 2017). The high chemical reactivity (Kefeni et al. 2017) increases the efficiency and fast kinetic adsorption of ions such as Ni^{2+}, Cu^{2+}, Co^{2+} $Cd^{2+,}$ and Cr (IV) (Guerra et al. 2018). Moreover, iron NPs are considered non-toxic to the environment or plants (Zuverza-Mena et al. 2017). These particles can be modified to improve their performance by including a catalytic element, like Ti or Pd; using coatings such as citrate or polymers, or soaking other materials such as active carbon or zeolites with NPs (Gens et al. 2016).

Table 6. Nanoparticles tested for soil remediation under different conditions.

NP	PTE	Action mode	Effect	Reference
Apatite with carboxymethyl cellulose stabilizer	Pb	Immobilization	Ratio 2:1 NPs: soil reduced the leachable Pb fraction from 66% to 10% after one month of NPs application.	Liu and Zhao (2013)
Hydroxyapatite	Pb	Immobilization	2 g kg^{-1} reduced the accumulation of Pb in *Brassica napus.*	Shaheen and Rinklebe (2015)
	Cd, Zn, Pb, Cu	Adsorption	0.2 g of NPs inhibited soil PTE desorption	(Chen et al. 2010)
Nano silicone	Pb	Stabilization	2.5 mmol L^{-1} increased the biomass of two rice cultivars and decreased foliar and grain Pb concentration.	Liu et al. (2015a)
Carbon Black	Cu, Zn	Immobilization	Soil Cu and Zn availability decreased between 47% to 80% and 17% to 43%, respectively when using 1, 3, and 5% NPs compared with no NPs addition. Zn and Cu proportion in the organic and sulfide soil fraction increased. Higher biomass of *Lolium multiflorum* and less plant Cu and Zn accumulation.	Wang et al. (2009)
Ca/CaO and Ca/PO_4	^{137}Cs	Immobilization	96% ^{137}Cs were immobilized.	Mallampati et al. (2012)
nZVI	Cr(VI)	Reagent material in a permeable reactive barrier for electro remediation	It was achieved to reduce 75-90% of the Cr(VI) in the soil. The total Cr removal efficiency rose to 42% compared with conventional electrokinetic treatment.	Shariatmadari et al. (2009)
	As, Hg	Immobilization	5% nZVI dose decreased 70 % exchangeable As concentration. 10% nZVI dose reduced the exchangeable Hg between 635 to 90%.	Gil-Díaz et al. (2017)
	Cd	Immobilization	150 mg nZVI kg^{-1}, *Salix alba*, and inoculation with *Pseudomonas fluorescens* and *Rhizophagus irregularis* increased the bioconcentration factor of Cd. 300 mg nZVI kg^{-1} inhibited *Salix alba* growth.	Mokarram-Kashtiban et al. (2019)
			The Cd concentration in the residual fraction increased from 15% to 57% after 30 d incubation of river sediments with sodium alginate modified nZVI at 0.1% (w/w).	Huang et al. (2016)

NP	PTE	Action mode	Effect	Reference
	Zn	Sorption	Extractable Zn concentration reduced the following use? from 0.5 to 4 mg kg^{-1}. No negative effects on soil microorganisms were found.	Anza et al. (2019)
	Pb, Zn, Cd	Immobilization	120 d after NPs application, 20% of Pb, and 8% of Zn were immobilized. The maximum immobilization reached was 15 d after NPs application.	Fajardo et al. (2020)
nZVI, FeS Fe_3O_4	As	Immobilization	The soil bioaccessible concentration of As decreased from 71% to 31%, 37%, and 30% when the soil was treated with nZVI, FeS, and Fe_3O_4 at a Fe/As molar ratio of 100:1, respectively.	Zhang et al. (2010)
nZVI, goethite	As	Immobilization and reduction	nZVI at dose 2% decreased 90% the As availability, while nGeothite at 0.2% dose decreased 83% the As available nZVI at dose 10% increased 1.4% the As^{3+} concentration.	Baragaño et al. (2020a)
Ɣ-Fe_2O_3	Zn	Immobilization	NPs and compost decreased 22% of the soluble Zn concentration and Zn accumulation in *Helianthus annuus*. Higher plant biomass was observed.	Martínez-fernández et al. (2015)
Fe_3O_4 coated with polyethyleneimine	Cs	Adsorption	Coated magnetic NPs at a dose of 0.05 g g^{-1} removed 82% of Cs.	Kim et al. (2020)
WO_3 coated with EDTA	Cd, Pb	Complexation	The dose of 10 mg NPs g^{-1} soil, removed from 60% to 80% of Cd and Pb in two different soil matrices.	Huang and Keller (2020)
TiO_2, CeO_2	Cu (II)	Adsorption	Soluble Cu soil concentration and toxic effects on rice plants decreased.	Wang et al. (2015)
Amorphous manganese oxide	Cd, Cu, Pb	Stabilization	Exchangeable soil fraction of Cd, Cu, and Pb decreased by around 92%.	Michálková et al. (2014)
	Fe, Al, Pb, Zn, Cu, y Cd	Immobilization	Soil neutralization reactions accelerated. Fe, Mn, and Al precipitate as secondary oxyhydroxides.	Vítková et al. (2015)
ZnO, Al_2O_3 (bare and modified with humic acids NPs)	Cd, Cu, Ni	Sorption	Leaching and bioavailability decreased after 56 d NPs addition. Order of metal removal Cu>Cd>Ni.	Mahdavi et al. (2015)
Hydroxyapatite, hematite, and magnetite	As, Pb, Sb	Sorption	Available As, Pb, and Sb soil concentrations decreased.	Arenas-Lago et al. (2019)

Modified from Pulimi and Subramanian (2016).

Zero-valent iron is one of the iron-NPs most studied for *in situ* soil remediation because it can reach sites that are inaccessible by other methods in a less destructive form and less time-consuming. Additionally, they can reduce and immobilize several redox-active PTE (Zhao et al. 2016). For instance, Gil-Díaz et al. (2016) evaluated the immobilizing effect of nZVI NPs to assist the phytoremediation of As polluted soils, from a metallurgical industrial site in Asturias, Spain. The authors carried out a growth chamber experiment with barley plants and nZVI at 1% and 10% (w/w). The results showed that the available As concentration decreased from 83 to 12 mg kg^{-1} with 10% nZVI treatment compared to the untreated soil. While the concentration in the residual fraction increased from 4,139 to 5,321 mg kg^{-1}, the leaching of As was significantly reduced. Posteriorly, Gil-Díaz et al. (Gil-díaz et al. 2019) in field experiments tested the application of 2.5% of nZVI to a highly polluted soil with As (43,300 mg kg^{-1}) and Hg (2,200 mg kg^{-1}).

These authors found that 72 h after nZVI application, the exchangeable As fraction decreased by 40% and in the leaching extract by 54%. Similarly, the Hg concentration in the leaching extract decreased by 39% from the Hg initial concentration. The immobilization of As and Hg remained stable after 24 months. A second application was required eight months after the first one. These authors also tested the application of nZVI in soils containing 7,280 mg kg^{-1} of As and 1,300 mg kg^{-1} of Hg. In this case, the As and Hg concentrations in the leachable extract were 70% and 80%, respectively, lower than the initial concentrations. Conditions still were stable after 24 months after the nZVI application.

NMs-assisted phytoremediation

Phytoremediation is one of the soil recovery cheap technologies and non-intrusive compared with the physical and chemical methods (González-Chávez et al. 2017; Thijs et al. 2017). Plants useful for phytoremediation encourage fixation of atmospheric CO_2, and increase soil biodiversity, and their biomass may have application in bioenergy production. Moreover, plant surfaces avoid the air dispersion of soil particles containing PTE (González-Chávez et al. 2017; Thijs et al. 2017; Sánchez-López et al. 2018a). However, their efficiency and success depend on the plants' ability to take up, tolerate, and accumulate PTE (Thijs et al. 2017). To overcome the limitations of phytoremediation,

biotechnology can be combined with other approaches such as the use of NMs as soil amendments or soil pretreatment (Zhu et al. 2019).

Metal NPs may enhance phytoremediation efficiency (Gong et al. 2018; Zhu et al. 2019) by reducing the availability of PTE (Figure 6). However, the excessive use of NMs may also produce contamination of soil and water resources. The addition of NMs to PTE-contaminated soil may be insufficient to help plant establishment because these altered soils often lack nutrients, and organic matter, and have a poor structure (Thijs et al. 2017). Hence, NMs-assisted phytoremediation can be combined with organic amendments to provide nutrients for plants and stimulate soil microbial communities, or with beneficial soil microorganisms to promote plant growth (Mokarram-Kashtiban et al. 2019; Baragaño et al. 2020b; Lacalle et al. 2020). For instance, mature compost, from olive mill waste and cow manure, at a rate of 14 g kg^{-1} combined with 1% of Ɣ-Fe_2O_3 NPs assisted phytoremediation with *Helianthus annuus* plants of a mine tailing from Murcia Spain. After 50 d, the reduction of the Zn concentration in the soil solution was 22% in comparison to the treatment without compost and NPs. Moreover, the foliar concentration of Zn, Cd, Cu, and Co significantly decreased while the root concentration of Al, Cu, and Pb were lower than this in the control plants. The plant dry aerial biomass increased due to the synergistic effect of compost and NPs (Martínez-fernández et al. 2015).

Biochar is another organic amendment that may be mixed with NMs. For example, through a greenhouse experiment, Baragaño et al. (2020b) assessed the effect of nZVI, compost-biochar, or a combination of these amendments to assist the phytoremediation with *Brassica juncea* L. of a PTE-polluted soil. After 75 d of amendments application, the mix of compost-biochar-nZVI, at a proportion of 15%, 5%, and 2% (w/w) respectively, lowered significantly the Cu, Pb, and Zn available concentrations in comparison with soil treated with nZVI and the control (without amendments).

Foliar spray of NMs may be used to promote structural stability, improve yield, and enhance the resistance of plants under PTE stress (Cui et al. 2020). Foliar spray of Si NPs in plants such as *Brassica chinensis* L., *Coriandrum sativum* L., and *Oryza sativa* L. reduced the accumulation of Pb and As in the aerial biomass of plants, stimulated the production of antioxidant enzymes in the plant, and also the soil microbial activity (Liu et

al. 2015; Cui et al. 2020; Fatemi et al. 2020; Tian et al. 2020). The reduced As rice plant accumulation was due to the improvement of pectin synthesis which chelated As and the mechanical force of the cell walls was enhanced by a higher thickness which kept the integrity of the cell and then ameliorated oxidative stress upon As exposure (Cui et al. 2020). While less Pb concentration by Si NPs was explained because Si induces root exudates which chelate metals and also due to silicates Pb complexes formation; therefore, reduced metal uptake was observed in coriander plants (Fatemi et al. 2020).

NMs and electrokinetic remediation

Another form to use NMs for soil treatment is to manufacture permeable reactive barriers (PRB) for electrokinetic remediation (EKR). The EKR-PRB is an attractive technique because it avoids secondary contaminants synthesis, in contrast with conventional EKR (Wang et al. 2021). It is also potentially applicable to several organic and inorganic pollutants. Moreover, it has a high removal efficiency and time-effectiveness in soils with low permeability (Souza et al. 2020). Figure 7 shows the mode of action of EKR-PBR.

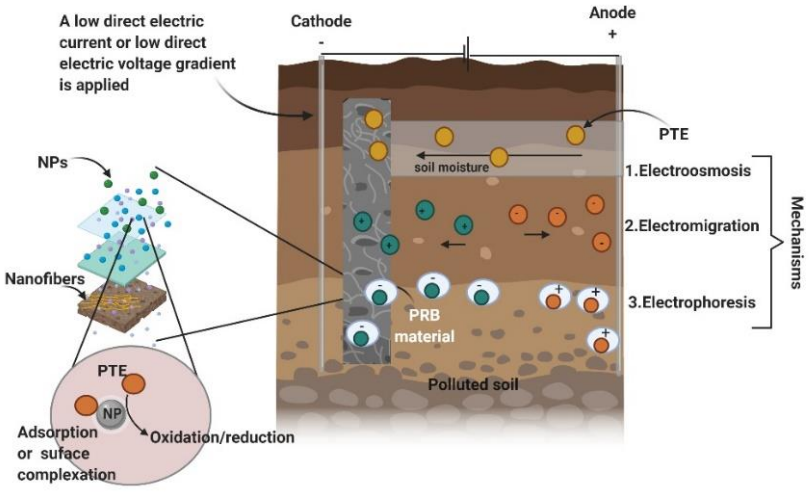

Figure 7. Fundamental mechanisms of permeable reactive barriers for electrokinetic remediation.

Permeable reactive barriers aim to intercept a contaminant plume and transform it into environmentally acceptable forms to attain the concentrations of chemical species safe for both environment and organisms (Andrade and dos Santos 2020). The PRB can be filled with NPs as reactive material (Souza et al. 2020; Wang et al. 2021) or

manufactured with nanofibers (Wang et al. 2021). Iron NPs such as nZVI has been used in the EKR-PRB to remove Cr(VI). Shariatmadari et al. (2009) found out the EKR-PRB can increase the removal efficiency of total Cr from 15% to 42% compared with EKR application in clayey soil. Nasiri et al. (2020) used Fe_3O_4 NPs as reactive material in PRB and assessed the use of chelating agents to remediate a Cr contaminated soil by EKR. The combination of EDTA and placing the PRB in the middle of the ER reactor removed around 70% of the initial Cr concentration (150 mg kg^{-1}). These authors found that Cr(VI) ions were reduced to Cr(III) when they passed through the PRB, so the NPs play a role in the Cr reduction. The Cr accumulation observed near the cathode section suggested that the mechanism of Cr removal was electromigration. Despite the high rate of Cr removal of EKR-PRB in comparison with EKR, the authors concluded that EKR-PRB may consume more energy than the traditional EKR process. Therefore, more experimental evidence to determine its cost-effectiveness in the long-term is necessary.

NMs for acid mine drainage treatment

In mining areas, both active or abandoned, acid mine drainage (AMD) is a source of PTE-soil and water pollution in addition to mining wastes (Atrei et al. 2019). Sulfide minerals oxidize when exposed to environmental conditions, particularly rain and atmospheric oxygen. As a result, protons are released, and AMD occurs. When sulfide minerals are oxidized, they produce acid iron and sulfate-rich waters that can dissolve other minerals that contain PTE, and release them into the environment (Kefeni et al. 2017; Atrei et al. 2019).

Once AMD occurs, its treatment can be expensive. Treating one ton of AMD with limestone can cost 60 dollars, while the treatment with caustic soda costs 1,240 dollars (Skousen 2014). The neutralization treatments of AMD are useful to remove PTE, however, they need to reach a pH above 10, and the proper disposal of the sludge that is generated after ADM neutralization (Kefeni et al. 2018). In contrast, treatments with NPs offer the opportunity to recover valuable resources that are impossible to recuperate from conventional treatments. Furthermore, treatment with NMs reduces secondary waste products as part of the AMD treatment process (Wei and Viadero 2007; Kefeni et al. 2018). For instance, $CoFe_2O_4$ and Fe_3O_4 NPs can remove 100% of Al, Mg, and Mn;

and up to 90% of Fe, Ni, and Zn from samples of AMD (pH adjusted to 7.05±0.35) from coal mines of Emalahleni and Randfontein in South Africa (Kefeni et al. 2017). α-Fe_2O_3 NPs can remove completely Al, Mg, and Mn up to 80% of Zn and Ni; and between 47% and 72% of Ca and Na (Kefeni et al. 2018). nZVI was used for the treatment of AMD from a uranium gold mine in Gauteng, South Africa. AMD-pH increased from 3.49 to 6.01, diminished the electrical conductivity from 0.59 Ohm m^{-1} to 0.13 Ohm m^{-1}, and decreased the total dissolved solids from 1683 mg L^{-1} to 384 mg L^{-1}. The removal capacity of PTE of nZVI followed this trend Li, Sr, Ba, B, Al, Na, and Co (Gilbert et al. 2019).

Some considerations for nanoremediation

Previous information resumes that NMs are a useful and effective alternative for the remediation of soils polluted with PTE. However; similar to the use of other soil amendments recommended for soil remediation (Carrillo-González et al. 2017), it is suggested that before the use of metal NPs, it is desirable to make an adequate characterization of the site. This includes geological conditions, types of contaminants and concentration, hydrology, soil composition, porosity, hydraulic conductivity, groundwater gradient, flow velocity, depth of the water table, and geochemical properties. All this information aims to make the action of the NPs efficient and prevent undesired effects after their application (Karn et al. 2009). For a successful application in the field, particulate agglomeration control, mobility in porous environments, reactivity, and longevity in the subsurface environment are all major controlling factors for the efficient remediation of contaminated sites under field conditions (Cecchin et al. 2017). Fulling mixing between NPs and soil is an important management step to guarantee successful remediation. In greenhouse experiments, Fajardo et al. (2020) and Gil-Diaz et al. (2016) used a commercial 5% nZVI w/w suspension applied to the soil, and mixed carefully obtained metal immobilization; which was dependent on soil properties and level of soil contamination. In a field experiment, Gil-Diaz et al. (2019) referred to the use of a commercial 2.5% nZVI suspension; which was diluted with water in equal proportions and uniformly dispersed on the soil surface. Then, NPs were incorporated with the topsoil surface layer to guarantee the depletion of As and Hg availability after only 72 h, which was stable during 32 months of monitoring. Liu et al. (2015) concluded that stabilized NPs

with low-cost materials, such as starch, chitosan, and carboxymethyl cellulose improve the dispersion in soils. Moreover, affinity, reactivity, and sorption capacity to target metals are improved for soil metal immobilization. To improve the combination of NP with soil, Moll et al. (2016) combined 300 g of a soil-sand mixture (1:1 w/w) with NPs on an overhead mixer in Schott bottles. Then, each pre-mixture was diluted with the mixture to a final volume of 30 kg and homogenized in a cement mixer for 6 h. This mixture with NPs was used for greenhouse experiments testing three types of NPs in pots.

Interaction metal NMs, plant, and soil beneficial microorganisms in remediation

Beneficial soil microorganisms improve several functions in the plant-soil system, such as plant protection, stability, productivity, growth, and phytoremediation (Khalid et al. 2021). Understanding the interactions between NPs, plants, and soil microorganisms are key to designing efficient NPs application methods for plant nutrition, soil remediation; and predicting the effect of NPs on ecosystems (Ma et al. 2010). Figure 5 summarizes the possible NPs interactions with microbial components of the plant-soil system and the effects for which there is evidence so far. The irrational use of NMs and their potential negative impact make them emergent contaminants, which may affect different organization levels in the environment.

Owing to the widespread and ecologically relevant of AM fungi as plant symbionts and key participants in global plant diversity, there is a significant interest to analyze their interaction with metal NMs. Results demonstrate that these fungi have an intricate interaction with bulk-sized metals and alleviate phytotoxicity in their host plant. Therefore, they may influence the fate, transformation, accumulation, and toxicity of NMs. Feng et al. (2013) observed that *G. caledonium* (*F. caledonium*) effectively ameliorated the effect of Ag NPs (20 nm) in a concentration-dependent manner. This is as Ag NP concentration enhanced (0.01, 0.1, and 1 mg kg^{-1}). Similarly, plants had higher root fungal colonization and P root absorption, but lower Ag shoots concentration. Siani et al. (Siani et al. 2017) evaluated the effect of inoculation of *R. irregularis* on *Trigonella foenumgrecum* plants when exposed to increasing concentrations of ZnO NPs (0, 125, 250, 375, and 500 mg kg^{-1}). The results showed that *R. irregularis* protected its host plant from the toxic effects of ZnO NPs at the dose of 500 mg kg^{-1}. The authors suggested that plant protection was

due to the secretion of glomalin, a glycoprotein produced mainly by AM fungi. Glomalin increased by 15% in comparison to the control treatment (without inoculation of *R. irregularis*). Similar results were found in *Zea mays* plants inoculated with *F. mosseae* and the addition of ZnO-NPs at 500 mg kg^{-1}. *F. mosseae* inoculation reduced the Zn bioavailability released from NPs, but increased available P, which depleted the toxic effect of the NPs (Wang et al. 2018b). Jing et al. (2016) also found the proper combination of P with AM fungi may lessen the effect of high NP toxicity.

Abundant information is available about the influence of beneficial soil microorganisms ameliorating toxic effects of bulk metals, and their relevance on phytoremediation, one of the utmost costs and environmentally friendly strategies, is now highly recognized. However, the interaction between these soil microorganisms and metal NMs and their participation in soil remediation is still very limited (Feng et al. 2013; Cao et al. 2020; Ogunkunle et al. 2020; Khalid et al. 2021). Research suggests that these microorganisms can protect plants from metallic NPs toxicity through regulation of NPs absorption, secretion of substances that act as chelating agents, providing nutrients to the plant, and protecting plants against toxicity and stress caused by metals.

Metal soil contamination, caused for common sources (fertilizers, pesticides, mining, etc.), may be solved by using NMs and beneficial soil microorganisms as a sophisticated assisted phytoremediation strategy. A cellular metal tolerance mechanism in plants and microorganisms may be convenient to deal with metal soil contamination, for example, structural-functional cell wall compounds, intercellular metal accumulation as electron-dense particles or granules, and efflux pumps of metal ions. In the case of plant growth-promoting bacteria, some microbial products (extracellular polymeric substances, hormones, organic acids, and enzymes) may interact with NMs modifying surface, bioavailability, and speciation (Ameen et al. 2021). Similarly, the fungal structures and glomalin (a glycoprotein produced by hypha under active growth) from AM fungi can sequester significant concentrations of metals, such as Cu, Cd, Pb, Mn, etc. (González-Chávez et al. 2004).

Ogunkunle et al. (2020) studied the interaction of an unidentified native fungal consortium of AM fungus with TiO_2 NPs, with size particles between 43 to 55 nm and 200

mg kg^{-1} of concentration, in a soil spiked with $CdCl_2$ (10 mg kg^{-1}) in the remediation of cowpea plants (*Vigna unguiculata*). These authors concluded that AM colonization promoted plant growth, chlorophyll pigments, antioxidative defense to plants stressed by Cd contamination, and lower Cd plant uptake (roots and shoots). TiO_2 NPs synergistically potentiated these effects; therefore, both alternatives may ameliorate the negative effects of Cd toxicity and improve plant fitness in contaminated soils. More efficient phytoremediation may be obtained when the synergistic contribution of NMs and AM fungi is achieved. Low NPs concentrations and a metal-tolerant fungal inoculum can facilitate phytoremediation and have prospective applications. Cheng et al. (2021) observed that the use of 100 mg kg^{-1} of nZVI (bare= B-nZVI or starch-stabilized= S-nZVI) and inoculation of sweet sorghum (*Sorghum bicolor*) with *Acaulospora mellea* was efficient in the nanoremediation of an acidic (pH=5) and multipollutant soil (DTPA-Cd=1.9, -Pb=413 and –Zn=239 mg kg^{-1}). Both types of NMs were not phytotoxic to sweet sorghum although decreased fungal root colonization; however, *A. mellea* still reduced soil Cd-, Pb-, and Zn-availability, their accumulation in plants and contributed to phytostabilization of these elements. These NMs immobilized Pb on their surface as well as Cd and Zn, especially when using S-nZVI there were several Pb minerals ($PbZnP_2O_4$, $PbFe_3(P_2O_7)_2$ explaining soil precipitation of this element; however, with B-nZVI these compounds were not observed. Moreover, *A. mellea* modified the speciation of Fe and decreased the occurrence of Pb, Cd, and Zn on the surface of S-nZVI, but a contrary effect with Cd and Pb was observed on B-nZVI.

Plant growth-promoting bacteria under metal-polluted soil conditions may improve growth and metal stress tolerance in plants. Shah et al. (2021) analyzed the mitigation effect of *Bacillus fortis* and ZnO NPs (20 mg kg^{-1}), single or combined application, on Cd toxicity (75 mg kg^{-1}) in *Cucumis melo*. These authors found that the independent use of *B. fortis* or ZnO NPs improves antioxidant enzyme activity (catalase, superoxide dismutase, and peroxidase). However, the combined application was more effective to enhance plant growth and decrease Cd plant concentration. Mokarram-Kashtiban et al. (2019) tested the white willow (*Salix alba*) assisted by *P. fluorescens*, *R. irregularis*, and nZVI at doses of 0, 150, and 300 mg kg^{-1}. The results showed that the treatment of 150 mg kg^{-1} of nZVI in combination with the inoculation of microorganisms increased root

length, leaf area, and root Cd concentration of white willow seedlings in comparison to plants without inoculation or addition of NPs. Although molecular mechanisms involved in metal tolerance were not analyzed and need to be understood, the synergistic use of NMs and beneficial soil microorganisms in the phytoremediation of metal-polluted soils is an unexplored research topic that promises to encourage environmental applications.

Currently, the potential co-occurrence of NPs and microplastics is another environmental concern. Yang et al. (2021) analyzed the effect of two kinds of microplastics (HDPE and PLA) and ZnO NPs (500 mg kg^{-1}) on AM fungi population and maize plant growth. Both contaminants influenced greatly the community composition and relative abundance of AM fungi and the effects were type and dose-dependent. Microplastics exerted a protective effect against ZnO NPs plant growth. These authors suggested that these contaminants have an intense ecological influence with undefined significance for agroecosystems.

Applications and challenges of nanotechnology in agriculture and soil remediation

Applications of NMs in agriculture and NMs-assisted phytoremediation soil are illustrated in Figure 3. In summary, NMs can release nutrients for plants, carry pesticides, be amendments to improve soil quality and degrade or stabilize soil pollutants. Despite the potential benefit of NPs application in agriculture and soil remediation, the NMs are not used on a large scale. There are no clear reasons for the slow development and use of NMs in agriculture. We need to find the limiting factor for technology transference from the laboratory to the field. The restrictive factors identification is difficult due to myriad aspects that must be considered (Figure 8), from different focuses: technological, environmental, economic, social, and political (Kah 2015; Dimkpa et al. 2018).

Essentially, scaling laboratory results to widespread field applications requires the design of processes and policies to transfer technology (Kim et al. 2018), safely and cheaply; p.e. to develop analytical methods to validate the chemical quality of nano agrochemicals. Monitoring transformation, and quantifying their concentrations in the environment is relevant (Dimkpa and Bindraban 2018), and to ensure that NMs do not

represent a danger to environmental and human health. Hence, one of the technical challenges is related to experimentation (Sharma et al. 2020).

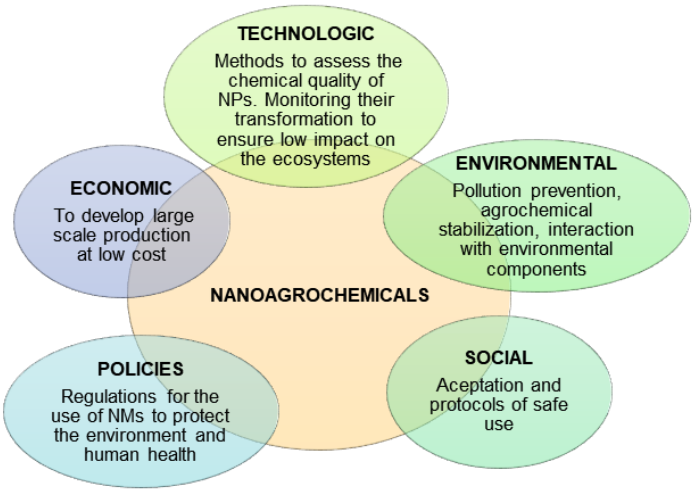

Figure 8. Concerns related to the use and commercialization of nano-agrochemicals on a large scale.

There is a need to carry out field and laboratory experiments to find safe NMs doses to reach sustainable crop production and mitigate soil pollution without damaging the soil quality and users' health (Sharma et al. 2020). Many of the reported studies were designed using high doses of NPs, short exposure times, and different media; therefore, the results may not be comparable. Moreover, experimental conditions do not reflect agricultural soil reality and complexity (Cao et al. 2017; Dimkpa and Bindraban 2018). Field-based studies to understand the life of NMs in agriculture systems are a critical requirement (Chen 2018).

To apply NMs at a wider scale and transfer nanotechnology, we should address social concerns, regulation, and legislative support (Corsi et al. 2018). There is an urgent need for policies for production and use to guarantee a low impact on the environment and the safety of human health. Acceptation of the NMs by potential consumers is transcendent. The NP interaction and transformation in the environment should be understood. Nanotechnology may have outstanding implications for sustainable development.

Conclusions

The metal NPs application for food production and soil remediation offers technological advantages. In the case of agriculture, MNs through precision farming techniques may promote efficiency in nutrient absorption, enhance crop yields and pest control avoiding environmental impact on soil and water resources. Furthermore, the agrochemical losses would reduce due to the properties of NMs and the slow release of an active ingredient. For soil remediation, metallic NPs act positively in combination with microorganisms and plants for the immobilization or stabilization of PTE. Moreover, these particles may solve the problems of both organic and inorganic pollutants. There are applications of nanotechnology to face agriculture and environmental issues. Nevertheless, it remains to select safe nanotechnologies for the environment and living organisms. In this regard, it is required to do convincing studies, using concentrations and conditions as realistic as possible, and evaluate long-term effects. The goal is to understand the complex networks of interactions between plants, soil microorganisms, the soil, and the NMs. Thus, we determine the variables that influence the toxicity of NMs, predict their fate after application, and design methods for their correct use.

CHAPTER 1. DISSOLUTION KINETICS OF CITRATE COATED $COFe_2O_4$ NANOPARTICLES IN SOIL SOLUTION[2]

1.1. ABSTRACT

Introducing nanomaterials in agriculture may help to transform the way we farm into a sustainable model by improving the efficiency of fertilizers and reducing the inputs. However, to make sure that these nanomaterials are safe for the environment and their users, the characterization of these nanomaterials and their interactions with the media are needed. Magnetic nanomaterials (such as those based on iron, iron oxides, cobalt ferrite, etc.) have been investigated for agricultural applications due to their ability to increase crop yield, photosynthetic rate, and plant biomass. In this context, this research addressed the dissolution rate of citrate-coated $CoFe_2O_4$ nanoparticles (NPs) at different pH values (5, 7, and 8) and short periods (to 0.25 until 168 h) in the soil solution of alkaline soil and artificial root exudates. Several equations were tested to fit the rate of dissolution, but the pseudo-second-order model was the best one to fit the release of Co (R^2 between 0.80 to 0.99) under all pH soil solution conditions. The k value at pH 5, 7, and 8, was 21.56, 10.52, and -31.33 L $mmol^{-1}$ h, respectively. Iron was not detected in soil solution experiments; in contrast, artificial root exudates released Fe from NPs. The best models to fit the Fe release from the NPs were the Higuchi and Korsmeyer-Peppas model (R^2 >0.92 and R^2 adjusted = 0.91). The k values were $4.33x10^{-5}$ mM $h^{1/2}$, and $9.88x10^{-3}$ h^{-n}, respectively. The main species formed from the elements released from the NPs by the ARE action were the complex of Fe and Co with malate (92 % of Fe as Fe-$malate^+$, 71% of Co as $CoH\text{-}Malate_{(aq)}$, and 14% of Co as $CoH\text{-}Malate^+$). The Fe contained in those complexes may be a Fe exchangeable source for plants. So, due to the poor water solubility of citrate-coated $CoFe_2O_4$ NPs and their dissolution by the action of artificial root exudates, these may be considered an option for slow-bio-release Fe fertilizer.

[2] Reproduced from Y. S. Perea-Vélez, Ma. D. C. A. González-Chávez, R. Carrillo-González and J. López-Luna, Environ. Sci.: Nano, 2022, 9, 2954 DOI: 10.1039/D2EN00330A, with the permission from the Royal Society of Chemistry

1.1.1. Environmental significance

Iron availability is one of the main constraints for plant nutrition in alkaline soils. Some nanomaterials may be suitable fertilizers for the controlled release of nutrients. It is important to assess the release of iron in soil solution and rhizospheric solution before the application to crops. This manuscript includes data from the dissolution of citrate-coated magnetite nanoparticles mimicking these conditions and demonstrates the controlled iron release under the influence of molecules found in root exudates. Nanoparticles may be a source of iron for plants with a low risk of Fe fixation in the soil, which could increase the efficiency of iron used by plants, and they could supply cobalt, a beneficial element for the plant with a low impact on the environment.

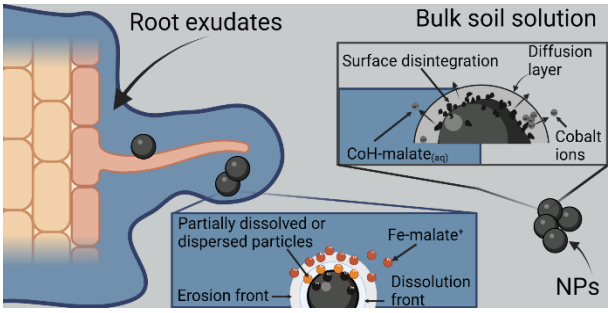

1.2. RESUMEN

Introducir nanomateriales en la agricultura puede ayudar a transformar la forma de cultivar en un modelo sostenible, mejorando la eficacia de los fertilizantes y reduciendo los insumos. Sin embargo, para asegurarnos de que estos nanomateriales son seguros para el medio ambiente y sus usuarios, es necesario caracterizarlos y conocer sus interacciones con el medio. Los nanomateriales magnéticos (como los basados en hierro, óxidos de hierro, ferrita de cobalto, etc.) se han investigado para aplicaciones agrícolas debido a su capacidad para aumentar el rendimiento de los cultivos, la tasa fotosintética y la biomasa de las plantas. En este contexto, esta investigación estudió la disolución de las nanopartículas (NPs) de $CoFe_2O_4$ recubiertas de citrato a diferentes valores de pH (5, 7 y 8) y períodos cortos (a 0,25 hasta 168 h) en la solución de suelo de un suelo alcalino y exudados radicales artificiales. Se probaron varias ecuaciones para ajustar la velocidad de disolución, pero el modelo de pseudo-segundo orden fue el que mejor se ajustó a la liberación de Co (R^2 entre 0,80 y 0,99) en todas las condiciones de pH de la solución del suelo. El valor de k a pH 5, 7 y 8, fue de 21,56, 10,52 y -31,33 L $mmol^{-1}$ h, respectivamente. El hierro no se detectó en los experimentos con la solución del suelo; en cambio, los exudados radicales artificiales liberaron Fe de las NPs. Los mejores modelos para ajustar la liberación de Fe de las NPs fueron el modelo de Higuchi y el de Korsmeyer-Peppas (R^2 >0,92 y R^2 ajustado = 0,91). Los valores de k fueron $4,33x10^{-5}$ mM $h^{1/2}$, y $9,88x10^{-3}$ h^{-n}, respectivamente. Las principales especies formadas a partir de los elementos liberados de las NPs por la acción de la ARE fueron los complejos de Fe y Co con malato (92% de Fe como Fe-malato$^+$, 71% de Co como CoH-Malato$_{(aq)}$, y 14% de Co como CoH-Malato$^+$). El hierro contenido en estos complejos puede ser una fuente intercambiable de Fe para las plantas. Así pues, debido a la escasa solubilidad en agua de las NPs de $CoFe_2O_4$ recubiertas de citrato y a su disolución por la acción de los exudados radiculares artificiales, éstas pueden ser consideradas como una opción de fertilizante de hierro de liberación lenta.

1.3. INTRODUCTION

Iron is one of the most abundant elements in nature. It is an essential nutrient for plants and animals (Angulo et al. 2021); however, crop species struggle for iron nutrition, the reason being the low Fe availability for plants (Bandyopadhyay and Prasad 2021). Iron bioavailability is strongly dependent on the chemical reactions with the soil components (Colombo et al. 2014). Alternatively, Co has been described as a benefic element, which means that low concentrations (0.01 to 10 mg kg^{-1}) stimulate plant growth, and yield, improve drought resistance, inhibit ethylene biosynthesis, and promote nitrogen fixation by increasing the number of nodules in legumes (Collins et al. 2010; Ma et al. 2021).

Iron and Co may be supplied in soluble chemical compounds to crops (Colombo et al. 2014). Chemical fertilizers containing these elements can enhance crop yield but, their excessive use in the long term may damage the soil microbial flora, disturb the soil mineral balance, and decrease the soil fertility (Pang et al. 2018). Further, more than half of the applied nutrients can be lost due to their transformation into insoluble forms in the soil or be leached to the subsoil (Solanki et al. 2015; Butt and Naseer 2020). For instance, the $FeSO_4$ soil application in calcareous soils is ineffective because Fe is quickly converted into unavailable Fe (III) forms like $Fe(OH)_3$ (Abadía et al. 2011), and using synthetic Fe chelates is an expensive option that is rarely 100% successful (Zuo and Zhang 2011). Calcic soils include more than 20 million hectares in México with Fe low availability (IUSS Working Group WRB 2006), where Fe availability may be a concern. In the case of Co, soil reserves of soluble and exchangeable Co regulate its bioavailability. In calcareous soils, the carbonate-bound fraction controls its availability. Co fertilization is commonly done as nitrate, chloride, and sulfate salts through soil application or foliar spraying. But, despite the positive effects of Co on plant performance for farmers, it is a neglected element due to a lack of knowledge about its fertilization doses and positive effects on plants (Banerjee and Bhattacharya 2021). Moreover, there is a scarcity of information about the management, advantages, and limitations of Co at a field level (Banerjee and Bhattacharya 2021; Hu et al. 2021).

In this context, the challenge is to develop efficient and cheap sources of nutrients for crops (Kah 2015). Hence, nano-based fertilizers seem to be an alternative (Shebl et al. 2020). A nano fertilizer is a nanomaterial (material with a physical diameter between 1 and 100 nm in at least one dimension, e.g. nanoparticles, NPs), or nano-enabled bulk materials used as fertilizers (Raliya et al. 2018). Due to the properties of nano fertilizers, such as small size, controlled solubility, surface reactivity, and surface area, theoretically, nanomaterials can supply nutrients to plants in a controlled way (Raliya et al. 2018; Butt and Naseer 2020). Due to the crystalline structure, in the case of Fe fertilization, the cobalt ferrite ($CoFe_2O_4$) NPs may be a poorly soluble source of Fe, at least the plant roots can solubilize the nanocrystals as has been observed with other NPs. Weilan Zhang et al. (Zhang et al. 2017) assessed the dissolution and plant uptake of CeO_2 NPs by radish plants. The authors found that CeO_2 NPs are dissolved at the root surface. The dissolution of NPs was primarily due to the action of the organic acid (succinic acid and malic acid) in the root solution. Therefore, ferrites can supply Fe to the plant, and also be a vehicle for other nutrients such as P, S, and Mo (Colombo et al. 2018). Moreover, $CoFe_2O_4$ NPs and other Fe-based magnetic materials (like $ZnFe_2O_4$, $MnFe_2O_4$, or terbium substituted $CoFe_2O_4$ NP_S) have been shown to induce earlier tomato seed germination (López-Moreno et al. 2016), enhance barley productivity (Tombuloglu et al. 2021), increase fresh and dry weight, and Zn and Fe content of *Pisum sativum* plants (Abdelhameed et al. 2021), improve plant resistance against abiotic stress (Zia-ur-Rehman et al. 2018), facilitate pest control (Sharma et al. 2017), and increase the symbiosis with nitrogen-fixing organisms (Ma et al. 2021). Previous investigations have reported a low potential toxic risk of $CoFe_2O_4$ NPs, and authors like López-Luna et al. (2018) found that the effective concentration of $CoFe_2O_4$ NPs that diminished root length of wheat plants by 50% is 1963 mg kg^{-1} for fresh NPs and 5023 mg kg^{-1} for powdered NPs. Miri et al. (2022) pointed out that $CoFe_2O_4$ NPs were nontoxic for cancer and normal cell lines. However, before using $CoFe_2O_4$ NPs in soil, it is necessary to mimic the release and try to predict the behavior of these NPs in the rhizosphere, because their effect on plant depends on the NP's characteristics, plant species' surrounding media (Perea Vélez et al. 2021).

An important desirable feature of nano fertilizers is the slow release of the active ingredient over time. When these are applied to the soil, plants can take up the maximum

amount of nutrients through their development. Moreover, losses of nutrients by leaching or fixation on the soil colloids can be avoided compared to bulk soluble fertilizers (Butt and Naseer 2020). These purposes can be achieved by adding coatings or by modifying the surface of the nano fertilizer (Solanki et al. 2015; Cartwright et al. 2020) to change its reactivity.

Soil application is the most common method of nutrient supplementation. However, to have a successful fertilization strategy, there is a need to know how soil chemical and biological factors will influence the properties of nano fertilizer once it is delivered, and how long it will last in the soil (Solanki et al. 2015). In this regard, testing the NPs dissolution can provide insights to develop guidelines on the appropriate dosage and storage of nano fertilizers in the case of NP suspension or dispersion, knowing their persistence in the environment, predicting the bioavailability of nutrients, and the right time to apply them, and thus enhance the efficiency of nano fertilizers (Timilsena et al. 2015). Moreover, the European Chemical Agency (ECHA) and the Environmental Protection Agency (EPA) are prioritizing the assessment of the dissolution rate as a key criterion for the evaluation of the risk potential of a nanomaterial. Hence, the dissolution rate can be used to compare different nanoforms of a substance from fast-dissolving to poorly soluble materials (Keller et al. 2020).

On the one hand, the dissolution of the NP and the release pattern of its ions constituents depends on its properties like particle size, composition, shape, crystallinity, specific surface area, and surface modifications (Miao et al. 2010; Misra et al. 2012; Utembe et al. 2015). It is generally assumed that solubility of NPs increases as particle size decreases (Misra et al. 2012; Avramescu et al. 2017) because the diffusion layer thickness decreases with particle size leading to faster transport of solvated molecules into the bulk solution. Also, the Gibbs-Thompson effect predicts that particles with a smaller radius and a convex surface curvature will have a high tendency to dissolve more than larger particles (Borm et al. 2006; Ely et al. 2014). However, experimentally it has also been observed that the NP-solubility may be size-dependent; which has been shown for NPs of SiO_2, ZnO, ZnS, AgNPs, and Fe_2O_4 (Zhang et al. 2011; Mudunkotuwa et al. 2012; Diedrich et al. 2012) but no difference between nano and microscopic particles

have been reported, and even dissolution can be inhibited by particle size reduction (Misra et al. 2012).

Moreover, the solvent properties such as pH, ionic strength, molecule solvation, temperature, presence of strong oxidants (such as oxygen, H_2O_2, HO_2^-, and OCl^-), sunlight, and organic ligands also influence the NP dissolution (Borm et al. 2006; Utembe et al. 2015; Cartwright et al. 2020). The interaction between NPs and media components can be dual-acting: either increasing the dissolution through ligand promoted process; reducing the dissolution of NPs through steric protection or inducing agglomeration/aggregation (Misra et al. 2012). The formation of agglomerates/aggregates can deplete dissolution by reducing the surface area. Modification of the specific surface can take part in the reduction of the dissolution process (Borm et al. 2006; Ely et al. 2014).

Experimental dissolution protocols for macroscopic materials can be adapted to assess the dissolution of NPs (Misra et al. 2012), while the Organization for Economic Cooperation and Development (OECD 2020) proposes the TG 105(OECD 1995) and ISO 19057 (ISO/TC 229 Nanotechnologies 2017) methods. The kinetic models are generally used to mimic the reaction rates, such as dissolution. The first-order and the pseudo-first-order rate equations have been suggested to describe the NP dissolution (Hedberg et al. 2019; OECD 2020) in many cases (Table 1.1). For example, in distilled water, the dissolution of citrate-coated Ag, CoO, and $Cu(OH)_2$ NPs followed a first-order kinetic model (Lee et al. 2012; Misra et al. 2014; Vencalek et al. 2016).

This research aimed to determine the dissolution rate of citrate-coated $CoFe_2O_4$ NPs at different pH values in the soil solution in short periods, and the effect of soil solution pH and root exudates on NP dissolution. Our hypotheses are I) NP dissolution is pH-dependent and II) citrate-coated $CoFe_2O_4$ NPs can be an option for the slow-release of the Fe nano fertilizer.

Table 1.1. Selected dissolution studies were performed on NPs in different conditions.

NP	Size (nm)	Media	Model kinetic	Rate constant	Conditions	Observation	Reference
Citrate coated AgNPs	13.3 and 60-100	Air-saturated DW	First-order kinetics	0.0278-0.073 h^{-1}	pH 5.5-5.8 22°C [NPs]: 0.05, 0.1, 1 mg L^{-1}	AgNPs dissolution reaches an equilibrium concentration after 48 h. The smaller rate constant is the result that the Ag^{+} rapidly reaches a critical concentration	Lee et al. (2012)
Citrate coated AgNPs	20-80	Quarter-strength Hoagland medium	Hard sphere theory (Arrhenius equation)	0.0127-0.055 h^{-1}	DO:7.8 mg L^{-1} pH: 5.6 [NPs]:300 and 600 µg L^{-1}	Ion release rates depended on primary particle size and concentration	Zhang et al. (2011)
ZnO	20	DW and artificial seawater (ASW)	$y = \frac{s * t}{t_{1/2} + t}$ y=Total [Zn] at time t s=maximum [Zn] $t_{1/2}$= time taken for y to reach half the maximum	$t_{1/2}$ in DW= 7.57 d $t_{1/2}$ in ASW: 0.09-0.25 d	[NPs]: 0.12-6.14 mM pH of • ASW:8 • DW:5.6	Ion release is mainly influenced by pH and the specific surface area of NPs.	Miao et al. (2010)
CuO,	7-270	$NaNO_3$ 1 M and serum-free cell-culture media	First-order Noyes-Witney	0.022-0.32 h^{-1}	[NPs]: 750 mg L^{-1}	The NP shape (spherical, rod, and spindle shape) affected the dissolution of NPs	Misra et al. (2014)
CuO, $Cu(OH)_2$	30-50	DW and natural water	Fickian diffusion model, First-order-diffusion	CuO: 0.0041-0.0104 h^{-1} $Cu(OH)_2$: 0.0091-0.3010 h^{-1}	pH: 5.8 and 7.7 [NPs]: 1 mg L^{-1} 20°C	Environmental conditions (pH, temperature, and biological activity) affect the dissolution rate	Vencalek et al. (2016)

CuO	<50	Soil	Surface area-normalized rate equation and modeled by a first-order kinetic	0.33 (pH 8.2)-6.42 (pH 5.3) and solubility ranged from 37.1-100.1 mg kg^{-1}	Soil moisture at 80% of the field water capacity pH soil: 4.9-8.4 OM: 12.2-54.2 g kg^{-1} Clay:11.1-39.9% [NPs]: 160 mg Cu kg^{-1}	The dissolution rate constant and solubility were positively correlated with the content of OM, clay, and Fe and Al oxides; and negatively correlated with soil pH.	Yang et al. (2022)
CeO_2	3 and 78	DW	Zero-order kinetic	0.0362-, and 0.0057-mM kg^{-1} h at pH 1.65, and 4.75, respectively (NPs size 33 nm). 0.0209- and 0.0084-mM kg-1 h at pH 1.65, and 4.75, respectively (NPs size 78 nm).	pH: 1.65,4.45, 7.45, and 12.40 [NPs]: 500 mg Ce L^{-1} Presence and absence of 100 µM P	The NPs dissolution was significant at pH<5 and inversely proportional to the surface area. After 120 h the Ce release was greater in large NPs than in small NPs.	Dahle et al. (2015)
Fe_3O_4	78	Stomach digestive fluid, duodenum digestive medium	First-order kinetic	k_1:4.37, k_2: 0.09 for pH 1.8 and k_1:3.80, k_2:0.07 for pH 5 conditions	pH: 1.8-2 (stomach media), and 4.5-5 (duodenum media)	The kinetic curve showed two linear intervals with different slopes indicating that the different mechanisms of the dissolution are specified by the size, shape, and state of the surface of the particles.	Tsykhanovska et al. (2019)

NP(s), nanoparticle(s); DW, deionized water; ASW, artificial seawater; DO, dissolved oxygen; OM, organic matter

1.4. EXPERIMENTAL

1.4.1 Synthesis and characterization of citrate-coated $CoFe_2O_4$ NPs

The synthesis of citrate-coated $CoFe_2O_4$ NPs was carried out following the methodology described by Martínez-Vargas et al. (2017b) and Silva-Silva et al.(2016). Briefly, in a 100 mL beaker, 8 mL $Fe(NO_3)_3\ 9H_2O$ 1 M and 4 mL $Co(NO_3)_2\ 6H_2O$ 1 M dissolved in 2 M HCl solution were mixed. 38 mL of NaOH 1.5 M was added dropwise with a peristaltic pump at a flow of 1.3 mL min^{-1}, under vigorous stirring. Subsequently, the mixture was heated at 90 °C under constant stirring for 1 h to induce crystallinity. Afterward, the ferrofluid was cooled down and soft magnetic decanted. The NPs were rinsed three times with deionized water. Then, 50 mL of sodium citrate 4 mM solution was added to the NPs. The mixture was heated for 30 min at 80 °C on continuous stirring. The NPs were rinsed with deionized water until the pH of the supernatant was 6.5-7.0 and suspended in deionized water (50 mL).

The morphology of NPs was obtained by transmission electronic microscopy (TEM). A sample of 5 µL of the ferrofluid was suspended in 240 µL acetone and sonicated for 30 min. Then, 30 µL of NP suspension was placed on a carbon and copper grid, and the solvent was left evaporated at room temperature for two h. The images were taken by a Tecnai Bio Twin, G2 Spirit 120 kV microscopy, and a WA-Vaketa camera. The hydrodynamic radius and potential Z were measured by dynamic light scattering (DLS) through a particle analyzer (Anton Paar Litesizer TM 500). For this analysis, the NPs were suspended in distilled water and sonicated with an ultrasonic probe for 2 min at 130 W and 90% amplitude. The elemental composition was assessed by SEM-EDX analysis. A minimal powder NP sample was placed in a sample holder with carbon tape. The micrographs were taken at 5kV while the EDS analysis was performed at 20 kV, 60 s live time, and resolution of 132.5 eV. The molar composition of NPs was corroborated by atomic absorption through the flame method with a Perkin Elmer, model 3110. X-ray diffraction analysis (XRD) was conducted using an Empyrean diffractometer in the 2Θ range of 4-80º with a step scan 0.003º min^{-1}.

1.4.2. Soil solution characterization

Topsoil samples (15 cm) were collected from the experimental field of Colegio de Postgraduados (19°30' N, 98°51' W). The soil solution was obtained by equilibrating field-moist soil in a solid-solution ratio of 1:2.5 on a rotator shaker at 20 rpm for 16 h (Degenkolb et al. 2019). Afterward, the mixture was centrifuged at 2500 rpm for 10 min and filtered with a Whatman No. 42 filter paper. The pH was analyzed by a pH meter (A420, Orion), and electrical conductivity (EC) was measured using a conductometer (Cl3, Conductronic). The concentration of SO_4^{2-} (turbidimetric), PO_4^{3-} (colorimetric), HCO_3^- and CO_3^- (Titration with H_2SO_4 solution), Cl^- (argentometric), Co, Fe, Ca^{2+} and Mg^{2+} (atomic absorption spectrophotometry), and Na^+ and K^+ (flame photometric) were measured in the extract. The ionic strength was calculated using Visual Minteq A ver. 3.1. Table S1 summarizes the properties of the soil solution.

1.4.3 The dissolution rate of $CoFe_2O_4$ NPs in soil solution as a function of pH and time

To assess the dissolution rate of citrate-coated $CoFe_2O_4$ NPs, kinetics experiments were carried out as a function of time at different pH levels. All the experiments were performed at room temperature and a total Fe concentration of 30 mg L^{-1} and 19 mg Co L^{-1} (equivalent to 81 mg NPs L^{-1}). The concentration was designed for a realistic scenario of the agronomic fortification of wheat. The pH range (5, 7, and 8) was selected to have different scenarios where the NPs can be applied, and the ion release kinetics understood. The pH of the soil solution was adjusted by adding a small volume of HCl 0.1 M or KOH 0.1 M solutions.

Separately, a stock suspension of $CoFe_2O_4$ NPs (500 mg Fe L^{-1}) was prepared by dispersing the NPs in deionized water and sonicated with an ultrasonic probe for 2 min at 130 W and 90% amplitude. Then, 1.2 mL of NPs stock suspension was mixed with 18.8 mL of soil solution pH adjusted in a Falcon tube of 50 mL. The mixture was equilibrated for 168 h on a rotating shaker at 20 rpm, and samples were taken at 0.25, 0.5, 1, 3, 6, 15, 24, 48, 72, and 168 h. The NPs were separated by centrifugation at 10 000 rpm for 8 min. Then, the slurry was magnetic decanted and filtered twice with a 0.2 µm nylon filter and

acidified with HCl. The concentration of Fe and Co in the extracts was analyzed by atomic absorption spectrophotometry (Perkin Elmer, model 3110) by the flame method. For Qa/Qc, the material used for the experiments was washed in a 0.25 M HCl solution to remove any traces of Fe and Co. All the reagents used were analytical grade (JT Baker, Merck, and Aldrich). All the experiments were carried out in triplicate. Standard solutions were prepared using certificated stock solutions.

1.4.4. Effect of pH in NPs dissolution

The pH of the soil solution was adjusted from 1 to 12 with HCl 0.1 M or KOH 0.1 M solutions. Then 18.8 mL of soil solution pH adjusted were mixed with 1.2 mL of citrate-coated $CoFe_2O_4$ NPs stock dispersion solution. The mixture was equilibrated for 3 h on a rotor shaker at 20 rpm. Then all the samples were filtrated and analyzed as mentioned above.

1.4.5. Effect of artificial root exudates in NPs dissolution

We use an ARE solution composed of succinic and malic acid, because these organic acids are ubiquitous in root exudates (LeFevre et al. 2013; Zhang et al. 2017; Peng et al. 2019). Furthermore, plant roots can release specific organic compounds depending on the soil conditions, for example, exudation of oxalate, acetate, and malate is often induced by soil nutrient deficient conditions. However, the specific composition and concentration of low molecular weight organic acids will depend on the plant species, the growth media, and the growing plant stage (Peng et al. 2019).

The ARE were prepared by mixing 50 mM glucose, 25 mM succinic acid, and 25 mM malic acid (Zhang et al. 2017). The ARE (18.8 mL, pH ARE solution= 4.2) was mixed with 1.2 mL of citrate-coated $CoFe_2O_4$ NPs stock dispersion at 500 mg Fe L^{-1} (prepared as described above) to get a final concentration of 30 mg Fe L^{-1}. The mixture was equilibrated on a shaker at 20 rpm for four days. Samples were taken at 0.25, 0.5, 1, 3, 6, 15, 24, 48, 72, and 96 h, centrifuged, filtrated, and analyzed as mentioned before.

1.4.6. Dissolution kinetics model

The chemical speciation of ions released from the citrate-coated $CoFe_2O_4$ NPs was determined by using the chemical speciation program, Visual Minteq ver. 3.1. The simulation was performed using the data of soil or ARE solution composition and the concentration of Co and Fe assessed after 168 h or 96 h of equilibrium with soil solution or ARE, respectively. Also, ANOVA to compare concentrations at a specific point in time was run using R Statistical Software version 4.0.3 (R Core Team 2020).

To simulate the release of Fe and Co, 13 different equations were tested to fit the rate dissolution (Table S2). The linear regression indices were calculated using R Statistical Software (R Core Team 2020). To examine the goodness of fit of the model, a test for the significance of the regression model was performed, and the determination coefficients (R^2) and their adjusted value (R^2 adjusted) were used to evaluate the fit adequacy of the regression model.

1.5. RESULTS AND DISCUSSION

1.5.1. Synthesis and characterization of citrate-coated $CoFe_2O_4$ NPs

A summary of the properties of citrate-coated $CoFe_2O_4$ NPs is given in Table 1.2. The TEM images (Figure 1.1a) indicated that $CoFe_2O_4$ NPs are semi-spherical in shape, and agglomerates were observed despite the NPs being dispersed with an ultrasonic bath (Figure 1.1a, b). The value of *Z* potential indicates that the NPs have low stability in water dispersions, which means that NPs tend to agglomerate. Coagulation could explain the size of hydrodynamic diameter because agglomerates tend to former even after the dispersion of NPs by an ultrasonic probe. The average primary size of $CoFe_2O_4$ NPs was 13.41 nm and particle sizes were distributed in the range of 4.69-29.81 nm (Figure 1.1c). Based on the EDX analysis, the ratio composition of NPs was 49.24 ± 2.38% Fe, 30.48 ± 1.48% Co, and 20.28 ± 3.84% O (Figure 1.1d). A similar composition was determined by the atomic absorption analysis. The X-ray diffraction (XRD) analysis confirmed that the NPs synthesized were $CoFe_2O_4$. The diffraction pattern of the sample could be assigned to the crystallized $CoFe_2O_4$ with intermediate crystallinity (Figure 1.1e).

Table 1.2. Properties of citrate-coated $CoFe_2O_4$ NPs.

Properties	Value
pH (supernatant)	6.44
Shape	Semi-spherical
Primary size (nm)	13.41±4.58
Hydrodynamic diameter (nm)	216.06±10.46
Polydispersity (%)	18.53±18.53
Zeta potential (mV, in DI water)	10.5 ±6.6
Point of zero charge (pH)	6.8
Fe composition (% by AAS)	48.48 ± 5.2
Co composition (% by AAS)	29.37 ± 1.8
Maximum repulsive potential (nm)	9

AAS, atomic absorption Spectrophotometry; DI, Deionized water

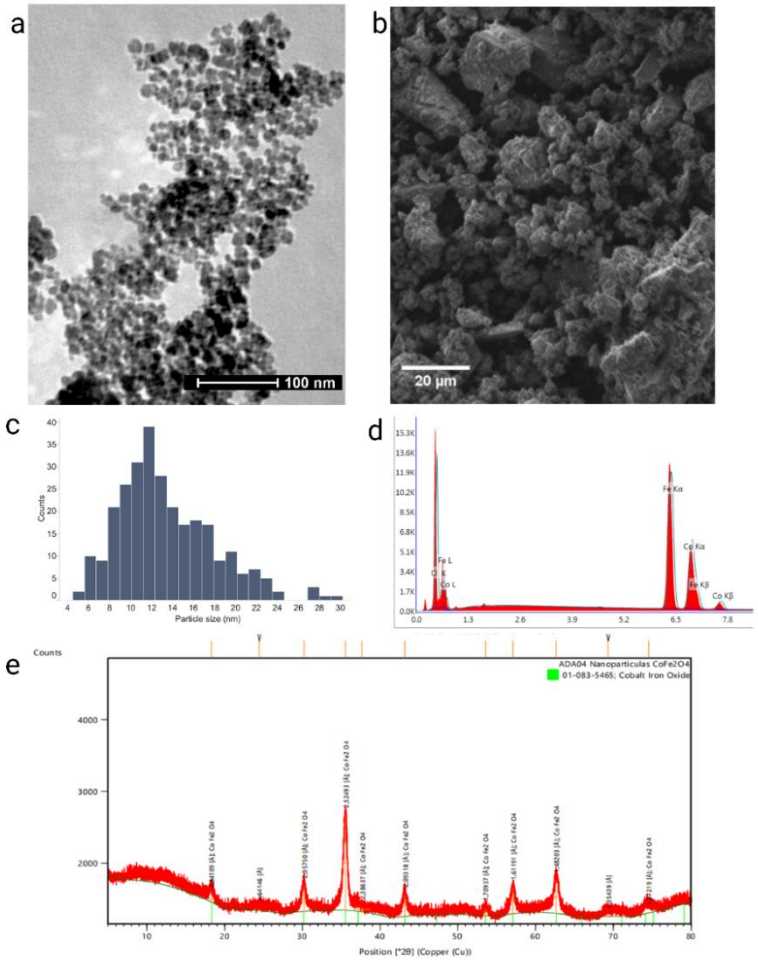

Figure 1.1. Morphology and composition of citrate-coated $CoFe_2O_4$ NPs. a) TEM and b) SEM images of NPs, c) the cobalt ferrite particle size distribution, d) EDX and e) XRD pattern for the composition of NPs.

1.5.2. Effect of pH soil solution on the dissolution of citrate-coated $CoFe_2O_4$ NPs and their dissolution rate

When we test the effect of the pH soil solution (from 1 to 12) on the dissolution of $CoFe_2O_4$ NPs, it was observed that the Co-release from NPs was pH-dependent. The maximum release was observed at pH 1 (17.5% of initial concentration; Figure 1.2). The minimum release was observed at pH 12 (0.38% of initial concentration). No significant changes in the concentration of Co-released from pH 6 to 8 (2.05%-1.80% of initial concentration) and 9 to 12 (0.82%-0.32% of initial concentration) were observed. This means that from slightly acid to alkaline soils the Co is slowly released from the $CoFe_2O_4$ NPs. The probability of plant uptake increases if the Co ions are in the soil solution. In contrast, Fe-release was only detected below pH 3, and the maximum dissolved fraction was observed at pH 1 (27.2% of initial concentration). The decrease in Fe fraction released per unit of pH was statistically different (p<0.001).

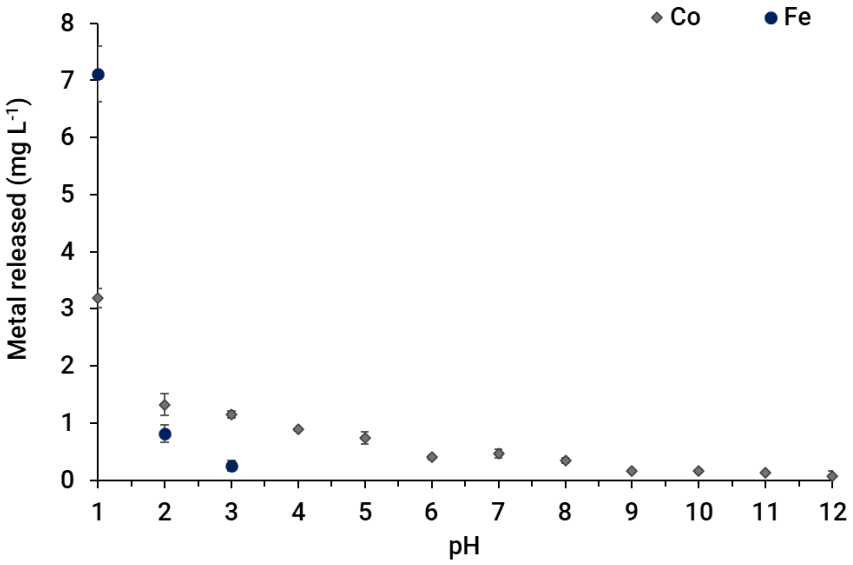

Figure 1.2. The effect of pH in Co and Fe dissolution from $CoFe_2O_4$ nanoparticles.

On the other hand, to assess the dissolution kinetic rate of $CoFe_2O_4$ NPs we carried out a time curse experiment at 5, 7, or 8 pH soil solution. Soluble Fe was not detected in the soil solution in any of the pH tested (5, 7, or 8). For this reason, only the data of the Co-release are presented. The release of Co from the NPs was pH-dependent (Figure 1.3). Fluctuations in Co concentrations were observed in the first 3 h (Figure 1.3).

From 0.25 h to 72 h, the Co concentration was superior in the pH 8 condition compared to that in the pH 7. At the end of monitoring, a significant (p<4.04x10^{-5}) reduction of the fraction of Co released was observed as the pH increased (Figure 1.3). Significant (p<0.001) changes in pH soil solution were observed at pH 5 and 7 initial conditions, from 5.01 to 6.48 ± 0.06, and from 7.01 to 7.97 ± 0.02, respectively. No significant changes were observed at pH 8 initial condition. The chemical species formed from the Co released from the NPs are shown in Table 1.3. At all pH analyzed, the species with the highest distribution was the Co^{2+} ion.

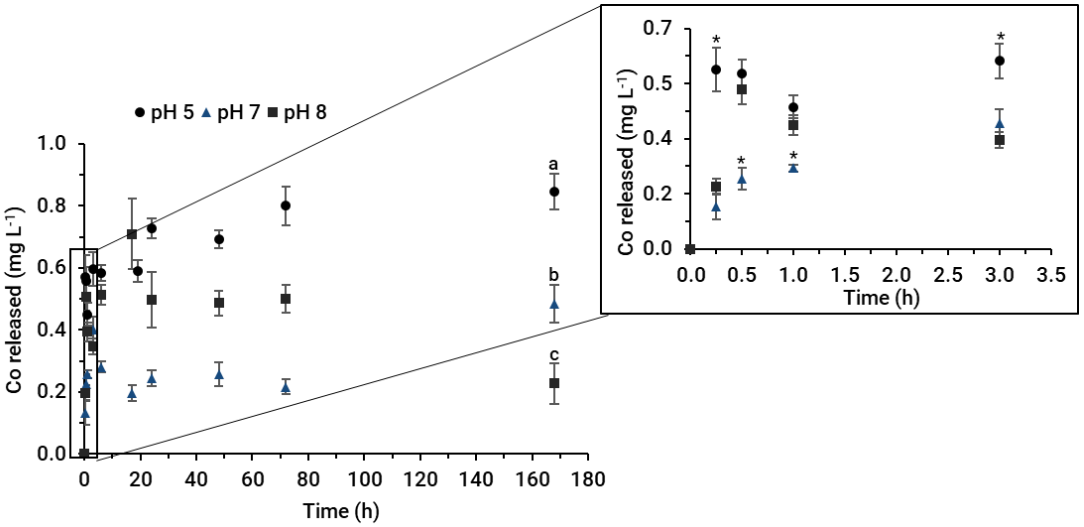

Figure 1.3. Kinetics of Co ions released from $CoFe_2O_4$ NPs in soil solutions at different pH levels. A close-up of the first 3.5 h of the time-course experiment. Bars represent standard deviations of three replicates. Lowercase letters and the * symbol indicate significant differences between pH conditions at a specific time according to Tukey's test (α=0.05).

Table 1.3. Percentage distribution among dissolved species of Co at different pH in soil solution

Component	pH		
	5	7	8
Co^{+2}	93.79	93.49	92.46
$CoSO_{4\,(aq)}$	6.07	6.05	5.99
$CoCl^{+}$	0.14	0.14	0.14
$CoOH^{+}$		0.11	1.09
$CoHPO_{4\,(aq)}$		0.21	0.25
$Co(OH)_{2\,(aq)}$			0.07

To model the Co-release mechanism from citrate-coated $CoFe_2O_4$ NPs, the pseudo-second-order equation was the best fit among the 13 models tested for the all-pH conditions with R^2 values between 0.80 and 0.99 (Figure 1.4a, Table S3). The highest goodness of fit in the experimental data was found in the pH 5 condition, with R^2 of 0.990 and R^2 adjusted at 0.989. Meanwhile, the goodness of fit for the experimental data decreased for pH 7 and 8 conditions with R^2 adjusted of 0.798 and 0.861, respectively. The slope and the intercept were statically significant for pH 5 and 7, while only the slope was significant for pH 8. From the linear equation of the pseudo-second-order dissolution reaction the kinetic constant (k), the theoretical saturation concentration ($[M]_s$), and the initial dissolution rate (V_d; $V_d=kc_s^2$) were calculated to mimic the Co-release in the soil solution, and the results are shown in Table 1.4. From those results, it can be observed that k, $[M]_s$, and V_d decrease with an increase in pH units, and the stability of NPs increases in alkaline conditions.

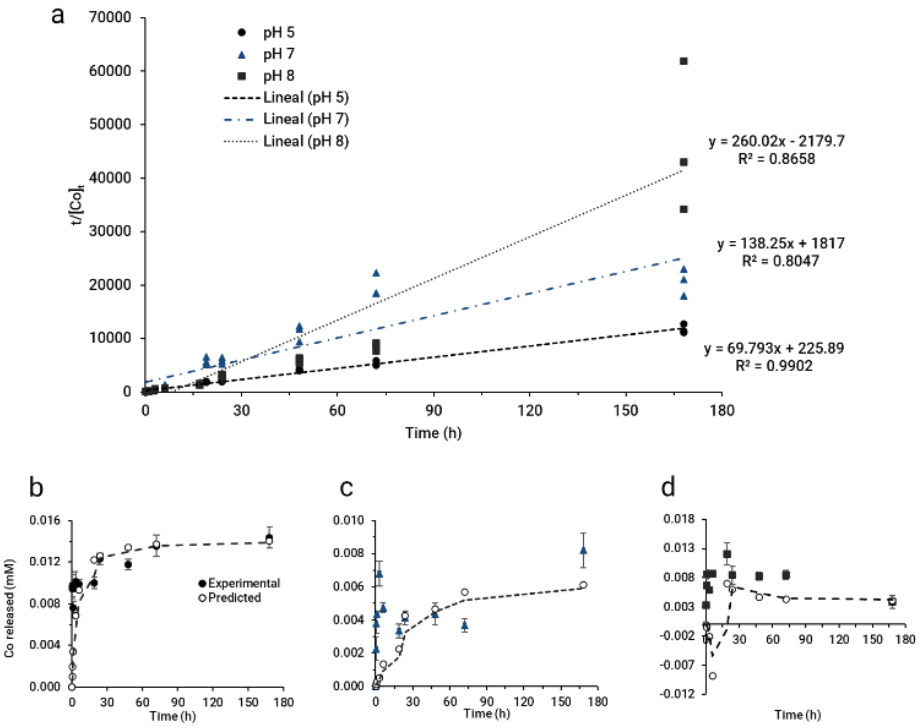

Figure 1.4. a) Pseudo-second-order kinetic plot of $CoFe_2O_4$ NPs dissolution, and experimental and predicted data from the dissolution model at b) pH 5, c) pH 7, and d) pH 8 soil solution. Bars represent the standard deviations of three replicates.

Table 1.4. Calculated parameters from the pseudo-second-order equation for Co ions released from the citrate-coated $CoFe_2O_4$ NPs in soil solution at different pH levels.

Fitting parameters	pH 5	pH 7	pH 8
k (L mol^{-1} h)	21.564	10.519	-31.327
$[M]_s$ (mM)	0.014	0.007	0.004
V_d (mM)	0.0044	0.0006	-0.0005

$[M]_{s;}$ theoretical saturation concentration, Vd initial dissolution rate

1.5.3. Effect of artificial root exudates in NPs dissolution

The concentration of Fe and Co ions released over time from citrate-coated $CoFe_2O_4$ NPs after four days of contact with ARE solution varied slightly with time (Figure 1.5 a). At the end of the kinetic test, 10.9% and 10.6% of initial concentrations of Fe and Co, respectively, were released. The released Fe was mainly bound to malate ion, while the predominant Co chemical species were $Co\text{-}Malate_{(aq)}$>$CoOH\text{-}Malate^{+}$>Co^{2+} (Figure 1.5 b and c).

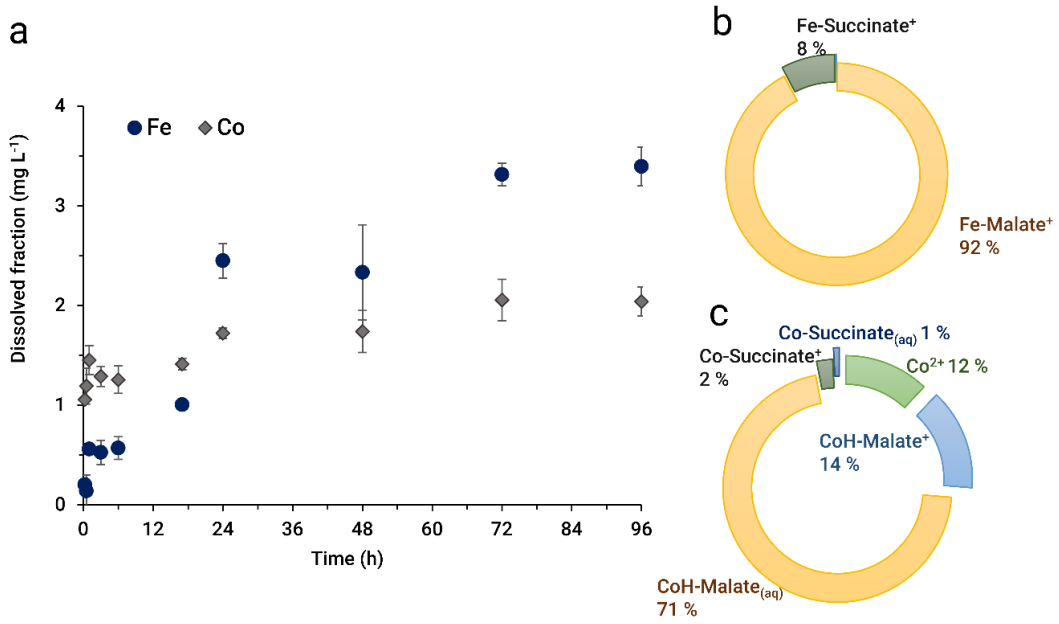

Figure 1.5. a) Concentration of metal ions released from citrate-coated $CoFe_2O_4$ NPs by the effect of artificial root exudate (ARE)s, and the b) Fe and c) Co chemical species formed in the ARE solution.

The best models to fit the release of Fe by the NPs were the Higuchi and Korsmeyer-Peppas (Table 1.6 Table S4) with R^2 >0.920 and R^2 adjusted=0.91. The pseudo-second-order model fails to predict the beginning of the reaction. In the case of Co-release, the best-fitted model was the pseudo-second-order with an R^2=0.981 and R^2 adjusted=0.98. The kinetic constant (k), and the theoretical saturation concentration ($[M]_s$) were calculated from the linear equation models.

Table 1.5. The fitting model parameters and the calculated parameters for ions released from the citrate-coated $CoFe_2O_4$ NPs according to different dissolution kinetic models.

Fitting parameters	Fe	Co
	Pseudo-second-order	
R^2	0.835	0.981
R^2 adjusted	0.829	0.981
Intercept	307.498*	82.462*
Slope	13.996*	28.801*
k (L mol^{-1} h)	0.637	10.059
$[M]_s$ (mM)	0.071	0.035
	Higuchi	
R^2	0.921	0.783
R^2 adjusted	0.918	0.775
Intercept	$-8.613x10^{-4}$*	0.019*
Slope	0.007*	$1.661x10^{-3}$*
k (mM $h^{1/2}$)	0.007	0.002
Ms (mM)	-0.001	0.019
	Korsmeyer-Peppas	
n	0.538	0.097
R^2	0.922	0.726
R^2 adjusted	0.919	0.712
Intercept	0.010*	-0.003
Slope	$9.879x\ 10^{-3}$*	0.067*
k (h^{-n})	$9.879\ x\ 10^{-3}$	0.067

$[M]_s$; theoretical saturation concentration, * Symbol indicates significance with an α=0.05.

1.5.4. Nanoparticle characterization and its dissolution by the effect of soil solution and artificial root exudates

During the last few years, one of the main objectives of nanotechnology in the agricultural sector has been to improve fertilizer efficiency. But, to develop new agrochemicals, we must show that a new product is safe for workers, the environment, crops, and food consumers. So, for this purpose, a new substance undergoes extensive tests, such as physicochemical properties, toxicology, residues, and eco-toxicology. This

study focuses on the NPs dissolution as part of the NP characterization and an integral part to understand the interactions between the NPs, the plants, and the abiotic surrounding media, if we think of a nanomaterial as a nano fertilizer. Our results showed that the shape and composition (Figure 1.1) of citrate-coated $CoFe_2O_4$ NPs synthesized were similar to those of $CoFe_2O_4$ NPs obtained by Martinez-Vargas et al. (2017) López-Luna et al. (2018) López-Moreno et al.(2016). Moreover, the XRD pattern of the citrate-coated $CoFe_2O_4$ NPs was in harmony with crystallographic data reported for other $CoFe_2O_4$ NPs (López-Moreno et al. 2016; Swatsitang et al. 2016; López-Luna et al. 2020). The XRD pattern (Figure 1.1e) of the NPs may be indexed to the spinel structure of ferrite because it occurs at nearly the same angle. No characteristic peaks for other impurities were detected.

The high chemical stability is one of the main features of Fe-based magnetic spinel nanomaterials, such as the $CoFe_2O_4$ NPs (Tombuloglu et al. 2021). This chemical stability makes the $CoFe_2O_4$ NPs poorly water-soluble nanomaterials, due to the strong Fe-Co interactions. The theoretical saturation concentration ($[M]_s$) calculated (from the time curse experiment and kinetic dissolution model) suggested that the citrate-coated $CoFe_2O_4$ NPs are poorly water-soil solution soluble at pH 5, 7, and 8 (Table 1.4). The [M]s in terms of mg Co L^{-1} were 3.29, 1.65, and 0.94 at pH 5, 7, and 8, respectively. So, if we consider these values as the solubility values of NPs, given the experimental conditions and the soil solution as the solvent, the NPs could be classified as very slightly soluble to practically insoluble according to the criteria of the United States Pharmacopeia (Con 1979; Savjani et al. 2012). Moreover, it was observed that the Co concentration in soil solution from pH 2 to 12 tends to decrease (Figure 1.2), while the Fe was only detected when the pH of the soil solution was below 3 (Figure 1.2). This chemical stability can be used as an advantage since the Fe contained in the particle will not be immediately fixed in the soil after the application of NPs; as occurs with other Fe fertilizers. For instance, after 1 h of the application of Fe-EDTA, Fe-DTPA, and Fe-EDDHA in alkaline soils (pH ≥ 7.9), almost 40% of applied Fe can be fixed, while in neutral soils 30% - 40% of applied Fe can be absorbed by the plants (Shaddox et al. 2019). In contrast, both Fe and Co can eventually be released from the nanoparticle by the effect of plant root

exudates as results showed that after four days 10% of the initial concentration of both elements was released (equivalent to 3 mg Fe L^{-1} and 1.9 mg Co L^{-1}).

The organic acids from the root exudates, such as oxalic, citric, and malic acid play an important role in the chelation, and dissolution of soil nutrients (Peng et al. 2019). Thus, it is expected that they may drive the transformation and bioavailability of ions from the NPs. In ARE solution the Fe concentration increased due to the lower pH (4.2) and the ligand concentrations. The citrate-coated NPs may react with H^+ from organic acids of ARE solution and release Fe and Co ions, meanwhile, the ions released combine with the carboxylic groups associated such as malate and succinate (Lv et al. 2019; Zhang et al. 2022). According to the speciation analysis carried out, the main species formed by the elements released by the NPs by the ARE action were the complex of Fe and Co with malate (92 % of Fe as Fe-malate$^+$, 71% of Co as CoH-Malate$_{(aq)}$, and 14% of Co as CoH-Malate$^+$). Meanwhile, a small portion of Fe and Co species is the complex formed with the succinate organic ligand (8% of Fe released as Fe-succinate, 2% and 1% of Co released as Co-succinate$^+$ and Co-succinate$_{(aq)}$, respectively) The Fe complex formed with organic acids, such as the malic and succinic acid, have a wide range (10^{3-20}) of stability constant (L-Fe^{III}) (Mimmo et al. 2014), indicating that the Fe contained in those complexes may be a source of exchangeable Fe which can be used by plants (strategy II). In the case of the strategy I plant if there is a sufficiently large redox potential for enzymatic reduction the Fe from the malate complex can be used as well (Mimmo et al. 2014). In the case of Co, the specific mechanisms of plant uptake and transport inside the plant system are still unknown to a great extent (Banerjee and Bhattacharya 2021), but it is known that the Co^{2+} form is uptake by the plant roots (Banerjee and Bhattacharya 2021; Hu et al. 2021). Collins et al. (2010) assessed the Co uptake and translocation in tomato and wheat plants. The authors reported that Co in the roots is complexed with carboxylic acids, suggesting that Co could also be complexed with other organic ligands such as citrate or malate. So, the Co species formed after the NPs dissolution could be absorbed by the plant roots. Moreover, from the results of NPs uptake studies (Stegemeier et al. 2015; Zhang et al. 2017), NP dissolution in the rhizosphere has been observed, suggesting that root exudates enhance the element bioavailability, and the

plant nutrient uptake from NPs by plants is attributed to the dissolution or partial dissolution of NPs.

Ideally, a perfect slow-release fertilizer would be one in which the nutrient release would not be controlled by hydrolysis or diffusion, but by the dissolution activities of the root itself (Chandra et al. 2009). Our results suggested that the dissolution of citrate-coated $CoFe_2O_4$ NPs by hydrolysis was slow at pH ≥ 6 because the Co-release fraction was 1.2% - 2.5% after 168 h, and similar results were observed in slow-release Fe fertilizer based on a polymeric phosphate structure, where 2% of initial Fe concentration was detected in water after 120 h (Chandra et al. 2009). Moreover, the citrate-coated $CoFe_2O_4$ NPs may be also considered a “bio-release fertilizer” or chelate reaction control, because the nutrients are released from an insoluble compound by the action of organic acid chelates (Chandra et al. 2009). The fact that Fe and Co may be controlled release from the NP by the effect of root exudates may provide a safer, economical, and efficient way to administer Fe or Co for a longer period and when the plant needs them. In consequence, this may help to improve the nutrient use efficiency by less frequent dosing of Fe fertilizers; reduce the environmental hazards by diminishing the amount of nutrients applied to the soil and their losses by the effect of runoff (Lawrencia et al. 2021), and decrease the energy, manpower or other resources used to operate the application of fertilizers (Kumar et al. 2021).

On the other hand, if we thought that the citrate-coated $CoFe_2O_4$ can be applied to soil as a nano fertilizer, its fast aggregation/agglomeration could result in significant deposition of the NPs in soil, but lower Fe and Co bioavailability (Cervantes-Avilés et al. 2021). Results showed that even though the NPs have a surface coating, these tend to agglomerate (Figure 1.1a and b). Even the value of zeta potential of NPs (10.5 ± 6.6 mV in distiller water) suggests that the NPs have low stability in water. The NPs agglomeration also can explain the poor dissolution of NPs in soil solution in addition to the nature of NPs. Cervantes-Aviles et al.(2021) observed metal dissolution from oxides in root exudates after six days of contact. Moreover, organic ligands may be adsorbed on the particle surface affecting aggregation. In addition, the agglomeration of metal oxide NPs, such as citrate-coated NPs, greatly reduces their movement in soils (Yang et al. 2022)

then reducing the NPs' migration to the subsoil, but investigation related to this topic is needed. Our work focused to assess the dissolution kinetic of $CoFe_2O_4$ NPs in soil solution and ARE as part of NP characterization and to know if they could be used as a Fe source for plants. Furthermore, the pH, ionic strength, and concentration of Ca^{2+} in soil solution affected the stability and dissolution of NPs. It has been observed that high ionic strength induces NP agglomeration due to the Van der Waals forces (attractive forces) being dominant (Kookana et al. 2014; Elhaj Baddar et al. 2019; Shrestha et al. 2020). For example, in ZnO NPs suspended in river water (pH 4-10), at any given pH, an increase in ionic strength (from 0.005 to 0.1 M) resulted in a less stable colloidal system (Domingos et al. 2013). Meanwhile, the high Ca^{2+} concentration in ion solution could act as a destabilizing agent (OECD 2020).

1.5.5. Modeling NPs dissolution in soil solution and ARE

The dissolution rate of a nanomaterial is recognized as a key parameter to understanding its environmental fate, persistence, and bioavailability (OECD 2020). From the fertility point of view, the nutrient release profile and rate are critical. The ideal fertilization pattern should coincide with the sigmoidal crop nutrient uptake pattern (Jange et al. 2021). The release of Co, from the NPs by the effect of soil solution and ARE fits the pseudo-second-order model (R^2 adjusted-soil solution pH 5, 7, and 8= 0.989, 0.798,0.861; R^2 adjusted-ARE= 0.981), in contrast to what has been observed in other nanomaterials that follow a first-order kinetic dissolution model (Lee et al. 2012; Misra et al. 2014; Vencalek et al. 2016; OECD 2020). On the one hand, the release mechanism can be assumed to proceed through two steps, surface disintegration followed by a diffusion step (Figure 1.6a). The dissolution process is only a function of solute concentration in the liquid phase irrespective of the solid phase concentration (Kumar et al. 2010). According to Mimmo et al. (2014), low molecular weight compounds in the rhizosphere are in low concentration but are continuously produced by the roots, then, the pseudo-second-order rate model may be used to mimic the Co dissolution.

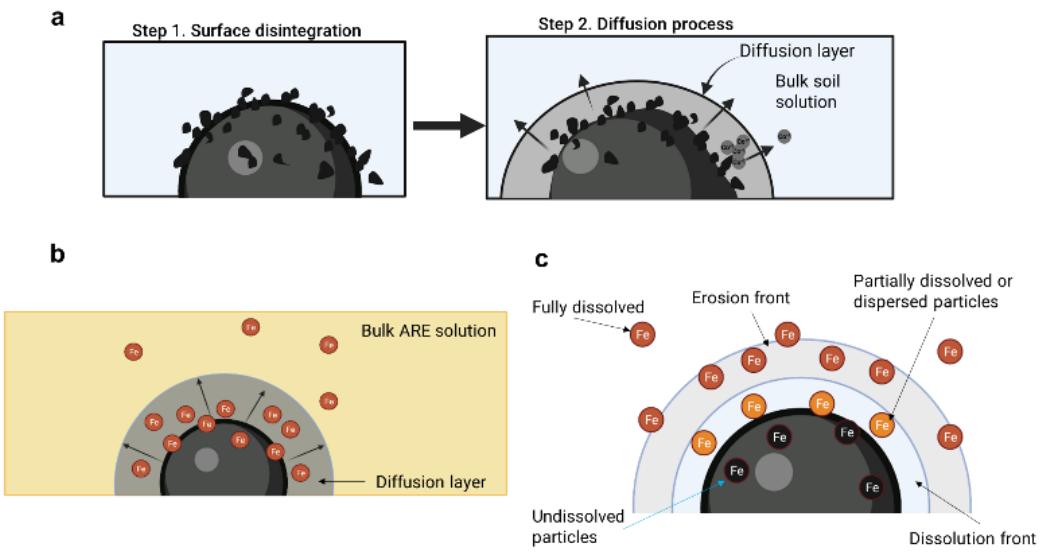

Figure 1.6. Graphic description of a) the pseudo-second-order dissolution model, b) the Higuchi dissolution model and c) the Korsmeyer-Peppas dissolution model to fit the Co and Fe release from citrate-coated $CoFe_2O_4$ NPs by the effect of soil solution and artificial root exudates.

1.6. CONCLUSIONS

The citrate-coated $CoFe_2O_4$ NPs were poorly water-soluble, but their low dissolution was pH-dependent, and their k values decreased with an increase in pH units. These results suggest that $CoFe_2O_4$ NPs are chemically stable in the soil solution and are an insoluble source of Fe and Co, and their release is controlled by the chelate reaction. Therefore, the citrate-coated $CoFe_2O_4$ NPs could be considered as an option for slow bio-release fertilizer that can be used in soils with an acid pH to an alkaline pH. The dissolution of Co from citrate-coated $CoFe_2O_4$ NPs in soil solution and the ARE-solution follows a pseudo-second-order model. In the case of Fe release, the dissolution model by the effect of ARE could be a Korsmeyer-Peppas equation, where the release of Fe is controlled by a diffusion and erosion model.

Our understanding of dissolution rates and mechanisms for citrate-coated NPs would be used to predict the bio durability and potential use of NPs as a soil fertilizer and to assess their lifetime in soil solution. However, as the dissolution is a complex process further experimentation is necessary to include the role of organic matter and the soil microorganisms in the NPs dissolution.

CHAPTER 2. CITRATE-COATED COBALT FERRITE NANOPARTICLES FOR THE NANO-ENABLED BIOFORTIFICATION OF WHEAT

2.1. ABSTRACT

A pot experiment was conducted in an open greenhouse to explore the use of citrate-coated cobalt ferrite nanoparticles ($CoFe_2O_4$ NPs) as a source for Fe fortification of three wheat lines (*Triticum aestivum* L.). Two of the three wheat lines tested differ in their efficiency concerning Zn storage in their grains (efficient and inefficient) and one with inefficient P-absorption. The NPs were supplied by foliar or soil application of Fe at 330 mg L^{-1}, and 46 or 68 mg kg^{-1} soil, respectively. A positive control (Fe-EDTA salt, a conventional iron fertilizer) and a negative control (no fertilization) were also included to compare the efficiency of NPs fertilization. Soil fertilization with NPs improved the grain yield and Fe- concentration in the grains compared to the foliar application of NPs and conventional Fe fertilizer. Application of soil NPs at 68 mg kg^{-1} increased the grain yield by 52% and 21% compared to the control and soil Fe-EDTA treatments, respectively. Likewise, grain Fe concentration increased by 96% and 72% compared to the control and soil Fe-EDTA treatments, respectively. The phytic acid concentration in grains and the phytic acid: Fe ratio decreased by 6% and 62%, respectively, due to the soil application of NPs (68 mg Fe kg^{-1}). The Fe-grain concentration of lines inefficient for Zn storage and P-uptake from plants soil fertilizer with NPs (68 mg Fe kg^{-1}) was 1.37 and 0.26 folds above the target biofortification concentration (60 g Fe kg^{-1}). Cobalt concentration in grains ranged from 9 to 16 mg kg^{-1}. These concentrations were below the maximum allowable limit of Co in grains (50 mg kg^{-1}) recommended by FAO and the WHO. Our results showed that Fe supply as NPs may improve the nutritional quality of wheat grains and economic yield. However, a long way forward to effective and cost-economic use of nanotechnology for wheat nutritional development remains.

Keywords: nutritional security, biofortification, micronutrient deficiency, precision nutrition, slow-bio-release fertilizer, cost-benefit nano-fertilization

2.2. RESUMEN

Un experimento en macetas en un invernadero abierto se realizó para explorar el uso de nanopartículas de $CoFe_2O_4$ recubiertas de citrato como fuente de Fe para biofortificación de tres líneas de trigo diferentes. Dos de las tres líneas de trigo difieren en su eficiencia en el almacenamiento de Zn en el grano (eficiente e ineficiente) y una en la absorción de P (ineficiente). Las NPs se aplicaron de manera foliar o al suelo a 330 mg de Fe L^{-1}, y 46 o 68 mg de Fe kg^{-1} al suelo, respectivamente. También se comparó la eficiencia de las NPs con el fertilizante Fe-EDTA (como testigo positivo). La fertilización al suelo mejoró el rendimiento de grano y la concentración de Fe en grano en comparación con la aplicación foliar de NPs y el fertilizante convencional de Fe. El rendimiento de grano de las plantas aumentó un 52 % y 51 % por la fertilización foliar con NPs y aplicación al suelo de NPs, respectivamente, en comparación con las plantas del tratamiento control. El tratamiento con NPs a 68 mg de Fe kg^{-1} de suelo aumentó la concentración de Fe en los granos en un 96% y 72% más en comparación con el control y el tratamiento con Fe-EDTA en el suelo, respectivamente. Además, la concentración de ácido fítico en los granos y la relación molar ácido fítico: Fe disminuyeron un 6% y un 62%, respectivamente, debido a la aplicación de NPs al suelo (68 mg Fe kg^{-1}). La concentración de Fe en los granos de las líneas ineficientes en almacenar Zn en grano e y absorción de P de las plantas fertilizadas al suelo con NPs (68 mg Fe kg^{-1}) fue 1,37 y 0,26 veces superior a la concentración objetivo de biofortificación (60 g Fe kg^{-1}). Las NPs de ferrita de cobalto recubiertas de citrato podrían considerarse un fertilizante alternativo para la biofortificación con Fe; sin embargo, habría que seguir investigando para asegurarse de que son seguras para los usuarios, el medio ambiente y los consumidores de alimentos.

Palabras clave: seguridad nutricional, biofortificación, deficiencia de micronutrientes, nutrición de precisión, fertilizante de bio-liberación lenta, costo-beneficio

2.3. INTRODUCTION

Iron (Fe) is considered the most essential microelement needed by different organisms because of its role in oxygen and electron transport, deoxyribonucleic acid synthesis, numerous redox reactions, and as a co-factor in enzymes (Abbaspour et al. 2014; Blanco-Rojo and Vaquero 2019). On one hand, Fe deficiency in humans can cause anemia affecting immunity mechanisms and cognitive development (Blanco-Rojo and Vaquero 2019). During pregnancy, Fe deficiency is associated with the risk of sepsis, maternal and perinatal mortality, and low birth weight (Abbaspour et al. 2014). The major causes of Fe deficiency in humans are the intake of inadequate foods that are low in Fe, and poor Fe absorption from diets rich in phytates (WHO 2008), since these compounds have a strong affinity with polyvalent cations (Bloot et al. 2021) especially Fe and Zn, thus decreasing their bioavailability for monogastric animals (Rose et al. 2013; Bilal et al. 2019).

On the other hand, when we talk about malnutrition, soil fertility is directly related to the nutritional quality of food produced (FAO 2022). Fe is abundant in the earth's crust, even though its deficiency in crops has become one of the most widespread abiotic stresses in alkaline and calcareous soils which account for 30% of global land (Rai et al. 2021; Yue et al. 2022). The reason why agricultural soils are Fe deficient, it's the Fe chemistry. In alkaline soils, most of the Fe is in the form of stable ferric hydroxide and carbonate, they are not available to plants (Aciksoz et al. 2011; Colombo et al. 2022). In addition, soluble Fe external sources in contact with oxygen form highly insoluble oxides that are not readily available for plant uptake (Abbaspour et al. 2014).

In this regard, the fortification of cereals can be a strategy to prevent Fe deficiency because they contribute approximately 50-60% of the dietary energy of the world's population (Prasad et al. 2014; Cakmak and Kutman 2018). Meanwhile, wheat is the staple food for 35% of the world's population (Cakmak and Kutman 2018), and its consumption is forecasted to increase by 46% by 2025 (Younas et al. 2020). However, modern wheat varieties are low in proteins and minerals (Murphy et al. 2008) but high in phytate (75-80% of the P content in grains is occurring in the phytate form). The high phytate content in grain affects negatively the grain quality for nutritional purposes (Rose

et al. 2013; Bilal et al. 2019). Nevertheless, a high P content in seeds is desirable to prevent P deficiency in early-growth seedling development (Bilal et al. 2019). Moreover, recent works highlight the role that phytic acid may play in the antioxidant system of plants and in preserving seed vitality (Škarpa et al. 2021; Colombo et al. 2022).

The mineral content of wheat grains can be improved through agronomic biofortification, the development of new genotypes with higher nutrient contents, or post-harvest food fortification (Borrill et al. 2014). The advantage of agronomic biofortification over conventional breeding programs is that it is an economical and short-term solution (Velu et al. 2014; Hassan et al. 2021). Furthermore, it can be a complementary approach to breeding programs (Velu et al. 2014; Solanki and Laura 2018). While post-harvest food fortification has the disadvantage of causing unacceptable sensory changes to foods when highly soluble Fe salts are added (Hurrell 2021), agronomic biofortification remains an option to increase the mineral content in wheat.

Agronomic biofortification is applying fertilizers by foliar spray or to the soil in order to increase the total and bioavailable concentration of micronutrients in the edible plant parts of crops, thus, increasing the dietary intake of a target mineral (de Valença et al. 2017). Biofortification success depends on micronutrient bioavailability, fertilizer chemical properties, formulation, time, and the form in which the fertilizer is applied (Elemike et al. 2019). However, adding or producing Fe-fortified food is the most difficult compared with other micronutrients like Zn (Blanco-Rojo and Vaquero 2019), because Fe is often a growth-limiting factor for plants (Aciksoz et al. 2011). Plant Fe homeostasis is tightly controlled to prevent Fe accumulation where it is not required, thus, the Fe redistribution to edible tissues may be limited (Connorton et al. 2017), and the fortification strategy fails. For example, foliar application of Zn fertilizers in wheat can improve grain Zn concentration by up to 2 or 3-fold, whereas increases in grain Fe concentration do not exceed 36% after foliar spray of $FeSO_4$ or Fe chelates (Aciksoz et al. 2011).

To improve Fe uptake and its translocation from the site of application to edible plant parts, inorganic Fe compounds, and synthetic Fe chelates have been used in a foliar spray, but contradictory results have been obtained. Nevertheless, some studies recommended the use of chelates over inorganic compounds due to their mobility

(Malhotra et al. 2020). In this regard, nanoparticles (NPs), due to their size and properties, could be an alternative to delivering Fe in a controlled and intelligent form. The small size of NPs may allow them to cross biological barriers and diffuse into the plant vascular system. Furthermore, the surface chemistry of NPs can be modified to provide new properties and functionalities to carry a target nutrient in the right place (Lowry et al. 2019). The targeted delivery system of NPs can also minimize the concentration of chemicals applied to crops that pollute the environment (Marzouk et al. 2019). Fe-chelate nano-fertilizers, carbon-coated Fe NPs, Fe_3O_4, and Fe_2O_3 NPs have been tested as Fe fertilizers on wheat plants (Chugh et al. 2022). The results of some studies demonstrate that Fe-NPs improved wheat yield, and protein, carbohydrate, and amino acid contents in wheat grains (Armin and Asgharipour 2011; Bakhtiari et al. 2015; Wang et al. 2019a).

Based on this information, this research aimed to explore the use of citrate-coated $CoFe_2O_4$ nanoparticles as a Fe source for the fortification of wheat. We evaluated the response of three wheat lines to foliar or soil application of iron NPs. Two of the wheat lines differed in their efficiency of Zn storage in the grains and one of P-absorption. We hypothesized that i) the Zn storage efficient line stores more Fe in its grains than the other lines, ii) the foliar application of citrate-coated $CoFe_2O_4$ NPs is more efficient than soil applications, and iii) through the NPs foliar application the target biofortification concentration in wheat grains can be reached compared to the Fe-EDTA fertilization.

2.4. MATERIALS AND METHODS

A pot experiment in an open greenhouse was conducted from April to September 2021. In the case of analytical determinations, for Qa/Qc, the material used was washed in a 0.25 M HCl solution to remove any traces of contaminating materials. All the reagents, enzymes, and bile salts used were of analytical grade (JT Baker, Merck, and Sigma Aldrich). All the determinations were carried out in triplicate. Standard solutions were prepared using certificated stock solutions.

2.4.1. Wheat lines

Spring wheat (*Triticum aestivum* L.) seeds were kindly provided by the International Maize and Wheat Improvement Center (CIMMYT, México). AF1104 is a line

efficient for Zn storage in the grains, whereas AF1116 is inefficient. On the other hand, MULTIAF2 is a P-uptake inefficient line.

2.4.2. Nanoparticle synthesis and properties

Citrate-coated $CoFe_2O_4$ NPs were synthesized by the coprecipitation method. Eight mL of $Fe(NO_3)_3$ 9 H_2O 1 M and 4 mL $Co(NO_3)_2$ 6 H_2O 1 M dissolved in 2M HCl solution were mixed. Sodium hydroxide 1.5 M (38 mL) was added dropwise to the mix of Fe and Co solution. The reaction mixture was stirred for one h at 80 °C. The product was then cooled to room temperature and washed three times with distilled water. The precipitate was mixed with 50 mL of sodium citrate four mM solution and heated for 30 min at 80 °C on continuous stirring. The NPs were rinsed with deionized water until the pH of the supernatant was 6.5-7.0 and suspended in deionized water. Table S1 presents the NPs characterization data.

2.4.3. Soil properties

The soil used in this experiment was clay soil, which was collected from the surface layer of the experimental field of Colegio de Postgraduados (19°30’ N, 98°51’ W). The soil was air-dried for at least 1 week in the shadow and sieved to <2 mm to remove debris. Soil pH and electrical conductivity were measured in soil samples in a 1:2.5 soil: water ratio slurry with a pH-meter (A420, Orion) and conductivity meter (24 h after equilibrium; Cl3, Conductronic), respectively. The organic matter content in the soil was performed by the Walkey and Black (1934) method described by Nelson and Sommers (1996), and the bioavailable micronutrient concentration was determined by the DTPA-TEA-$CaCl_2$ method.(Lindsay and Norvell 1978) The total nitrogen (Bremner 2016a) and inorganic nitrogen (Bremner 2016b) concentrations were assessed according to the Kjeldahl method. The relative bioavailability of inorganic P was determined by the Olsen method (Olsen and Sommers 1982). The concentration of exchangeable cations (Ca^{2+}, Mg^{2+}, Na^{+}, and K^{+}) was determined by the ammonium acetate extraction method(Chapman 2016) and atomic absorption spectroscopy (Perkin Elmer, model 3110), and flame photometry (Jenway, PFP7). Table S2 summarized the properties of the soil.

2.4.4. Experimental design

The experiment was set up in a completely randomized experimental design with six treatments and three replicates each. The treatments were:

1) control without application of NPs (negative control)

2) soil application of Fe-EDTA at 46 mg Fe kg^{-1} (positive control)

3) soil application of NPs at 46 mg Fe kg^{-1} (equivalent to 98 mg NPs kg^{-1})

4) soil application of NPs at 68 mg Fe kg^{-1} (equivalent to 145 mg NPs kg^{-1})

5) foliar application of Fe-EDTA at 330 mg Fe L^{-1} (equivalent to 0.25 % w/v, positive control),

6) foliar application of NPs at 330 mg Fe L^{-1} (equivalent to 0.07% w/v).

We tried to follow the 4R approach (right source, right rate, right time, and right place) when the experiment was designed, which means that the concentration of the rate of soil applications was chosen based on a Fe-fixation test (Table S3). From that test, we found that after the application of 45-68 mg Fe kg^{-1} (as iron sulfate), the Fe DTPA extractable was 9 -13 mg Fe kg^{-1}, reaching an adequate concentration of Fe in soil according to the Mexican norm for soil fertility NOM-021-RECNAT-2000(SEMARNAT 2000).

2.4.5. $CoFe_2O_4$ NPs and Fe-EDTA application to soil

The dried NPs were applied before seed sowing. The respective amount of citrate-coated $CoFe_2O_4$ NPs was weighed and added to the soil. The mixture of soil and NPs was homogenized in a cement mixer for one h. Fe-EDTA fertilizer (TradeCorp®) was used to compare the effect of $CoFe_2O_4$ NPs on the fortification of wheat. The corresponding amount of Fe-EDTA was diluted in 500 L of water and added to the soil before sowing seeds.

2.4.6. $CoFe_2O_4$ suspension preparation and their application for foliar spray

A $CoFe_2O_4$ NPs suspension at 330 mg Fe L^{-1} concentration was prepared in deionized water and sonicated with an ultrasonic probe for 2 min at 130 W and 90% amplitude. Four foliar spray applications were done. The first foliar application was done when half of the inflorescence emerged (Zadoks' scale 5.5), the second one, when the inflorescence completely emerged (Zadoks' scale 5.9), the third one at the beginning of anthesis (Zadoks' scale 6.0), and the last one at the milk development (Zadoks' scale 7.3). A volume of 10 mL of $CoFe_2O_4$ NPs suspension per pot was evenly sprayed (at the end of the experiment a total of 13.2 mg of Fe per pot were supplied). To avoid the entry of NPs into the substrate, the pot's upper surface was covered with a plastic bag and the foliar spraying was done carefully with a manual sprayer by spraying continued until the volume of 10 mL runoff. A similar protocol of application was performed for the foliar spray of Fe-EDTA solution at 330 mg Fe L^{-1}. The spray was realized during sunrise.

2.4.7. Growth conditions and plant management

Wheat seeds were soaked for 5 min in a 3% (v/v) NaClO solution to disinfect the seeds' surface. The seeds were then rinsed 5 times with abundant sterile distilled water. The floating seeds were discarded.(López-Luna et al. 2020) Ten disinfested seeds were sown at 1 cm depth in a pot containing 8 kg of soil. After emergence, eight seedlings were kept per pot. The plants were grown in an open greenhouse at an average temperature of 19.4 °C (27 °C max temperature and 12 °C low temperature) and humidity of 68%. Plants were watered daily at ~60% of their field moisture capacity. A recommended dose of N (80 kg N ha^{-1}) was applied 15 days after the emergence.

2.4.8. Evaluation of physiological traits

The plant height was measured when plants reached the Zadoks' scale 7.3 growth state. Samples of the flag leaves were collected 48 h after the last foliar fertilization and prepared for photosynthetic pigments extraction and analysis of stress markers (H_2O_2 and proline). The determination of photosynthetic pigments was performed according to Lichtenthaler (Lichtenthaler 1987). For the extraction, circles of 5 mm diameter were placed into 5 mL acetone 80% (v/v) and incubated in darkness at 4°C for 72 h. The

absorbance of extracts was measured at 470, 646.8, and 663.2 nm wavelengths. The H_2O_2 concentration in leaves was performed according to Velikova et al. (2000). For the extraction, 150 mg of fresh tissue was macerated with 5 mL of trichloroacetic acid solution 0.1% (w/v). The extract was centrifuged at 1200 rpm for 10 min. Then, 0.5 mL of the supernatant was mixed with 0.5 mL 10 mM potassium phosphate buffer (pH 7), and 1 mL of KI 1M solution. The absorbance of the reaction mixture was measured at 390 nm (Varian Cary 50 Scan UV-Vis), and the concentration of H_2O_2 was calculated by calibrating the curve function from 15 to 70 µM H_2O_2. The proline concentration was conducted according to the method described by Carillo et al. (2008) and Gibon et al. (2000). For the extraction, 150 mg of macerated fresh tissue was mixed with 2 mL of ethanol 40% (v/v) solution, and incubated overnight at 4 °C. The extract was then centrifuged at 1200 rpm for 5 min. A 100 µL aliquot of the extract was mixed with 1 mL of 1% (w/v) solution of ninhydrin in 60% (v/v) acetic acid. The reaction mixture was then heated at 95 °C for 20 min. After cooling at room temperature, the chromophore was extracted with 3 mL of toluene. The absorbance of the upper phase was measured at 520 nm (Varian Cary 50 Scan UV-Vis). The proline concentration was calculated through a calibrating curve function from 2 to 50 µM.

2.4.9. Evaluation of agronomic components

At the harvest, the yield components determined were biological yield (plant biomass), grain yield per pot, number of spikes per pot, number of grains per pot, and 1000 grains weight. The harvest index was calculated as the ratio of grain yield to biological yield (Ghafari and Razmjoo 2015).

2.4.10. Nutritional quality in wheat grains

The wheat grains nutritional quality involved various analyses such as elemental analysis, biofortification, soluble Fe and Zn, phytic acid analysis, phytic acid: Fe and Zn molar ratios, nutrients bioaccessibility, protein content, and soluble sugars and free amino acids. Elemental analysis in plant tissues was also analyzed.

Grain samples and aerial parts were ground into powder and acid digested. Elemental analysis was performed using atomic absorption by the flame method (Perkin Elmer,

model 3110). Meanwhile, the P concentration in grains was performed by the vanadomolybdo phosphoric acid colorimetric method (Kitson and Mellon 1944). The degree of biofortification was expressed as a percentage, and it was calculated according to the following formula (Dolijanović et al. 2022):

$$\text{Degree of biofortification} = \left(\frac{\text{FeF} * 100}{\text{FeC}}\right) - 100$$

Where: FeF: Fe content in grains from plants fertilized; FeC: Fe content in grains from control plants.

For soluble Fe and Zn in grains, samples of 500 mg of ground wheat grain were extracted with 25 mL of Tris HCl buffer (50 mM, pH 7.5) in Falcon tubes by shaking at 120 oscillations per min for 18 h at 37 °C. Afterward, the samples were centrifuged at 13 000 rpm for 10 min. The supernatant was filtered through a 0.2 µm membrane filter and stored until its analysis (Eagling et al. 2014). Elemental analysis was performed using atomic absorption by the flame method (Perkin Elmer, model 3110).

The phytic acid determination was performed by the modified colorimetric Wade reagent method (Gao et al. 2007). For the extraction, a sample of 0.5 g of powdered grain was mixed with 10 mL of 2.4% HCl solution (v/v) in a Falcon tube and agitated at 220 rpm for 16 h. The acid extract was centrifuged at 3000 rpm at 10 °C for 20 min. The supernatant was transferred to a Falcon tube containing 1 g NaCl and shaken at 350 rpm for 20 min. The mixture was then allowed to settle at 4 °C for 60 min. The mixture was then centrifuged at 3000 rpm at 10 °C for 20 min. One mL of supernatant was diluted 25 times in a centrifuge tube with deionized water. Three mL of this diluted sample was combined with one mL of modified Wade reagent (0.03% $FeCl_3$ $6H_2O$ + 0.3% sulfosalicylic acid), one mL of deionized water. The reaction mixture was vortexed for 30 s and centrifuged. The absorbance of the reaction mixture was measured at 500 nm after 15 min on a spectrophotometer (Varian, Cary 50 Scan UV-Vis). The concentration of phytic acid in the extract was estimated using a calibration curve of sodium phytate from 3 to 48 mg L^{-1}. After the interpolation with a standard curve of phytic acid, the result obtained was multiplied by 0.282 to express the content of phytate phosphorus in the sample because

this constant corresponds to the molar ratio of P in the phytic acid molecule (Naves et al. 2014).

The relative bioavailability of Fe and Zn in the grains was estimated by the molar ratios of phytate: Fe (Phy: Fe), and Phy: Zn. The concentrations of phytic acid, Fe, and Zn were converted into moles by dividing their respective molar mass and atomic weights. The molecular weight of the phytate used was 660.04 g mol^{-1}, and the atomic weights 55.84 g Fe mol^{-1} and 65.38 g Zn mol^{-1} were used (Magallanes-López et al. 2017; Castro-Alba et al. 2019).

The Fe, Zn, Cu, Se, and P *in-vitro* bioaccessibility was measured by the digestion method according to the INFOGEST protocol (Brodkorb et al. 2019). For this test, we analyzed the grains obtained from the AF116 and MULTIAF2 lines that were soil fertilized with NPs at 68 mg Fe kg^{-1}. Those treatments showed the highest Fe concentration in grain and low phytic acid-Fe molar ratio. Grains from the control, Fe-EDTA soil fertilization, and local commercial wheat grains (From Texcoco local market) were analyzed as well, to compare the mineral bioaccessibility. A sample of 5 g of whole grain was boiled at 95 ± 5 °C with drinking water with a ratio of 1:12 (w:w grain:water) until wheat grains were soft. Through the extraction procedure, the temperature was kept at 37 ± 2 °C, and constant mixing conditions were obtained by placing the tubes in an orbital incubator at speed of 55 rpm. The proportion of electrolytic stock solutions, enzymes, bile salts, and Ca^{2+} that were added in each extraction phase is detailed in the supplementary information (Table S4). The mastication process was simulated by placing a sample of soft wheat grain and 5 mL of simulated saliva fluid (SSF), in a manual mincer. The grains were minced to a paste with a similar consistency to the mustard. The swallowable bolus was then incubated for 2 min at 37± 2 °C. Afterward, the bolus (from the oral phase) was mixed with simulated gastric fluid (SGF), and the pH of the sample was adjusted to pH 3 with HCl 5 M solution. Distilled water was added to the sample to obtain a final ratio of food to SGF of 1:1 (v/v). The tubes containing the sample were incubated for 2 h. For Fe bioaccessibility in the gastric phase, the samples were centrifuged at 4000 rpm for 5 min, and the supernatant was filtered through a 0.2 µm nylon membrane filter. The filtrates were then placed in boiling water for 5 min, to stop the digestion reaction and freeze for

further analysis. On the other hand, the gastric chyme was mixed with simulated intestinal fluids (SIF) to achieve a final ratio of 1:1 (v/v). The pH of the mix of gastric chyme and SIF was adjusted to 7, and the mixture was then incubated for two h. Finally, the digestion mixture was centrifuged at 4000 rpm for 5 min. The supernatant was filtrated through a 0.2 µm nylon micro filter. The elemental analysis was done within 24 h by ICP-MS (ICP-OES, Agilent 725-ES).

The protein concentration of wheat grains was determined using the Kjeldahl method. An aliquot of 5 mL of the acid-digested grain sample was mixed with 30 mL of distilled water, and 20 mL of NaOH. The sample was distilled and titrated with 0.01 N H_2SO_4 solution (Suzanne N.S. 2010). The protein content was calculated by multiplying the amount of total nitrogen with the conversion factor of 6.25 which assumes the nitrogen content of proteins in foodstuffs is 16% (Mariotti et al. 2008).

Soluble sugars and free amino acids were analyzed in a 50 mg sample of powdered wheat grains and extracted with 2 mL of ethanol 80% (v/v) in a water bath at 80°C for 40 min. The extract was then cooled and centrifuged at 13,000 rpm for 10 min. The supernatant was kept at 4 °C until its analysis, and it was used to determine the concentrations of both soluble sugars and free amino acids. The concentration of soluble sugars (glucose, fructose, sucrose) was determined using an enzymatic method, through a microplate reader assay (Viola and Davies 1992), while the free amino acids concentration was determined following the method described by Jones et al. (2002).

2.4.11. Iron and zinc distribution in wheat grains

Iron distribution in wheat grains was determined by Perls' Prussian blue staining. It is a rapid method to screen iron distribution in grains (Velu et al. 2008). Dry wheat seed samples were placed for one h in deionized water before excision. Dissected wheat seeds were rinsed with deionized water and stained for 45 min with a Prussian blue solution of 2% (w/v) potassium hexacyanoferrate (II) and 2% (v/v) hydrochloric acid (1:1). Stained seeds were then rinsed with deionized water and dried with tissue paper. The samples were mounted on a microscope slide and qualitatively analyzed using a reflectance light

microscope (Carl Zeiss Stereo V20), and pictures were taken with a digital camera Canon 5D.

Zinc distribution in wheat grains was performed in dissected wheat seeds, which were stained for 30 min in a diphenyl thiocarbazone solution (concentration 500 mg L^{-1} in methanol). Then, the stained seeds were rinsed thoroughly in water and gently dried with tissue paper (Ozturk et al. 2006). The samples were mounted on a microscope slide and analyzed as described in the above section.

2.4.12. NPs localization in wheat foliar tissues

The localization of NPs on the leaf surface was done by environmental scanning electron microscope (ESEM; Carl Zeiss EVO LS10, Jena, Germany) and an x-ray detector (EDX; Bruker, Quantax 200, Germany). Dried flag leaf samples from the control and NPs foliar sprayed plants were mounted on double-sided carbon conductive tape and observed with an acceleration voltage of 30 kV, a pressure of 80 Pa of water vapor, a backscattered electron detector, and the x-ray mapping technique, a non-destructive method that uses colors to represent the spatial distribution of chemical elements on a photomicrograph captured with an electron microscope.

In addition, hyperspectral darkfield microscopy-enhanced (HDFM) imaging was also performed. The flag leaf samples from the control and NPs foliar sprayed plants were washed with tap water and then twice with distilled water. The excess water was removed with the help of paper tissue. Next, a sample of 4 cm^2 was fixed in FAA solution (Formaldehyde: Alcohol: Acetic acid, 10%:50%:5% +35% water) for 48 h at 4 °C. The samples were then washed with distilled water for 15 min and preserved in 50% ethanol solution (v/v). Shoot transverse sections (30-50 µm) were then made with a manual microtome. All samples were analyzed using the CytoViva Enhanced Darkfield Hyperspectral Microscope system. The hyperspectral data were collected from 400 to 1000 nm and analyzed by the ENVI 4.8 (Harris) software. All samples were imaged with a 60x oil immersion objective. The spectral library of the citrate-coated $CoFe_2O_4$ NPs (Figure S1) was used to identify positive $CoFe_2O_4$ NPs spectra in all the exposed leaf sections. The Spectral Angle Mapping algorithm (SAM) was used to identify these spectra

in the samples. Any pixel that contained these spectra from the filtered library was pseudo-colored RED.

2.4.13. Nutrient/fertilizer use efficiency measurements

The use/efficiency-related attributes (or nutrient efficiency measures) were calculated by following equations (Fixen et al. 2015; Akram et al. 2020):

$$\text{Partial factor productivity (PFP, kg g}^{-1}) = \frac{\text{Units of crop yield (kg)}}{\text{Unit of nutrient applied (g)}}$$

$$\text{Agronomic efficiency (AE, kg g}^{-1}) = \text{GY}_\text{f} - \frac{\text{GY}_\text{c}}{\text{N}_\text{ap}}$$

$$\text{Apparent nutrient recovery efficiency (ARE, \%)} = \frac{\text{N}_\text{f} - \text{N}_\text{C}}{\text{N}_\text{af}} \times 100\%$$

$$\text{Physiological efficiency (PE, kg g}^{-1}) = \frac{\text{BY}_\text{f} - \text{BY}_\text{c}}{\text{TAc}_\text{f} - \text{TAc}_\text{c}}$$

Where: GY_f: grain yield treated pots with NPs or Fe-EDTA; GY_c: grain yield of control pots; N_{ap}: Quantity of Fe applied as NPs or Fe-EDTA; BY_f: biomass yield from NPs or Fe-EDTA treated pots; BY_c: biomass yield from control pots; TAc_f: Total Fe accumulation from NPs or Fe-EDTA treated pots; TAc_c: total Fe accumulation in control; Nf: nutrient uptake from NPs or Fe-EDTA treated pots in straw and grain; Nc: nutrient uptake from control pots in straw and grain.

2.4.14. Economic evaluation

The economic analysis was performed using the following economic indicators (Sarwar et al. 2007; Dhaliwal et al. 2022a):

$$\text{Gross income} = \text{yield (t ha}^{-1}) \times \text{grain price}$$

$$\text{Profitable return(PR)} = \text{gross income} - \text{total production cost}$$

$$\text{PR over control} = \text{PR} - \text{control treatments}$$

$$\text{Cost} - \text{benefit ratio (CBR)} = \frac{\text{PR over control}}{\text{Total production cost}}$$

$$\text{Investment factor (IF)} = \frac{\text{Gross income}}{\text{Total production cost}}$$

To estimate the gross income the guaranteed price of bread wheat in 2021 in Mexico (MXN 6400 t^{-1}) (SADER 2022) was used. To report the economic indicators in terms of USD, the exchange rate used was 19.96 MXN/USD (International Monetary Fund 2021), which was an average of the exchange rates between 1 and 15 September 2021. In the case of the cost of sowing, irrigation, pest control, harvesting, commercialization, labor costs, and other costs, the data of the top three Mexican states producing wheat was applied based on the statistics of the Trust Funds for Rural Development (FIRA in Spanish, and for more details see Table S5). The cost of NPs production at the laboratory scale (Table S6) was calculated and the market price of cobalt ferrite NPs was used as the cost of fertilization.

2.4.15. Data analysis

The data were analyzed with the statistical software R version 4.0.3 (R Core Team 2020). The verification of compliance with the assumptions of normality and homogeneity of variances was performed through Shapiro's and Bartlett's tests, respectively. Data that did not comply with the assumptions (normality and homogeneity of variance) were transformed using the log (H_2O_2 concentration in the leaves, Fe and Zn concentration in the SIF), square root (proline leave concentration), and box cox (iron concentration in grain) transformation. An analysis of variance was then performed to detect that at least one of the treatments was different (α=0.05). To detect differences between treatments the Tukey honest significant difference test was performed (α=0.05). The Wilcoxon rank-sum test and the post hoc Bonferroni test were also used to compare the grain yield by the effect of treatment, data of degree of biofortification, and nutrient efficiency measurements. The existence of correlations between variables was also verified and principal component analysis (PCA) was carried out to detect trends present. A hierarchical cluster analysis was carried out to explore similarities between the lines, and the distant matrix was computed by the Euclidian method.

2.5. RESULTS AND DISCUSSION

2.5.1. Effect of NPs fertilization on the physiological and agronomic traits

The three wheat lines differ significantly in their physiological and agronomic traits. In general, the AF1104 and AF1116 lines showed similar responses (Figures 2.1, and 3.2a, b, f), and the MULTIAF2 line was segregated from them. The AF1104 line (Zn grain-storage efficient) was characterized by taller plants, high harvest index, grain yield, nutrient efficient ratio (NER), phytic: Fe molar ratio, and having the heaviest seeds compared to the other lines (53±5 g for thousand kernels; Figure 2.1a). The AF1116 line (Zn-grain storage inefficient) was featured by taller plants, high harvest index, SPAD units, and heavy seeds (50±3 g weight of thousand kernels). The MULTIAF2 line (P-uptake inefficient) showed the highest biological yield, numbers of tillers, spikes, and grains; a low NER, and lightweight seeds (38±4 g for thousand kernels Figure 2.1a and 3.2 a-d). Moreover, the kernels of the AF1104 and AF116 lines were similar. The grains of both lines were yellow, with an average length of 6.45±0.7 mm and width of 3.2±0.5 mm. In contrast, the kernels of the MULTIAF2 line were red-light in color, short, and thinner (5.7± 0.6 mm length and 2.7± 0.4 mm width) compared to those of the AF1104 and AF1116 lines (Figure 2.1a).

No remarkable effects were observed on the physiological traits of wheat plants at the flowering stage (Table 2.1) by the addition of NPs compared to the control treatment (without fertilization) and the fertilization treatments with Fe-EDTA. In contrast, at the end of the experiment, significantly higher grain yields compared to the control treatment were obtained after soil NPs fertilization at 68 mg Fe kg^{-1} and foliar fertilization with NPs and Fe-EDTA (Table 2.2). The results of the foliar treatments agree with those reported by Bakhtiari et al. (2015) They evaluated the responses of wheat growth, yield, and quality after the foliar application of Fe NPs (the authors did not provide any information about NPs features). They found that the foliar application of Fe NPs at 0.03 and 0.04 % (w/v) increased the biological and grain yield by 6-7% and 11-14% compared to the control treatment (without fertilization). Al-juthery et al. (2019) also studied the responses of wheat plants to foliar application of Fe NPs only or in combination with Zn and Co NPs. The experiment was carried out on loam soil with a pH of 7.7. The authors found an

enhancement in grain yield (8.9% to 28.5%) by Fe NPs application (single or in combination) compared to the control.

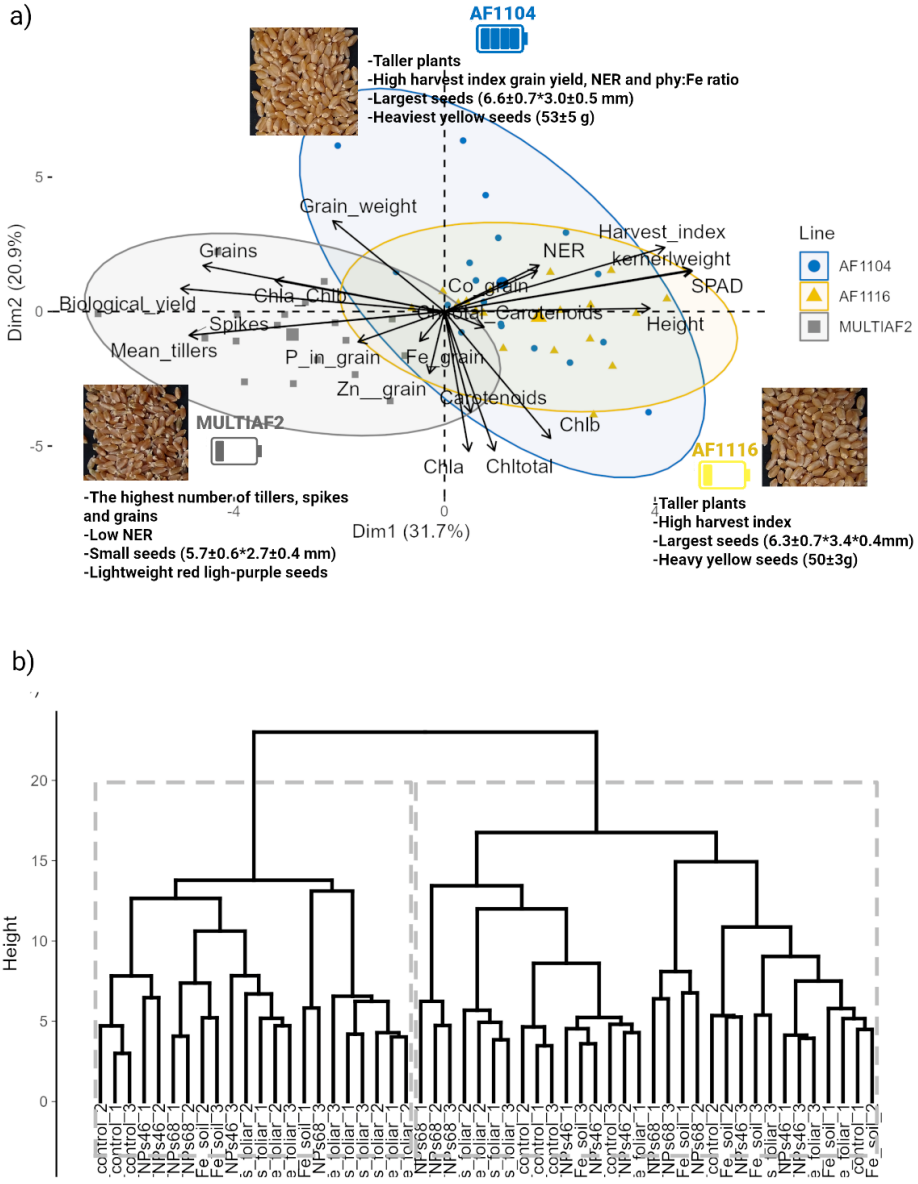

Figure 2.1. Principal component analysis (PCA) and dendrogram clustering of the response variables evaluated on wheat lines to the application of citrate-coated $CoFe_2O_4$ NPs, and Fe-EDTA salt by soil or foliar application. a) PCA biplot showing the loading and the scores of the physiological and agronomic variables evaluated in wheat plants fertilized with NPs or Fe-EDTA. b) Hierarchical cluster dendrogram.

Table 2.1. Physiological traits of wheat plants (at the flowering stage) treated with citrate-coated $CoFe_2O_4$ NPs and Fe-EDTA salt by soil or foliar applications.

Application	Treatment	Plant height (cm)	Chla	Chlb	Chlt	Caro	Chla/b ratio	Chlt/Caro ratio	H_2O_2	Proline
			($\mu g\ cm^{-2}$)						($\mu mol\ g^{-1}$)	
Soil	Control	64.5±10	47.4±11.9 ab	17.5±5.3 a	65.0±16.9 ab	12.2±2.1 a	2.7±0.3	5.3±0.9	2.9±1.3 b	1.8±0.5 a
	Fe-EDTA	65.6±8.6	49.9±7.4 ab	18.7±3.3 a	68.6±10.0 ab	11.3±2.3 a	2.7±0.3	6.2±1.0	3.4±0.7 ab	2.4±1.1 a
	NPs 46	64.4±6.6	51.2±9.0 a	19.1±3.9 a	70.3±12.5 a	12.1±2.9 a	2.7±0.3	5.9±1.0	3.0±1.2 b	1.5±0.8 a
	NPs 68	60.3±4.9	39.1±13.3 b	14.3±5.3 a	53.4±18.5 b	8.7±3.1 a	2.8±0.4	6.2±0.7	3.2±1.3 ab	0.6±0.2 b
Foliar	Fe-EDTA	63.7±8.7	43.7±6.4 ab	15.0±3.0 a	58.7±8.7 ab	10.6±2.0 a	3.0±0.4	5.6±1.1	3.4±1.2 ab	2.3±0.9 a
	NPs	62.9±4.3	40.6±7.8 ab	14.5±2.9 a	55±10.1 ab	11.8±4.0 a	2.8±0.4	5.1±1.7	4.2±1.1 a	2.2±1.4 a

Mean ± standard deviation of n=3. Different letters represent significant differences between treatments (Tukey α=0.05)
NPs, nanoparticles; Chla,b or t chlorophyll a, b, or total, Caro, carotenoids

Table 2.2. Agronomic traits of wheat plants treated with citrate-coated $CoFe_2O_4$ NPs and Fe-EDTA salt by soil or foliar applications.

		Treatment	Mean tillers per plant	Spikes number per pot	Biological yield per pot (g)	Grains number per pot	Grain yield per pot (g)	Thousand kernel weight (g)	Harvest index (%)
Application	Soil	Control	4±2 c	32± 13 c	89±28 c	796±223 b	39±7.3 c	50±7.4 a	45±8.5 ab
		Fe-EDTA	5±2 abc	43±17 abc	120±41 ab	1012±320 ab	48±8.1 bc	50±9.5 a	43±9.6 ab
		NPs 46	5±1 bc	41±8 bc	99±22 bc	875±220 b	41±13.5 c	47±7.6 ab	42±9.7 b
		NPs 68	5±2 bc	39±13 bc	124±27 ab	1219±270 a	59±17.4 a	48±6.1 a	48±11.2 a
	Foliar	Fe-EDTA	7±2 a	55±17 a	130±34 a	1251±381 a	51±6.6 ab	43±7.6 b	41±7.4 b
		NPs	6±2 ab	45±15 ab	118±34 abc	1149±245 a	52±5.2 ab	46±6.8 ab	46±8.7 ab

Mean ± standard deviation of n=3. Different letters represent significant differences between treatments (Tukey α=0.05)

When comparing the effect of NPs application (Figure 2.2), in the case of the AF1104 line, fertilization with NPs had no significant effect on the numbers of tillers and spikes (Figure 2.2a, b). However, plants fertilized with NPs at 68 mg Fe kg^{-1} had higher grain yield than control plants (Figure 2.2e). Meanwhile, for plants of the AF1116 line, foliar fertilization with NPs increased the numbers of tillers, spikes, and biological yield compared to those in the control treatment. But NPs fertilization did not increase the grain yield compared to that control or Fe-EDTA fertilization. For the MULTIAF2 line, NPs fertilization (soil or foliar) had a similar effect to the control and Fe-EDTA treatments on the agronomic variables (Figure 2.2a, c, d). The improvement of some agronomic variables by the effect of NPs fertilization agrees with the findings observed by the application of other Fe oxide NPs. Al-Amri et al. (2020) evaluated the effects of Fe_2O_3 NPs at 500 mg L^{-1} on the growth of wheat plants. The authors reported an increase in wheat biomass from treatments with Fe_2O_3 NPs despite using a hydroponics system and a short evaluation time. Rostamizadeh et al. (2021) found that supplementing Fe_2O_3 (20-40 nm size) through the irrigation solution at 200-400 mg L^{-1} improved the fresh and dry weights of wheat plants after 21 d. Jhanzab et al. (2022) evaluated the effect on wheat of foliar application of Fe NPs (5 mg NPs $L^{-1)}$ blended with nicotinic acid, tryptophan, and myoinositol. NPs were applied at the tillering growth stage. The chlorophyll concentration (16%), leaf area (59%), plant height (31%), and fresh and dry biomass were significantly higher than for the control treatment (without foliar fertilization).

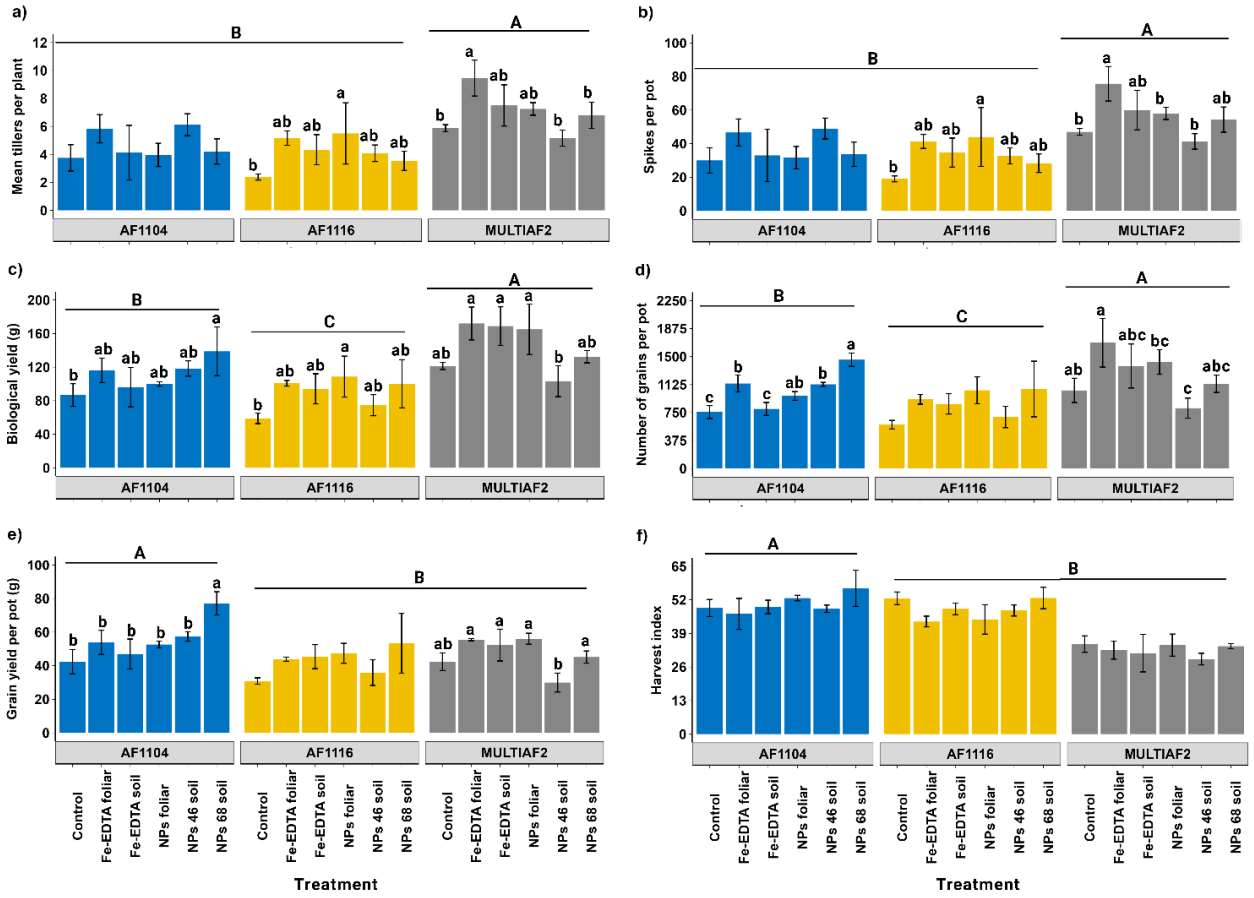

Figure 2.2. Comparison of the agronomic traits of wheat plants treated with citrate-coated $CoFe_2O_4$ NPs and Fe-EDTA salt by soil or foliar applications: a) mean tillers, b) the number of spikes, c) biological yield, d) the number of grains, e) grain yield, and f) harvest index. Different lowercase letters represent significant differences (Tukey α=0.05) between treatments within the line. Capital letters represent significant differences between lines.

2.5.2. Impact of NPs fertilization on the biofortification of wheat grains

Soils are crucial in micronutrient deficiencies and access to more nourishing food because ~95% of our food nutrients come from soils (FAO 2022). The ability of soil to provide nutrients depends on its properties and management, but in the case of micronutrient availability, soil pH and redox potential are the most important. In general, micronutrients are most available in acid-to-neutral soils (Riaz et al. 2020). Therefore, in alkaline soils, micronutrient availability is often an issue. We used moderately alkaline soil (pH 7.71±0.01) with a marginal concentration of Fe (DTPA extraction 3.23±0.31 mg kg^{-1}). Thus, the supply of extra Fe was reasonable. Thereby an increase in grain Fe

concentration was expected. However, knowing the best way to apply NPs to achieve our objective was the question. Biofortification depends on ensuring the availability of micronutrients when the plant requires them. Thus, the mode of fertilization influences the success of agronomic biofortification (Dhaliwal et al. 2022b).

Traditionally, in the case of alkaline soils, foliar fertilization is highly recommended to avoid nutrient losses and to facilitate the mobilization of nutrients (Fageria et al. 2009). Surprisingly, when comparing the effect of the treatments, the grain Fe concentration of plants fertilized with 68 mg Fe kg^{-1} as NPs was significantly higher compared to the Fe concentration in the grains of the control treatment and the foliar fertilization with Fe-EDTA or NPs (Figure 2.3a). For the AF1116 and MULTIAF2 lines, fertilization with NPs at 68 mg Fe kg^{-1} increased grain Fe concentration by 1.37 and 0.26 folds (Figure 2.4a) above the target concentration for biofortification (60 mg kg^{-1}).

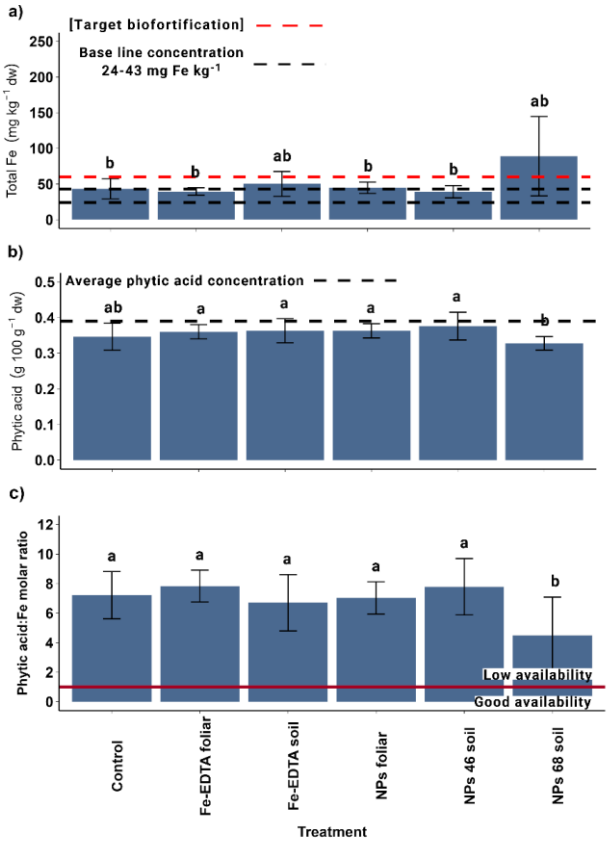

Figure 2.3. Average response of a) Fe grain concentration, b) phytic acid concentration, and c) phytic acid:Fe molar ratios by the effect of type of fertilization of three wheat lines. Different lowercase letters represent significant differences (Tukey α=0.05) between treatments.

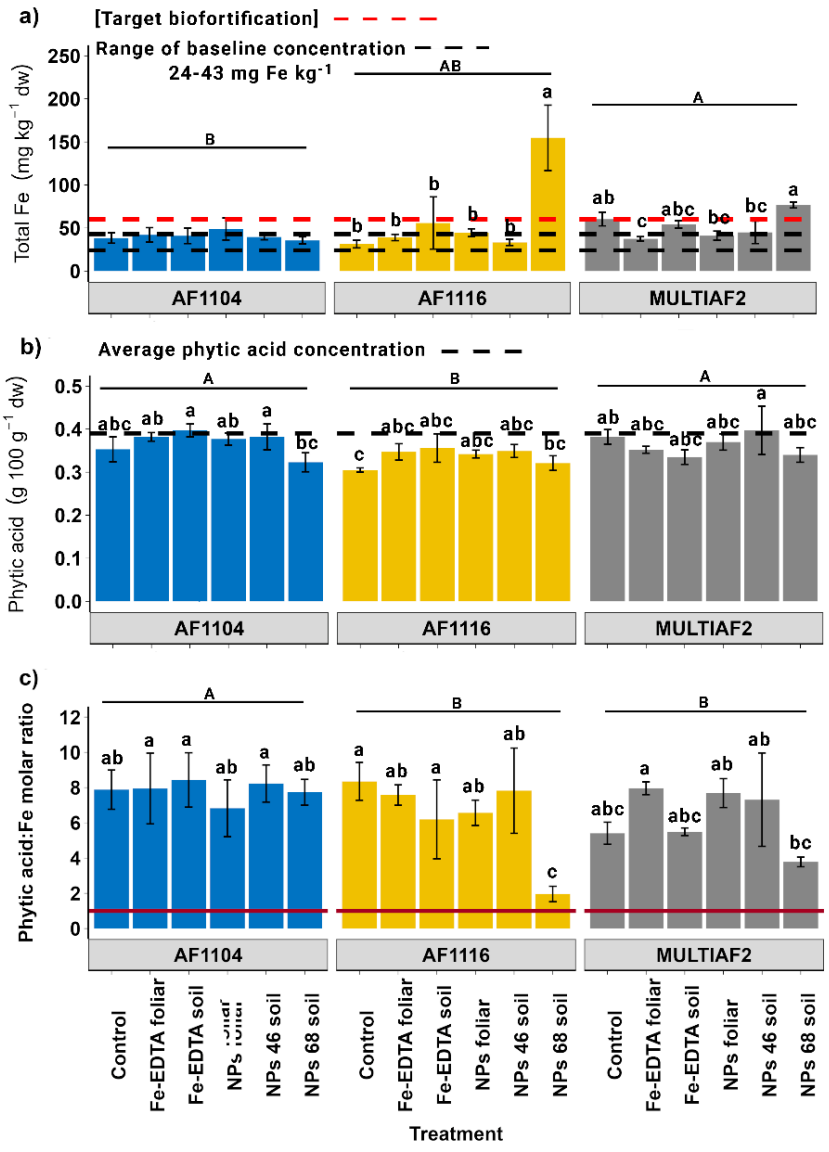

Figure 2.4 The concentration of a) Fe, and b) phytic acid in grains of three wheat lines fertilizers with citrate-coated $CoFe_2O_4$ NPs and Fe-EDTA salt by soil or foliar applications, and their c) phytic acid:Fe molar ratios. Values of the molar ratio of phytic acid:Fe <1 (red line) indicate good Fe availability, preferably values less than 0.5 are required (Castro-Alba et al. 2019). Different lowercase letters represent significant differences (Tukey α=0.05) between treatments within the line. Capital letters represent significant differences between lines.

AF1116 was interesting among the wheat lines because it is an inefficient line to store Zn in its grains, a low concentration of Zn and Fe in grains was expected, as has been reported in other studies. For instance, Hafeez et al.(2021) assessed the agronomic biofortification of two wheat lines that differ in their features. The cultivar Zincol-16 was claimed as a Zn-efficient with low yield potential, while Anaj-17 was considered Zn

inefficient with high-yield potential. Both cultivars were grown in sandy clay loam soil with a pH of 7.5 to 7.7, which was fertilized with Fe at 12 kg ha^{-1} ($FeSO_4$). The cultivar Zncol-16 (Zn-efficient) accumulated more Fe in its grains than Anaj-17 (Zn-inefficient). However, when comparing lines, Fe (Figure 2.4a) and Zn grain (Table 2.3) concentrations of grains of the AF1116 (inefficient) line were not different from those of the grains of the AF1104 (efficient) line. When comparing treatments within the line, the grain Fe concentration of plants fertilized with 68 mg Fe kg^{-1} as NPs was significantly higher than the control (Figure 2.3), and the soil application of Fe-EDTA and foliar application of NPs by 4.5, 2.5, and 3.21 folds, respectively. The degree of biofortification in this line by the NPs application ranged between 6% and 394% over the control (Table S7). Significant differences in the Zn concentration in grains were observed when comparing the type of fertilization. The highest Zn concentration was observed in grains from the plant's soil fertilized with Fe-EDTA (34.77±3.65 mg kg^{-1}). The NPs fertilization (both foliar and soil) did not increase the Zn grain concentration compared to the grains from the control treatment (27.77±2.43 mg kg^{-1}). The interaction between Fe and Zn is complex due to the chemical similarity between their divalent cations and transporter proteins. Antagonists (Rai et al. 2021) and synergistic (Tipu et al. 2022) relationships between Fe and Zn have been documented. However, in wheat Zn-deficient plants, Zn concentration in the growth medium influences the Fe uptake. When an adequate Zn concentration was supplied, higher Fe in shoots was observed than in Zn-sufficient plants (Imtiaz et al. 2003). Inversely, an excess of Zn in the medium may cause a deficiency of Fe (Rai et al. 2021).

In contrast, the null improvement in Fe grain concentration in the AF1104 line compared to the control and the average Fe grain concentration of wheat cultivars (Figure 2.4a), even with the application of Fe-chelate, agrees with the results reported by Aciksoz et al.(Aciksoz et al. 2011) They argued that some gramineous species, like wheat, may not respond to Fe soil fertilization due to adaptive reactions of the roots. Plants with Fe uptake strategy II can overcome the Fe-deficiency conditions by secreting phytosiderophores at a sufficient rate to satisfy their Fe demand.

Table 2.3. Mineral and protein concentration in wheat grains of three different wheat lines fertilized with Fe-EDTA or citrate-coated $CoFe_2O_4$ NPs by soil or foliar applications.

Wheat line	Type application	Treatment	Total mineral concentration (mg kg^{-1})			Soluble mineral (mg kg^{-1})		Protein (%)
			Co	Zn	P	Fe	Zn	
AF1104		Control	14.3±2.2	29.0±2.4 ab	98.4±65.2 b	3.8±1.4	3.2±0.3	11.8±1.3
	Soil application	Fe-EDTA	14.1±2.1	32.6±4.3 a	37.5±14.0 b	3.1± 1.0	3.8±0.3	13.8±1.0
		NPs 46	14.7±2.0	27.1±1.0 ab	290.1±30.1 a	3.3±1.5	4.0±0.5	13.1±1.6
		NPs 68	15.5±1.5	24.1±1.4 b	56.8±12.3 b	3.7±1.2	3.2±0.3	13.2±0.4
	Foliar application	Fe-EDTA	14.2±2.3	26.7±0.7 ab	87.5±71.2 b	4.3±1.5	3.2±0.8	14.0±0.5
		NPs	12.4±1.4	28.1±3.3 ab	285.1±52.3 a	4.2±0.8	3.3±0.3	11.8±1.9
	Mean		14.2±1.9 A	27.9±3.4	142.6±114.5 B	3.7±1.1	3.4±0.5 B	13.0±1.4 B
AF1116		Control	12.7 ± 0.2	25.7±2.5	219.1±20.1	3.0±1.3	4.1±0.3	17.3±1.4
	Soil application	Fe-EDTA	11.4 ± 1.7	35.6±4.5	230.0±27.0	4.3±1.3	4.5±0.5	11.3±3.1
		NPs 46	11.4 ± 0.2	26.3±4.2	251.7±48.0	3.8±2.7	4.2±1.2	13.8±3.5
		NPs 68	10.7 ± 2.0	29.2±9.4	190.0±63.0	4.8±1.9	4.0±1.0	15.6±2.4
	Foliar application	Fe-EDTA	11.7 ± 2.4	31.3±3.1	226.0±28.7	3.2±1.0	4.3±0.3	17.5±1.6
		NPs	15.0± 1.7	34.6±3.1	198.0±15.7	3.2±1.2	5.0±0.9	15.7±1.6
	Mean		12.1±2.0 AB	30.4±5.7	219.1±38.0 A	3.7±1.6	4.4±0.7 A	15.2±3.0 A
MULTIAF2		Control	9.6± 4.1	28.7±1.3 bc	203.0±75.0	1.2±1.1	5.1±0.8 a	14.0±3.5
	Soil application	Fe-EDTA	10.4± 6.5	36.1±2.0 a	64.2±5.0	2.5±1.4	4.5±0.9 a	9.9±0.9
		NPs 46	14.8± 5.0	29.9±2.8 bc	159.5±121.8	3.2±0.8	4.3±0.3 ab	11.3±2.3
		NPs 68	9.0± 3.5	33.2±3.2 ab	233.4±21.0	2.5±0.7	2.8±0.6 bc	9.2±2.1
	Foliar application	Fe-EDTA	9.3±2.0	26.4±0.8 c	263.0±41.4	3.1±1.0	2.6±0.3 c	13.2±1.3
		NPs	13.8±1.1	27.7±0.7 c	118.1±19.4	4.0±1.5	2.7±0.3 c	12.8±1.2
	Mean		11.1±4.2 B	30.3±3.9	176.6±86.7 B	3.2±1.1	3.7±1.1 B	12.0±2.8 B

Mean± standard deviation of n=3. Different lowercase letters represent significant differences (Tukey α=0.05) between treatments within lines. Different capital letters show significant differences between lines.

Despite the drawbacks of soil application of micronutrients in alkaline soils (like higher production cost and environmental challenges due to the misuse and overuse of fertilizers)(Khan et al. 2021a), we decided to test the soil application of NPs because the advantage of applying NPs in the soil is that Fe will become gradually available to the plant due to its slow release. Our earlier results suggested that Fe will eventually release from the NPs by the effects of root exudates(Perea-Velez et al. 2022). In the case of the success of NPs applications in soil, we hypothesize that the wheat plant may utilize Fe from NPs due to the dissolution of NPs by root exudates. Nevertheless, more studies are needed to understand the mechanisms of NPs uptake by plants in complex systems such as soils. Even though research in hydroponic systems(Iannone et al. 2016; Al-Amri et al. 2020) or inert substrates such as sand (López–Luna et al. 2018; López-Luna et al. 2020) demonstrated that iron oxide NPs could be taken up by root plants; the plant-NPs interaction is also highly dependent on the surrounding environment (Perea Vélez et al. 2021).

The increment of the Fe concentration in grains due to the NPs soil application at 68 mg Fe kg^{-1} (Figure 2.3a) was contrary to other studies where the foliar application of iron NPs resulted in higher Fe concentrations compared to the control treatments. For instance, the foliar spraying of nZVI (23.7% Fe) with urea (2% w/v) applied three times (Zadoks 3.1, 4.5, and 6.5) in wheat cultivar “Bezostaja-1” increased the grain Fe concentration from 26.3.0±0.8 (control) to 35.7±0.5 mg kg^{-1} (nZVI+urea), and from 33.1±1.0 to 37.4±0.8 mg kg^{-1}. That field experiment was carried out in two soils, one of them was clay soil with a pH of 7.9, and the other one was clay loam soil with a pH of 7.34 (Taskin and Gunes 2022) The behavior of Fe inside the plant may explain the lack of enrichment of Fe in the grains by foliar applications; for Fe-EDTA fertilization, it must be reduced before moving into the cytoplasm (Rios et al. 2016) for NPs, their absorption does not necessarily mean that they may be translocated to other parts of the plants; it even may be a “dead-end” (Avellan et al. 2021). The possible routes of NPs foliar uptake are the stomata, cuticle, and hydathode pores; among them, the stomata pathway has been described as the principal route (Avellan et al. 2021). After the NPs enter into stomata, their dissolution is expected (Avellan et al. 2021), and Fe ions may then get distributed in the wheat plants, as has been observed with other NPs such as

ZnO.(Deshpande et al. 2017). Our results demonstrated that NPs could be taken up; the HDFM-enhanced images show that NPs were mainly detected in the cuticle and epidermis of the leaf (Figures 2.5b and f). A small number of pixels, located in the palisade cells and phloem, matched with the NPs spectral library (Figures 2.5b-d), indicating the presence of NPs inside the leaf; the ESEM-EDX imaging analysis supported these results. Particle uptake may occur through stomata, Figure 2.6b shows a particle inside the stomatal pore, and EDX mapping analysis shows the presence of Co and Fe in that particle (Figures 2.6b). On the leaf transverse section, agglomerates of particles were also observed; these particles contained Fe and Co (Figures 2.6d-e). However, the fate of the citrate-coated $CoFe_2O_4$ NPs after being taken up by the wheat leaves was beyond the objectives of this research. Future research should be performed to improve the foliar applications of NPs.

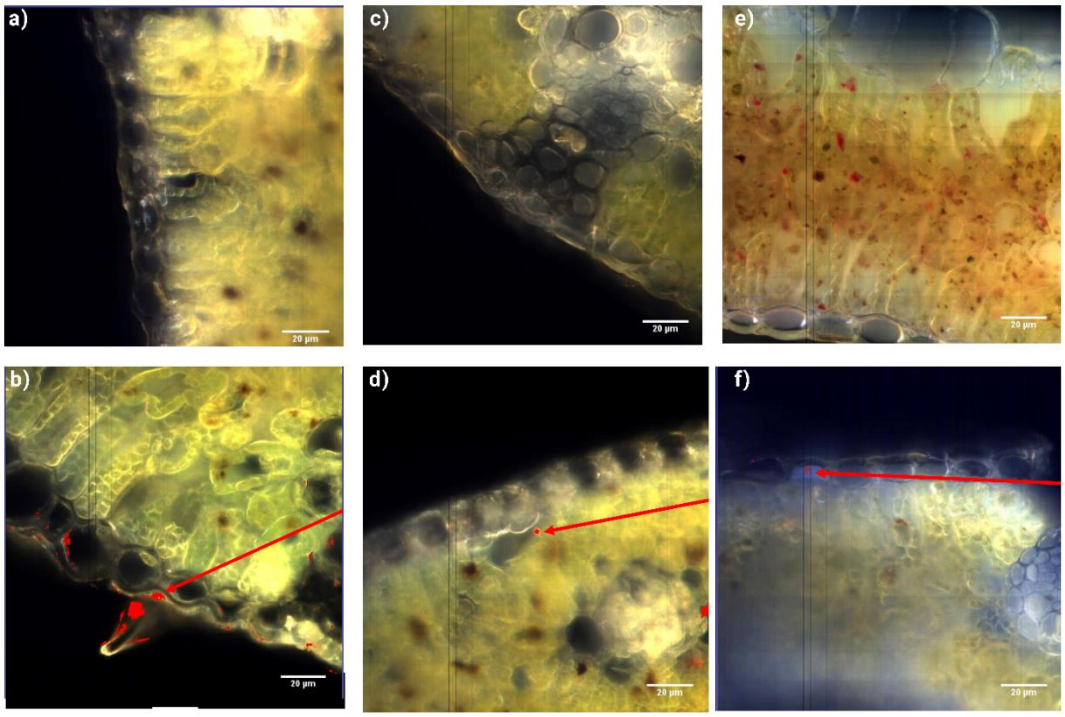

Figure 2.5. Hyperspectral darkfield microscopy (HDFM) enhanced images (60x) of shoot transverse sections of flag leaf of wheat plant foliar fertilized with citrate-coated $CoFe_2O_4$ NPs and their control treatment. Control and leaf exposed to NPs of plants of a, b) line AF1104, c, d) line AF1116, and e, f) line MULTIAF2. The red pixels represent the pixel that matched the spectra of citrate-coated $CoFe_2O_4$ NPs.

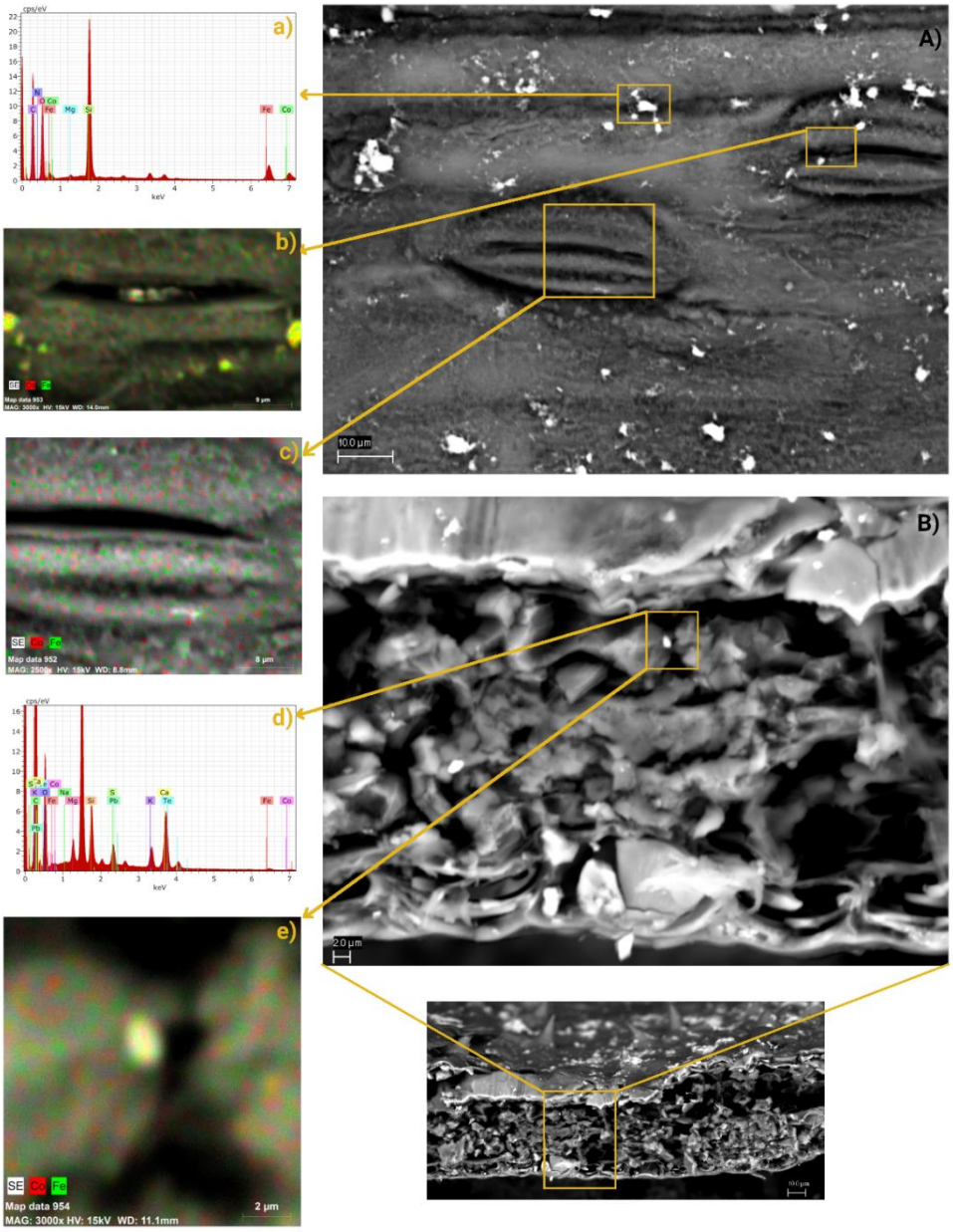

Figure 2.6. ESEM images of the adaxial (A) and transverse section (B) of the flag leaf of wheat plants (AF1116) that were foliar fertilized with citrate-coated $CoFe_2O_4$ NPs. a) and d) EDX pattern of an agglomerate of NPs; b), c) and d) EDX mapping analysis of a selected area, red pixels indicate the presence of Co, while green pixels indicate the presence of Fe in the analyzed area.

The efficiency of foliar-applied fertilizers depends on parameters related to the formulation, such as compound stability, the ability to penetrate through leaf cuticle, the mobility/translocation following diffusion into leaf tissue (Fatima et al. 2021); and the leaf morphology, such as trichomes, stomata, and hydathode pores (Avellan et al. 2021). In

this regard, the low water stability of citrate-coated $CoFe_2O_4$ NPs (Perea-Velez et al. 2022) may play a role in the efficiency of foliar applications because the NPs tend to form agglomerates/aggregates (216.06±10.46 nm of size) (Perea-Velez et al. 2022); thus the size of those agglomerates may inhibit the uptake of NPs through stomata. The adhesion of NPs on the surface of wheat leaf was observed (Figure 2.6A); the average size of these agglomerates of NPs was 2.6 ± 1.2 µm. The NPs size (13.4±4.5 nm primary size) also may explain the NPs' adhesion on the leaf surface. It has been observed higher adhesion for smaller NPs than large NPs sizes due to their higher specific surface area (Avellan et al. 2021).

The Fe concentration in grains is not the final goal in biofortification, but its bioavailability should be high enough. Because of the possibility of strong chelation between the phytic acid and the minerals, the phytic acid concentration in grains is an interesting parameter to assess the relative bioavailability of Fe and Zn. Some studies suggested that the phytate had more influence on Fe bioavailability than the total Fe content in seeds (Magallanes-López et al. 2017). The phytic acid concentration (Figures 2.3b and 2.4b) in the kernels was below the lower limit (0.39-1.5 g 100 g^{-1}) of the average concentration of phytic acid in wheat grains (Schlemmer et al. 2009). The lowest phytic acid concentration was found in kernels of line AF1116 (Zn storage inefficient; when comparing lines); and in those from plants fertilized with NPs at 68 mg Fe kg^{-1} compared to the Fe-EDTA or NPs foliar fertilization. The molar ratio of phytic acid and Fe is an indirect form to predict the bioavailability of Fe; despite the molar ratios of phytic acid and Fe being above the desirable value (<1), a 1.96 value was observed in grains of AF1116 line from plants soil fertilized with NPs at 68 mg Fe kg^{-1} (Figure 2.4c). Changes in phytate concentration in wheat seeds due to exogenous Fe application (chelate compounds and $FeSO_4$) have been reported. Tipu et al.(2022) evaluated soil and foliar application of Zn and Fe, alone or in combination, both elements in their non-chelated and chelated forms. They found that all the chemical types of Fe and Zn fertilizers and their mixtures significantly decreased the phytate contents in grains compared to the control. The phytate ranged from 0.87 g 100 g^{-1} to 0.83 g 100 g^{-1}. The foliar fertilization of wheat with

$FeSO_4$ (0.25% w/v) + Zn-EDTA (0.5% w/v) and Fe-EDTA (0.25% w/v) + Zn-EDTA (0.5%w/v) reduced the phytate content in seeds by 5% compared to the control.

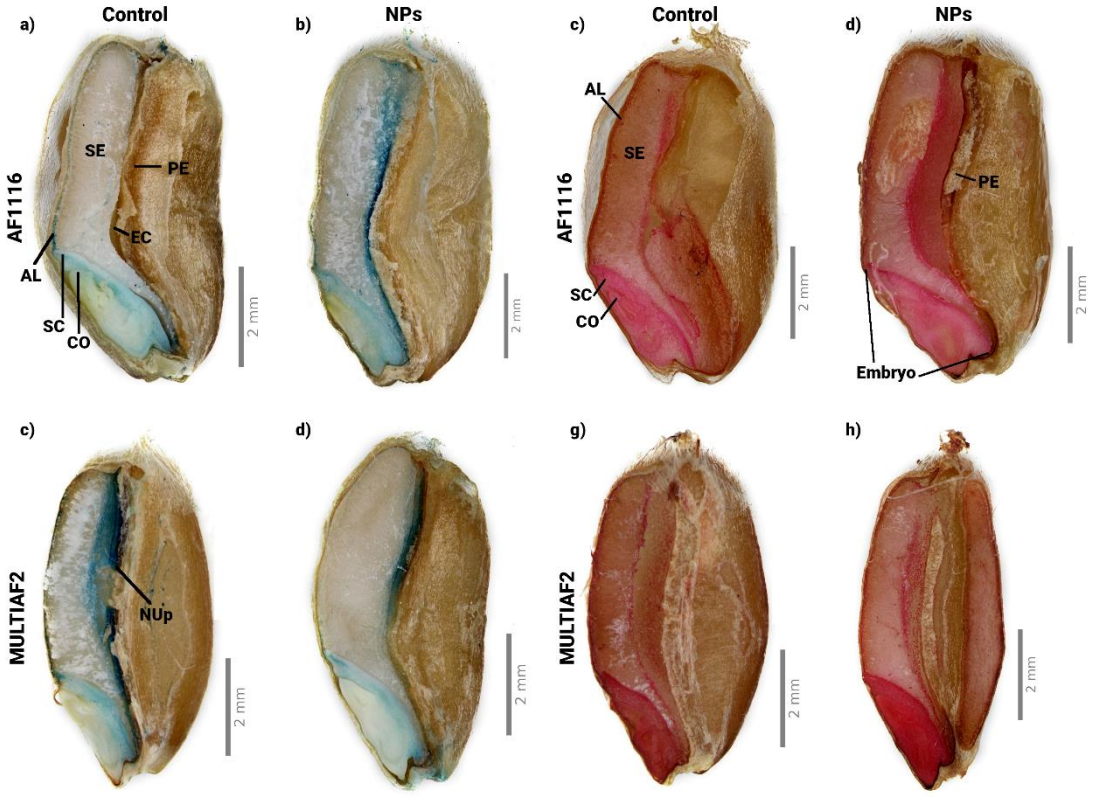

Figure 2.7. Localization of Fe (blue staining, by Prussian blue) and Zn (red staining, by dithizone staining) in mature grains of wheat lines AF1116 (a-d) and MULTIAF2 (e-h) from control plants and soil NPs fertilized plants at 68 mg Fe kg^{-1}. SE, starchy endosperm; AL, aleurone layer; SC, scutellum; CO; coleoptile; PE, pericarp increase region; EC, Endosperm cavity; NUp; Nucellar projection.

The distribution of Fe in grains may explain why the high Fe concentration and low phytic iron molar ratios were observed in seeds from plants fertilized with NPs. In wheat grains, Fe ligands can be phytate and non-phytate ligands. The phytate ligands are predominantly present in the aleurone layer, scutellum, and embryo, and the non-phytate ligands (such as citrate, nicotinamide, sulfate, oxide-hydroxide) are found in the nucellar projection and pericarp. Assuming that Fe bioavailability depends on those Fe-ligands, Pongrac et al.(2020) proposed that the Fe-speciation is tissue specific. In this regard, for seeds of the AF1104 line from plants soil fertilized with NPs, the intensity of the blue staining was stronger in the scutellum and the nucellar projection in the groove region

compared to the control seeds (Figures 2.7a-b). In the case of grains of MULTIAF2, no differences were found between the control seeds and those from plants after applying NPs to the soil (Figures 2.7e-f). Zn was most concentrated in the embryo and the aleurone layer (Figures 2.7c, d, g, and h). The seed embryo from MULTIAF2 plants appeared to stain stronger than those of the AF1116. These observations agree with what was reported by Balk et al. (2019) and Wu et al. (2013).

As mentioned above, more of a micronutrient in the kernel does not necessarily mean a greater bioavailability/bioaccessibility ratio. Bioavailability refers to the fraction of an ingested nutrient that reaches the systemic circulation and specific sites where it can exert its biological action. Meanwhile, the bioaccessibility of a nutrient refers to the amount of an ingested nutrient that is available for absorption in the gut after digestion (Galanakis and Drago 2022). In this regard, analyzing the soluble fraction of Fe and Zn in the grains provides information about the potential bioaccessibility of those micronutrients. The average soluble Fe in grains was 3.54 mg kg^{-1}, and no significant changes were found due to the fertilization ($p=0.981$) or line type ($p=0.380$). The soluble Zn concentrations ranged from 12% to 16%, and the soluble Zn of grains of the AF1116 line (Zn storage inefficient) was significantly higher than that of the genotype AF1104 (Zn storage efficient). Cobalt was not detected in the soluble fraction.

The bioavailability/bioaccessibility ratio of a nutrient is affected by the food matrix, food processing, digestive enzymes, and digestion microbiota (Rodrigues et al. 2022). That is why we used the *in vitro* digestion model to predict the mineral bioaccessibility of the wheat grains that exhibited high Fe concentration, low phytic acid, and relatively high bioavailability/bioaccessibility. The concentrations of microelements and P after the *in vitro* digestion are shown in Table 2.4. In the simulated gastric fluid (SGF), no significant changes in the Cu, Fe, Zn, and P concentrations were observed due to the type of fertilization or line. For the Se concentrations in SGF, the highest Se concentration was found in SGF from the grains from the Fe-EDTA treatment (0.84±0.19 mg kg^{-1}), while the lowest Se concentration was observed in the grains from NPs treatment (0.49±0.21 mg kg^{-1}). When comparing the mineral concentrations of grains obtained from the treatments tested over the commercial wheat grains, significant differences were observed for the P

concentrations between the control treatment and the commercial wheat grains. The P concentration in commercial wheat grains was 1.26-1.53 folds higher than that of grains obtained in this experiment. In general, the mineral concentration tendency in both lines in the SGF was P>Zn>Se>Fe>Cu. In contrast, in the simulated intestinal fluid (SIF) only Fe, Zn, and P were detected. The types of fertilization and line have a significant effect on the concentration of Fe, Zn, and P in SIF.

When comparing treatments, the highest Fe concentration in the SIF was observed in samples from plants fertilized with NPs. These results support that the soil NPs fertilization at 68 mg Fe kg^{-1} may enhance the bioavailability of Fe in whole wheat grains, and the higher bioaccessibility of Fe in grains from NPs treatment in comparison to that from the control and Fe-EDTA treatments could be related to the low phytic acid concentration (Figure 2.3). Meanwhile, comparing the lines with each other, the highest Fe concentration was observed in grains of the MULTIAF2 line. For the AF1116 line, the highest Fe concentration in SIF was found in samples from the Fe-EDTA treatment; in contrast, NPs treatment resulted in the highest Fe concentration in SIF in the MULTIAF2 line. Moreover, in both lines and treatments, Fe in the SIF was significantly higher than that from the commercial wheat grains.

The Zn concentration in the SIF from AF1116 line was higher than that of the MULTIAF2 line. No significant differences were observed in the Zn concentration in the SIF between treatments and the commercial wheat samples. For P, significant differences were observed between treatments within lines and the commercial wheat grains. For the AF1116 line, the SIF from Fe-EDTA treatment had a higher P concentration than that of the SIF from commercial wheat. For the MULTIAF2 line, control and NPs treatments showed a higher P bioaccessibility compared to commercial wheat. Positive correlations were found between P and Fe in the SIF for both lines ($p=0.67$ and $p=0.55$, respectively).

Table 2.4. Bioaccessible concentration of mineral nutrients in two wheat lines fertilized with FeEDTA or citrate-coated $CoFe_2O_4$ NPs, and their comparison with commercial wheat grains.

Simulated fluid	Wheat line	Treatment	Cu	Fe	Se	Zn	P
			(mg kg^{-1})				(g kg^{-1})
Gastric	AF1116	Control	0.18±0.04 a	0.53±0.17 a	0.53±0.17 a	1.30±0.07 a	0.19±0.03 ab
		Fe-EDTA soil	0.21±0.12 a	0.30±0.29 a	0.78±0.21a	1.79±0.32 a	0.16±0.02 b
		NPs 68 soil	0.25±0.10 a	0.63±0.30 a	0.53±0.07 a	1.59±0.58 a	0.19±0.03 ab
		Mean	0.21±0.09	0.49±0.26	0.61±0.18	1.56±0.39	0.18±0.03
	MULTIAF2	Control	0.11± 0.09 a	0.48±0.25 a	0.87±0.12 a	0.75±0.37 a	0.11±0.02 b
		Fe-EDTA soil	0.28± 0.17 a	0.53±0.38 a	0.90±0.18 a	2.07±1.10 a	0.19±0.04 ab
		NPs 68 soil	0.15± 0.06 a	0.27±0.18 a	0.45±0.32 a	0.56±0.60 a	0.17±0.06 ab
		Mean	0.18±0.12	0.43±0.27	0.74±0.28	1.12±0.96	0.15±0.05
	Commercial wheat grains		0.38±0.05 a	0.36±0.08 a	0.52±0.30 a	2.17±0.27 a	0.24±0.02 a
Intestinal	AF1116	Control	ND	0.15±0.09 b	ND	0.54±0.05 a	0.28±0.02 b
		Fe-EDTA soil	ND	0.49±0.12 a	ND	0.49±0.18 a	0.38±0.04 a
		NPs 68 soil	ND	0.21±0.08 b	ND	0.42±0.12 a	0.31±0.05 ab
		Mean		0.28±0.17 B		0.48±0.12 A	
	MULTIAF2	Control	ND	0.22±0.04 b	ND	0.19±0.00 a	0.32±0.05 a
		Fe-EDTA soil	ND	0.19±0.03 b	ND	0.28±0.14 a	0.26±0.02 ab
		NPs 68 soil	ND	0.87±0.23 a	ND	0.26±0.02 a	0.33±0.01 a
		Mean		0.43±0.35 A		0.24±0.08 B	
	Commercial wheat grains		ND	0.09±0.04 b	ND	0.38±0.17 a	0.22±0.02 b
				Treatment comparison			
		Control	ND	0.19±0.07 b	ND	0.37±0.19	0.30±0.04
		Fe-EDTA soil	ND	0.34±0.18 b	ND	0.39±0.18	0.32±0.07
		NPs 68 soil	ND	0.54±0.39 a	ND	0.34±0.11	0.32±0.03

Mean±standard deviation of n=3. ND, no detected. Different lowercase letters show significant differences (Tukey α=0.05) between treatments within lines and their comparison with the commercial wheat grains, or between treatments. Different capital letters show significant differences between lines.

The protein concentration in the kernels was between the average protein concentration (10-15%) reported by Govindan et al. (2022) in wheat grains from different cultivars. The protein content in grains of the AF1116 line was higher than the protein content of grains of the MULTIAF2 line but similar to that of the grains of genotype AF1104 (Table 2.3). Concerning P concentrations in the grains, significant differences were observed in the AF1104 line. The treatments with soil NPs at 68 mg Fe kg^{-1} and foliar spray of NPs significantly increased the P grain concentration compared to either control plants or those fertilized with Fe-EDTA. When comparing between lines, the grains from the AF1116 line showed the highest P concentration. The Co grain concentration was between 11.14 to 14.21 mg kg^{-1}. These Co concentrations were below the maximum allowable limit in grains (50 mg kg^{-1}) recommended by FAO and the WHO (Ejaz et al. 2022). Alternatively, the NPs fertilization or Fe-EDTA fertilization did not alter the concentration of soluble polysaccharides and free amino acids (Table S8).

2.5.3. Influence of NPs fertilization on efficiency-related attributes and economic evaluation

Significant effects by the type of fertilization were observed in the partial factor productivity (PFP, $p=1.29e^{-6}$), agronomic efficiency (AE, $p=1.016e^{-6}$), and apparent efficiency recovery (AER, p=0.0040). For foliar fertilization with NPs and Fe-EDTA, high values of PFP, AE, and AER were obtained (Figure 2.8 a-c). However, significant differences in the function of different wheat lines were also observed in the AER (p= 0.001), and no significant differences by the effect of treatment or line on the physiological efficiency (PE, p= 0.623, 0.111, respectively) index.

The PFP and AE indexes focused on the economic yield. On the one hand, the PFP is an index that helps to know how productive a cropping system is compared to its nutrient input. (Fixen et al. 2015) Meanwhile, AE determines how much productivity improvement was achieved by adding a nutrient.(Fixen et al. 2015; Kumar et al. 2022) The PFP for foliar NPs fertilization was between 30 and 41 fold higher than the NPs or Fe-EDTA soil fertilization, meaning that the lower amount of Fe supplied by foliar spray (13.2 mg Fe per pot) may produce a greater grain yield than the other types of fertilization (368 and 544 mg Fe per pot). But Fe inputs, either foliar or soil application, improved the

yield compared to the control (Figure 2.8a and Table 2.2). The AE index indicated that foliar fertilization (NPs or Fe-EDTA) significantly increased the economic yield compared to soil fertilization. However, this index is a short-term indicator of the fertilization effect (Fixen et al. 2015). Thus, the AE values for soil fertilization (0.007-0.037 kg g^{-1}) should not be ignored; on the contrary, they suggest that changes in crop management could improve yield and plant response to fertilization or reduce fertilizer input (Fixen et al. 2015). AER and PE are indicators that center on the plant's ability to absorb a nutrient (from an external source), and turn it into economic yield (Fixen et al. 2015; Kumar et al. 2022). AER index answers to how much of the nutrient applied did the plant take up? (Fixen et al. 2015). According to this index, AF1104 and AF1116 lines took up more Fe than the plants of line MULTIAF2. The highest levels of AER for foliar NPs fertilization (Figure 8c) suggest a better Fe absorption by the plant than the soil fertilization; nevertheless, these values may be over-estimated because the image analysis of flag leaves (at Zadoks' scale 7.3) revealed that NPs remain adhered on the leaf surface (Figure 2.6A). In contrast, AER values for the soil NPs application treatments were ~2 folds higher than that of the Fe-EDTA soil fertilization. The PE index answers the question "What is the ability of the plant to transform nutrients acquired from the source applied into economic yield?" (Fixen et al. 2015). The PE values obtained ranged from -14 to 8 kg g^{-1} when comparing wheat line*treatment, and from -4 to 4 kg g^{-1} when comparing treatments. Both cases were below the common values (40-60) observed among cultivars and cultural practices (Fixen et al. 2015). Although, evaluations in the short term often lead to an underestimation of this index (and the same for the AER index) due to the lack of observation of the residual effects of the nutrients applied in the long term (Fixen et al. 2015).

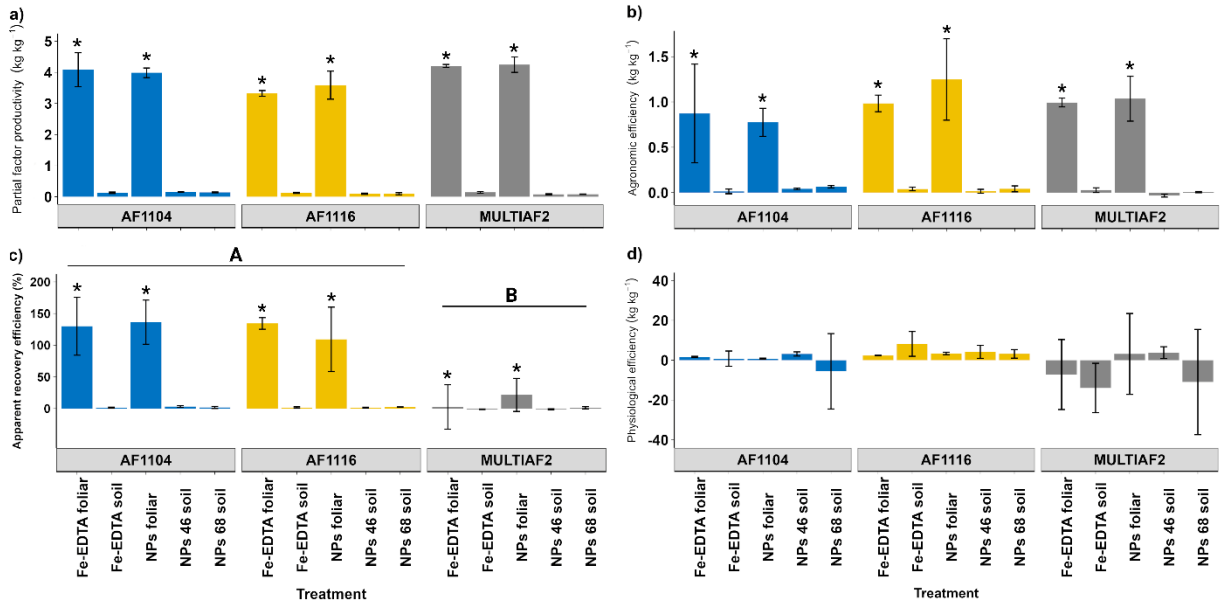

Figure 2.8. Nutrient efficiency measures for the evaluation of crop production through conventional fertilization (Fe-EDTA salt) and Fe nano-fertilizer (coated-citrated $CoFe_2O_4$ NPs). a) Partial factor productivity, b) agronomic efficiency, c) apparent recovery efficiency, and d) physiological efficiency. * shows significant differences (Tukey α=0.05) between treatments within the wheat lines (AF1104, AF1116 MULTIAF2). Different capital letters show significant differences between lines.

The high grain yield of treatments with soil NPs at 68 mg Fe kg^{-1} and the application of NPs or Fe-EDTA by foliar spraying compared to the control treatment resulted in a relatively high gross income (Table 2.5). The gross income with soil NPs at 68 mg Fe kg^{-1} was 21.4% more than the soil Fe-EDTA fertilization, for the foliar treatments, the NPs foliar fertilization resulted in a 1.8% higher gross income than the foliar Fe-EDTA one. Among the lines, the highest increase in the gross income by NPs fertilization was observed with AF1104: the soil NPs treatments resulted in 22% and 64% higher gross income than that of the soil Fe-EDTA fertilization. Nevertheless, for the AF1116 line, NPs treatment by soil (68 mg kg^{-1}) and foliar application increased by 17% and 8% of the gross income, respectively, compared to the Fe-EDTA fertilization. Meanwhile, in MULTIAF2, only the NPs foliar fertilization led to an increase compared to the soil applications, as the gross income was 1% higher compared to the Fe-EDTA fertilization. However, the high cost of production due to the Fe soil fertilization reduced the profitable return. The estimated cost of Fe soil fertilization per ha was 8,204.6 USD for soil Fe-EDTA supplement, 44,283.0 USD in the case of NPs at 46 mg Fe kg^{-1}, and 65,522.9 USD for

NPs at 68 mg kg^{-1}. Thus, the Fe-EDTA fertilization reduced the profitable return by 6,000 USD, and the NPs fertilization at the rate of 48 mg Fe kg^{-1} and 68 mg Fe kg^{-1} by 42,000 and 62,000, respectively. The profitable return over the control treatment was positive only in the cases of the Fe-EDTA foliar treatments.

The cost-benefit ratio was positive in only the foliar Fe-EDTA fertilization in all the wheat lines. However, it was less than 1 in all cases meaning that the cost of agronomic biofortification outweighs the economic benefits compared to the control treatment. The highest investment factors were also found in the case of the Fe-EDTA foliar treatments. Among the NPs treatments, it was also the foliar supplement that resulted in the highest investment factor (1.3) compared to the soil applications (0.1). The highest results were observed in the MULTIAF2 line: 2.8 for Fe-EDTA, and 1.4 for NPs foliar fertilization.

When the efficiency of NPs fertilization was evaluated through the nutrient efficiency measurement, the PFP, and AE indicated that NPs foliar fertilization was the best option, because the system was more productive compared to the control treatment, and soil application of both NPs and Fe-EDTA. These conclusions may be reinforced by the economic analysis, where positive profitable return and low cost-benefit ratio were observed with foliar NPs fertilization compared to the soil application. Undoubtedly, foliar fertilization is a visible economic form to supplement nutrients to plants compared to soil fertilization.(Fageria et al. 2009) Moreover, a foliar application will not only decrease the production cost but also reduce the runoff of soil-applied nutrients.(Fageria et al. 2009) However, as was discussed in the previous section, foliar fertilization with NPs did not improve the grain Fe concentration, which was our goal. In contrast, the target iron concentration for biofortification was reached in the lines AF1104 and MULTIAF2 by the soil application of NPs.

Table 2.5. Economic evaluation of different Fe fertilization for agronomic biofortification.

Wheat line	Application	Treatment	Gross income (USD)	Cost of production (USD)	Profitable return (USD)	PR over control (USD)	Cost-benefit ratio	Investment factor
			Wheat lines comparison					
AF1104		Control	2,661.6	940.2	1,721.4			2.8
	Soil	Fe-EDTA	2,948.5	9,144.9	-6,196.3	-7,917.7	-0.9	0.3
		NPs 48 mg	3,603.6	45,223.3	-41,619.7	-43,341.1	-1.0	0.1
		NPs 68 mg	4,843.0	66,463.1	-61,620.2	-63,341.6	-1.0	0.1
	Foliar	Fe-EDTA	3,385.5	1,234.9	2,150.6	429.2	0.3	2.7
		NPs	3,303.9	2,492.9	811.0	-910.4	-0.4	1.3
AF1116		Control	1,939.8	940.2	999.6			2.1
	Soil	Fe-EDTA	2,850.2	9,144.9	-6,294.7	-7,294.3	-0.8	0.3
		NPs 48 mg	2,253.1	45,223.3	-42,970.2	-43,969.8	-1.0	0.0
		NPs 68 mg	3,349.1	66,463.1	-63,114.0	-64,113.6	-1.0	0.1
	Foliar	Fe-EDTA	2,755.0	1,234.9	1,520.0	520.4	0.4	2.2
		NPs	2,973.9	2,492.9	480.9	-518.7	-0.2	1.2
MULTIAF2		Control	2,662.5	940.2	1,722.2			2.8
	Soil	Fe-EDTA	3,283.8	9,144.9	-5,861.0	-7,583.3	-0.8	0.4
		NPs 48 mg	1,880.2	45,223.3	-43,343.1	-45,065.4	-1.0	0.0
		NPs 68 mg	2,834.3	66,463.1	-63,628.9	-65,351.1	-1.0	0.0
	Foliar	Fe-EDTA	3,486.0	1,234.9	2,251.1	528.8	0.4	2.8
		NPs	3,520.7	2,492.9	1,027.8	-694.5	-0.3	1.4
			Treatment comparison					
		Control	2,421.3	940.2	1,481.1			2.6
	Soil	Fe-EDTA	3,027.5	9,144.9	-6,117.3	-7,598.4	-0.8	0.3
		NPs 48 mg	2,579.0	45,223.3	-42,644.3	-44,125.4	-1.0	0.1
		NPs 68 mg	3,675.4	66,463.1	-62,787.7	-64,268.8	-1.0	0.1
	Foliar	Fe-EDTA	3,208.8	1,234.9	1,973.9	492.8	0.4	2.6
		NPs	3,266.2	2,492.9	773.2	-707.9	-0.3	1.3

The AER indicator for the soil NPs application was ~2 folds higher than that for the Fe-EDTA soil fertilization (Figure 2.8), meaning a better absorption of Fe from the NPs than the Fe-EDTA source. Nutrient efficiency measures are a critical concept in the evaluation of crop production systems and indicate the potential for nutrient losses to the environment from cropping systems. Their interpretation must be carefully considered since they do not measure nutrient loss, so their interpretation must be done within a known context (Fixen et al. 2015). In this regard, we should consider that a residual effect after the NPs soil application may reduce the cost of production because Fe fertilization may not be required for the next crop. However, further investigation related to this topic should be addressed.

The high cost of production (Table 2.5) is related to the high cost of the NPs, this opens an opportunity to improve the current methods to produce $CoFe_2O_4$. Likewise, the high production cost of NPs may be related to Co prices, as this is a critical element. The price of many critical minerals has recently soared due to the combination of rising demand, disrupted supply chains, and concerns about tightening supply (Kim 2022). For example, according to the International Energy Agency (IEA), the price of cobalt from January 2021 to March 2022 has increased by 156%. On the other hand, micronutrient deficiencies in the population not only affect the burden of disease, but also work productivity, the cost of health system usage, and the success of the education system via cognition (Horton 2004). So, the indirect cost due to the micronutrient deficiencies in the population may be greater than the cost of production of more nutritious food.

2.6. CONCLUSIONS

Nutritional security is a threat faced by many developing countries, and micronutrient deficiencies in their populations are related to limited access to a diversified diet. In this endeavor, this work was motivated by the idea to propose an innovative approach to increase the Fe concentration in wheat grains using NPs as an alternative source of Fe in agronomic biofortification. Surprisingly, the highest Fe concentration was observed in grains of lines AF1104 (inefficient in Zn storage) and MULTIAF2 (phosphorus inefficient), specifically after soil fertilization with NPs at 68 mg kg^{-1}. Likewise, the target concentration of Fe biofortification (60 mg kg^{-1}) was achieved. After soil fertilization with

NPs (68 mg kg^{-1}), the Fe concentration in grains of Zn storage inefficient and P-uptake inefficient lines was respectively 1.37 and 0.26 folds above the target biofortification concentration. Thus, based on those results the original hypotheses were rejected. On the other hand, the application of citrate-coated $CoFe_2O_4$ NPs for biofortification purposes, and as fertilizer to enhance crop production is at level 3 of the technology readiness level. Despite the high-cost estimate for the use of NPs, our results showed the potential of NPs fertilization to improve the economic yield of the crop and the nutritional quality of wheat grains. Understanding several aspects related to the safe usage of nanomaterials and their future perspectives may enhance their successful utilization in terms of economic and fulfillment of nutritional requirements following wheat nano-biofortification.

CHAPTER 3. NANO-PRIMING WITH CITRATE-COATED COBALT FERRITE NANOPARTICLES ON *Phaseolus vulgaris*

3.1. ABSTRACT

Nano-priming is one of the less explored applications of nanotechnology in agriculture. This technique is based on seed priming, but nanoparticles are used as a priming agent instead of conventional substances (water, phytohormones, microorganisms, etc.). This study assessed the effect of nano-priming with citrate-coated cobalt ferrite nanoparticles (10, 20, and 40 mg NPs L^{-1}) on the life cycle of *Phaseolus vulgaris* cultivar OTI from April to Jun of 2022. No significant effect of the nano-priming was observed on the germination variables, the vegetative growth parameters, and the nutritional status of plants at the flowering stage (51 d after sowing). The plant growth, from V1 to R6, from nano-primed seeds (20 and 40 mg NPs L^{-1}) was significantly higher than that of the control plants. Native *Rhizobium* root colonization kept occurring in plants from primed seeds after flowering. The change in the number of total nodules between the flowering stage and the plant maturity was 3.38 and 2.74 folds for the nano-priming at 20 mg and 40 NPs L^{-1}, respectively. Plants from the seeds treated with 40 mg NPs L^{-1} exhibited a large number total number of nodules and the heaviest nodules were observed in plants from the nano-primed seeds at 20 mg NPs L^{-1}. At the harvesting (81 d after sowing), no significant differences in the agronomic traits were observed between the plants from primed and unprimed seeds. However, the seed nutrient content was positively affected by the nano-priming seeds treatment. The nano-primed treatment at 20 mg NPs L^{-1} increased the K concentration in seeds compared to that of the control and hydroprimed treatment, and the seed P concentration compared to that of the hydroprimed treatment. The Zn concentration of offspring seeds of plants from nano-primed seeds at 10 and 40 mg NPs L^{-1} was significantly higher compared to those seeds from the plants from the control and hydroprimed seeds. Even the Zn concentration in the seeds was 2-2.4 folds above the average seed Zn concentration reported for Mexican bean varieties (27-40 mg Zn kg^{-1}). The calculated cost of nano-priming bean seeds per ha ranged from 121 to 143 USD. In this regard, the nano-priming of bean seeds with citrate-coated $CoFe_2O_4$ NPs could be a low input, cheaper environmentally friendly

approach to improve the Zn, P, and K concentrations in seeds without the addition of an external supply of micronutrients. However, further research is needed to create a standard protocol for a deeper evaluation of the benefits of seed priming.

Keywords: nano-biofortification, iron and zinc biofortification, plant-nutrition, micronutrients.

3.2. RESUMEN

Nano-priming es una de las aplicaciones menos exploradas de la nanotecnología en la agricultura. Esta técnica se basa en seed priming, pero las nanopartículas se usan como agente para el seed primg en lugar de sustancias convencionales como (agua, fitohormonas, microorganismos, etc.). Se evaluó el efecto del nano-priming con nanopartículas de ferrita de cobalto recubiertas de citrato (10, 20 y 40 mg NPs L^{-1}) en el ciclo de vida de *Phaseolus vulgaris* variedad OTI de abril a junio de 2022. No se observó ningún efecto significativo del nano-priming sobre las variables de germinación, los parámetros de crecimiento vegetativo y el estado nutricional de las plantas en la fase de floración (51 d después de la siembra). El crecimiento vegetativo, de V1 a R6, de las semillas que se trataron con nano-priming (20 y 40 mg NPs L^{-1}) fue significativamente superior al de las plantas testigo. La colonización de raíces por *Rhizobium* nativo siguió produciéndose en las plantas procedentes de semillas con nano-priming después de la floración. El cambio en el número de nódulos totales entre la fase de floración y la madurez de la planta fue de 3.38 y 2.74 veces para el nano-priming a 20 mg y 40 NPs L^{-1}, respectivamente. Las plantas de las semillas tratadas con 40 mg de NPs L^{-1} mostraron el mayor número total de nódulos y los nódulos más pesados se observaron en las plantas de las semillas con nano-priming a 20 mg de NPs L^{-1}. En la cosecha (81 d después de la siembra), el número total de nódulos fue 3.38 y 2.74 veces mayor que en la floración. En la cosecha (81 días después de la siembra), no se observaron diferencias significativas en los rasgos agronómicos entre las plantas procedentes de semillas con nano-priming, hidropriming y testigo. Sin embargo, el tratamiento con nano-priming afecto positivamente el contenido en nutrientes de las semillas. El tratamiento con nano-priming a 20 mg NPs L^{-1} aumentó la concentración de K en las semillas en comparación con el control y el tratamiento de hidropriming, y la concentración de P en las semillas en comparación con el tratamiento de hidropriming. La concentración de Zn de las semillas descendientes de las plantas procedentes de las semillas con nano-priming a 10 y 40 mg NPs L^{-1} fue significativamente mayor en comparación con las semillas de las plantas procedentes de control e hidropriming. Incluso la concentración de Zn en grano fue 2-2.4 veces superior a la concentración media de Zn en grano registrada para las variedades

mexicanas (27-40 mg Zn kg^{-1}). El coste calculado por hectárea para el tratamiento de nano-priming de semillas de frijol osciló entre 121 y 143 USD. En este sentido, el nano-priming de semillas de frijol con NPs de $CoFe_2O_4$ recubiertas de citrato podría ser un enfoque de bajo insumo, más barato y amigable con el medio ambiente para mejorar la concentración de Zn, P y K en las semillas de frijol sin la adición de un suministro externo de micronutrientes. Sin embargo, es necesario seguir investigando para crear un protocolo estándar que permita una evaluación más profunda de los beneficios del seed priming

Keywords: nano-biofortification, iron and zinc biofortification, plant-nutrition, micronutrients.

3.3. INTRODUCTION

The introduction of nanomaterials (NMs) in agriculture can potentially contribute to the transition to a more sustainable agri-food system (Dutta 2018) and improve the nutritional quality of the crops. The idea of using NMs in agriculture is to reduce the application of fertilizers to crops by improving their efficiency, to enhance the tolerance of crops to biotic and abiotic stress, and to increase the crop yield while exerting less pressure on soil and water resources (do Espirito Santo Pereira et al., 2021; Perea Velez et al., 2021).

The application of nanotechnology in agriculture has been focusing on the development of nano-fertilizers, but other less explored options like seed priming (nano-priming) could be also attractive and may help to address the issue of sustainability in agriculture (Dutta 2018; do Espirito Santo Pereira et al. 2021). The seed priming technique is a low input, and pre-sowing seed treatment. It allows synchronized germination and maturity of crops, improve the germination time and water use efficiency, increases the nutrient uptake and the tolerance of a plant to biotic and abiotic stresses (Dutta 2018; Chandrasekaran et al. 2020). Seed priming is generally defined as the controlled hydration of the seeds to the level to allow pre-germinative metabolic activity without radical protrusion (Sher et al. 2019; Shah et al. 2021b). After the seed hydration, the seed is dried again to its original weight (Sher et al. 2019; Shelar et al. 2021).

Conventional seed priming mainly employs water or solutions containing substances, like nutrients, hormones, microorganisms, or biopolymers (Chandrasekaran et al. 2020). For seed nano-priming, the media used are nanoparticle (NPs) suspensions or nano-formulations, where the NPs may or may not be taken up by the seed, or may be retained on/in the seed coat (do Espirito Santo Pereira et al. 2021). Examples of metallic NPs tested as seed priming agents are Fe, Ag, Au, Cu NPs, TiO_2, FeS_2, Fe_2O_3, ZnO (Perea Vélez et al. 2021), and some carbon-based NPs as carbon nanotubes (Mahakham et al. 2017; Shukla et al. 2019). The reported effects of NPs on plant germination and plant development are diverse. For example, a significant enhanced germination rate, reduced average germination time, and increased yield (from 32% to 36% more than unprimed seeds) have been observed in watermelon seeds primed with AgNPs (Acharya

& Pal, 2020). Sundaria et al. (2019) reported an increase in germination percentage and shoot length in two wheat varieties (high and low iron-efficient) after nano-priming treatment with Fe_2O_4 NPs of the grains. Despite the positive results observed by nano-priming, the molecular mechanisms behind those effects on seed germination and plant development have not been described well until now (Shukla et al. 2019). It is assumed that NPs internalization promotes the fast water uptake (stage I of the seed priming process) by the seed. Then, the pre-germinative seed metabolism is stimulated (stage II or activation phase of seed priming process) by the action of NPs internalization. It means that NPs can also induce the production and accumulation of reactive oxygen species (ROS) and phytohormones, which will act as signal molecules and promote protein synthesis, activation of enzymes and antioxidant systems, DNA repair, and formation of new mitochondria (Rai-Kalal et al. 2021; Shelar et al. 2021).

On the other hand, *Phaseolus vulgaris* (common bean) is one of the major widespread and important legumes worldwide (Petry et al. 2015). It represents 65% of the total protein consumed and 35% source of energy for people (more than 300 million) from Latin America Caribbean and Eastern Africa (Petry et al. 2015). It was characterized as a nearly perfect food because of its high protein, fiber, prebiotic, vitamins (A, C, and folate), and mineral content (Ca, Mg, K, Cu, Fe, and Zn). Likewise, the biofortification of beans could contribute to combating the prevalence of iron deficiency anemia (IDA) in populations of rural and marginalized areas (Ramírez-Jaspeado et al. 2020) of countries of Latin America, the Caribbean, and East Africa without having to modify the population's consumption patterns. The highest IDA prevalence is found in Africa, South Asia, and Latin America, representing 23.9%, 37.5%, and 33.9% of global anemia cases, respectively (Glahn and Noh 2021).

Research efforts to produce Fe biofortified beans have been done since 2003, and in Africa, Fe biofortified beans have been proclaimed a "nutrition success story" (Glahn and Noh 2021). However, the biofortification of staple crops remains a big challenge, because a higher Fe concentration does not always result in more bioavailable Fe delivered for absorption due to the high concentrations of substances like phytic acid and polyphenols, considered antinutrient substances (Glahn and Noh 2021). Common bean

has an average high Fe concentration compared to other crops such as wheat, rice, and maize (Petry et al. 2015). The average Fe concentration in bean seeds varies depending on the region. E.g., 55 mg Fe kg^{-1} from the collection of the Center Tropical Agriculture (CIAT, Colombia), 71 mg Fe kg^{-1} seed collection from the breeders of East Africa, and 69 mg Fe kg^{-1} from collections of Brazil and Latin America (Glahn and Noh 2021).

The bioavailability of Fe in beans is a function of the seed coat polyphenolic profile, phytic acid concentration, and the cotyledon cell walls. The phytic acid and the cotyledon cell walls are the major inhibitory factors for Fe delivery. In general, a high molar ratio of phytic acid:Fe (10:1) means a low Fe bioavailability. However, the use of nano-fertilizers has been shown to induce changes in the nutraceutical properties of grains like wheat. For example, Perea-Vélez et al. (2023) observed changes in the molar ratio of phytic acid and Fe of wheat seeds obtained from plants fertilized with cobalt ferrite NPs compared to the grains of non-fertilized plants, and plants fertilized with Fe-EDTA salt. They also observed a significant increase in the grain Fe concentration and grain yield.

Another interesting aspect to consider is that the common bean is a crop that enriches the soil through biological nitrogen fixation, which is based on symbiosis with bacteria, such as the *Rhizobium leguminosarium bv. Phaseoli* (Murube et al. 2021). Recent research showed that cobalt ferrite ($CoFe_2O_4$) NPs can significantly enhance the symbiotic nitrogen fixation efficiency by 260% in *Glycine max* (L.) Merr (Ma et al. 2021).

In this context, this research aimed to assess the effect of nano-priming of OTI variety *Phaseolus vulgaris* L. with citrate-coated cobalt ferrite ($CoFe_2O_4$) NPs. We hypothesized that: (1) the seed-nano-priming treatment may improve the germination traits compared to the unprimed seeds, and (2) enhance the yield, and (3) the nutritional quality of bean grains.

3.4. MATERIALS AND METHODS

Two experiments were conducted to assess the effect of nano-priming on *Phaseolus vulgaris* cultivar OTI with citrate-coated $CoFe_2O_4$ NPs. One was analyzed at the germination stage and the second one at the end of bean harvest under greenhouse

conditions. For quality assurance and quality control in analytical measurements, the material used was washed in 0.25 M HCl solution to remove any traces of contaminating materials. All the reagents used were of analytical grade (J.T. Baker, Merck, and Sigma Aldrich). All the measurements were carried out in triplicate. Standard solutions were prepared using certificated stock solutions.

3.4.1. Experiment 1. Assessment of the effect of nano-priming on the germination of bean

A completely randomized experimental design was set up to assess the effect of nano-priming on the germination traits of the *Phaseolus vulgaris* cultivar OTI bean. The seeds were primed with citrate-coated $CoFe_2O_4$ NPs dispersed in distilled water at 10, 20, and 40 mg NPs L^{-1}. To differentiate the effects of water and NPs, seeds were primed with distilled water (hydro priming or positive control), and unprimed seeds were considered a negative control. Three replicates per treatment were performed.

3.4.2. Plant material

The *P. vulgaris* cultivar OTI seeds were obtained from the Program of Genetic Resources and Productivity of Colegio de Postgraduados. OTI is an improved bean cultivar adapted to the central high valleys of the Mexican Republic. Some of its main characteristics are the cooking time (61-85 min), its yield (2.5 t ha^{-1}), and its high resistance to *Colletotrichum lindemuthianum, Sclerotinia* sp., and *Rhizoctonia solani*; medium resistance to *Uromyces appendiculathus* var. *appendiculatus*; and moderate tolerance to *Pseudomonas phaceolicola.* The seed coat of the OTI bean is a light brown background with bright purple spots (Estrada-Gómez et al. 2004).

3.4.3. Citrate-coated $CoFe_2O_4$ NPs and preparation of priming suspension

Citrate-coated $CoFe_2O_4$ NPs were synthesized by the coprecipitation method. The synthesis procedure was done following the methodology described by Martinez-Vargas et al. (2017) and Silva-Silva et al. (2016). The NPs characterization data were published by Perea-Velez et al. (2022). The main NPs features are semi-spherical shape, average

primary size of 13±5 nm, hydrodynamic diameter of 216±10 nm, 48% Fe and 29% Co composition.

For seed priming, suspensions of citrate-coated $CoFe_2O_4$ NPs at 10, 20, and 40 mg NPs L^{-1} (equivalent to 3.5, 7.5, 15 mg Fe L^{-1}; and 2.4, 4.5. and 9.5 mg Co L^{-1}, respectively) were freshly prepared in sterilized deionized water. The NPs suspension was sonicated with an ultrasonic probe for 2 min at 130 W and 90% amplitude. The concentrations of the nano-priming suspensions were chosen to ensure the dispersion of NPs and avoid their fast agglomeration.

3.4.4. Seed priming method

To determine the seed priming time, the seed water uptake curve was previously assessed (Figure S1). After setting the imbibition time, bean seeds were surface sterilized by soaking them in a 3% (v/v) sodium hypochlorite solution for 10 min and then carefully rinsed with sterilized deionized water to remove all the chloride. Afterward, the seeds were soaked in the NPs suspension for 2 h 30 min at room temperature (20-25 °C) with constant agitation on a rotor shaker (30 turns per minute). The primed seeds were then dried back to their original moisture content, for this the seeds were placed in sterilized paper bags and dried in an oven at 25 °C for 3d. Dried seeds were then stored at 4 °C until further use.

3.4.5. Quantitative estimation of Fe and Co content in nano-primed seeds

0.5 g of ground dried nano-primed seeds was acid digested (1 mL H_2O_2, and 4mL $HClO_4$:H_2SO_4; 4:1 v/v), and the digested sample was diluted to 25 mL with deionized water. The concentration of Fe and Co was determined by flame atomic absorption spectroscopy (Perkin Elmer, model 3110).

3.4.6. Localization of NPs and iron in nano-primed seeds

As a first attempt to detect the NPs in the seeds, the Perls' Prussian blue staining (Velu et al. 2008) was used. Briefly, dried nano-primed seeds were placed for 1 h in distilled water. The partially hydrated nano-primed seeds were then stained for 1 h with

Prussian blue solution (mixture of 2% (w/v) potassium hexacyanoferrate (II) and 2% (v/v) hydrochloric acid relation 1:1). Then, stained seeds were rinsed with distilled water, and the excess of water was removed with a paper tissue. The samples were mounted on a microscope slide and qualitatively analyzed using a reflectance light microscope (Carl Zeiss Stereo V20), and pictures were taken with a digital camera Canon 5D.

To confirm the presence of NPs on the seeds, environmental scanning electron microscopy-EDX analysis was performed. The dried nano-primed seeds were mounted on double-sided carbon conductive tape and observed by an ESEM, Carl Zeiss EVO LS10 (Jena, Germany) microscope, and X-ray detector (Bruker, Quantax 200, Germany). The images were taken at 30kV and 80 Pa of water vapor pressure.

3.4.7. Seed germination assay

Ten seeds were placed into a surface-disinfected plastic container which contained a bed of sterilized cotton and two sterile disks of filter paper. The seeds were moistened with 15 mL of sterile distilled water and kept in dark for germination at 20-23 °C for 7 d. Germinating seeds were counted based on 2 mm radical emergence (Rai-Kalal and Jajoo 2021), and germination was recorded daily. The germination percentage (GP), energy period (EP), germination energy (GE), germination rate (GR), and mean germination time (MGT) (Feizi et al. 2012; Antony et al. 2021) were calculated based on the following equations:

$$GP = \frac{number\ of\ seeds\ germinated}{total\ number\ of\ seeds\ placed\ for\ germination\ test} \times 100$$

$$EP = Days\ after\ starting\ the\ germination\ test\ to\ reach\ \geq 50\%\ og\ germinated\ seeds$$

$$GE = \frac{Cumulative\ daily\ total\ of\ germinated\ seeds\ at\ day\ 4}{Number\ of\ seeds\ set\ to\ germinate} \times 100$$

$$GR = \left(\frac{a}{1}\right) + \left(\frac{b-a}{2}\right) + \left(\frac{c-b}{3}\right) + \cdots + \left(\frac{n-n_{-1}}{D}\right)$$

$$mean\ germination\ time\ (MGT) = \frac{\sum(D \times n)}{\sum n}$$

Where a, b, c, … n is the number of seeds germinated on day 1, 2, 3, …, D; and D is the number of days counted from the beginning of the test.

At the end of the germination experiment (7 d), the fresh and dry weights of the seedlings were determined. Further, the stem height and root length were measured with the help of ImageJ software. The germination index (GI) and the relative seed germination (RSG) were calculated according to the following equations (Del Buono et al. 2022).

$$GI = (G \times L)/(Gw \times Lw)$$

$$RSG = \frac{Seeds\ germinated\ in\ the\ treating\ solution}{Number\ of\ seeds\ germinated\ in\ water\ or\ control\ treatment} \times 100$$

Where G and L are the germination and radicle length recorded for a specific treatment; Gw and Lw are the values recorded for control seeds.

The seedling vigor was calculated based on the following equation (Feizi et al. 2012):

$$Vigor\ index\ = germination\% \times seedling\ weight\ (root + shoot)$$

3.4.8. Evaluation of seedlings

Normal seedlings were considered those seedlings that developed a primary root and seminal roots; hypocotyl and two cotyledons with good development without tissue damage. Seedlings with defects were considered those showing impaired primary roots, without the development of secondary roots, little vigor without crossing the seed coat, negative geotropism, hypocotyl without development, enlarged, twisted; and cotyledons deformed, necrotic, or damaged.

3.4.9. Experiment 2. Effect of nano-priming on the growth of bean plants (from VE to R2 growth stage) and nodulation (greenhouse experiment)

A completely randomized experimental design was used. The treatments were: negative control (unprimed seeds), positive control (hydroprimed seeds), and nano-primed seeds at 10, 20, and 40 mg NPs L^{-1}. Each treatment had 10 replicates.

The soil used in this experiment was clay soil, collected from the surface layer of the experimental field of Colegio de Postgraduados (19°30'N, 98°51'W). The soil properties are presented in Table S1. Two seeds were sown in pots containing 8 kg of soil. Seedling emergence was recorded, and a seedling was considered as emerged when the cotyledons were completely raised above the soil. At the V2 growth stage (second trifoliate leaf established), one of the seedlings was removed. The plant height was recorded once a week after the plant's emergence. The plants were grown in an open greenhouse from April to June 2022 at an average temperature of 21 °C (27° C maximum temperature and 14° C minimum temperature). Plants were watered daily with tap water to keep ~60% of soil field moisture capacity.

To assess the effect of nano-priming on the nodulation four plants were harvested carefully 51 d after their sowing (R2 plant growth stage), and shoots were separated from the roots. Shoots were used to determine the leaf area and plant nutrition, while fresh nodules were collected, and the nodule fresh weight and the number of active nodules (pink pigmented) or inactive ones (brown dark-green) per plant root were determined.

3.4.10. Nitrogenase activity

The nitrogenase activity was determined by acetylene reduction. For plants at the R2 growth stage (51 d after sowing), samples of roots with nodules were transferred into a plastic hermetic closed container; the excess adhered soil was removed carefully before placing the roots in the container. The serum stopper was inserted and 10% of the air was replaced with acetylene and incubated for 1h (Hashem et al. 2016; Senthilkumar et al. 2021). The gas samples were analyzed in a gas chromatograph (Clarus 400, Perkin Elmer).

3.4.11. Foliar area

Digital images (Moto g6 camera) of leaves arranged on a white background and bright lighted conditions were taken. The images were analyzed with the ImageJ analysis software.

3.4.12. Evaluation of plant nutrition

The plant aerial part was dried in an oven at 70 °C for 3 d, then it was ground into powder. An aliquot of 500 mg was acid digested (1 mL H_2O_2 and 4 mL $HClO_4$: H_2SO_4, 4:1 v/v) on a digest block for 16 h at 90 °C. The digested samples were then made up to 25 mL with deionized water and filtered. The Ca, Mg, Fe, and Zn concentrations were determined by flame atomic absorption spectroscopy (Perkin Elmer, model 3110). The N concentration was estimated by the Kjeldahl method (Kjeldahl 1883), while the P and K concentration was determined using the vanadomolybdo phosphoric acid colorimetric method (Kitson and Mellon 1944), and flame photometry (Jenway, PFP7), respectively.

3.4.13. Assessment of the effects of nano-priming on the agronomic traits and grain nutritional quality of bean plants

Plants (6 experimental units) were harvested when they reach their maturity (R9, 81 days after sowing). The agronomic variables evaluated were the number of pods per plant, the weight of pods, the number of seeds per pod and plant, seed yield (weight of seeds per plant), seed index (100 seed weight), and harvest index.

The macro (Ca, Mg, K, and P) and micronutrient concentrations (Fe, Zn, and Cu) in seeds were determined by atomic absorption spectroscopy (Perkin Elmer, model 3110) or flame photometry (Jenway PFP7), respectively. While the P concentration in seeds was determined by the vanamolybdo phosphoric acid colorimetric method (Kitson and Mellon, 1944). The protein concentration in seeds was evaluated using the Kjeldahl method (Kjeldahl 1883). The protein content was calculated by multiplying the amount of total nitrogen with the conversion factor of 6.25 which assumes the nitrogen content of proteins in foodstuffs is 16% (Mariotti et al. 2008). The phytic acid concentration in seeds was estimated by the colorimetric Wade reagent method modified as described by Gao et al. (2007). The molar ratio of phytic acid: Fe and Zn were calculated by converting the concentrations of Fe (55.84 g mol^{-1}), Zn (65.38 g mol^{-1}), and phytic acid (660.04 g mol^{-1}) into moles.

3.4.14. Economic evaluation of nano-priming seed treatment

The economic analysis was performed using the economic indicators described by Dhaliwal et al. (2022) and Sarwar et al. (2007):

$$Gross\ income = yield\ (t\ ha^{-1}) \times grain\ price$$

$$Profitable\ return(PR) = gross\ income - total\ production\ cost$$

$$PR\ \ over\ control = PR - control\ treatment$$

$$Cost\ benefit\ \ ratio\ (CBR) = \frac{PR\ over\ control}{Total\ production\ cost}$$

$$Investment\ factor\ (IF) = \frac{Gross\ income}{Total\ production\ cost}$$

The guaranteed price of beans in 2022 in Mexico was used to estimate the gross income indicator (MXN 16000 t^{-1}) (SADER 2022). The cost of production was calculated based on the data of the top five Mexican states producing beans, which were obtained from the Trust Funds for Rural Development (FIRA in Spanish, Table S2). The NPs price used for estimating the cost of the nano-primed treatment was 5750 USD (Perea-Velez et al 2023). To report the economic indicators in terms of USD, the exchange rate used was 19.9 MXN/USD (International Monetary Fund, 2022), which was an average of the exchange rates between 1 and 15 June 2022.

3.4.15. Data analysis

The data were analyzed with the statistical software R version 4.0.3 (R Core Team 2020). The germination data were analyzed through a time-to-event model (Onofri et al. 2018; Romano and Stevanato 2020) because this type of analysis provides more reasonable inferences considering that the germination event did not occur at the specific time of evaluation, but during the interval between evaluations. The parametric and the non-parametric approach were applied to the data analysis. The goodness of fit model was evaluated graphically from the observed versus the predicted values. In the case of the parametric time-to-event model, the likelihood ratio test was performed to compare

the time-to-event models between the different treatments. The model optimization was performed using Akaike Information Criterion (AIC), where the selected model was the one with the lowest AIC. While in the case of no parametric approach to modeling the effect of the experimental factor a Wilcoxon-type statistic was carried out (Onofri et al. 2022). The plant growth (plant height) data were analyzed through repeated measures ANOVA. Afterward, pairwise comparisons between time points at each group level and between group levels were performed using the Bonferroni p-adjust method. On the other hand, an analysis of variance was performed (α=0.05) to compare the effect of seed priming on germination traits, agronomic traits, and seed nutritional quality. Before the ANOVA analysis, the verification of compliance with the assumptions of normality and homogeneity of variances was performed through Shapiro's and Bartlett's tests, respectively. Data that did not observe the assumptions of normality and homogeneity of variance (GP, GR, EP, GE, MGT, relative seed germination *vs* control treatment, number of nodules, fresh weight of nodules) were analyzed through the Kruskal Wallis rank sum test. The data of phytic acid and P grain concentration were box cox transformed. The Tukey honest significant difference test (α=0.05) and the Bonferroni test were used to detect differences between treatments.

3.5. RESULTS AND DISCUSSION

3.5.1. Nano-priming of OTI bean and its effects on the germination variables

The seed Fe concentration, after nano-priming treatment at 10, 20, and 40 mg NPs L^{-1}, were 53.31±3.58, 53.72±6.31, and 57.27±2.99 mg kg^{-1}, respectively. The seed Fe concentration was not significantly (p=0.0571) different from that of unprimed (60.90±0.22) and hydroprimed (53.73±2.99) seeds. Cobalt was not detected in the acid digestion extracts of primed seeds. After a nano-priming treatment, the NPs may or may not be taken up by the seeds. It had been suggested that after nano-priming most of the NPs may remain on the seed surface (Acharya & Pal, 2020; Khan et al., 2023). In this regard, histochemical staining and microscopy analyses were used to confirm that the NPs remained on the seed surface or entered the seeds. Those analyses complemented the information from the atomic absorption analysis since the differences in Fe seed

concentration were not significant compared to the unprimed seeds. By comparing the intensity of the staining, we deduced that NPs were in the hilum (Figure 3.1d-e) and the seed coat (Figure 3.1d). The intensity of blue staining of the cotyledons increased as the NPs concentration increased (Figure 3.1g), and the elemental mapping analysis confirms the presence of Fe and Co in the cotyledons of seeds (Figure 3.1f, and h).

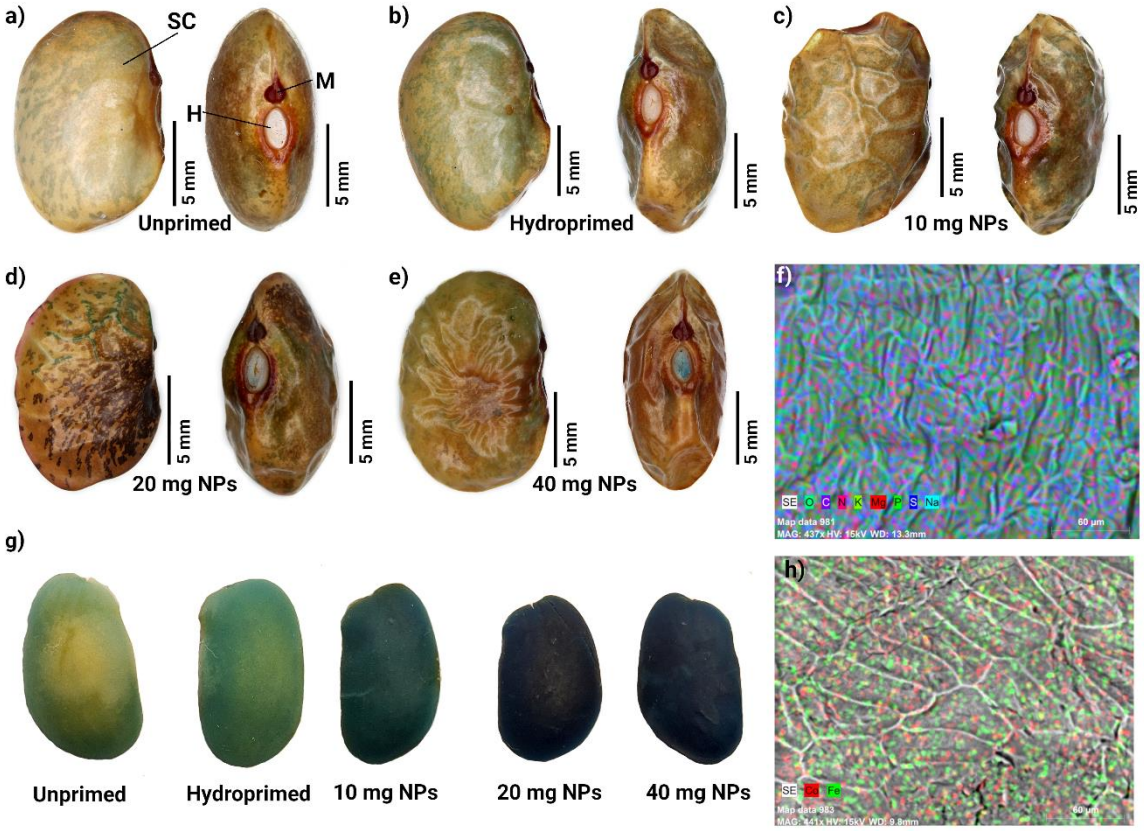

Figure 3.1. Localization of Fe by the Perls' Prussian blue staining and ESEM images of the seed coat and cotyledons. The pictures a-e) the blue stain among the seed coats from the unprimed and primed seeds. Picture g) shows variations in the staining intensity among the cotyledons. Pictures f) and h) show the EDX mapping analysis of the cotyledons of unprimed seed (f), and nanoprimed (h) seed at 40 mg NPs. SC, seed coat; H, hilum; M, micropyle.

On the other hand, the seed water uptake after nano-priming treatment was from 40% ± 3% to 48% ± 4%, but no significant changes (p=0.101) were observed compared to the hydropriming treatment (52.3% ± 5.2%). These results are in contrast with other studies where nano-priming promoted faster water uptake compared to conventional seed priming techniques. For example, Afzal et al. (2021) reported 50% more water

uptake in rice grains imbibed with 20 and 40 mg FeO NPs L^{-1} for 24 h compared to hydropriming and $FeSO_4$ solution (20 mg L^{-1}). Similar results have been observed with other types of NPs as priming agents and other seeds. For instance, the nano-priming of rapeseeds (*Brassica napus* variety Zhongshuang 11) with polyacrylic acid-coated nanoceria (0.1 mM) increased the water uptake by 52% compared to the priming treatment with TES buffer in the first hour of the priming treatment. The increment of water uptake in nanoprimed seeds after 3 and 8 h of imbibition was 14% and 12% more compared to the observed with TES buffer treatment (Khan et al. 2021b). In wheat grains, the nano-priming with ZnO NPs (10 mg L^{-1}) increased the water uptake by 51% compared to the hydropriming treatment after 12 h of imbibition (Rai-Kalal and Jajoo 2021). It had been pointed out that nano-priming accelerates the seed water uptake, however, the mechanisms of water uptake into the seed under the influence of nanomaterials are still unknown (Ighaiee Oskoiee et al. 2021). Moreover, the effects of NPs on plant or seed performance depends on the NPs' properties and concentration, the plant species, and the seed properties (Ighaiee Oskoiee et al. 2021; Khan et al. 2023).

The results of the germination variables are shown in Table 3.1. According to these results and following a traditional approach to evaluate the effect of nano-priming on the germination of OTI beans (using the germination variables, GP, GI, RSG, EP, MGT, and GR), the nano-priming did not affect the germination of OTI beans compared to the hydropriming and control (unprimed seeds) treatments (Table 3.1). In contrast, the time-to-event analysis allowed us to detect differences between treatments on the germination curves. Time-to-event no parametric curves (Figure 3.2c) of control seeds and the nano-primed seed at 10 mg NPs L^{-1} are different from the other treatments, and the Wilcoxon scores confirmed this observation. The sum of the Wilcoxon scores for the control and the nano-primed seeds at 10 mg NPs L^{-1} was 7.57 and 3.57, respectively, while negative values were observed for the hydroprimed seeds (-2.08), and the nano-primed seeds at 20 mg NPs L^{-1} (-2.54), and 40 mg NPs L^{-1} (-6.52). Hence, the germination of the control and nano-primed seeds at 10 mg NPs L^{-1} was, on average, the fastest compared to the other treatments. A similar conclusion can be made from the parametric time-to-event curves because the lowest median germination time estimated was that from the control and the nano-primed seeds at 10 mg of NPs L^{-1} (Table 3.2). In general, the parametric

approach of time-to-event models is well suited to make inferences about the underlying biological mechanisms of the process, in this case, germination (Onofri et al. 2022). On the other hand, the likelihood ratio test for the parametric log-logic time-to-event model curves of the treatments (p-value= 0.0164) indicated that the germination curves are different from one another (Figure 3.2b). And according to the AIC criterion, the best model in descending order is control > 10 mg NPs > hydropriming >40 mg NPs >20 mg NPs curves, meaning that the control seeds germinated faster than those with priming treatments.

Table 3.1. Influence of nano-priming with citrate-coated $CoFe_2O_4$ NPs on the seed water uptake and germination variables of OTI bean.

Variable	Treatment				
	Control	Hydropriming	10 mg NPs	20 mg NPs	40 mg NPs
Seed water uptake after nano-priming (%)	—	52 ± 5.2	47 ± 7.5	48 ± 4.1	40 ± 3.4
Final germination (%)	97 ± 5.8	93 ± 5.8	100 ± 0.0	93 ± 5.8	90 ± 0.0
Germination index	—	0.79 ± 0.29	1.13 ± 0.86	0.75 ± 0.20	0.91 ± 0.25
Relative seed germination I * (%)	—	—	107 ± 0.0 a	100 ± 6.2 ab	96 ± 0.0 b
Relative seed germination II * (%)	—	97 ± 6.0	103 ± 0.0	97 ± 6.0	93 ± 0.0
Energy period (d)	2.7 ± 0.6	3.0 ± 0.0	3.0 ± 0.0	3.0 ± 0.0	3.3 ± 0.6
Germination energy (%)	97 ± 5.8	90 ± 10.0	100 ± 0.0	87 ± 15.3	90 ± 0.0
Mean germination time (d)	2.5 ± 0.2	3.0 ± 0.3	2.7 ± 0.2	3.0 ± 0.1	3.1 ± 0.4
Germination rate	3.9 ± 0.1	3.3 ± 0.5	3.8 ± 0.2	3.3 ± 0.3	3.0 ± 0.5

Mean ± standard deviation of n=3. Different letters represent significant differences between treatments (Tukey α=0.05).

*The relative germination (RSG) I considered the number of germinated seeds in the hydropriming treatment, while RSG II considered the germinated seeds in the control treatment.

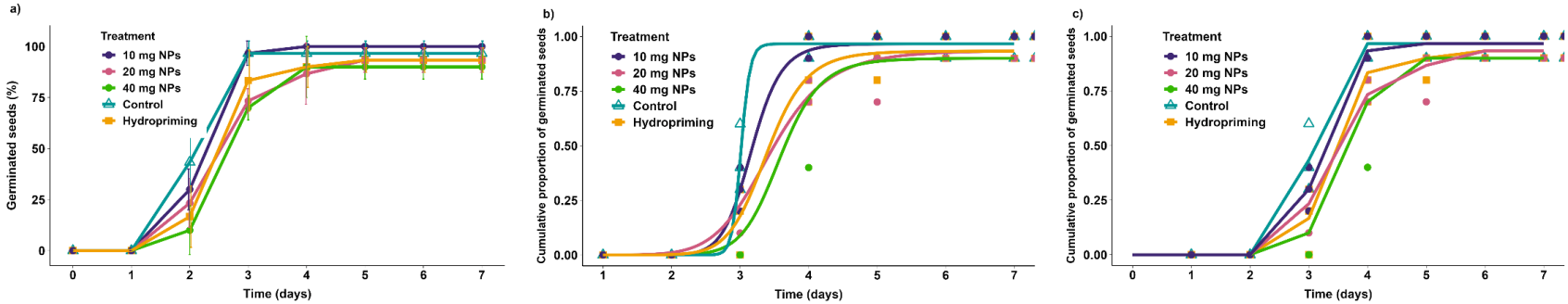

Figure 3.2. Effect of nanopriming on the germination of OTI bean. a) The germination curve of OTI bean, b) the fitted parametric log-logistic model time-to-event, and c) the no parametric model time-to-event. For the time-to-event curves, markers represent the observed data and lines show the time-to-event model fit.

Table 3.2. Parameter estimates from the time-to-event model fitted and the Akaike Information Criterion (AIC) indicator for the germination of OTI beans after priming treatment.

Parameter	Treatment				
	Control	Hydropriming	10 mg NPs	20 mg NPs	40 mg NPs
Slope	27.40 (29.26)	11.77* (2.19)	14.67* (2.58)	8.21* (1.52)	12.37* (2.35)
Germinate fraction	0.97* (0.03)	0.93* (0.05)	0.97* (0.03)	0.94* (0.05)	0.90* (0.05)
Median germination time†	3.01* (0.13)	3.39* (0.11)	3.17* (0.09)	3.44* (0.15)	3.59* (0.12)
AIC indicator	90.69	106.62	94.79	123.15	108.45

† Mean germination time for the germinate fraction; * indicates that the estimate was significant according to the parametric time-to-event model at α=0.05; data in parentheses are standard errors of estimates.

The phenotypic characteristics of seedlings developed from all nano-primed seeds were normal without visible signs of toxicity (Figure S2). The nano-priming treatment had not affected the fresh (p=0.066), and dry weight (p=0.176) of seedlings, the average root length (p=0.068), the root diameter (p=0.195), and the number of roots (p=0.313; Table 3). No significant differences (p=0.061) were found between the vigor index of seedlings from the nano-primed treatment and the control treatment (Table 3.3). Our observations contrast with the studies that stated that the nano-priming accelerates or enhances germination, and improves seedling growth and vigor in different plant species (Ighaiee Oskoiee et al. 2021; Kandhol et al. 2022). In rice, nano-priming with FeO NPs at 20 and 40 mg L^{-1} increased radicle length by 50% and plumule length by 22% compared to the hydroprimed treatment (Afzal et al. 2021). Pawar et al. (2019) found that Fe_2O_3 NPs at 4-8 mg L^{-1} significantly enhanced the radicle length and plumule length of chickpea (*Cicer arietinum* L variety Digvijay) seedlings.

Table 3.3. Phenotypic characteristics of seedlings developed from unprimed or nano-primed seeds.

Variable	Treatment				
	Control	Hydropriming	10 mg NPs	20 mg NPs	40 mg NPs
Fresh weight seedling (g)	0.8 ± 0.1	0.8 ± 0.1	1.0 ± 0.0	0.8 ± 0.1	0.9 ± 0.1
Average root length (cm)	19.4 ± 7.7	16.0 ± 6.5	29.3 ± 2.1	15.2 ± 4.6	19.0 ± 5.1
Primary root length (cm)	5.5 ± 1.1 a	3.9 ± 0.8 ab	5.5 ± 0.1 a	3.5 ± 0.6 b	4.2 ± 1.0 ab
Root diameter (cm)	0.20 ± 0.01	0.18 ± 0.02	0.21 ± 0.01	0.17 ± 0.02	0.21 ± 0.04
Number of roots	10 ± 2	12 ± 0	13 ± 3	9 ± 2	12 ± 3
Cotyledon length (cm)	1.5 ± 0.0	1.6 ± 0.1	1.6 ± 0.1	1.5 ± 0.2	1.6 ± 0.1
Dry seedling weight (g)	0.17 ± 0.09	0.19 ± 0.01	0.20 ± 0.00	0.17 ± 0.02	0.18 ± 0.01
Vigor index (%)	16 ± 0.98 ab	18 ± 2.47ab	17 ± 0.80 a	16 ± 1.73 b	20 ± 0.18 ab

Mean ± standard deviation of n=10. Different letters represent significant differences between treatments (Tukey α=0.05).

3.5.2. Effect of nano-priming on the life cycle of OTI bean plants and the agronomic traits

From seeds that were primed, between 80% and 100% seedling emergence was observed 8 days after sowing (Figure 3.3a). 100% of seedling emergence was recorded 11 days after sowing. Overall, the plants (from unprimed and primed seeds) had a shorter growing duration (81-83 days after sowing) compared to the varietal description (110-130 days after sowing), and the flowering occurred 11 days before the expected time (Figure 3.3b).

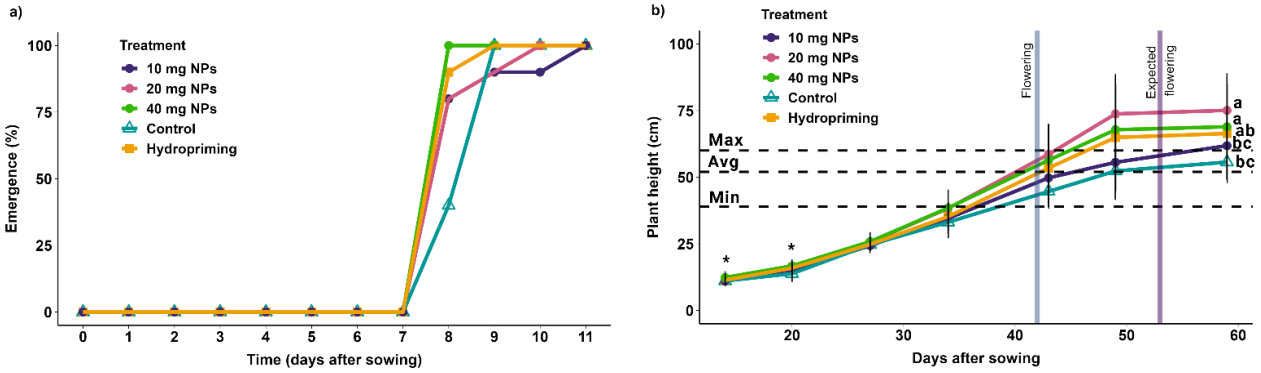

Figure 3.3. Effect of nano-priming on the emergence and plant growth of OTI bean. a) Emergence curve, and b) growth curve. The dotted line represents the Max, maximum; Avg, average; and Min, minimum plant height reported in the varietal description. * symbol represents that the simple main effect of nano priming treatment was significant according to the repeated measures analysis. Different letters represent significant differences between growth curves according to the Bonferroni p-adjusted method.

Plant height (R2, flowering) from primed seeds was higher than the maximum reported in the varietal description (Figure 3.3b). The simple main effect of nano-priming treatment was significant on day 14 (p-value=0.018) and 20 (p-value=0.013), among treatments with NPs at 10 and 20 mg L^{-1} (Figure 3.3b). When comparing the plant growth curve (Figure 3.3b), plants from treatments with NPs at 20 and 40 mg L^{-1} were taller than those of the control and NPs treatment at 10 mg L^{-1}. On the other hand, in terms of the vegetative growth parameters (Table 3.4), the plant performance until the flowering stage was not affected by the nano-priming treatment compared to the control or hydropriming treatment ($p>0.1$).

Table 3.4. Vegetative growth parameters of OTI bean plants from primed seeds at the flowering stage (R2, 51 days after sowing).

Treatment	Plant height (cm)	FW aerial part (g)	FW root (g)	Foliar area (m^2)	DW root (g)	DW aerial (g)	FW nodules (g)	Number of active nodules
Control	43.9 ± 5.1	120.3 ± 19.9	33.8 ± 16.4	0.26 ± 0.02	3.8 ± 0.8	15.8 ± 2.5	0.4 ± 0.3	32 ± 20
Hydropriming	49.1 ± 6.6	125.5 ± 7.8	39.8 ± 3.7	0.28 ±0.02	4.0 ± 0.6	15.7 ± 1.4	1.1 ± 1.7	34 ± 21
10 mg NPs	57.6 ± 13.2	141.8 ± 12.6	45.1 ± 9.5	0.31 ± 0.02	4.4 ± 0.8	17.3 ± 2.8	1.6 ± 2.4	99 ± 133
20 mg NPs	53.6 ± 11.1	132.1 ± 3.1	32.2 ± 2.8	0.30 ±0.03	3.7 ± 0.7	15.8 ± 0.6	0.6 ± 0.9	31 ± 6
40 mg NPs	56.4 ± 12.5	129.8 ± 30.8	37.3 ± 8.9	0.29 ± 0.04	3.8 ± 1.2	17.3 ± 3.8	0.7 ± 0.7	50 ± 17

Mean ± standard deviation of n=4. FW, fresh weight; DW, dry weight.

Table 3.5. Nutritional status of plants of OTI bean at the flowering stage (R2, 51 days after sowing), and reference values.

Treatment	N	P	K	Ca	Mg	Zn	Fe	Cu
			(%)				mg kg^{-1}	
Control	28.6 ± 5.4	0.3 ± 0.0	3.7 ± 0.1	6.8 ± 1.6	1.1 ± 0.1	47.1 ± 0.3 ab	487.3 ± 152	15.3 ± 2.5
Hydropriming	28.8 ± 3.8	0.3 ± 0.0	3.8 ± 0.4	6.0 ± 1.4	1.0 ± 0.1	47.5 ± 2.4 ab	418.5 ± 95	11.4 ± 7.0
10 mg NPs	28.5 ± 3.7	0.3 ± 0.0	3.8 ± 0.7	6.6 ± 0.9	0.9 ± 0.1	45.1 ± 3.6 b	472.3 ± 125	10.3 ± 3.4
20 mg NPs	25.2 ± 2.5	0.3 ± 0.0	3.4 ± 0.3	5.9 ± 1.5	0.9 ± 0.1	57.9 ± 9.4 a	305.7 ± 230	12.4 ± 5.2
40 mg NPs	29.3 ± 3.8	0.3 ± 0.0	3.3 ± 0.4	4.9 ± 1.7	0.9 ± 0.1	47.6 ± 4.0 ab	510.6 ± 160	8.1 ± 1.7
				Reference values				
Sufficient or normal	4.25 – 6.0[†]	0.30 – 6.00[†]	>2.0[†]	0.8 – 3.0[†]	>0.30[†]	25.0 – 150.0[δ]	25.0 – 300.0[†]	5.0 – 30.0 [δ]

Mean ± standard deviation of n=4. Different letters represent significant differences between treatments (Tukey α=0.05).
Reference values for interpreting plant analyses according to [δ] Kabata-Pendias (2010), and [†]Plank and Kissel (1989).

The nutritional status of plants at the flowering stage (R2, 51 d after sowing) was within the normal values of reference for macro and micronutrients for soybean and other beans (Table 3.5), except for N, Ca, Mg, and Fe; the concentration of these elements were higher than the common values found for beans. When comparing the plants from the nano-priming treatments with the control and hydropriming treatments, no significant differences were observed in the concentration of macronutrients (N, P, K, Ca, and Mg) and Fe, and Cu. Nevertheless, the Zn concentration in the leaves of plants from the treatment with 20 mg NPs L^{-1} was higher than that in plants from the treatment with 10 mg L^{-1} of NPs.

Regarding nodule formation at the flowering stage (51d after sowing), the number of active nodules and their fresh weight were statistically similar between the treatments (Table 3.4). A negative correlation between the number of active nodules, their fresh weight (p= -0.64), and K in leaves (p= -0.64) was found. It is worth mentioning that the observed nodules were the product of the native rhizobia present in the soil. The soil used has a history of growing maize plants, and symbiotic bacteria like *Rhizobium etli* are naturally associated with the rhizosphere of maize and inside their roots (Rosenblueth & Martínez-Romero, 2004). On the other hand, the reduction of acetylene (to C_2H_4) was only detected in nodules of plants from the 40 mg kg^{-1} nano-primed seeds. The produced C_2H_4 was 2.57±0.01 moles h^{-1} $plant^{-1}$.

At the R9 stage (81 d after sowing), the plants from the 40 mg L^{-1}nano-primed seeds had the largest number of total nodules compared to the control plants, and the plants from the hydropriming treatment (Table 3.6). Meanwhile, the heaviest nodules were observed in plants from the 20 mg L^{-1} nano-primed seeds compared to that from the control plants (Table 3.6). The change in the number of total nodules between the flowering stage and the plant maturity was 0.25 folds in control plants, 1.47 in plants from the hydropriming treatment, 0.36 folds in plants from the nano-priming at 10 mg L^{-1}, 3.38 folds in plants from the nano-priming at 20 mg NPs L^{-1}, and 2.74 folds in plants from the nano-priming treatment at 40 mg L^{-1}. Root infection kept occurring in plants from the nano-priming treatments and hydropriming between the flowering and plant maturity, however, a destructive sampling is recommended to ensure that those new nodules were active in

that period since the root nodules have a short life span (12-18 d; Fedorova et al., 2021), and 28 days passed between flowering and harvesting. Promotion of the nodulation and extension of the nodulation period on soybean and common bean plants by ferrite NPs and Fe_3O_4 treatments has been observed by Ma et al. (2021), Ma et al. (2022), Wang et al. (2022), and De Souza-Torres et al. (2021). Ma et al. (2021) evaluated the effect of Fe and Fe-Co-based NPs on the nodulation of soybean plants (*Glicine max* L. Meer "Williams 82" 28 days old plants). The plant growth substrate (sand) was amended with NPs at a dose from 1 to 100 mg kg^{-1}. The authors reported a significant enlargement of nodules (~30%) and a large number of total nodules (~30%) after treatment with $CoFe_2O_4$ (10 mg kg^{-1}) compared to the control treatment (without amendment of NPs). De Souza-Torres et al. (2021) assessed the effects of Fe_3O_4 NPs or in combination with *Rhizobium leguminosarum* CF1 strain inoculation on nodulation, nitrogen fixation, and growth of common bean (cv. Red Guama, *Phaseolus vulgaris*). This study was a pot experiment (pot capacity ~484 cm^3), and loam soil was used. The NPs were added through the irrigation water at a concentration of 40 mg L^{-1} per day over 35 d. The authors found that treatment with NPs increased the number of active nodules per plant by 59%, and the nodule dry weight by 40% compared to the control. Ma et al. (2022) evaluated the effect of $MnFe_2O_4$ NPs on the nodulation of soybean plants. The NPs (0.1-100 mg L^{-1}) were mixed with the plant growth substrate (vermiculite), and the inoculation of *Rhizobium* was done one week after planting the seedlings. The NPs treatment significantly increased the number of nodules and the nodule weight by 61% and 51%, respectively, compared to the control treatment (without NPs). The NPs treatment (10-100 mg L^{-1}) enhanced the nitrogen fixation (evaluated by the analyzing the reduction of acetylene) by 1.99 to 2.51 times relative to the control treatment. The transcriptomic analysis showed that genes related to the nodulation were upregulated 12 d post inoculation of *Rhizobium*, meaning an extending period of the nodulation by the effect of the NPs. Wang et al. (2022) evaluated the effect of foliar application of Fe_3O_4 NPs on soybean (*Glycine max).* The foliar application of Fe_3O_4 NPs increased the number of root nodules by 35% compared to the control (unexposed). The studies mentioned above are not seed-priming experiments, and it is hard to compare results since they differ in the experimental conditions, crops, and practices to supply the NPs. However, they illustrate the potential

effect of NPs on nodulation. Once again, it should be highlighted that the impact of NPs on the plant depends on the properties of the NPs, their concentration, application method, time of application, plant species, and the surrounding medium.

At harvesting time (81 d after sowing), the nano-priming and hydropriming treatments did not have significant effects on the dry weight of the plants ($p=0.947$), stem diameter ($p=0.754$), and agronomic traits (Table 3.6). On the other hand, the number of pods per plant and the grain yield per plant were ~37 % below the reported data in the varietal description. The pod size, the number of seeds per pod, and the seed index (the weight of 100 seeds) were within the values reported in the varietal description.

Table 3.6. Physiological and agronomic traits of OTI bean plants (R9 stage, 81 days after sowing) from unprimed and primed seeds.

Variable	Treatment					Varietal description†
	Control	Hydropriming	10 mg NPs	20 mg NPs	40 mg NPs	
DW plant aerial part (g)	16.6 ± 3.6	15.8 ± 3.3	12.8 ± 3.1	16.4 ± 5.3	14.8 ± 0.2	—
DW root (g)	4.3 ± 0.7	4.5 ± 0.9	4.2 ± 0.9	4.6 ± 1.6	4.6 ± 0.4	—
Stem diameter (mm)	6.9 ± 0.3	6.8 ± 0.6	6.2 ± 1.3	6.8 ± 0.8	6.8 ± 0.4	—
Total nodules	40 ± 25 c	84 ± 55 bc	123 ± 56 abc	136 ± 40 ab	187 ± 35 a	—
Nodules weight (g)	0.6 ± 0.4 b	1.1 ± 0.7 ab	1.0 ± 0.7 ab	2.8 ± 1.9 a	2.2 ± 0.2 ab	—
Pods per plant	20 ± 1	22 ± 2	21 ± 1	20 ± 4	19 ± 3	54
Pod length (cm)	11.2 ± 0.3	11.1 ± 0.3	11.0 ± 0.0	10.9 ± 0.9	11.0 ± 0.3	10.5
Pod width (cm)	1.1 ± 0.0	1.1 ± 0.1	1.0 ± 0.0	1.0 ± 0.1	1.0 ± 0.0	0.9
Seeds per pod	5 ± 1	4 ± 0	5 ± 3	4 ± 1	4 ± 0	5
Number of seeds per plant	95 ± 11	93 ± 10	96 ± 35	88 ± 21	82 ± 10	—
Grain yield per plant (g)	24.9 ± 3.1	22.8 ± 2.4	22.0 ± 5.2	23.0 ± 4.2	22.7 ± 1.4	48-93 Average 63
Seed index	26.1 ± 2.3	24.6 ± 2.5	23.0 ± 7.5	26.4 ± 1.8	27.9 ± 1.4	26-33
Harvest index	1.5 ± 0.2	1.5 ± 0.4	1.8 ± 0.8	1.5 ± 0.5	0.8 ± 0.9	—

Mean ± standard deviation of n=6. Different letters represent significant differences between treatments (Tukey α=0.05). DW, dry weight. †Data from Estrada-Gómez et al. (2004)

3.5.3. Effect of nano-priming on the nutritional quality of OTI bean seeds

Beans are featured by their high protein and mineral content compared to cereals (Chávez-Mendoza and Sánchez 2017; Jaspers et al. 2019). In the present research, the protein content overall treatments ranged between 106% and 137%. Despite the lack of significant differences between offspring seeds from the primed seeds (nano and hydroprimed), the control, and the original seed, the protein concentration was higher than the reported protein content in Mexican beans varieties (14% and 33% (Chávez-Mendoza and Sánchez 2017). In addition, the protein content in seeds from the nano-priming treatment was 28%-30% less than that of the high Fe from bean varieties of the HarvestPlus program.

The nano-priming had a significant effect on the mineral composition of bean seeds (Table 3.7). The offspring seeds of plants from nano-primed seeds at 20 mg NPs L^{-1} had higher K concentration than that from plants of the hydropriming or control treatment, and higher P seed concentration compared to the hydroprimed treatment. Unexpectedly, the highest Zn grain concentration was found in the offspring seeds from plants grown from 10 and 40 mg NPs L^{-1} nano-primed seeds compared to that from the control, hydroprimed, and original seeds. The Zn concentration observed in seeds was higher than the value range for the Mexican bean varieties (Table 3.7), and the average Zn in beans (28 - 31 mg kg^{-1}) from other regions around the globe (Huertas et al. 2022). Even the Zn concentration in beans from the nano-primed treatments was 29% higher than extreme values observed in beans, such as 77 mg Zn kg^{-1} (Huertas et al. 2022). The target level for Zn biofortification is 17 mg kg^{-1} above the local materials (Beebe 2020). Thus, offspring seeds from the primed seeds can be considered biofortified, because the Zn concentration was between 32 and 59 mg kg^{-1} above the average Zn concentration for Mexican bean varieties. In addition, the Zn concentration in offspring seeds from the 10 and 40 mg NPs L^{-1} primed seeds compares with those found in animal products where the Zn concentration range between 23 and 170 mg kg^{-1}, dry weight basis (Huertas et al. 2022).

Table 3.7. Mineral composition, phytic acid concentration, and phytic acid: iron or zinc (phy:Fe, phy:Zn) molar ratio of OTI bean seeds from plants of primed or unprimed seeds.

Treatment	Ca	Mg	K	P	Protein	Fe	Zn	Cu	Phytic acid	Phy:Fe molar ratio	Phy:Zn molar ratio
	(%)					(mg kg^{-1})					
Control	0.06±0.01 ab	0.18±0.01	1.71±0.15 c	15.7±1.4 ab	106.9±14.2	67.2±1.9	78.9±14.3 b	5.4±0.8	0.47±0.04 a	5.7±0.5	5.96±0.97 a
Hydropriming	0.10±0.03 ab	0.17±0.01	1.91±0.14 abc	12.8±3.0 b	135.3±39.1	70.7±4.1	77.8±5.2b	4.9±0.8	0.43±0.05 ab	5.2±1.0	5.56±0.82 a
10 mg NPs	0.09±0.02 ab	0.17±0.01	1.76±0.06 ab	17.2±2.7 ab	127.4±12.3	62.9±2.1	100.1±1.3 a	4.2±0.9	0.35±0.08 ab	4.9±1.5	3.51±0.86 b
20 mg NPs	0.11±0.03 a	0.18±0.01	1.98±0.06 a	22.1±4.5 a	136.7±18.8	68.1±7.01	84.1±6.8 ab	4.4±0.1	0.38±0.01 ab	5.1±1.1	4.72±0.93 ab
40 mg NPs	0.10±0.00 ab	0.18±0.00	1.93±0.06 ab	14.0±1.7 b	133.2±18.1	74.9±9.2	82.8±7.6 a	5.0±0.5	0.40±0.07 ab	4.6±0.8	4.85±0.93 ab
Original seed	0.08±0.01 ab	0.17±0.01	1.85±0.08 abc	14.0±10.3 b	135.6±10.6	73.2±0.3	78.9±0.6 b	4.9±0.0	0.47±0.01 a	5.4±0.1	5.91±0.11 a
Reference values											
Mexican varieties*, δ	0.11–0.57	0.11–0.13	0.85–0.95	0.27–0.36	14–33	35–58	27–41	1.14–2.02	0.98–2.16		
HarvestPlust†					190–230	64–119					

Reference values of the mineral composition of bean seeds for Mexican varieties according to *Chávez-Mendoza and Sánchez (2017), and δEspinoza-García et al. (2016).
†Reference values for protein and Fe reported for the bean varieties of the HarvestPlus program (HarvestPlus 2022)

In contrast, no significant effects due to the nano-priming treatment were observed on the Ca, Mg, Fe, and Cu concentrations in the offspring seeds. Nevertheless, the Fe seed concentrations among treatments were higher than the average Fe concentration reported for seeds of Mexican bean varieties (35-58 mg kg^{-1}), but below the target concentration for biofortification (140 mg kg^{-1}). According to the CIAT, the target Fe concentration for beans must be at least 94 mg Fe kg^{-1} above the concentration of local varieties (Huertas et al. 2022).

In this experiment, no external source of macro or micronutrients was added to the soil, because soil nutrient content (Table S-1) was high enough to fulfill the nutrient demands of beans (53 kg N t^{-1}, 8 kg P t^{-1}, 55 kg K t^{-1}, 40 kg Ca t^{-1}, 8 kg Mg t^{-1}, 271 g Fe t^{-1}, 90 g Cu t^{-1}, and 192 g Zn t^{-1}; Ayala Garay et al., 2021). However, the combination of the seed priming technique with adequate fertilization for biofortification objectives may enhance the Fe content in seeds. The effectiveness of agronomic biofortification depends on a variety of variables, such as, the state of soil micronutrients and their availability, cropping system, nutrient-allocation and translocation of nutrient to the edible parts of crops (Jan et al. 2020). For instance, in wheat, the combination of seed priming with Zn solutions and Zn soil fertilization increased the Zn grain concentration over the control by 36% (Umar and Hussain 2022). NPs soil fertilization demonstrated an increase in the Fe grain concentration in wheat seeds by 1.37 and 0.26 folds above the target Fe concentration for biofortification (60 mg kg^{-1}) of wheat (Perea-Vélez et al., 2023). On the other hand, the success of fortification strategies needs a comprehensible understanding of how Fe acquisition in plants is affected (Rai et al. 2021), and despite the extensive knowledge, relatively little information is available on Fe (and also Zn) uptake process in common bean (Huertas et al. 2022).

The potential nutritional impact of consuming fortified beans depends on their concentration of anti-nutritional compounds, like phytic acid, polyphenols, lectins, and tannins. Among those compounds, it is suggested that phytic acid is one of the major and significant inhibitors of mineral bioavailability (and thus uptake) from beans, followed by polyphenols (Hummel et al. 2020). The phytic acid concentrations (PA) ranged from 0.35 to 0.40 g 100 g^{-1} for the offspring seeds of the plants grown from nano-primed seeds. The

PA concentration observed between the control treatment and the primed treatments were statistically similar. However, the PA concentration of tested seeds was below the average phytic acid concentration reported for Mexican bean varieties, and bean seeds around the world (from 0.4 to 2.6 g $100g^{-1}$) (Petry et al. 2015). The relative bioavailability of Fe and Zn was determined based on the phytic acid to mineral molar ratios. In the case of Fe, the PA:Fe molar ratio was 5:1 on average, and no significant effect was found of the nano-priming treatment. Likewise, these PA:Fe ratios were lower than the range (from 6:1 to 33:1) observed in different bean seeds around the world (Petry et al. 2015). For Zn, the lowest ratio (3:1) was observed in seeds from the plants from primed 10 mg NPs L^{-1}seeds. Both values can be interpreted as low bioavailability compared to the recommended values (1:1) for adequate bioavailability (Castro-Alba et al. 2019).

3.5.4. Economic evaluation, benefits, and challenges of nano-priming seed treatment

The gross income estimated for the primed treatments was from 3,590.79 to 3,139.75 USD per ha (Table 3.8). Meanwhile, the gross income from unprimed seeds was 3,521.79 USD. No significant differences ($p=0.83$) were observed in the gross income by the effect of primed treatments. However, the profitable return of nano-priming treatments over the control (unprimed seeds) was between 163.08 and 524.70 USD less. The negative profitable return of nano-priming treatments over the unprimed control can be explained by the relatively low (but not statically significant) grain yield (Table 3.6) of plants from the nano-primed seeds.

Seed priming can be a commercially viable form of incorporating NPs into agriculture because it is inexpensive and easier to implement compared to the soil or foliar application of nano-fertilizers. For example, our calculated cost of nano-priming bean seeds (with citrate-coated $CoFe_2O_4$ NPs) ranged from 121 to 143 USD per ha and used a concentration suspension from 10 to 40 mg NPs L^{-1}. For wheat fortification, the estimated cost ranged from 44,283 to 65,523 USD per ha for soil fertilization (98-145 mg $CoFe_2O_4$ NPs kg^{-1}), and 1,553 USD for foliar fertilization per ha (Perea-Vélez et al., 2023). It should be highlighted that the cost of soil fertilization depends greatly on the nutritional

status of soils (FAO 2022), and the residual effect of NPs in soil should be considered too (Perea-Vélez et al., 2023).

Table 3.8. Economic indicators for the economic evaluation of the nano-priming seed treatment of OTI bean per hectare of cultivated land.

Treatment	Gross income (USD)	Cost of production (USD)	Profitable return (USD)	Profitable return over control (USD)	Benefit-cost ratio	Investment factor
Control	3,521.78	936.89	2,584.89			3.76
Hydropiming	3,590.79	937.65	2,653.14	68.25	0.07	3.83
10 mg NPs	3,479.80	1,057.99	2,421.82	-163.08	-0.15	3.29
20 mg NPs	3,421.55	1,065.18	2,356.38	-228.52	-0.21	3.21
40 mg NPs	3,139.75	1,079.56	2,060.19	-524.70	-0.49	2.91

The potential cost of nanotechnology is a key concern among farmers, and one of the main factors considered to invest in this new technology (Siimes et al. 2022). Farmers from the wine industry of New Zealand expressed acceptance of this novel technology if the nanotechnology can significantly reduce the cost of production, or the production time, or increase the quality without increasing cost. Indeed, they also expressed that the profitable return could be sacrificed in pursuit of quality (Siimes et al. 2022). As mentioned above, nano-priming is a cheaper approach for implementing the use of NPs to improve seed germination, seedling establishment, and the complete life cycle of the plant compared to the foliar or soil supply of NPs. For OTI bean cultivar, we found that nano-priming of the seeds did not affect the germination, but the plant height, total number of nodules, and seed P, K, and Zn concentrations were higher than those for the unprimed control. These results might be attractive for farmers.

The effects of nano-priming on other bean varieties should be assessed to know their responses and to improve the nano-priming technology since some studies have reported that seed priming did not affect the germination of seeds, but it may burst in plant development throughout the life cycle of the plant (do Espirito Santo Pereira et al. 2021; Ighaiee Oskoiee et al. 2021), and our results agree with those observations. For instance, Acharya et al. (2020) examined the effects of nano-priming with AgNPs on two varieties of watermelon (*Citrullus lanatus*) seeds in three locations over three years (2017-2019).

In 2017, no significant differences were observed in the days required for 50% seed germination, final germination percentage, and the emergence percentage of the Riverside variety watermelon compared to the unprimed seeds. However, in 2017, seed priming of Riverside watermelon increased significantly the yield compared to that of the plants from unprimed seeds, meanwhile, the fruit quality was not modified.

On the other hand, despite the up costs of nano-priming of seeds treatment compared to the control (unprimed), the benefits may be greater in the long term. For example, if seed priming can extend the period of nodulation without threatening the vegetative growth of plants while improving agronomic traits or food quality; an opportunity is opened to lower the environmental impact of agriculture because global legume-rhizobial symbioses are estimated to fix 21 Mt of N annually, representing approximately one-tenth of ammonia applied annually synthesized by the Haber-Bosch process (Huertas et al. 2022). Moreover, scope 2 emissions, indirect greenhouse emissions associated with bean cropping, may be reduced, due to the global legume-rhizobial symbioses estimated to save CO_2 emissions of over 150 Mt annually (Huertas et al. 2022). Improving the life quality of the population of rural and marginalized areas can be another impact of the nano-priming seeds. In the case of the common bean, the land dedicated to its production is ~33 M hectares globally. In Africa, 5 million hectares of the bean are cultivated by smallholder farmers, most of whom are women (Huertas et al. 2022). The average consumption of common beans in Latin America ranges from 10 to 18 kg per person annually, meanwhile, in Africa, it can reach 50 kg per person per year (Huertas et al. 2022). Thus, nano-priming could be a complementary approach to producing beans, while enriching the soils via biological nitrogen fixation and enhancing the nutritional quality of bean grains.

Despite the benefits of nano-priming, one of the drawbacks of the seed priming technique is that there is no standard protocol that can be followed blindly (Paul et al. 2022). It requires standardization before application to determine the appropriate “stop-time”, and re-drying (Paul et al. 2022) because these variables greatly depend on the plant species and properties of seeds. Thus, the lack of standardization of the priming

technique prevents a convincing evaluation of the benefits of seed priming. Therefore, the main challenge of seed priming is standardization.

3.6. CONCLUSIONS

The nano-priming technique may be a complementary tool for the biofortification of beans. We obtained encouraging results although no external source of nutrients was added to the bean plants. We cannot confirm the hypothesis that nano-priming may improve the germination traits compared to the unprimed seeds and enhance the yield of bean plants. The effects of nano-priming with citrate-coated $CoFe_2O_4$ NPs affected the plant growth curve, nodulation, and mineral content of bean seeds. Nano-priming improved the nutritional quality of bean seeds in terms of Zn, P, and K concentration. A low phytic acid:Zn molar ratio was observed for offspring seeds from the 10 mg L^{-1}nano-priming treatment. In addition, the low cost of nano-priming of seeds may be a feasible approach to enhance the mineral content of beans and potentially contribute to the transition to a more sustainable agri-food system; as well as to enhance the nutritional security in rural and marginalized areas because it is an easy and low-cost tool. However, for its agronomical adoption and more homogenous plant response, standardization of the protocols is highly recommendable, not only for conventional seed priming but also for seed nano-priming.

GENERAL DISCUSSION

Citrate-coated $CoFe_2O_4$ NPs as nano-fertilizer: tiny particles, big questions

Nanotechnology offers potential solutions for sustainable agriculture, such as boosting the efficacy of agricultural inputs while reducing its environmental footprint, saving labor costs, increasing the nutrient efficiency of crops, improving the efficacy of pest management, or enhancing the nutritional quality of food (Perea Vélez et al. 2021; Rahman et al. 2021; Agrawal et al. 2022). Laboratory studies of these promising results were presented in Chapter 1 of this work. However, the potential of nano-enabled plant agriculture is still in the stage of development (Raliya et al. 2018; Kah et al. 2019; Hofmann et al. 2020).

Hofmann et al., (2020) and Siimes et al., (2022) highlighted several major barriers to field-scale delivery of nanomaterials such as the regulatory and safety concerns, the economic feasibility, and consumer acceptance which prevent wide-scale application and the full potential of nanotechnology for agriculture. In this regard, this research addressed some of these key topics, related to application methods and economic feasibility, bearing in mind that this work aimed at the agronomic biofortification of wheat and bean.

For nano-fertilizers, soil, and foliar application are the conventional methods of delivery, and limited information exists about their applications at the field scale (Hofmann et al. 2020). The characterization of nanomaterials and the matrix where they will be delivered are fundamental for choosing the application method, even designing the formulation (nano-fertilizer as NPs suspension or as dry powder). For citrate-coated $CoFe_2O_4$ NPs, I observed that their application on soil could be successful because of their chemical stability in soil solution, and their dissolution by the effect of artificial root exudates. On the one hand, I found that the citrate-coated $CoFe_2O_4$ NPs are slightly soluble to practically insoluble in the soil solution at pH 5, 7, and 8. In contrast, the dissolution of NPs was observed by the effect of artificial root exudates. Hence, it can be expected that the Fe contained in the particle will not be immediately fixed in the soil after their application compared to the soluble Fe fertilizers or Fe-chelates, because the Fe and Co release will be controlled by the dissolution activities of the plant root instead of

hydrolysis or diffusion mechanism (Chandra et al. 2009; Perea-Velez et al. 2022). However, further information about the role of soil microorganisms in the NPs solution or the fate and NPs transformation after their application in soil should be generated. On the other hand, the aggregation/agglomeration of NPs for soil applications could result in significant deposition of the NPs in soil, but lower Fe and Co bioavailability (Cervantes-Avilés et al. 2021; Perea-Velez et al. 2022). Meanwhile, for the foliar applications, aggregation/agglomeration of NPs (216±10 nm) could be a problem since size exclusion of NPs may occur, because stomata have been suggested as the principal route for NPs uptake (Avellan et al. 2021). Another issue related to using nano-suspensions for foliar application is the potential deposition of agglomerates/aggregates on the leaf surface (Dimkpa and Bindraban 2018).

Environmental friendliness of nano-fertilizers is part of the safety concerns (Siimes et al. 2022), this issue is also related to the fertilizer rate, the fertilizer efficiency, and the nutrient use efficiency (NUE) of crops (Rahman et al. 2021; Zahra et al. 2022). Using a proper fertilizer in the right amount is one of the most important strategies to increase fertilizer efficiency (Rawal et al. 2022). Therefore, I tried to follow the 4R approach (right source, right rate, right time, and right place), which means that the concentration of NPs applied was chosen based on the capacity of the soil to fix iron. The rate of NPs application was 98 and 145 mg NPs kg^{-1}. As conventional fertilizers, the judicious use of nano-fertilizers may contribute to preventing soil degradation through soil contamination. Hence, it is recommended to establish fertilization rates based on the relevant soil characteristics, crops and cultivars to be grown, and previous crops grown (FAO 2019).

Concerning NUE for soil and foliar fertilization, the partial factor productivity (PFP); agronomic efficiency (AE); apparent efficiency recovery (AER), and physiological efficiency (PE) indexes were estimated. High NUE (PFP, AE, and AER) indexes were obtained for foliar fertilization compared to those for soil fertilization, meaning that a lower amount of Fe supplied by foliar spray (13.2 mg Fe per pot) may produce a greater grain yield and better Fe uptake by the plant than the soil fertilization (368 and 544 mg Fe per pot). Nevertheless, these values may be over-estimated because NPs remain adhered on the leaf surface (Figure 4.6a).

When comparing the NUE indexes of NPs with Fe-EDTA fertilization, for foliar fertilization, the NUE index (PFP, AE, and AER) was statistically similar. However, for soil fertilization, ARE index was ~ 2-fold higher than that for the Fe-EDTA fertilization, meaning a better absorption of Fe from the NPs than the Fe-EDTA source. A low NUE is usually regarded as the active compound of fertilizer that has a faster release than plant absorption capacity or changes in nutrient types that are not available to plants (Rahman et al. 2021). Nonetheless, their interpretation must be carefully considered since the NUE does not measure nutrient loss (Fixen et al. 2015). In this regard, the residual effect of NPs soil application in successive cropping should be analyzed in a future investigation to design appropriate dosage of NPs for wheat biofortification and estimate the cost-saving effects.

Specific risks for agricultural applications and potential effects of the citrate-coated $CoFe_2O_4$ NPs need to be known. This research focused on the effects of direct and obvious endpoints like crop yield, and the nutritional content of seeds (which are discussed in the following sections of this Chapter). However, it is recommended to investigate soil quality after the NPs application, and subtler endpoints, for example, changes in the meta-transcriptome, proteome, and metabolome of plants and soils after the NPs applications for a more holistic understanding of benefits and prevent the negative impacts of nano-fertilizers (Hofmann et al. 2020).

Are the citrate-coated $CoFe_2O_4$ NPs a novel approach to boosting micronutrients in staple crops to achieve nutritional security?

The main goal of this research was to explore the use of citrate-coated $CoFe_2O_4$ NPs for the Fe fortification of wheat and bean. I agree with other authors (Chugh et al. 2022) that nanotechnology could provide a tool to produce nutritional food while promoting a sustainable agri-food system because in both experiments, wheat, and bean the application of NPs enhanced the Fe, and Zn concentration in grains, respectively. Moreover, the nano-enable biofortification of staple foods may be a sustainable and cost-effective strategy to alleviate the hidden hunger and achieve the United Nations 2030 Sustainable Development Goals (SDG 2 “no hunger” and SDG 3 “good health and well-being”) (Hefferon et al. 2021).

In Chapter 3 of this work, I mentioned that agronomic biofortification success depends on micronutrient bioavailability, fertilizer chemical properties, formulation, time, and form in which the fertilizer is applied (Elemike et al. 2019). Thus, I tested three ways of applying the NPs, soil, foliar applications, and seed priming. For the wheat experiment, surprisingly, the Fe concentration in the grains was significantly higher after soil fertilization with NPs compared to the control and the Fe-EDTA fertilization (both soil and foliar) and foliar application of NPs. For the Zn storage inefficient wheat line (AF1116) fertilized by soil NPs applications, the Fe grain concentration was 1.37 times higher than the target Fe concentration for biofortification (60 mg kg^{-1}), meanwhile for the P uptake inefficient line (MULTIAF2) was 0.26-fold above biofortification target concentration. In the MULTIAF2 line, the bioaccessible Fe concentration of whole grain was higher in the simulated intestinal fluid (SIF) than that observed in the SIF of grains from the Fe-EDTA soil fertilization, commercial wheat grain, and the control treatment (unfertilized). These results were different from other studies where the foliar application of Fe-NPs resulted in higher Fe concentrations (Taskin and Gunes 2022). For conventional Fe fertilizers, soil fertilization is not recommended due to low NUE because Fe is readily converted to insoluble Fe^{3+} after its release in soil (Abbaspour et al. 2014; Dhaliwal et al. 2022b). Thus, foliar feeding of Fe fertilizers is highly suggested (Dhaliwal et al. 2022b) because Fe is readily available and more easily utilized by the plant than Fe from the soil. However, the success behind soil fertilization could be attributed to the NPs dissolution. The citrate-coated $CoFe_2O_4$ NPs dissolution is controlled by the chelate reaction, and according to the findings of Chapter 2, the Fe-malate$^+$ complex is the predominant species formed by the Fe released from the NPs and the artificial root exudates (Perea-Velez et al. 2022). These Fe-malate$^+$ complexes may be a source of exchangeable Fe which can be used by plants' strategy II Fe uptake (Mimmo et al. 2014). Then, the hypothesis was that the wheat plant may utilize Fe from NPs due to the dissolution of NPs by root exudates as illustrated in Figure 9.

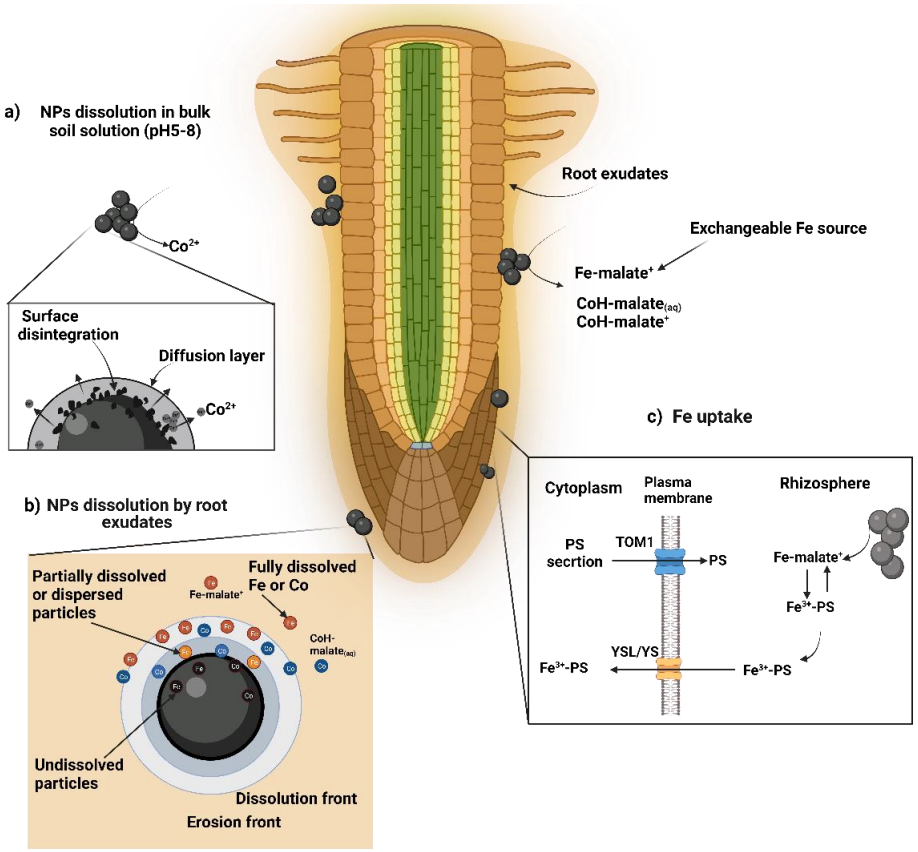

Figure 9. Proposed Fe uptake pathway for wheat roots after soil fertilization with citrate-coated $CoFe_2O_4$ NPs. a) The NPs are chemically stable in soil solution from pH 5 to 8. Co ions may be released in the soil solution due to the low water-soluble particle properties. b) The dissolution of the NPs is mainly controlled by the root exudates and Fe release following a combination of diffusion and erosion-controlled events. The citrate shell may undergo an erosion process allowing the root exudates to diffuse through until they reach the bare NP. The diffusion process then occurs. c) Fe released from the NP may form new chemical species with the compounds of root exudates, for example, the malate complex of Fe. This complex of Fe with root exudates may be an exchangeable source of Fe with the phytosiderophores (PS) of wheat plants. Once the Fe is chelated by the PS, the Fe-PS chelate could be transported inside the root cell by the yellow stripe-like transporter (YSL/YS). TOM1, Transporter of mugineic acid family phytosiderophores.

On the other hand, the foliar fertilization with NPs in wheat increased the grain yield compared to the control treatment; however, no enrichment of Fe in the grains was observed. I found that the NPs uptake occurred through stomata (Figures 3.5 and 3.6), yet, their absorption does not mean that they may be translocated to other parts of the plant or dissolved (Deshpande et al. 2017; Avellan et al. 2021). The fate and transformation of the citrate-coated $CoFe_2O_4$ NPs after being absorbed were beyond the objectives of this research, but future research should be performed to improve foliar fertilization with NPs.

For beans, the seed priming treatment significantly increased the K, P, and Zn concentration in grains compared to the offspring seeds from hydroprimed and control plants. These results agree with the positive effects of NPs by altering or enhancing nutrient content in plants (Hofmann et al. 2020; Perea Vélez et al. 2021). The grain Zn concentration ranged from 83 to 100 mg kg^{-1} in the plants from nano-priming treatments; meanwhile, for the control (unprimed seeds) and hydroprimed treatments, it was 78-79 mg kg^{-1}. Seeds from the primed seeds treatments can be considered biofortified because the Zn concentration was between 32 and 59 mg kg^{-1} above the average Zn concentration for Mexican bean varieties (27-41 mg kg^{-1}). The target level for Zn biofortification is 17 mg kg^{-1} above the local materials (Beebe 2020). The relative bioavailability of Zn in the bean seeds from the nano-priming treatment at 10 mg kg^{-1} was higher than that of the seeds from the control and unprimed treatments. These findings are interesting since beans biofortification was mainly focusing on Fe (Cichy et al. 2022). On the other hand, the average seed Fe concentration (69 mg kg^{-1}) was higher than those reported for Mexican bean varieties (35-58 mg kg^{-1}), and within the range reported for fortified beans (64 to 119 mg kg^{-1}). However, no significant differences in seed Fe concentration among treatments were observed in this study.

Economic feasibility of citrate-coated $CoFe_2O_4$ NPs for nano-enable biofortification of wheat and bean

The agronomic benefits of nano-fertilizers and their impact on the grain mineral content, production cost, and affordability to farmers are some of the key factors in convincing the industry to invest in nano-fertilizer production (Dimkpa and Bindraban 2018) and their wide-scale application (Siimes et al. 2022). The comparison of the cost, positive effects, and drawbacks for the different forms to apply NPs in agriculture are shown in Table 7.

Table 7. Comparison of the cost, positive effects, and drawbacks for the different forms to apply NPs in agriculture over the Fe-EDTA fertilization.

Technology	Concentration† (mg kg^{-1} or L^{-1})	mg Fe kg^{-1} or L^{-1}	Cost of fertilization or treatment (USD)	Gross income (USD)	Positive effects	Drawbacks
Nano-priming	10, 20, 40	3.5, 7.5, 15	121, 128, and 143	3,140 to 3,480	Enhance mineral content of offspring seeds and plant height An extended period of nodulation The low phytic acid concentration in seeds No negative effects on germination and plant performance Low input technology	Requires standardization to determine the imbibition time and re-drying
NPs soil application	98, 145	48, 68	44,283 to 65,523	2,579 to 3,675	May increase the grain yield, while reaching the target Fe concentration for biofortification Increased the Fe concentration, and their relative bioavailability in grains Increase the Fe bioaccessible concentration of whole grain The low phytic acid concentration in seeds	Improve the application method to scale it up to the field Expensive cost due to the cost of NPs production The residual effect needs to be assessed
NPs foliar application	676	330	1,553	3,266	Increase the grain and biological yield. Potential high NUE Cheaper compared to the soil application Relative low input technology	Agglomeration/aggregation of NPs Adhesion of NPs on the leaf surface Low water stability of NPs Improve application method

Technology	Concentration† (mg kg^{-1} or L^{-1})	mg Fe kg^{-1} or L^{-1}	Cost of fertilization or treatment (USD)	Gross income (USD)	Positive effects	Drawbacks
Fe-EDTA soil fertilization	348	48	8,204	3,027	May increase the Fe concentration in grains	Fe losses due to their fixation in soil Expensive
Fe-EDTA foliar fertilization	2.5	330	294	3,208	Increase the grain yield Low input technology Cheaper compared to soil fertilization	

† Concentrations base on NPs or Fe-EDTA concentration.

According to the findings from Chapters 3 and 4, seed priming is the cheaper and more environmentally friendly form of nano-enable biofortification, followed by foliar and soil applications. Notably, the amount of NPs required for seed priming treatments is inherently lower compared to soil or foliar applications, potentially shifting the economic scale for feasibility (Hofmann et al. 2020).

Currently, the high production cost of NPs may still delay the implementation of soil and foliar application of NPs (Dimkpa and Bindraban 2018; Hofmann et al. 2020). The cost of NPs in the market ranges from 5,750 to 145,620 USD per kg of $CoFe_2O_4$ (Perea-Velez et al, 2023; Chapter 3, Table S6). Whereas, the estimated cost of citrate-coated $CoFe_2O_4$ NPs, used in this research, at laboratory scale was 25,109 USD kg^{-1}. The cost of magnetic NPs (such as magnetite, and Fe oxides) reported in the literature varies from 800 to 120,000 USD per kg of NPs (Delfani et al. 2014b; Correa et al. 2021). In this regard, to gain traction in $CoFe_2O_4$ NPs as fertilizers for large field applications and global adoption, NPs should be produced industrially in tons amounts per unit of time, at a reasonable cost (Dimkpa and Bindraban 2018).

The cost of soil fertilization with NPs may be lower due to the residual effect of successive cropping. However, no demonstration of such residual effects have been reported yet, as well as their impact on crop production (Dimkpa et al. 2018). I recommend that this issue be considered in future research. In addition, indirect effects should also be taken into account in the assessment of the feasibility of NPs in the fortification of staple foods. Such as the burden of micronutrient deficiencies, low labor productivity, the cost of health system usage, the success of the education system via cognition (Horton 2004), reduction of the scope 2 emissions associated with bean cropping (Huertas et al. 2022)

Finally, according to Hofmann et al. (2020), the technology-readiness level (TRL) for nanoscale micronutrients is relatively high, because they have been demonstrated improving plant productivity at the laboratory and greenhouse scale, using low doses of application. It is now important to validate the laboratory observations in the field and to optimize the production cost of NPs to make this technology feasible and applicable. Whereas the TRL for nano-priming is deemed low due to very few rigorous studies (lack

of standardized methods) of the beneficial effects of nano-priming, meaning we need to address further research to maxim the outcomes of nano-priming because, among the forms to apply NPs, this form seems potentially economic feasible for wide-scale application.

GENERAL CONCLUSIONS

The results from this thesis have provided information about the potential use and feasibility of citrate-coated $CoFe_2O_4$ NPs for the biofortification of wheat and bean. The main outcomes were:

- The citrate-coated $CoFe_2O_4$ NPs are chemically stable in soil solutions at a pH from 5 to 8. The dissolution of NPs and the release of Fe and Co is controlled by the chelate reaction. Based on those results, the citrate-coated $CoFe_2O_4$ NPs could be considered as an option for slow-bio-release fertilizer that can be used in soils with an acid pH to an alkaline one.
- The release of Co from the NPs by the effect of ARE and soil solution fits the pseudo-second-order dissolution model (R^2 adjusted soil solution pH 5, 7, and 8= 0.98, 0.79, 0.86; R^2 adjusted-ARE=0.98). This dissolution model proposes a two steps process, first, the surface disintegration of the NP followed by a diffusion step.
- The release of Fe from the NPs by the effect of ARE fits the Higuchi model (R^2 adjusted= 0.91) and the Korsmeyer-Peppas model (R^2 adjusted= 0.91). The Kormeyer-Peppas model explains that the citrate shell is eroded, allowing the ARE solution diffuses through until reaches the bare NP. Then, a diffusion process occurs.
- Foliar application of NPs increased wheat grain yield by 52% over the control; however, it did not change the Fe grain concentration. The cost of NPs fertilization was estimated at 3,266 USD per ha. It was cheaper compared to the cost of soil fertilization.
- Soil fertilization with NPs at 68 mg kg^{-1} increased the Fe grain concentration by 96% and 71% over the control and Fe-EDTA soil fertilization, for the inefficient Zn grain storage and P uptake wheat lines.
- Target Fe concentration for biofortification was achieved after the soil application of NPs at 68 mg kg^{-1}, 1.37 folds above the target biofortification concentration for the line Zn-grain storage inefficient (AF1116), and 0.26 times for the line P uptake inefficient (MULTIAF2).

- Seed priming increased the K, P, and Zn concentration in grains compared to the offspring seeds from the plants from the hydroprimed and control treatments.
- The grain Zn concentration ranged from 83 to 100 mg kg^{-1}.
- Seeds from the nano-primed treatments can be considered biofortified because Zn concentration was between 32 and 59 mg kg^{-1} above the average Zn concentration for Mexican bean varieties (27-41 mg kg^{-1}).
- Reduction of the phytic acid concentration in grains by the effect of NPs fertilization (soil and foliar) and seed priming was observed. Thus, the relative bioavailability of Fe and Zn increased compared to the control treatments.
- Seed priming was the cheaper form of applying NPs for the nano-enabled biofortification compared to the soil and foliar applications. Indeed, the amount of NPs required for seed priming treatments is inherently lower compared to soil or foliar applications.

According to these findings, the general hypothesis is accepted, because of the application of NPsenhanced Fe and Zn concentrations in wheat grains and beans. These encouraging findings show the potential of nano-fertilizers to enhance the mineral content of two of the most consumed staple foods, and potentially contribute to the transition to a sustainable agri-food system; as well as to achieve nutritional security in rural and marginalized areas.

On the other hand, the agronomic biofortification of staple food is an economic and fast approach (compared to plant breeding) to produce food with better nutritional quality to combat malnutrition in a vulnerable population. The major cause of malnutrition is the poor intake of micronutrients due to the lack of a diversified diet. However, the success of agronomic biofortification depends on the fertilizer characteristics, application form, and the type of crop. In this regard, concerns related to the improvement of application methods of NPs recommended dose, and greenhouse results validation at the field scale should be investigated. In addition, nano-fertilizers should be proven to promote the sustainability of our agri-food system before a wide-use of NPs. For last concern, topics

that must be studied in the future are the effect of NPs on the soil after being applied, the fate of NPs after their applications, the ecotoxicology of NPs, recommended doses according to the application form, and the economic cost of production and NPs application.

REFERENCES

Abadía J, Vázquez S, Rellán-Álvarez R, et al (2011) Towards a knowledge-based correction of iron chlorosis. Plant Physiol Biochem 49:471–482. https://doi.org/10.1016/j.plaphy.2011.01.026

Abbaspour N, Hurrell R, Kelishadi R (2014) Review on iron and its importance for human health. J Res Med Sci 19:164–174

Abd-alla MH, Nafady NA, Khalaf DM (2016) Assessment of silver nanoparticles contamination on faba bean- *Rhizobium leguminosarum bv. viciae* - *Glomus aggregatum* symbiosis : Implications for induction of autophagy process in root nodule. Agriculture, Ecosyst Environ 218:163–177. https://doi.org/10.1016/j.agee.2015.11.022

Abdel Latef AAH, Srivastava AK, El-sadek MSA, et al (2018) Titanium dioxide nanoparticles improve growth and enhance tolerance of broad bean plants under saline soil conditions. L Degrad Dev 29:1065–1073. https://doi.org/10.1002/ldr.2780

Abdelhameed R, Abu-Elsaad N, Abdel Latef A, Metwally R (2021) Tracking of zinc ferrite nanoparticle effects on pea (*Pisum sativum* L.) plant growth, pigments, mineral content and arbuscular mycorrhizal colonization. Plants 10:583. https://doi.org/10.3390/plants10030583

Acharya A, Pal PK (2020) Agriculture nanotechnology: Translating research outcome to field applications by influencing environmental sustainability. NanoImpact 19:100232. https://doi.org/10.1016/j.impact.2020.100232

Acharya P, Jayaprakasha GK, Crosby KM, et al (2020) Nanoparticle-mediated seed priming improves germination, growth, yield, and quality of watermelons (*Citrullus lanatus*) at multi-locations in Texas. Sci Rep 10:5037. https://doi.org/10.1038/s41598-020-61696-7

Aciksoz SB, Yazici A, Ozturk L, Cakmak I (2011) Biofortification of wheat with iron through soil and foliar application of nitrogen and iron fertilizers. Plant Soil 349:215–225. https://doi.org/10.1007/s11104-011-0863-2

Adisa IO, Rawat S, Pullagurala VLR, et al (2020) Nutritional status of tomato (*Solanum lycopersicum*) fruit grown in fusarium-infested soil: impact of cerium oxide nanoparticles. J Agric Food Chem 68:1986–1997. https://doi.org/10.1021/acs.jafc.9b06840

Afzal S, Sharma D, Singh NK (2021) Eco-friendly synthesis of phytochemical-capped iron oxide nanoparticles as nano-priming agent for boosting seed germination in rice (*Oryza sativa* L.). Environ Sci Pollut Res. 28: 40275-40287. https://doi.org/10.1007/s11356-020-12056-5

Agrawal S, Kumar V, Kumar S, Shahi SK (2022) Plant development and crop protection using phytonanotechnology: A new window for sustainable agriculture.

Chemosphere 299:134465. https://doi.org/10.1016/j.chemosphere.2022.134465

Ahmed B, Ameen F, Rizvi A, et al (2020) Destruction of cell topography, morphology, membrane, inhibition of respiration, biofilm formation, and bioactive molecule production by nanoparticles of Ag, ZnO, CuO, TiO_2, and Al_2O_3 toward beneficial soil bacteria. ACS Omega 5:7861–7876. https://doi.org/10.1021/acsomega.9b04084

Akram MA, Depar N, Irfan M (2020) Agronomic zinc biofortification of wheat to improve accumulation, bioavailability, productivity and use efficiency. Eurasian J Soil Sci 9:75–84. https://doi.org/10.18393/ejss.647585

Al-Amri N, Tombuloglu H, Slimani Y, et al (2020) Size effect of iron (III) oxide nanomaterials on the growth, and their uptake and translocation in common wheat (*Triticum aestivum* L.). Ecotoxicol Environ Saf 194:110377. https://doi.org/10.1016/j.ecoenv.2020.110377

Al-juthery HWA, Hassan AH, Kareem FK, et al (2019) The response of wheat to foliar application of nano-micro nutrients. Plant Arch 19:827–831

Alsharef JMA, Taha MR, Firoozi AA, Govindasamy P (2016) Potential of using nanocarbons to stabilize weak soils. Appl Environ Soil Sci 2016:5060531. https://doi.org/10.1155/2016/5060531

Alston JM, Pardey PG (2014) Agriculture in the global economy. J Econ Perspect 28:121–146. https://doi.org/10.1257/jep.28.1.121

Ameen F, Alsamhary K, Alabdullatif JA, ALNadhari S (2021) A review on metal-based nanoparticles and their toxicity to beneficial soil bacteria and fungi. Ecotoxicol Environ Saf 213:112027. https://doi.org/10.1016/j.ecoenv.2021.112027

Andrade DC, dos Santos EV (2020) Combination of electrokinetic remediation with permeable reactive barriers to remove organic compounds from soils. Curr Opin Electrochem 22:136–144. https://doi.org/10.1016/j.coelec.2020.06.002

Angulo M, García MJ, Alcántara E, et al (2021) Comparative study of several Fe deficiency responses in the *Arabidopsis thaliana* ethylene insensitive mutants *ein2-1* and *ein2-5.* Plants 10:262. https://doi.org/10.3390/plants10020262

Antony D, Yadav R, Kalimuthu R (2021) Accumulation of phyto-mediated nano-CeO_2 and selenium doped CeO_2 on *Macrotyloma uniflorum* (horse gram) seed by nano-priming to enhance seedling vigor. Biocatal Agric Biotechnol 31:101923. https://doi.org/10.1016/j.bcab.2021.101923

Anza M, Salazar O, Epelde L, et al (2019) The Application of nanoscale zero-valent iron promotes soil remediation while negatively affecting soil microbial biomass and activity. Front Environ Sci 7:19. https://doi.org/10.3389/fenvs.2019.00019

Aqua-Yield® (2021) Aqua-Yield® NanoShield® Technology. https://www.aquayield.com/. Accessed 5 Jan 2021

Arenas-Lago D, Abreu MM, Andrade Couce L, Vega FA (2019) Is nanoremediation an effective tool to reduce the bioavailable As, Pb and Sb contents in mine soils from iberian pyrite belt? CATENA 176:362–371. https://doi.org/10.1016/j.catena.2019.01.038

Armin M, Asgharipour MR (2011) Effect of time and concentration of boron foliar application on yield and quality of sugar beet. Asian J Plant Sci 10:307–311. https://doi.org/10.3923/ajps.2011.307.311

Arumugam G, Velayutham V, Shanmugavel S, Sundaram J (2016) Efficacy of nanostructured silica as a stored pulse protector against the infestation of bruchid beetle, *Callosobruchus maculatus* (Coleoptera: Bruchidae). Appl Nanosci 6:445–450. https://doi.org/10.1007/s13204-015-0446-2

Askary M, Amirjani MR, Saberi T (2017) Comparison of the effects of nano-iron fertilizer with iron-chelate on growth parameters and some biochemical properties of *Catharanthus roseus*. J Plant Nutr 40:974–982. https://doi.org/10.1080/01904167.2016.1262399

Atkins P, De Paula J (2006) Atkins' Physical Chemistry. Oxford University Press, Oxford, New York.

Atrei A, Fiorani M, Bellingeri A, et al (2019) Remediation of acid mine drainage-affected stream waters by means of eco-friendly magnetic hydrogels crosslinked with functionalized magnetite nanoparticles. Environ Nanotechnology, Monit Manag 12:100263. https://doi.org/10.1016/j.enmm.2019.100263

Auffan M, Achouak W, Rose J, et al (2008) Relation between the redox state of iron-based nanoparticles and their cytotoxicity toward *Escherichia coli*. Environ Sci Technol 42:6730–6735. https://doi.org/10.1021/es800086f

Avellan A, Yun J, Morais BP, et al (2021) Critical review: Role of inorganic nanoparticle properties on their foliar uptake and in planta translocation. Environ Sci Technol 55:13417–13431. https://doi.org/10.1021/acs.est.1c00178

Avramescu M-L, Rasmussen PE, Chénier M, Gardner HD (2017) Influence of pH, particle size and crystal form on dissolution behaviour of engineered nanomaterials. Environ Sci Pollut Res 24:1553–1564. https://doi.org/10.1007/s11356-016-7932-2

Awasthi G, Singh T, Tiwari Y, et al (2020) A review on nanotechnological interventions for plant growth and production. Mater Today Proc 31:685–693. https://doi.org/10.1016/j.matpr.2020.07.255

Aziz N, Pandey R, Barman I, Prasad R (2016) Leveraging the attributes of *Mucor hiemalis*-derived silver nanoparticles for a synergistic broad-spectrum antimicrobial platform. Front. Microbiol. 7:1984. https://doi.org/10.3389/fmicb.2016.01984

Bakhtiari M, Moaveni P, Sani B (2015) The Effect of iron nanoparticles spraying time and concentration on wheat. Biol Forum - An Int J 7:679–683

Balk J, Connorton JM, Wan Y, et al (2019) Improving wheat as a source of iron and zinc for global nutrition. Nutr Bull 44:53–59. https://doi.org/10.1111/nbu.12361

Bandyopadhyay T, Prasad M (2021) IRONing out stress problems in crops: a homeostatic perspective. Physiol Plant 171:559–577. https://doi.org/10.1111/ppl.13184

Banerjee P, Bhattacharya P (2021) Investigating cobalt in soil-plant-animal-human system: dynamics, impact and management. J Soil Sci Plant Nutr 21:2339–2354. https://doi.org/10.1007/s42729-021-00525-w

Baragaño D, Alonso J, Gallego JR, et al (2020a) Zero valent iron and goethite nanoparticles as new promising remediation techniques for As-polluted soils. Chemosphere 238:124624. https://doi.org/10.1016/j.chemosphere.2019.124624

Baragaño D, Forján R, Fernández B, et al (2020b) Application of biochar, compost and ZVI nanoparticles for the remediation of As, Cu, Pb and Zn polluted soil. Environ Sci Pollut Res. 27: 33681–33691. https://doi.org/10.1007/s11356-020-09586-3

Bardos P, Kvapil P, Koschitzky H (2018) Status of nanoremediation and its potential for future deployment : risk-benefit and benchmarking appraisals. Remediation J 28:43–56. https://doi.org/10.1002/rem.21559

Barisik M, Atalay S, Beskok A, Qian S (2014) Size dependent surface charge properties of silica nanoparticles. J Phys Chem C 118:1836–1842. https://doi.org/10.1021/jp410536n

Baruah S, Dutta J (2009) Nanotechnology applications in pollution sensing and degradation in agriculture. Environ. Chem. Lett. 7:191–204. https://doi.org/10.1007/s10311-009-0228-8

Batsmanova L, Taran N, Konotop Y, et al (2020) Use of a colloidal solution of metal and metal oxide-containing nanoparticles as fertilizer for increasing soybean productivity. J Cent Eur Agric 21:311–319. https://doi.org/10.5513/jcea01/21.2.2414

Bayat H, Kolahchi Z, Valaey S, et al (2018) Novel impacts of nanoparticles on soil properties: tensile strength of aggregates and compression characteristics of soil. Arch Agron Soil Sci 64:776–789. https://doi.org/10.1080/03650340.2017.1393527

Beddow J, Stolpe B, Cole P, et al (2014) Effects of engineered silver nanoparticles on the growth and activity of ecologically important microbes. Environ Microbiol Rep 6:448–458. https://doi.org/10.1111/1758-2229.12147

Beebe S (2020) Biofortification of common bean for higher iron concentration. Front Sustain Food Syst. https://doi.org/10.3389/fsufs.2020.573449

Belal E, El-Ramady H (2016) Nanoparticles in water, soils and agriculture. In: Rajan S, Dasgupta N, Lichtfouse E (eds) Nanoscience in Food and Agriculture 2. Sustainable Agriculture Reviews. Springer, Cham, pp 311–358. https://doi.org/10.1007/978-3-319-39306-3_10

Ben-Moshe T, Dror I, Berkowitz B (2010) Transport of metal oxide nanoparticles in saturated porous media. Chemosphere 81:387–393. https://doi.org/10.1016/j.chemosphere.2010.07.007

Bilal HM, Aziz T, Maqsood MA, Farooq M (2019) Grain phosphorus and phytate contents of wheat genotypes released during last 6 decades and categorization of selected genotypes for phosphorus use efficiency. Arch Agron Soil Sci 65:727–740. https://doi.org/10.1080/03650340.2018.1521957

Bio Nano. https://bionano-egy.com/works/nano-cu/. Accessed 5 Jan 2021

Blanco-Rojo R, Vaquero MP (2019) Iron bioavailability from food fortification to precision nutrition. A review. Innov Food Sci Emerg Technol 51:126–138. https://doi.org/10.1016/j.ifset.2018.04.015

Bloot APM, Kalschne DL, Amaral JAS, et al (2021) A Review of phytic acid sources, obtention, and applications. Food Rev Int 1–20. https://doi.org/10.1080/87559129.2021.1906697

Boehlje M, Broring S (2011) The increasing multifunctionality of agricultural raw materials: three dilemmas for innovation and adoption. Int. Food Agrobusiness Manag. Rev.14:1–16

Borm P, Klaessig FC, Landry TD, et al (2006) Research strategies for safety evaluation of nanomaterials, part V: role of dissolution in biological fate and effects of nanoscale particles. Toxicol Sci 90:23–32. https://doi.org/10.1093/toxsci/kfj084

Borrill P, Connorton J, Balk J, et al (2014) Biofortification of wheat grain with iron and zinc: integrating novel genomic resources and knowledge from model crops. Front Plant Sci 5:53. https://doi.org/10.3389/fpls.2014.00053

Boxi SS, Mukherjee K, Paria S (2016) Ag doped hollow TiO_2nanoparticles as an effective green fungicide against *Fusarium solani* and *Venturia inaequalis* phytopathogens. Nanotechnology 27:85103. https://doi.org/10.1088/0957-4484/27/8/085103

Bratovcic A, Hikal WM, Said-Al Ahl HAH, et al (2021) Nanopesticides and nano-fertilizers and agricultural development: scopes, advances and applications. Open J Ecol 11:301–316. https://doi.org/10.4236/oje.2021.114022

Bravo Cadena M, Preston GM, Van der Hoorn RAL, et al (2018) Enhancing cinnamon essential oil activity by nanoparticle encapsulation to control seed pathogens. Ind Crops Prod 124:755–764. https://doi.org/10.1016/j.indcrop.2018.08.043

Bremner JM (1965a) Total Nitrogen. In: A.G. Norman (ed) Methods of Soil Analysis, ASA, Madison, WI, USA. pp 1149–1178

Bremner JM (1965b) Inorganic Forms of Nitrogen. In: A.G. Norman (ed) Methods of Soil Analysis, ASA, Madison, WI, USA. pp 1179–1237

Brodkorb A, Egger L, Alminger M, et al (2019) INFOGEST static *in vitro* simulation of gastrointestinal food digestion. Nat Protoc 14:991–1014. https://doi.org/10.1038/s41596-018-0119-1

Bruemmer GW, Gerth J, Herms U (1986) Heavy metal species, mobility and availability in soils. Zeitschrift für Pflanzenernährung und Bodenkd 149:382–398. https://doi.org/10.1002/jpln.19861490404

Bruschi ML (2015) Mathematical models of drug release. In: Bruschi ML (ed) Strategies to modify the drug release from pharmaceutical systems. Elsevier, Cambridge, UK. pp 63–86. https://doi.org/10.1016/B978-0-08-100092-2.00005-9

Bundschuh M, Filser J, Lüderwald S, et al (2018) Nanoparticles in the environment: where do we come from, where do we go to? Environ Sci Eur 30:6. https://doi.org/10.1186/s12302-018-0132-6

Burman U, Saini M, Kumar P (2013) Effect of zinc oxide nanoparticles on growth and antioxidant system of chickpea seedlings. Toxicol Environ Chem 95:605–612. https://doi.org/10.1080/02772248.2013.803796

Buteler M, Lopez Garcia G, Stadler T (2018) Potential of nanostructured alumina for leaf-cutting ants *Acromyrmex lobicornis* (Hymenoptera: Formicidae) management. Austral Entomol 57:292–296. https://doi.org/10.1111/aen.12277

Butt BZ, Naseer I (2020) Nanofertilizers. In: Javad S (ed). Nanoagronomy. Springer, Cham, pp 125–152. https://doi.org/10.1007/978-3-030-41275-3_8

Cai L, Cai L, Jia H, et al (2020) Foliar exposure of Fe_3O_4 nanoparticles on *Nicotiana benthamiana:* Evidence for nanoparticles uptake, plant growth promoter and defense response elicitor against plant virus. J Hazard Mater 393:122415. https://doi.org/10.1016/j.jhazmat.2020.122415

Cakmak I, Kutman UB (2018) Agronomic biofortification of cereals with zinc: a review. Eur J Soil Sci 69:172–180. https://doi.org/10.1111/ejss.12437

Cao J, Feng Y, He S, Lin X (2017) Silver nanoparticles deteriorate the mutual interaction between maize (*Zea mays* L.) and arbuscular mycorrhizal fungi : a soil microcosm study. Appl Soil Ecol 119:307–316. https://doi.org/10.1016/j.apsoil.2017.04.011

Cao J, Feng Y, Lin X, et al (2016) Iron oxide magnetic nanoparticles deteriorate the mutual interaction between arbuscular mycorrhizal fungi and plant. J Soils Sediments. https://doi.org/10.1007/s11368-016-1561-8

Cao J, Feng Y, Lin X, Wang J (2020) A beneficial role of arbuscular mycorrhizal fungi in influencing the effects of silver nanoparticles on plant-microbe systems in a soil matrix. Environ Sci Pollut Res 27:11782–11796. https://doi.org/10.1007/s11356-020-07781-w

Carillo P, Mastrolonardo G, Nacca F, et al (2008) Nitrogen metabolism in durum wheat under salinity: accumulation of proline and glycine betaine. Funct Plant Biol 35:412–426. https://doi.org/10.1071/FP08108

Caroline V, Antônio T (2019) Sustainability in life cycle analysis of nanomaterials applied in soil remediation. In: Zhan L, Chen Y, Bouazza A (eds) Proceedings of the 8th International Congress on Environmental Geotechnics Volume 3. Springer Singapore, Singapore, pp. 537–543 https://doi.org/10.1007/978-981-13-2227-3_66

Carrillo-González R, Perea-Vélez YS, González-Chávez MC. (2017) Fitoremediación asistida con enmiendas y fitoestabilización de elementos potencialmente tóxicos. Agroproductividad 10:15–20

Cartwright A, Jackson K, Morgan C, et al (2020) A Review of metal and metal-oxide nanoparticle coating technologies to inhibit agglomeration and increase bioactivity for agricultural applications. Agronomy 10:1018. https://doi.org/10.3390/agronomy10071018

Castro-Alba V, Lazarte CE, Bergenståhl B, Granfeldt Y (2019) Phytate, iron, zinc, and calcium content of common Bolivian foods and their estimated mineral bioavailability. Food Sci Nutr 7:2854–2865. https://doi.org/10.1002/fsn3.1127

Cecchin I, Reddy KR, Thomé A, et al (2017) Nanobioremediation: integration of nanoparticles and bioremediation for sustainable remediation of chlorinated organic contaminants in soils. Int Biodeterior Biodegradation 119:419–428. https://doi.org/10.1016/j.ibiod.2016.09.027

Cervantes-Avilés P, Huang X, Keller AA (2021) Dissolution and aggregation of metal oxide nanoparticles in root exudates and soil leachate: implications for nanoagrochemical application. Environ Sci Technol. 55:13443-13451. https://doi.org/10.1021/acs.est.1c00767

Chakraborty U, Kaur G, Chaudhary G (2021) Development of environmental nanosensors for detection monitoring and assessment. In: Kumar, R., Kumar, R., Kaur, G. (eds) New Frontiers of Nanomaterials in Environmental Science, Springer Singapore, Singapore, pp. 91–143 https://doi.org/10.1007/978-981-15-9239-3_5

Chandra P, Ghosh K, Varadachari C (2009) A new slow-releasing iron fertilizer. Chem Eng J 155:451–456. https://doi.org/10.1016/j.cej.2009.07.017

Chandrasekaran U, Luo X, Wang Q, Shu K (2020) Are there unidentified factors involved in the germination of nanoprimed seeds? Front Plant Sci 11. https://doi.org/10.3389/fpls.2020.00832

Chang R (2005) Physical chemistry for the biosciences. University Science Books, Sausalito

Chapman HD (1965) Total exchangeable bases. In: A.G. Norman (ed) Methods of Soil Analysis, ASA, Madison, WI, USA.pp 902–904

Chavan S, Nadanathangam V (2019) Effects of nanoparticles on plant growth-promoting bacteria in indian agricultural soil. Agron. 9:140. https://doi.org/10.3390/agronomy9030140

Chávez-Mendoza C, Sánchez E (2017) Bioactive compounds from mexican varieties of the common bean (*Phaseolus vulgaris*): implications for health. Molecules 22:1360. https://doi.org/10.3390/molecules22081360

Chen C, Unrine JM, Hu Y, et al (2020) Responses of soil bacteria and fungal communities to pristine and sulfidized zinc oxide nanoparticles relative to Zn ions. J Hazard Mater 405:124258. https://doi.org/10.1016/j.jhazmat.2020.124258

Chen H (2018) Metal based nanoparticles in agricultural system: behavior, transport, and interaction with plants. Chem Speciat Bioavailab 30:123–134. https://doi.org/10.1080/09542299.2018.1520050

Chen J, Sun L, Cheng Y, et al (2016) Graphene oxide-silver nanocomposite: novel agricultural antifungal agent against *Fusarium graminearum* for crop disease prevention. ACS Appl Mater Interfaces 8:24057–24070. https://doi.org/10.1021/acsami.6b05730

Chen J, Wang Y, Zhou D, et al (2010) Adsorption and desorption of Cu(II), Zn(II), Pb(II), and Cd(II) on the soils amended with nanoscale hydroxyapatite. Environ Prog Sustain Energy 29:233–241. https://doi.org/10.1002/ep.10371

Cheng P, Zhang S, Wang Q, et al (2021) Contribution of nano-zero-valent iron and arbuscular mycorrhizal fungi to phytoremediation of heavy metal-contaminated soil. Nanomater. 11:1264. https://doi.org/10.3390/nano11051264

Choudhary RC, Kumaraswamy R V, Kumari S, et al (2019) Zinc encapsulated chitosan nanoparticle to promote maize crop yield. Int J Biol Macromol 127:126–135. https://doi.org/10.1016/j.ijbiomac.2018.12.274

Chugh G, Siddique KHM, Solaiman ZM (2022) Iron fortification of food crops through nanofertilisation. Crop Pasture Sci. 73:736-748. https://doi.org/10.1071/CP21436

Cichy K, Chiu C, Isaacs K, Glahn R (2022) Dry bean biofortification with iron and zinc. In: Kumar S, Dikshit HK, Mishra GP, Singh A (eds). Biofortification of staple crops. Springer, Singapore, pp 225–270. https://doi.org/10.1007/978-981-16-3280-8_10

Collins RN, Bakkaus E, Carrière M, et al (2010) Uptake, localization, and speciation of cobalt in *Triticum aestivum* L. (wheat) and *Lycopersicon esculentum* M. (tomato). Environ Sci Technol 44:2904–2910. https://doi.org/10.1021/es903485h

Colombo C, Iorio E di, Liu Q, et al (2018) Iron oxide nanoparticles in soils: environmental and agronomic importance. J Nanosci Nanotechnol 18:761–761. https://doi.org/10.1166/jnn.2018.15294

Colombo C, Palumbo G, He J-Z, et al (2014) Review on iron availability in soil: interaction of Fe minerals, plants, and microbes. J Soils Sediments 14:538–548. https://doi.org/10.1007/s11368-013-0814-z

Colombo F, Sangiorgio S, Abruzzese A, et al (2022) The potential of low phytic acid1-1 mutant in maize (*Zea mays* L.): a sustainable solution to non-renewable phosphorus. Front Biosci 27:284. https://doi.org/10.31083/j.fbl2710284

Cominelli E, Pilu R, Sparvoli F (2020) Phytic acid and mineral biofortification strategies: from plant science to breeding and biotechnological approaches. Plants 9:553. https://doi.org/10.3390/plants9050553

Compant S, Samad A, Faist H, Sessitsch A (2019) A review on the plant microbiome: ecology, functions, and emerging trends in microbial application. J Adv Res 19:29–37. https://doi.org/10.1016/j.jare.2019.03.004

Con USPC (1979) The United States Pharmacopeia. Rockville Md.

Connorton JM, Balk J, Rodríguez-Celma J (2017) Iron homeostasis in plants-a brief overview. Metallomics 9:813–823. https://doi.org/10.1039/c7mt00136c

Conway JR, Keller AA (2016) Gravity-driven transport of three engineered nanomaterials in unsaturated soils and their effects on soil pH and nutrient release. Water Res 98:250–260. https://doi.org/10.1016/j.watres.2016.04.021

Correa T, Presciliano R, Abreu F (2021) Why does not nanotechnology go green? Bioprocess simulation and economics for bacterial-origin magnetite nanoparticles. Front Microbiol 12. https://doi.org/10.3389/fmicb.2021.718232

Corsi I, Winther-Nielsen M, Sethi R, et al (2018) Ecofriendly nanotechnologies and nanomaterials for environmental applications: key issue and consensus recommendations for sustainable and ecosafe nanoremediation. Ecotoxicol Environ Saf 154:237–244. https://doi.org/10.1016/j.ecoenv.2018.02.037

Costa P, Sousa Lobo JM (2001) Modeling and comparison of dissolution profiles. Eur J Pharm Sci 13:123–133. https://doi.org/10.1016/S0928-0987(01)00095-1

Cui J, Li Y, Jin Q, Li F (2020) Silica nanoparticles inhibit arsenic uptake into rice suspension cells via improving pectin synthesis and the mechanical force of the cell wall. Environ Sci Nano 7:162–171. https://doi.org/10.1039/C9EN01035A

Dahle JT, Livi K, Arai Y (2015) Effects of pH and phosphate on CeO_2 nanoparticle dissolution. Chemosphere 119:1365–1371. https://doi.org/10.1016/j.chemosphere.2014.02.027

Das CK, Srivastava G, Dubey A, et al (2016) Nano-iron pyrite seed dressing: a sustainable intervention to reduce fertilizer consumption in vegetable (beetroot, carrot), spice (fenugreek), fodder (alfalfa), and oilseed (mustard, sesamum) crops. Nanotechnol Environ Eng 1:2. https://doi.org/10.1007/s41204-016-0002-7

Davarpanah S, Tehranifar A, Davarynejad G, et al (2016) Effects of foliar applications of zinc and boron nano-fertilizers on pomegranate (*Punica granatum* cv. Ardestani) fruit yield and quality. Sci Hortic (Amsterdam) 210:57–64. https://doi.org/10.1016/j.scienta.2016.07.003

de Oliveira Pereira FS, Agarrayua DA, Quines CB, Ávila D (2020). Risk assessment of nano-fertilizers and nanopesticides. In: Fraceto LF, S.S. de Castro VL, Grillo R, et al. (eds). Nanopesticides. Springer, Cham, pp 299–316. https://doi.org/10.1007/978-3-030-44873-8_10

De Souza-Torres A, Govea-Alcaide E, Gómez-Padilla E, et al (2021) Fe_3O_4 nanoparticles and *Rhizobium* inoculation enhance nodulation, nitrogen fixation and growth of common bean plants grown in soil. Rhizosphere 17:100275. https://doi.org/10.1016/j.rhisph.2020.100275

de Valença AW, Bake A, Brouwer ID, Giller KE (2017) Agronomic biofortification of crops to fight hidden hunger in sub-Saharan Africa. Glob Food Sec 12:8–14. https://doi.org/10.1016/j.gfs.2016.12.001

Debnath P, Mondal A, Sen K, et al (2020) Genotoxicity study of nano Al_2O_3, TiO_2 and ZnO along with UV-B exposure: an *Allium cepa* root tip assay. Sci Total Environ 713:136592. https://doi.org/10.1016/j.scitotenv.2020.136592

Degenkolb L (2021). Mobility and transport mechanisms of engineered nanoparticles in soils and water-saturated sediments. Dissertation, Technische Universität Berlin. https://doi.org/10.14279/depositonce-10833

Degenkolb L, Kaupenjohann M, Klitzke S (2019) The variable fate of Ag and TiO_2 nanoparticles in natural soil solutions—sorption of organic matter and nanoparticle stability. Water, Air, Soil Pollut 230:62. https://doi.org/10.1007/s11270-019-4123-z

Del Buono D, Luzi F, Tolisano C, et al (2022) Synthesis of a lignin/zinc oxide hybrid nanoparticles system and its application by nano-priming in maize. Nanomater. 12:568. https://doi.org/10.3390/nano12030568

Delfani M, Baradarn Firouzabadi M, Farrokhi N, Makarian H (2014) Some physiological responses of black-eyed pea to iron and magnesium nano-fertilizers. Commun Soil Sci Plant Anal 45:530–540. https://doi.org/10.1080/00103624.2013.863911

Deshpande P, Dapkekar A, Oak MD, et al (2017) Zinc complexed chitosan/TPP nanoparticles: a promising micronutrient nanocarrier suited for foliar application. Carbohydr Polym 165:394–401. https://doi.org/10.1016/j.carbpol.2017.02.061

Dhaliwal SS, Sharma V, Shukla AK, et al (2022a) Biofortification of soybean (*Glycine max* L.) through $FeSO_4 \cdot 7H_2O$ to enhance yield, iron nutrition and economic outcomes in sandy loam soils of india. agriculture 12:586. https://doi.org/10.3390/agriculture12050586

Dhaliwal SS, Sharma V, Shukla AK, et al (2022b) Biofortification—a frontier novel approach to enrich micronutrients in field crops to encounter the nutritional security. Molecules 27:1340. https://doi.org/10.3390/molecules27041340

Díaz J, Rendueles M, Díaz M (2010) Straining phenomena in bacteria transport through natural porous media. Environ Sci Pollut Res 17:400–409. https://doi.org/10.1007/s11356-009-0160-2

Diedrich T, Dybowska A, Schott J, et al (2012) The dissolution rates of SiO_2 nanoparticles as a function of particle size. Environ Sci Technol 46:4909–4915. https://doi.org/10.1021/es2045053

Dimkpa CO (2018). Soil properties influence the response of terrestrial plants to metallic nanoparticles exposure. Curr Opin Environ Sci Heal 6:1–8. https://doi.org/10.1016/j.coesh.2018.06.007

Dimkpa CO, Bindraban PS (2018) Nano-fertilizers: new products for the industry? J. Agric. Food Chem. 66:6462-6473. https://doi.org/10.1021/acs.jafc.7b02150

Dimkpa CO, Fugice J, Singh U, Lewis TD (2020) Development of fertilizers for enhanced nitrogen use efficiency – Trends and perspectives. Sci Total Environ 731:139113. https://doi.org/10.1016/j.scitotenv.2020.139113

Dimkpa CO, Singh U, Bindraban PS, et al (2018) Exposure to weathered and fresh nanoparticle and ionic zn in soil promotes grain yield and modulates nutrient acquisition in wheat (*Triticum aestivum* L.). J. Agric. Food Chem. 66:9645-9656. https://doi.org/10.1021/acs.jafc.8b03840

Dinesh R, Anandaraj M, Srinivasan V, Hamza S (2012) Engineered nanoparticles in the soil and their potential implications to microbial activity. Geoderma 173–174:19–27. https://doi.org/10.1016/j.geoderma.2011.12.018

do Espirito Santo Pereira A, Caixeta Oliveira H, Fernandes Fraceto L, Santaella C (2021) nanotechnology potential in seed priming for sustainable agriculture. Nanomater. 11:267. https://doi.org/10.3390/nano11020267

Dolijanović Ž, Nikolić SR, Dragicevic V, et al (2022) Mineral composition of soil and the wheat grain in intensive and conservation cropping systems. Agronomy 12:1321. https://doi.org/10.3390/agronomy12061321

Domingos RF, Rafiei Z, Monteiro CE, et al (2013) Agglomeration and dissolution of zinc oxide nanoparticles: role of pH, ionic strength and fulvic acid. Environ Chem 10:306–312. https://doi.org/10.1071/EN12202

Du W, Sun Y, Ji R, et al (2011) TiO_2 and ZnO nanoparticles negatively affect wheat growth and soil enzyme activities in agricultural soil. J Environ Monit 13:822–828. https://doi.org/10.1039/C0EM00611D

Du W, Yang J, Peng Q, et al (2019) Comparison study of zinc nanoparticles and zinc sulphate on wheat growth: from toxicity and zinc biofortification. Chemosphere 227:109–116. https://doi.org/10.1016/j.chemosphere.2019.03.168

Dubchak S, Ogar A, Mietelski JW, Turnau K (2010) Influence of silver and titanium nanoparticles on arbuscular mycorrhiza colonization and accumulation of radiocaesium in *Helianthus annuus*. Span. J. Agric. Res. 8:103–108. https://doi.org/10.5424/sjar/201008S1-1228

Dutta P (2018) Seed priming: new vistas and contemporary perspectives. In: Rakshit A, Singh HB (eds). Advances in seed priming. Springer, Singapore, pp. 3–22. https://doi.org/10.1007/978-981-13-0032-5_1

Eagling T, Neal AL, McGrath SP, et al (2014) Distribution and speciation of iron and zinc in grain of two wheat genotypes. J Agric Food Chem 62:708–716. https://doi.org/10.1021/jf403331p

Ejaz A, Ahmad K, Khan ZI, et al (2022) Assessment of cobalt in wheat grains as affected by diverse fertilizers: implications for public health. Environ Sci Pollut Res 29:34558–34574. https://doi.org/10.1007/s11356-022-18528-0

Elemike EE, Uzoh IM, Onwudiwe DC, Babalola OO (2019) The role of nanotechnology in the fortification of plant nutrients and improvement of crop production. Appl Sci 9:1–32. https://doi.org/10.3390/app9030499

Elhaj Baddar Z, Matocha CJ, Unrine JM (2019) Surface coating effects on the sorption and dissolution of ZnO nanoparticles in soil. Environ Sci Nano 6:2495–2507. https://doi.org/10.1039/C9EN00348G

Elmer WH, White JC (2016) The use of metallic oxide nanoparticles to enhance growth of tomatoes and eggplants in disease infested soil or soilless medium. Environ Sci Nano 3:1072–1079. https://doi.org/10.1039/c6en00146g

Ely DR, Edwin García R, Thommes M (2014) Ostwald–Freundlich diffusion-limited dissolution kinetics of nanoparticles. Powder Technol 257:120–123. https://doi.org/10.1016/j.powtec.2014.01.095

Ermolin M, Fedyunina N, Katasonova O (2019) Mobility and fate of cerium dioxide, zinc oxide, and copper nanoparticles in agricultural soil at sequential wetting-drying cycles. Mater. 12:1270. https://doi.org/10.3390/ma12081270

Espinoza-García N, Martínez-Martínez R, Chávez-Servia JL, et al (2016) Contenido de minerales en semilla de poblaciones nativas de frijol común (*Phaseolus vulgaris* L.). Rev Fitotec Mex 39:215–223.

Estrada-Gómez JA, Estrada-Trejo V, Hernández-Livera A, et al (2004) OTI, una nueva variedad de frijol para el valle de méxico. Rev Fitotec Mex 27:115. https://doi.org/10.35196/rfm.2004.1.115

Etefagh R, Azhir E, Shahtahmasebi N (2013) Synthesis of CuO nanoparticles and fabrication of nanostructural layer biosensors for detecting A*spergillus niger fungi.* Sci Iran 20:1055–1058. https://doi.org/10.1016/j.scient.2013.05.015

Fageria NK, Filho MPB, Moreira A, Guimarães CM (2009) Foliar fertilization of crop plants. J Plant Nutr 32:1044–1064. https://doi.org/10.1080/01904160902872826

Fajardo C, Saccà ML, Costa G, et al (2014) Impact of Ag and Al_2O_3 nanoparticles on soil organisms: *In vitro* and soil experiments. Sci Total Environ 473–474:254–261. https://doi.org/10.1016/j.scitotenv.2013.12.043

Fajardo C, Sánchez-Fortún S, Costa G, et al (2020) Evaluation of nanoremediation strategy in a Pb, Zn and Cd contaminated soil. Sci Total Environ 706:136041. https://doi.org/10.1016/j.scitotenv.2019.136041

Fan R, Huang YC, Grusak MA, et al (2014) Effects of nano-TiO_2 on the agronomically-relevant *Rhizobium*–legume symbiosis. Sci Total Environ 466–467:503–512. https://doi.org/10.1016/j.scitotenv.2013.07.032

FAO (2021) World Food and Agriculture – Statistical Yearbook 2021. FAO, Rome

FAO (2022) Soils for nutrition: state of the art. FAO, Rome

FAO (2019) The international code of conduct for the sustainable use and management of fertilizers. FAO, Rome

FAO, IFAD, UNICEF, et al (2022) The State of Food Security and Nutrition in the World 2022. FAO, Rome

FAO, IFAD, UNICEF, et al (2020) The State of Food Security and Nutrition in the World 2020. FAO, IFAD, UNICEF, WFP and WHO, Rome

Fatemi H, Esmaiel Pour B, Rizwan M (2020) Foliar application of silicon nanoparticles affected the growth, vitamin C, flavonoid, and antioxidant enzyme activities of coriander (*Coriandrum sativum* L.) plants grown in lead (Pb)-spiked soil. Environ Sci Pollut Res. https://doi.org/10.1007/s11356-020-10549-x

Fatima F, Hashim A, Anees S (2021) Efficacy of nanoparticles as nanofertilizer production: a review. Environ Sci Pollut Res 28:1292–1303. https://doi.org/10.1007/s11356-020-11218-9

Fedorova EE, Coba de la Peña T, Lara-Dampier V, et al (2021) Potassium content diminishes in infected cells of *Medicago truncatula* nodules due to the mislocation of channels MtAKT1 and MtSKOR/GORK. J Exp Bot 72:1336–1348. https://doi.org/10.1093/jxb/eraa508

Feizi H, Rezvani Moghaddam P, Shahtahmassebi N, Fotovat A (2012) Impact of bulk and nanosized titanium dioxide (TiO_2) on wheat seed germination and seedling growth. Biol Trace Elem Res 146:101–106. https://doi.org/10.1007/s12011-011-9222-7

Feng Y, Cui X, He S, et al (2013) The role of metal nanoparticles in influencing arbuscular mycorrhizal fungi effects on plant growth. Environ Sci Technol 47:9496-9504. https://doi.org/10.1021/es402109n

FIRA (2022) Agrocostos Interactivo. https://www.fira.gob.mx/agrocostosApp/AgroApp.jsp Accessed 13 Oct 2022

FIRA (2023) Agrocostos Interactivo, https://www.fira.gob.mx/agrocostosApp/AgroApp.jsp Accessed 3 Jan 2023.

Fixen P, Brentrup F, Bruulsema T, et al (2015) Nutrient/fertilizer use efficiency: measurement, current situation and trends. In: Drechsel P, Heffer P, Magen H, et al. (eds). Managing water and fertilizer for sustainable agricultural intensification. International Fertilizer Industry Association(IFA), International Water Management Institute (IWMI), International Plant Nutrition Institute (IPNI), and International Potash Institute (IPI), Paris, France, pp 8–38

Freiberg S, Zhu XX (2004) Polymer microspheres for controlled drug release. Int J Pharm 282:1–18. https://doi.org/https://doi.org/10.1016/j.ijpharm.2004.04.013

Galanakis CM, Drago SR (2022) Introduction. In: Galanakis CM (ed). Nutraceutical and functional food components. Academic Press, London, UK pp 1–18. https://doi.org/10.1016/B978-0-323-85052-0.00003-9.

Gao Y, Shang C, Saghai Maroof MA, et al (2007) A modified colorimetric method for phytic acid analysis in soybean. Crop Sci 47:1797–1803. https://doi.org/10.2135/cropsci2007.03.0122

García-Gómez C, García S, Obrador AF, et al (2018) Effects of aged ZnO NPs and soil type on Zn availability, accumulation and toxicity to pea and beet in a greenhouse experiment. Ecotoxicol Environ Saf 160:222–230. https://doi.org/10.1016/j.ecoenv.2018.05.019

Gatoo MA, Naseem S, Arfat MY, et al (2014) Physicochemical properties of nanomaterials: implication in associated toxic manifestations. Biomed Res Int 2014:498420. https://doi.org/10.1155/2014/498420

Ge Y, Priester JH, Van De Werfhorst LC, et al (2014) Soybean plants modify metal oxide nanoparticle effects on soil bacterial communities. Environ Sci Technol 48:13489–13496. https://doi.org/10.1021/es5031646

Gens A., Roos J., Koschitzky H.-P., Joner E., Coutris C., Bardos P., Braun J., van Gaans P., Oughton D., Nathanail P., Limasse E. (2016) NanoRem 1: Nanotechnology for contaminated land remediation – possibilities and future trends resulting from the nanorem project. CL:AIRE and NanoRem 4:1–6 Ghafari H, Razmjoo J (2015) Response of durum wheat to foliar application of varied sources and rates of iron fertilizers. J Agric Sci Technol 17:321–331.

Ghareeb RY, Alfy H, Fahmy AA, et al (2020) Utilization of *Cladophora glomerata* extract nanoparticles as eco-nematicide and enhancing the defense responses of tomato plants infected by *Meloidogyne javanica*. Sci Rep 10:19968. https://doi.org/10.1038/s41598-020-77005-1

Ghori MU, Conway BR (2015) Hydrophilic Matrices for Oral Control Drug Delivery. Am J Pharmacol Sci 3:103–109. https://doi.org/10.12691/ajps-3-5-1

Ghormade V, Deshpande M V, Paknikar KM (2011) Perspectives for nano-biotechnology enabled protection and nutrition of plants. Biotechnol Adv 29:792–803. https://doi.org/10.1016/j.biotechadv.2011.06.007

Giannousi K, Avramidis I, Dendrinou-Samara C (2013) Synthesis, characterization and evaluation of copper based nanoparticles as agrochemicals against Phytophthora infestans. RSC Adv 3:21743–21752. https://doi.org/10.1039/C3RA42118J

Gibon Y, Sulpice R, Larher F (2000) Proline accumulation in canola leaf discs subjected to osmotic stress is related to the loss of chlorophylls and to the decrease of mitochondrial activity. Physiol Plant 110:469–476. https://doi.org/10.1111/j.1399-3054.2000.1100407.x

Gil-Díaz M, Alonso J, Rodríguez-Valdés E, et al (2017) Comparing different commercial zero valent iron nanoparticles to immobilize As and Hg in brownfield soil. Sci Total Environ 584–585:1324–1332. https://doi.org/10.1016/j.scitotenv.2017.02.011

Gil-Díaz M, Diez-Pascual S, González A, et al (2016) A nanoremediation strategy for the recovery of an As-polluted soil. Chemosphere 149:137–145. https://doi.org/10.1016/j.chemosphere.2016.01.106

Gil-díaz M, Rodríguez-valdés E, Alonso J, et al (2019) Nanoremediation and long-term monitoring of brown field soil highly polluted with As and Hg. Sci Total Environ 675:165–175. https://doi.org/10.1016/j.scitotenv.2019.04.183

Gilbert C, Ayanda OS, Fatoba OO, et al (2019) A novel method of using iron nanoparticles from coal fly ash or ferric chloride for acid mine drainage remediation. Mine Water Environ 38:617–631. https://doi.org/10.1007/s10230-019-00605-5

Glahn RP, Noh H (2021) Redefining bean iron biofortification: a review of the evidence for moving to a high fe bioavailability approach. Front Sustain Food Syst 5:682130. https://doi.org/10.3389/fsufs.2021.682130

Gohari G, Mohammadi A, Akbari A, et al (2020) Titanium dioxide nanoparticles (TiO_2 NPs) promote growth and ameliorate salinity stress effects on essential oil profile and biochemical attributes of *Dracocephalum moldavica*. Sci Rep 10:912. https://doi.org/10.1038/s41598-020-57794-1

Gomes DG, Pelegrino MT, Ferreira AS, et al (2021) Seed priming with copper-loaded chitosan nanoparticles promotes early growth and enzymatic antioxidant defense of maize (*Zea mays* L.) seedlings. J Chem Technol Biotechnol: https://doi.org/10.1002/jctb.6738

Gong X, Huang D, Liu Y, et al (2018). Remediation of contaminated soils by biotechnology with nanomaterials : bio-behavior, applications, and perspectives. Crit Rev Biotechnol 3:455–468. https://doi.org/10.1080/07388551.2017.1368446

González-Chávez MC, Carrillo-González R, Wright SF, Nichols KA (2004) The role of glomalin, a protein produced by arbuscular mycorrhizal fungi, in sequestering potentially toxic elements. Environ Pollut 130:317–323. https://doi.org/10.1016/j.envpol.2004.01.004

González-Chávez MCA, Carrillo González R, Sánchez-López AS, Ruiz-Olivares A (2017) Alternativas de fitorremediación de sitios contaminados con elementos potencialmente tóxicos. Agroproductividad. 10:8–14.

Govindan V, Michaux KD, Pfeiffer WH (2022) Nutritionally enhanced wheat for food and nutrition security. In: Reynolds MP, Braun H-J (eds) Wheat Improvement. Cham, pp 195–214. https://doi.org/10.1007/978-3-030-90673-3_12

Graham JH, Johnson EG, Myers ME, et al (2016) Potential of nano-formulated zinc oxide for control of citrus canker on grapefruit trees. Plant Dis 100:2442–2447. https://doi.org/10.1094/PDIS-05-16-0598-RE

Grieger KD, Hjorth R, Rice J, et al (2015) Nano-remediation : tiny particles cleaning up big environmental problems. DTU Orbit. http://cmsdata.iucn.org/downloads/nanoremediation.pdf. Accessed 23 May 2021

Grillo R, Mattos BD, Antunes DR, et al (2021) Foliage adhesion and interactions with particulate delivery systems for plant nanobionics and intelligent agriculture. Nano Today 37:101078. https://doi.org/10.1016/j.nantod.2021.101078

Guan X, Gao X, Avellan A, et al (2020) CuO Nanoparticles alter the rhizospheric bacterial community and local nitrogen cycling for wheat grown in a calcareous soil. Environ Sci Technol 54:8699–8709. https://doi.org/10.1021/acs.est.0c00036

Guerra FD, Attia MF, Whitehead DC, Alexis F (2018) Nanotechnology for environmental remediation: Materials and applications. Molecules 23:1–23. https://doi.org/10.3390/molecules23071760

Hafeez MB, Ramzan Y, Khan S, et al (2021) Application of zinc and iron-based fertilizers improves the growth attributes, productivity, and grain quality of two wheat (*Triticum aestivum*) cultivars. Front Nutr 8: 779595. https://doi.org/10.3389/fnut.2021.779595

Hashem A, Abd_Allah EF, Alqarawi AA, et al (2016) The Interaction between Arbuscular Mycorrhizal Fungi and Endophytic Bacteria Enhances Plant Growth of *Acacia gerrardii* under Salt Stress. Front Microbiol 7: 1089. https://doi.org/10.3389/fmicb.2016.01089

HarvestPlus (2022) Hight iron beans. a food that can change your business and the world naturally. https://www.harvestplus.org/wp-content/uploads/2022/01/Iron-Beans.pdf. Accessed 16 november 2022.

Hassan MU, Aamer M, Nawaz M, et al (2021) Agronomic bio-fortification of wheat to combat zinc deficiency in developing countries. Pakistan J Agric Res 34:201–217. https://doi.org/10.17582/journal.pjar/2021/34.1.201.217

He L, Liu Y, Mustapha A, Lin M (2011a) Antifungal activity of zinc oxide nanoparticles against *Botrytis cinerea* and *Penicillium expansum*. Microbiol Res 166:207–215. https://doi.org/https://doi.org/10.1016/j.micres.2010.03.003

He S, Feng Y, Ren H, Zhang Y (2011b) The impact of iron oxide magnetic nanoparticles on the soil bacterial community. J Soils Sediments 11:1408–1417. https://doi.org/10.1007/s11368-011-0415-7

Hedberg J, Blomberg E, Odnevall Wallinder I (2019) In the search for nanospecific effects of dissolution of metallic nanoparticles at freshwater-like conditions: a critical review. Environ Sci Technol 53:4030–4044. https://doi.org/10.1021/acs.est.8b05012

Hedge J, Wilson DJ (2016) Practical approaches for detecting selection in microbial genomes. PLOS Comput Biol 12:e1004739. https://doi.org/10.1371/journal.pcbi.1004739

Hefferon KL, Downs S, Oliu GO, De Steur H (2021) Editorial: sustainable development goals (SDGs): impact on nutrition. Front Nutr 8:. https://doi.org/10.3389/fnut.2021.676080

Hofmann T, Lowry GV, Ghoshal S, et al (2020) Technology readiness and overcoming barriers to sustainably implement nanotechnology-enabled plant agriculture. Nat Food 1:416–425. https://doi.org/10.1038/s43016-020-0110-1

Hoppe M, Mikutta R, Utermann J, et al (2014) Retention of sterically and electrosterically stabilized silver nanoparticles in soils. Environ Sci Technol 48:12628–12635. https://doi.org/10.1021/es5026189

Horton S (2004) The economic impact of micronutrient deficiencies. In: J.M. Pettifor, and S. Zlotkin (eds). Micronutrient Deficiencies during the weaning period and the first years of life Nestlé Nutrition Institute Workshop Series. Nestle Ltd, Vevey/S, Karger AG, Basel, pp 187–202. https://doi.org/10.1159/000080611

Hu X, Wei X, Ling J, Chen J (2021) Cobalt: an essential micronutrient for plant growth? Front Plant Sci 12:. https://doi.org/10.3389/fpls.2021.768523

Huang B, Chen F, Shen Y, et al (2018) Advances in targeted pesticides with environmentally responsive controlled release by nanotechnology. Nanomater. 8:102. https://doi.org/10.3390/nano8020102

Huang D, Xue W, Zeng G, et al (2016) Immobilization of Cd in river sediments by sodium alginate modified nanoscale zero-valent iron: Impact on enzyme activities and microbial community diversity. Water Res 106:15–25. https://doi.org/10.1016/j.watres.2016.09.050

Huang Y, Keller AA (2020) Remediation of heavy metal contamination of sediments and soils using ligand-coated dense nanoparticles. PLoS One 15:e0239137. https://doi.org/10.1371/journal.pone.0239137

Huang YC, Fan R, Grusak MA, et al (2014) Effects of nano-ZnO on the agronomically relevant *Rhizobium*-legume symbiosis. Sci Total Environ 497–498:78–90. https://doi.org/10.1016/j.scitotenv.2014.07.100

Huertas R, Karpinska B, Ngala S, et al (2022) Biofortification of common bean (*Phaseolus vulgaris* L.) with iron and zinc: achievements and challenges. Food Energy Secur 00:e406. https://doi.org/https://doi.org/10.1002/fes3.406

Hummel M, Talsma EF, Taleon V, et al (2020) Iron, zinc and phytic acid retention of biofortified, low phytic acid, and conventional bean varieties when preparing common household recipes. Nutrients 12:658. https://doi.org/10.3390/nu12030658

Huo C, Ouyang J, Yang H (2014) CuO nanoparticles encapsulated inside Al-MCM-41 mesoporous materials via direct synthetic route. Sci Rep 4:3682. https://doi.org/10.1038/srep03682

Hurrell RF (2021) Iron fortification practices and implications for iron addition to salt. J Nutr 151:3S-14S. https://doi.org/10.1093/jn/nxaa175

Iannone MF, Groppa MD, de Sousa ME, et al (2016) Impact of magnetite iron oxide nanoparticles on wheat (*Triticum aestivum* L.) development: evaluation of oxidative damage. Environ Exp Bot 131:77–88. https://doi.org/10.1016/j.envexpbot.2016.07.004

Iavicoli I, Leso V, Fontana L, Calabrese EJ (2018) Nanoparticle exposure and hormetic dose–responses: an update. Int. J. Mol. Sci. 19: 805. https://doi.org/10.3390/ijms19030805

Ighaiee Oskoiee A, Ghanbari AA, Mirhadi MJ (2021) Effects of iron nanoparticles on seed germination of bean genotypes. SSRN Electron J. https://doi.org/10.2139/ssrn.3899301

Imtiaz M, Alloway BJ, Shah KH, et al (2003) Zinc nutrition of wheat: ii: interaction of zinc with other trace elements. Asian J Plant Sci 2:156–160. https://doi.org/10.3923/ajps.2003.156.160

Ingram J (2020) Nutrition security is more than food security. Nat Food 1:2. https://doi.org/10.1038/s43016-019-0002-4

International Monetary Fund (2021) Representative exchange rates for selected currencies for september 2021. https://www.imf.org/external/np/fin/data/rms_mth.aspx?SelectDate=2021-09-30&reportType=REP. Accessed 9 Oct 2022

ISO/TC 229 Nanotechnologies (2017) ISO/TR 19057:2017 Nanotechnologies- Use and application of acellular in vitro test and methodologies to assess nanomaterial biodurability. ISO website. Accessed 18 Nov 2021.

IUSS Working Group WRB (2006) World reference base for soil resources 2006 A framework for international classification, correlation and communication, 2nd edn. FAO, Rome

Jacoby R, Peukert M, Succurro A, et al (2017) The role of soil microorganisms in plant mineral nutrition—current knowledge and future directions. Front Plant Sci 8:1617. https://doi.org/10.3389/fpls.2017.01617

Jagana D, R. Hegde Y, Lella R (2017) Green nanoparticles - A novel approach for the management of banana anthracnose aused by *colletotrichum musae*. Int J Curr Microbiol Appl Sci 6:1749–1756. https://doi.org/10.20546/ijcmas.2017.610.211

Jahani M, Khavari-Nejad RA, Mahmoodzadeh H, Saadatmand S (2019) Effects of foliar application of cobalt oxide nanoparticles on growth, photosynthetic pigments, oxidative indicators, non-enzymatic antioxidants and compatible osmolytes in canola (*Brassica napus* L.). Acta Biol Cracoviensia s Bot 61:29–42. https://doi.org/10.24425/abcsb.2019.127736

Jahani S, Saadatmand S, Mahmoodzadeh H, Khavari-Nejad RA (2018) Effects of cerium oxide nanoparticles on biochemical and oxidative parameters in marigold leaves. Toxicol Environ Chem 100:677–692. https://doi.org/10.1080/02772248.2019.1587443

Jan B, Bhat TA, Sheikh TA, et al (2020) Agronomic bio-fortification of rice and maize with iron and zinc: a review. Int Res J Pure Appl Chem 28–37. https://doi.org/10.9734/irjpac/2020/v21i1630257

Jange CG, Wassgren CR, Ambrose RPK (2021) Disintegration and release kinetics of dry compacted urea composites: a formulation and process design study. EFB Bioeconomy J 1:100020. https://doi.org/10.1016/j.bioeco.2021.100020

Jaspers C, Fraune S, Arnold AE, et al (2019) Resolving structure and function of metaorganisms through a holistic framework combining reductionist and integrative approaches. Zoology 133:81–87. https://doi.org/10.1016/j.zool.2019.02.007

Jhanzab HM, Qayyum A, Bibi Y, et al (2022) Fe nanoparticles effect on growth, physiochemical and yield traits of wheat (*Triticum aestivum*). Agronomy 12:757. https://doi.org/10.3390/agronomy12040757

Jing X-X, Su Z-Z, Xing H-E, et al (2016) Biological effects of zno nanoparticles as influenced by arbuscular mycorrhizal inoculation and phosphorus fertilization. Huan jing ke xue= Huanjing kexue 37:3208–3215. https://doi.org/10.13277/j.hjkx.2016.08.049

Jones D (2002) Simple method to enable the high resolution determination of total free amino acids in soil solutions and soil extracts. Soil Biol Biochem 34:1893–1902. https://doi.org/10.1016/S0038-0717(02)00203-1

Joseph S, Anawar HM, Storer P, et al (2015) Effects of enriched biochars containing magnetic iron nanoparticles on mycorrhizal colonisation, plant growth, nutrient uptake and soil quality improvement. Pedosphere 25:749–760. https://doi.org/10.1016/S1002-0160(15)30056-4

Jośko I, Oleszczuk P, Dobrzyńska J, et al (2019) Long-term effect of ZnO and CuO nanoparticles on soil microbial community in different types of soil. Geoderma 352:204–212. https://doi.org/10.1016/j.geoderma.2019.06.010

Juárez-Maldonado A, Tortella G, Rubilar O, et al (2021) Biostimulation and toxicity: the magnitude of the impact of nanomaterials in microorganisms and plants. J Adv Res. 31:113-126. https://doi.org/10.1016/j.jare.2020.12.011

Judy JD, Kirby JK, Creamer C, et al (2015) Effects of silver sulfide nanomaterials on mycorrhizal colonization of tomato plants and soil microbial communities in biosolid-amended soil. Environ Pollut 206:256–263. https://doi.org/10.1016/j.envpol.2015.07.002

Judy JD, Kirby JK, McLaughlin MJ, et al (2016) Symbiosis between nitrogen-fixing bacteria and *Medicago truncatula* is not significantly affected by silver and silver sulfide nanomaterials. Environ Pollut 214:731–736. https://doi.org/10.1016/j.envpol.2016.04.078

Kabata-Pendias A (2010) Trace Elements in Soils and Plants. CRC Press

Kah M (2015) Nanopesticides and nano-fertilizers: emerging contaminants or opportunities for risk mitigation? Front Chem 3:1–6. https://doi.org/10.3389/fchem.2015.00064

Kah M, Kookana RS, Gogos A, Bucheli TD (2018) A critical evaluation of nanopesticides and nanofertilizers against their conventional analogues. Nat Nanotechnol 13:677–684. https://doi.org/10.1038/s41565-018-0131-1

Kah M, Tufenkji N, White JC (2019) Nano-enabled strategies to enhance crop nutrition and protection. Nat Nanotechnol 14:532–540. https://doi.org/10.1038/s41565-019-0439-5

Kandhol N, Singh VP, Ramawat N, et al (2022) Nano-priming: Impression on the beginner of plant life. Plant Stress 5:100091. https://doi.org/10.1016/j.stress.2022.100091

Kanhed P, Birla S, Gaikwad S, et al (2014) *In vitro* antifungal efficacy of copper nanoparticles against selected crop pathogenic fungi. Mater Lett 115:13–17. https://doi.org/10.1016/j.matlet.2013.10.011

Karn B, Kuiken T, Otto M (2009) Nanotechnology and *in situ* remediation: a review of the benefits and potential risks. Environ. Health Perspect. 117:1823–1831. https://doi.org/10.1289/ehp.0900793

Karunakaran G, Suriyaprabha R, Manivasakan P, et al (2013) Effect of nanosilica and silicon sources on plant growth promoting rhizobacteria, soil nutrients and maize seed germination. IET nanobiotechnology 7:70–77. https://doi.org/10.1049/iet-nbt.2012.0048

Kaushik H., Dutta P. (2017) Chemical synthesis of zinc oxide nanoparticle: its application for antimicrobialactivity and plant health management. In: Paper presented at the 109th Annual Meeting of the American Phytopathological Society, San Antonio, TX, August

Kefeni KK, Mamba BB, Msagati TAM (2017) Magnetite and cobalt ferrite nanoparticles used as seeds for acid mine drainage treatment. J Hazard Mater 333:308–318. https://doi.org/10.1016/j.jhazmat.2017.03.054

Kefeni KK, Msagati TAM, Nkambule TTI, Mamba BB (2018) Synthesis and application of hematite nanoparticles for acid mine drainage treatment. J Environ Chem Eng 6:1865–1874. https://doi.org/10.1016/j.jece.2018.02.037

Keller J, Peijnenburg W, Werle K, et al (2020) Understanding dissolution rates via continuous flow systems with physiologically relevant metal ion saturation in lysosome. Nanomaterials 10:311. https://doi.org/10.3390/nano10020311

Khalid M, Ur-rahman S, Hassani D, et al (2021) Advances in fungal-assisted phytoremediation of heavy metals: a review. Pedosphere 31:475–495. https://doi.org/10.1016/S1002-0160(20)60091-1

Khan MK, Pandey A, Hamurcu M, et al (2021) Insight into the prospects for nanotechnology in wheat biofortification. Biol. 10:1123. https://doi.org/10.3390/biology10111123

Khan MN (2016) Nano-titanium dioxide (Nano-TiO_2) mitigates NaCl stress by enhancing antioxidative enzymes and accumulation of compatible solutes in tomato (*Lycopersicon esculentum* Mill.). J Plant Sci 11:1–11. https://doi.org/10.3923/jps.2016.1.11

Khan MN, Fu C, Li J, et al (2023) Seed nanopriming: how do nanomaterials improve seed tolerance to salinity and drought? Chemosphere 310:136911. https://doi.org/10.1016/j.chemosphere.2022.136911

Khan MN, Li Y, Khan Z, et al (2021b) Nanoceria seed priming enhanced salt tolerance in rapeseed through modulating ROS homeostasis and α-amylase activities. J Nanobiotechnology 19:276. https://doi.org/10.1186/s12951-021-01026-9

Khosroyar S, Akbarzade A, Arjoman M, et al (2012) Ferric–saccharate capsulation with alginate coating using the emulsification method. African J Microbiol Res 6:2455–2461. https://doi.org/10.5897/ajmr11.1514

Khot LR, Sankaran S, Maja JM, et al (2012) Applications of nanomaterials in agricultural production and crop protection: a review. Crop Prot 35:64–70. https://doi.org/10.1016/j.cropro.2012.01.007

Kim D-Y, Kadam A, Shinde S, et al (2018) Recent developments in nanotechnology transforming the agricultural sector: a transition replete with opportunities. J Sci Food Agric 98:849–864. https://doi.org/10.1002/jsfa.8749

Kim J-H, Kim S-M, Yoon I-H, et al (2020) Selective separation of Cs-contaminated clay from soil using polyethylenimine-coated magnetic nanoparticles. Sci Total Environ 706:136020. https://doi.org/10.1016/j.scitotenv.2019.136020

Kim MS, Kim GW, Park TJ (2015) A facile and sensitive detection of organophosphorus chemicals by rapid aggregation of gold nanoparticles using organic compounds. Biosens Bioelectron 67:408–412. https://doi.org/10.1016/j.bios.2014.08.073

Kim T-Y (2022) Critical minerals threaten a decades-long trend of cost declines for clean energy technologies. In: 18 May 2022. https://www.iea.org/commentaries/critical-minerals-threaten-a-decades-long-trend-of-cost-declines-for-clean-energy-technologies. Accessed 12 Oct 2022

Kitson RE, Mellon MG (1944) Colorimetric determination of phosphorus as molybdivanadophosphoric acid. Ind Eng Chem Anal Ed 16:379–383. https://doi.org/10.1021/i560130a017

Kjeldahl J (1883) Neue methode zur bestimmung des stickstoffs in organischen körpern. zeitschrift für. Anal Chemie 22:366–382. https://doi.org/10.1007/BF01338151

Knijnenburg JTN, Hilty FM, Oelofse J, et al (2018) Nano- and pheroid technologies for development of foliar iron fertilizers and iron biofortification of soybean grown in South Africa. Chem Biol Technol Agric 5:26. https://doi.org/10.1186/s40538-018-0138-8

Kookana RS, Boxall ABA, Reeves PT, et al (2014) Nanopesticides: guiding principles for regulatory evaluation of environmental risks. J Agric Food Chem 62:4227–4240. https://doi.org/10.1021/jf500232f

Kothari R, Wani KA (2018) Environmentally friendly slow release nano-chemicals in agriculture. In Poonia R, Gao X., Raja L., Sharma S., Vyas S. (eds) Smart farming technologies for sustainable agricultural development. IGI Global, pp 220–240. https://doi.org/10.4018/978-1-5225-5909-2.ch010

Kottegoda N, Sandaruwan C, Priyadarshana G, et al (2017) Urea-hydroxyapatite nanohybrids for slow release of nitrogen. ACS Nano 11:1214–1221. https://doi.org/10.1021/acsnano.6b07781

Kumar A, Choudhary A, Kaur H, et al (2021) Smart nanomaterial and nanocomposite with advanced agrochemical activities. Nanoscale Res Lett 16:156. https://doi.org/10.1186/s11671-021-03612-0

Kumar KV, Khaddour IA, Gupta VK (2010) A pseudo second-order kinetic expression for dissolution kinetic profiles of solids in solutions. Ind Eng Chem Res 49:7257–7262. https://doi.org/10.1021/ie1010228

Kumar P, Burman U, Santra P (2015) Effect of nano-zinc oxide on nitrogenase activity in legumes: an interplay of concentration and exposure time. Int Nano Lett 5:191–198. https://doi.org/10.1007/s40089-015-0155-6

Kumar S, Nehra M, Dilbaghi N, et al (2019) Nano-based smart pesticide formulations: emerging opportunities for agriculture. J Control Release 294:131–153. https://doi.org/10.1016/j.jconrel.2018.12.012

Kumar S, Sharma SK, Thakral SK, et al (2022) Integrated nutrient management improves the productivity and nutrient use efficiency of *Lens culinaris* Medik. Sustainability 14:1284. https://doi.org/10.3390/su14031284

Kwak S-Y, Wong MH, Lew TTS, et al (2017) Nanosensor technology applied to living plant systems. Annu Rev Anal Chem 10:113–140. https://doi.org/10.1146/annurev-anchem-061516-045310

Laboratories SR (2022) Cobalt iron oxide nanopowder. https://www.srlchem.com/products/compound/Cobalt-Ferrite-Nanopowder/31570. Accessed 9 Nov 2022

Lacalle RG, Garbisu C, Becerril JM (2020) Effects of the application of an organic amendment and nanoscale zero-valent iron particles on soil Cr(VI) remediation. Environ Sci Pollut Res 27 :31726–31736. https://doi.org/10.1007/s11356-020-09449-x

Lal R (2020) The role of industry and the private sector in promoting the “4 per 1000” initiative and other negative emission technologies. Geoderma 378:114613. https://doi.org/10.1016/j.geoderma.2020.114613

Land Green and Technology Co (2020) Novaland Nano Fertilizers. https://www.lgt.tw/novaland. Accessed 5 Jan 2021

Lawrencia D, Wong SK, Low DYS, et al (2021) Controlled release fertilizers: a review on coating materials and mechanism of release. Plants 10:238. https://doi.org/10.3390/plants10020238

Le Van N, Ma C, Shang J, et al (2016) Effects of CuO nanoparticles on insecticidal activity and phytotoxicity in conventional and transgenic cotton. Chemosphere 144:661–670. https://doi.org/10.1016/j.chemosphere.2015.09.028

Lee Y-J, Kim J, Oh J, et al (2012) Ion-release kinetics and ecotoxicity effects of silver nanoparticles. Environ Toxicol Chem 31:155–159. https://doi.org/https://doi.org/10.1002/etc.717

LeFevre GH, Hozalski RM, Novak PJ (2013) Root exudate enhanced contaminant desorption: an abiotic contribution to the rhizosphere Effect. Environ Sci Technol 47:11545–11553. https://doi.org/10.1021/es402446v

Li X, Gui X, Rui Y, et al (2014) Bt-transgenic cotton is more sensitive to CeO_2 nanoparticles than its parental non-transgenic cotton. J Hazard Mater 274:173–180. https://doi.org/10.1016/j.jhazmat.2014.04.025

Li Y, Liang L, Li W, et al (2021) ZnO nanoparticle-based seed priming modulates early growth and enhances physio-biochemical and metabolic profiles of fragrant rice against cadmium toxicity. J Nanobiotechnology 19:75. https://doi.org/10.1186/s12951-021-00820-9

Lichtenthaler HK (1987) [34] Chlorophylls and carotenoids: pigments of photosynthetic biomembranes. Methods Enzymol. 148:350–382. https://doi.org/10.1016/0076-6879(87)48036-1

Lin D, Xing B (2008) Root uptake and phytotoxicity of ZnO nanoparticles. Environ Sci Technol 42:5580–5585. https://doi.org/10.1021/es800422x

Lin S, Reppert J, Hu Q, et al (2009) Uptake, translocation, and transmission of carbon nanomaterials in rice plants. Small 5:1128–1132. https://doi.org/10.1002/smll.200801556

Lindsay WL, Norvell WA (1978) Development of a DTPA soil test for zinc, iron, manganese, and copper. Soil Sci Soc Am J 42:421–428. https://doi.org/10.2136/sssaj1978.03615995004200030009x

Liu J, Cai H, Mei C, Wang M (2015) Effects of nano-silicon and common silicon on lead uptake and translocation in two rice cultivars. Front Environ Sci Eng 9:905–911. https://doi.org/10.1007/s11783-015-0786-x

Liu R, Lal R (2014) Synthetic apatite nanoparticles as a phosphorus fertilizer for soybean (*Glycine max*). Sci Rep 4:5686. https://doi.org/10.1038/srep05686

Liu R, Zhao D (2013) Synthesis and characterization of a new class of stabilized apatite nanoparticles and applying the particles to in situ Pb immobilization in a fire-range soil. Chemosphere 91:594—601. https://doi.org/10.1016/j.chemosphere.2012.12.034

Liu W, Zeb A, Lian J, et al (2020) Interactions of metal-based nanoparticles (MBNPs) and metal-oxide nanoparticles (MONPs) with crop plants: a critical review of research progress and prospects. Environ Rev 28:294–310. https://doi.org/10.1139/er-2019-0085

López-Luna J, Cruz-Fernández S, Mills DS, et al (2020) Phytotoxicity and upper localization of Ag@$CoFe_2O_4$ nanoparticles in wheat plants. Environ Sci Pollut Res 27:1923–1940. https://doi.org/10.1007/s11356-019-06668-9

López-Moreno ML, Avilés LL, Pérez NG, et al (2016) Effect of cobalt ferrite ($CoFe_2O_4$) nanoparticles on the growth and development of *Lycopersicon lycopersicum* (tomato plants). Sci Total Environ 550:45–52. https://doi.org/10.1016/j.scitotenv.2016.01.063

López–Luna J, Camacho–Martínez MM, Solís–Domínguez FA, et al (2018) Toxicity assessment of cobalt ferrite nanoparticles on wheat plants. J Toxicol Environ Heal Part A 81:604–619. https://doi.org/10.1080/15287394.2018.1469060

Louie SM, Spielman-Sun ER, Small MJ, et al (2015) Correlation of the physicochemical properties of natural organic matter samples from different sources to their effects on gold nanoparticle aggregation in monovalent electrolyte. Environ Sci Technol 49:2188–2198. https://doi.org/10.1021/es505003d

Lowry G V, Avellan A, Gilbertson LM (2019) Opportunities and challenges for nanotechnology in the agri-tech revolution. Nat Nanotechnol 14:517–522. https://doi.org/10.1038/s41565-019-0461-7

Lv J, Christie P, Zhang S (2019) Uptake, translocation, and transformation of metal-based nanoparticles in plants: recent advances and methodological challenges. Environ Sci Nano 6:41–59. https://doi.org/10.1039/C8EN00645H

Ma J, Song Z, Yang J, et al (2021) Cobalt ferrite nanozyme for efficient symbiotic nitrogen fixation via regulating reactive oxygen metabolism. Environ Sci Nano 8:188–203. https://doi.org/10.1039/D0EN00935K

Ma J, Zhou Y, Li J, et al (2022) Novel approach to enhance *Bradyrhizobium diazoefficiens* nodulation through continuous induction of ROS by manganese ferrite nanomaterials in soybean. J Nanobiotechnology 20:168. https://doi.org/10.1186/s12951-022-01372-2

Ma X, Geiser-lee J, Deng Y, Kolmakov A (2010). Interactions between engineered nanoparticles (ENPs) and plants : phytotoxicity , uptake and accumulation. Sci Total Environ 408:3053–3061. https://doi.org/10.1016/j.scitotenv.2010.03.031

Magallanes-López AM, Hernandez-Espinosa N, Velu G, et al (2017) Variability in iron, zinc and phytic acid content in a worldwide collection of commercial durum wheat cultivars and the effect of reduced irrigation on these traits. Food Chem 237:499–505. https://doi.org/10.1016/j.foodchem.2017.05.110

Mahajan P, Dhoke SK, Khanna AS (2011) Effect of nano-ZnO particle suspension on growth of mung (*Vigna radiata*) and Gram (*Cicer arietinum*) seedlings using plant agar method. J Nanotechnol 2011:696535. https://doi.org/10.1155/2011/696535

Mahakham W, Sarmah AK, Maensiri S, Theerakulpisut P (2017) Nanopriming technology for enhancing germination and starch metabolism of aged rice seeds using phytosynthesized silver nanoparticles. Sci Rep 7:8263. https://doi.org/10.1038/s41598-017-08669-5

Mahawar H, Prasanna R (2018) Prospecting the interactions of nanoparticles with beneficial microorganisms for developing green technologies for agriculture. Environ Nanotechnology, Monit Manag 10:477–485. https://doi.org/10.1016/j.enmm.2018.09.004

Mahdavi S, Afkhami A, Jalali M (2015) Reducing leachability and bioavailability of soil heavy metals using modified and bare Al_2O_3 and ZnO nanoparticles. Environ Earth Sci 73:4347–4371. https://doi.org/10.1007/s12665-014-3723-6

Mahmoodzadeh H, Nabavi, M., and Kashefi, H. (2013). Effect of nanoscale titanium dioxide particles on the germination and growth of canola (*Brassica napus*). J Ornam Hortic.3:25–32

Malhi GS, Kaur M, Kaushik P (2021) Impact of climate change on agriculture and its mitigation strategies: a review. Sustain. 13: 1318. https://doi.org/10.3390/su13031318

Malhotra H, Pandey R, Sharma S, Bindraban PS (2020) Foliar fertilization: possible routes of iron transport from leaf surface to cell organelles. Arch Agron Soil Sci 66:279–300. https://doi.org/10.1080/03650340.2019.1616288

Mallampati SR, Mitoma Y, Okuda T, et al (2012) High immobilization of soil cesium using ball milling with nano-metallic Ca/CaO/NaH_2PO_4: implications for the remediation of radioactive soils. Environ Chem Lett 10:201–207. https://doi.org/10.1007/s10311-012-0357-3

Maqbool A, Abrar M, Bakhsh A, et al (2020) Biofortification under climate change: the fight between quality and quantity. In: Fahad S, Hasanuzzaman M, Alam M, et al. (eds) Environment, climate, plant and vegetation growth. Springer, Cham, pp 173–227. https://doi.org/10.1007/978-3-030-49732-3_9

Mariotti F, Tomé D, Mirand PP (2008) Converting nitrogen into protein—beyond 6.25 and Jones' Factors. Crit Rev Food Sci Nutr 48:177–184. https://doi.org/10.1080/10408390701279749

Martínez-Fernández D, Vítková M, Bernal MP, Komárek M (2015) Effects of nano-maghemite on trace element accumulation and drought response of *Helianthus annuus* L. in a contaminated mine soil. Pollut 226:101. https://doi.org/10.1007/s11270-015-2365-y

Martinez-Vargas S, Martínez AI, Hernández-Beteta EE, et al (2017) Arsenic adsorption on cobalt and manganese ferrite nanoparticles. J Mater Sci 52:6205–6215. https://doi.org/10.1007/s10853-017-0852-9

Marzouk NM, Abd-Alrahman HA, EL-Tanahy AMM, Mahmoud SH (2019) Impact of foliar spraying of nano micronutrient fertilizers on the growth, yield, physical quality, and nutritional value of two snap bean cultivars in sandy soils. Bull Natl Res Cent 43:84. https://doi.org/10.1186/s42269-019-0127-5

Masrahi A, VandeVoort AR, Arai Y (2014) Effects of silver nanoparticle on soil-nitrification processes. Arch Environ Contam Toxicol 66:504–513. https://doi.org/10.1007/s00244-013-9994-1

Mastronardi E, Tsae P, Zhang X, et al (2015) Strategic role of nanotechnology in fertilizers: potential and limitations. In: Rai M, Ribeiro C, Mattoso L, Duran N (eds) Nanotechnologies in food and agriculture. Springer, Cham., pp 25–67. https://doi.org/10.1007/978-3-319-14024-7_2

Mazarji M, Minkina T, Sushkova S, et al (2021) Effect of nanomaterials on remediation of polycyclic aromatic hydrocarbons-contaminated soils: a review. J Environ Manage 284:112023. https://doi.org/10.1016/j.jenvman.2021.112023

Mendes R, Garbeva P, Raaijmakers JM (2013) The rhizosphere microbiome: significance of plant beneficial, plant pathogenic, and human pathogenic microorganisms. FEMS Microbiol Rev 37:634–663. https://doi.org/10.1111/1574-6976.12028

Miao A-J, Zhang X-Y, Luo Z, et al (2010) Zinc oxide–engineered nanoparticles: dissolution and toxicity to marine phytoplankton. Environ Toxicol Chem 29:2814–2822. https://doi.org/10.1002/etc.340

Michálková Z, Komárek M, Šillerová H, et al (2014) Evaluating the potential of three Fe- and Mn-(nano)oxides for the stabilization of Cd, Cu and Pb in contaminated soils. J Environ Manage 146:226–234. https://doi.org/10.1016/j.jenvman.2014.08.004

Michels C, Perazzoli S, M. Soares H (2017) Inhibition of an enriched culture of ammonia oxidizing bacteria by two different nanoparticles: silver and magnetite. Sci Total Environ 586:995–1002. https://doi.org/10.1016/j.scitotenv.2017.02.080

Milani N, McLaughlin MJ, Stacey SP, et al (2012) Dissolution kinetics of macronutrient fertilizers coated with manufactured zinc oxide nanoparticles. J Agric Food Chem 60:3991–3998. https://doi.org/10.1021/jf205191y

Mimmo T, Del Buono D, Terzano R, et al (2014) Rhizospheric organic compounds in the soil–microorganism–plant system: their role in iron availability. Eur J Soil Sci 65:629–642. https://doi.org/10.1111/ejss.12158

Miri A, Sarani M, Najafidoust A, et al (2022) Photocatalytic performance and cytotoxic activity of green-synthesized cobalt ferrite nanoparticles. Mater Res Bull 149:111706. https://doi.org/10.1016/j.materresbull.2021.111706

Misra SK, Dybowska A, Berhanu D, et al (2012) The complexity of nanoparticle dissolution and its importance in nanotoxicological studies. Sci Total Environ 438:225–232. https://doi.org/10.1016/j.scitotenv.2012.08.066

Misra SK, Nuseibeh S, Dybowska A, et al (2014) Comparative study using spheres, rods and spindle-shaped nanoplatelets on dispersion stability, dissolution and toxicity of CuO nanomaterials. Nanotoxicology 8:422–432. https://doi.org/10.3109/17435390.2013.796017

Mokarram-Kashtiban S, Hosseini SM, Tabari Kouchaksaraei M, Younesi H (2019) The impact of nanoparticles zero-valent iron (nZVI) and rhizosphere microorganisms on the phytoremediation ability of white willow and its response. Environ Sci Pollut Res Int 26:10776–10789. https://doi.org/10.1007/s11356-019-04411-y

Moll J, Gogos A, Bucheli TD, et al (2016) Effect of nanoparticles on red clover and its symbiotic microorganisms. J Nanobiotechnology 14:36. https://doi.org/10.1186/s12951-016-0188-7

Mondal A, Dubey BK, Arora M, Mumford K (2021) Porous media transport of iron nanoparticles for site remediation application: A review of lab scale column study, transport modelling and field-scale application. J Hazard Mater 403:123443. https://doi.org/10.1016/j.jhazmat.2020.123443

Monreal CM, DeRosa M, Mallubhotla SC, et al (2016) Nanotechnologies for increasing the crop use efficiency of fertilizer-micronutrients. Biol Fertil Soils 52:423–437. https://doi.org/10.1007/s00374-015-1073-5

Morales-Díaz A.B., Ortega-Ortíz H., Juárez-Maldonado A., Cadenas-Pliego G., González-Morales S. Benavides-Mendoza A. (2017) Application of nanoelements in plant nutrition and its impact in ecosystems. Adv Nat Sci: Nanosci Nanotechnol 8:013001. https://doi.org/10.1088/2043-6254/8/1/013001

Mourão HAJL, Malagutti AR, Ribeiro C (2010) Synthesis of TiO_2-coated $CoFe_2O_4$ photocatalysts applied to the photodegradation of atrazine and rhodamine B in water. Appl Catal A Gen 382:284–292. https://doi.org/10.1016/j.apcata.2010.05.007

Moussout H, Ahlafi H, Aazza M, Maghat H (2018) Critical of linear and nonlinear equations of pseudo-first order and pseudo-second order kinetic models. Karbala Int J Mod Sci 4:244–254. https://doi.org/10.1016/j.kijoms.2018.04.001

Mudunkotuwa IA, Rupasinghe T, Wu C-M, Grassian VH (2012) Dissolution of ZnO nanoparticles at circumneutral ph: a study of size effects in the presence and absence of citric acid. Langmuir 28:396–403. https://doi.org/10.1021/la203542x

Mukhopadhyay SS (2014) Nanotechnology in agriculture: prospects and constraints. Nanotechnol Sci Appl 7:63–71. https://doi.org/10.2147/NSA.S39409

Murphy KM, Reeves PG, Jones SS (2008) Relationship between yield and mineral nutrient concentrations in historical and modern spring wheat cultivars. Euphytica 163:381–390. https://doi.org/10.1007/s10681-008-9681-x

Murube E, Beleggia R, Pacetti D, et al (2021) Characterization of nutritional quality traits of a common bean germplasm collection. Foods 10:1572. https://doi.org/10.3390/foods10071572

Nanochemazone (2022) Cobalt Ferrite Nanoparticles. https://www.nanochemazone.com/product/cobalt-ferrite-nanoparticles/. Accessed 13 Oct 2022

Nasiri A, Jamshidi-Zanjani A, Khodadadi Darban A (2020) Application of enhanced electrokinetic approach to remediate Cr-contaminated soil: effect of chelating agents and permeable reactive barrier. Environ Pollut 266:115197. https://doi.org/10.1016/j.envpol.2020.115197

Naves L de P, Rodrigues PB, Bertechini AG, et al (2014) Comparison of methodologies to quantify phytate phosphorus in diets containing phytase and excreta from broilers. Asian-Australasian J Anim Sci 27:1003–1012. https://doi.org/10.5713/ajas.2013.13538

Nehra M, Dilbaghi N, Marrazza G, et al (2021) Emerging nanobiotechnology in agriculture for the management of pesticide residues. J Hazard Mater 401:123369. https://doi.org/10.1016/j.jhazmat.2020.123369

Nelson DW, Sommers LE (1996) Total carbon, organic carbon, and organic matter. In: D.L Sparks et al (eds.) Methods of Soil Analysis, ASA, Madison, WI, USA.. pp 961–1010

Nima ZA, Lahiani MH, Watanabe F, et al (2014) Plasmonically active nanorods for delivery of bio-active agents and high-sensitivity SERS detection in planta. RSC Adv 4:64985–64993. https://doi.org/10.1039/C4RA10358K

Noori A, White JC, Newman LA (2017) Mycorrhizal fungi influence on silver uptake and membrane protein gene expression following silver nanoparticle exposure. J Nanoparticle Res 19:66. https://doi.org/10.1007/s11051-016-3650-4

O'Day PA, Vlassopoulos D (2010) Mineral-based amendments for remediation. Elements 6:375–381. https://doi.org/10.2113/gselements.6.6.375

OECD (2020) Guidance document for the testing of dissolution and disspersion stability of nanomaterials and the use of the data for further environmental testing and assement strategies. Series on testing and assessment No. 318. 52. OECD Website. Accessed 17 Nov 2021.

OECD (1995) Test No. 105: Water Solubility. OECD Website. Accessed 17 Nov 2021.

Ogunkunle CO, Ahmed El-Imam AM, Bassey E, et al (2020) Co-application of indigenous arbuscular mycorrhizal fungi and nano-TiO_2 reduced Cd uptake and oxidative stress in pre-flowering cowpea plants. Environ Technol Innov 20:101163. https://doi.org/10.1016/j.eti.2020.101163

Olsen SR, Sommers LE (1982) Phosphorus. In: A. L. Page et al. (ed) Methods of soil analysis: Part 2. Chemical and microbiological properties., 2nd edn. ASA and SSSA, Madison, WI., pp 403–430.

Onofri A, Benincasa P, Mesgaran MB, Ritz C (2018) Hydrothermal-time-to-event models for seed germination. Eur J Agron 101:129–139. https://doi.org/10.1016/j.eja.2018.08.011

Onofri A, Mesgaran MB, Ritz C (2022) A unified framework for the analysis of germination, emergence, and other time-to-event data in weed science. Weed Sci 70:259–271. https://doi.org/10.1017/wsc.2022.8

Ozturk L, Yazici MA, Yucel C, et al (2006) Concentration and localization of zinc during seed development and germination in wheat. Physiol Plant 128:144–152. https://doi.org/10.1111/j.1399-3054.2006.00737.x

Palchoudhury S, Jungjohann KL, Weerasena L, et al (2018) Enhanced legume root growth with pre-soaking in α-Fe_2O_3 nanoparticle fertilizer. RSC Adv 8:24075–24083. https://doi.org/10.1039/c8ra04680h

Panda KK, Achary VMM, Krishnaveni R, et al (2011) *In vitro* biosynthesis and genotoxicity bioassay of silver nanoparticles using plants. Toxicol Vitr 25:1097–1105. https://doi.org/10.1016/j.tiv.2011.03.008

Pandohee J, Basu R, Dasgupta S, et al (2023) Applications of multi-omics approaches for food and nutritional security. In: Prakash CS, Fiaz S, Nadeem MA, et al. (eds). Sustainable Agriculture in the Era of the OMICs Revolution. Springer International Publishing, Cham, pp 103–118. https://doi.org/10.1007/978-3-031-15568-0_5

Pang W, Hou D, Wang H, et al (2018) Preparation of microcapsules of slow-release NPK compound fertilizer and the release characteristics. J Braz Chem Soc 29:2397–2404. https://doi.org/10.21577/0103-5053.20180117

Park S, Croteau P, Boering KA, et al (2012) Trends and seasonal cycles in the isotopic composition of nitrous oxide since 1940. Nat Geosci 5:261–265. https://doi.org/10.1038/ngeo1421

Paul S, Dey S, Kundu R (2022) Seed priming: an emerging tool towards sustainable agriculture. Plant Growth Regul 97:215–234. https://doi.org/10.1007/s10725-021-00761-1

Pavela R, Murugan K, Canale A, Benelli G (2017) Saponaria officinalis-synthesized silver nanocrystals as effective biopesticides and oviposition inhibitors against *Tetranychus urticae* Koch. Ind Crops Prod 97:338–344. https://doi.org/10.1016/j.indcrop.2016.12.046

Pawar VA, Ambekar JD, Kale BB, et al (2019) Response in chickpea (*Cicer arietinum* L.) seedling growth to seed priming with iron oxide nanoparticles. Int J Biosci 14:82–91. https://doi.org/10.12692/ijb/14.3.82-91

Peng C, Tong H, Yuan P, et al (2019) Aggregation, sedimentation, and dissolution of copper oxide nanoparticles: influence of low-molecular-weight organic acids from root exudates. Nanomaterials 9:841. https://doi.org/10.3390/nano9060841

Perea-Velez YS, González Chávez M del CA, Carrillo-González R, Lopez-Luna J (2022) Dissolution kinetics of citrate coated $CoFe_2O_4$ nanoparticles in soil solution. Environ Sci Nano. 9:2954–2965. https://doi.org/10.1039/D2EN00330A

Perea Vélez YS, Carrillo-González R, González-Chávez M del CA (2021) Interaction of metal nanoparticles–plants–microorganisms in agriculture and soil remediation. J Nanoparticle Res 23:206. https://doi.org/10.1007/s11051-021-05269-3

Perea-Vélez YS, González Chávez M del CA, Carrillo-González R et al. (2023) Citrate-coated cobalt ferrite nanoparticles for the nano-enabled biofortification of wheat. Manuscript submitted for publication.

Pérez-de-Luque A (2017) Interaction of nanomaterials with plants: what do we need for real applications in agriculture? Front Environ Sci 5:12. https://doi.org/10.3389/fenvs.2017.00012

Pérez-Hernández H, Fernández-Luqueño F, Huerta-Lwanga E, et al (2020) Effect of engineered nanoparticles on soil biota: do they improve the soil quality and crop production or jeopardize them? L Degrad Dev 31:2213–2230. https://doi.org/10.1002/ldr.3595

Pestovsky YS, Martínez-Antonio A (2017) The use of nanoparticles and nanoformulations in agriculture. J Nanosci Nanotechnol 17:8699–8730. https://doi.org/10.1166/jnn.2017.15041

Petry N, Boy E, Wirth JP, Hurrell RF (2015) Review: The potential of the common bean (*Phaseolus vulgaris*) as a vehicle for iron biofortification. Nutr. 7:1144-1173; https://doi.org/10.3390/nu7021144

Pitambara, Archana, Shukla YM (2019) Nanofertilizers: a recent approach in crop production. In: Panpatte DG, Jhala YK (eds). Nanotechnology for agriculture: crop production and protection. Springer, Singapore, pp 25–58. https://doi.org/10.1007/978-981-32-9374-8_2

Plank CO, Kissel DE (1989) Plant Analysis Handbook for Georgia. http://aesl.ces.uga.edu/publications/plant/. Accessed 12 Sep 2022

Pongrac P, Arčon I, Castillo-Michel H, Vogel-Mikuš K (2020) Mineral element composition in grain of awned and awnletted wheat (*Triticum aestivum* L.) cultivars: tissue-specific iron speciation and phytate and non-phytate ligand ratio. Plants 9:79. https://doi.org/10.3390/plants9010079

Prasad R, Bhattacharyya A, Nguyen QD (2017) Nanotechnology in sustainable agriculture: recent developments, challenges, and perspectives. Front Microbiol 8:1014. https://doi.org/10.3389/fmicb.2017.01014

Prasad R, Shivay YS, Kumar D (2014) Agronomic biofortification of cereal grains with iron and zinc. Adv. Agron. 125:55–91. https://doi.org/10.1016/B978-0-12-800137-0.00002-9

Prasad TNVK V, Sudhakar P, Sreenivasulu Y, et al (2012). Effect of nanoscale zinc oxide particles on the germination, growth and yield of peanut. J Plant Nutr 35:905–927. https://doi.org/10.1080/01904167.2012.663443

Prerna DI, Govindaraju K, Tamilselvan S, et al (2021) Influence of nanoscale micro-nutrient α-Fe_2O_3 on seed germination, seedling growth, translocation, physiological effects and yield of rice (*Oryza sativa*) and maize (*Zea mays*). Plant Physiol Biochem 162:564–580. https://doi.org/10.1016/j.plaphy.2021.03.023

Pulimi M, Subramanian S (2016) Nanomaterials for soil fertilisation. Nanosci Food Agric 1:229–246. https://doi.org/10.1007/978-3-319-39303-2

Qian ZS, Shan XY, Chai LJ, et al (2014) DNA nanosensor based on biocompatible graphene quantum dots and carbon nanotubes. Biosens Bioelectron 60:64–70. https://doi.org/10.1016/j.bios.2014.04.006

Qiu W, Yang D, Xu J, et al (2016) Efficient removal of Cr (VI) by magnetically separable $CoFe_2O_4$/activated carbon composite. J Alloys Compd 678:179–184. https://doi.org/10.1016/j.jallcom.2016.03.304

Qureshi A, Singh DK, Dwivedi S (2018) Nano-fertilizers: a novel way for enhancing nutrient use efficiency and crop productivity. Int J Curr Microbiol Appl Sci 7:3325–3335. https://doi.org/10.20546/ijcmas.2018.702.398

R Core Team (2020) R: A language and environment for statistical computing. Vienna, Austria.

Raffi MM, Husen A (2019) impact of fabricated nanoparticles on the rhizospheric microorganisms and soil environment. In: Husen A, Iqbal M (eds). Nanomaterials and plant potential. Springer, Cham, pp 529–552. https://doi.org/10.1007/978-3-030-05569-1_21

Rahi AA, Anjum MA, Iqbal Mirza J, et al (2021) Yield enhancement and better micronutrients uptake in tomato fruit through potassium humate combined with micronutrients mixture. Agric. 11: 357. https://doi.org/10.3390/agriculture11040357

Rahman MS, Chakraborty A, Mazumdar S, et al (2020) Effects of poly(vinylpyrrolidone) protected platinum nanoparticles on seed germination and growth performance of *Pisum sativum*. Nano-Structures and Nano-Objects 21:100408. https://doi.org/10.1016/j.nanoso.2019.100408

Rai-Kalal P, Jajoo A (2021) Priming with zinc oxide nanoparticles improve germination and photosynthetic performance in wheat. Plant Physiol Biochem 160:341–351. https://doi.org/10.1016/j.plaphy.2021.01.032

Rai-Kalal P, Tomar RS, Jajoo A (2021). H_2O_2 signaling regulates seed germination in ZnO nanoprimed wheat (*Triticum aestivum* L.) seeds for improving plant performance under drought stress. Environ Exp Bot 189:104561. https://doi.org/10.1016/j.envexpbot.2021.104561

Rai S, Singh PK, Mankotia S, et al (2021) Iron homeostasis in plants and its crosstalk with copper, zinc, and manganese. Plant Stress 1:100008. https://doi.org/10.1016/j.stress.2021.100008

Raj D, Maiti SK (2020) Sources, bioaccumulation, health risks and remediation of potentially toxic metal(loid)s (As, Cd, Cr, Pb and Hg): an epitomised review. Environ Monit Assess 192:108. https://doi.org/10.1007/s10661-019-8060-5

Rajput V, Minkina T, Sushkova S, et al (2020) ZnO and CuO nanoparticles: a threat to soil organisms, plants, and human health. Environ Geochem Health 42:147–158. https://doi.org/10.1007/s10653-019-00317-3

Rajput VD, Minkina T, Sushkova S, et al (2018) Effect of nanoparticles on crops and soil microbial communities. J Soils Sediments 18:2179–2187. https://doi.org/10.1007/s11368-017-1793-2

Raliya R, Saharan V, Dimkpa C, Biswas P (2018) Nanofertilizer for precision and sustainable agriculture: current state and future perspectives. J Agric Food Chem 66:6487–6503. https://doi.org/10.1021/acs.jafc.7b02178

Raliya R, Tarafdar JC (2013). ZnO Nanoparticle biosynthesis and its effect on phosphorous-mobilizing enzyme secretion and gum contents in clusterbean (*Cyamopsis tetragonoloba* L.). Agric Res 2:48–57. https://doi.org/10.1007/s40003-012-0049-z

Raliya R, Tarafdar JC, Biswas P (2016) Enhancing the mobilization of native phosphorus in the mung bean rhizosphere using ZnO nanoparticles synthesized by soil fungi. J Agric Food Chem 64:3111–3118. https://doi.org/10.1021/acs.jafc.5b05224

Ramírez-Jaspeado R, Palacios-Rojas N, Nutti M, Pérez S (2020). Estados potenciales en méxico para la producción y consumo de frijol biofortificado con hierro y zinc. Rev Fitotec Mex 43:11. https://doi.org/10.35196/rfm.2020.1.11

Rashid MI, Shahzad T, Shahid M, et al (2017) Toxicity of iron oxide nanoparticles to grass litter decomposition in a sandy soil. Sci Rep 7:41965. https://doi.org/10.1038/srep41965

Rasouli H, Popović-Djordjević J, Sayyed RZ, et al (2020) Nanoparticles: a new threat to crop plants and soil rhizobia?. In: Hayat S, Pichtel J, Faizan M, Fariduddin Q (eds). Sustainable agriculture reviews, vol. 41: nanotechnology for plant growth and development. Springer, Cham, pp 201–214. https://doi.org/10.1007/978-3-030-33996-8_11

Rastogi A, Zivcak M, Sytar O, et al (2017) Impact of metal and metal oxide nanoparticles on plant: a critical review. Front Chem 5:1–16. https://doi.org/10.3389/fchem.2017.00078

Ren H-X, Liu L, Liu C, et al (2011) Physiological investigation of magnetic iron oxide nanoparticles towards Chinese mung bean. J Biomed Nanotechnol 7:677–684. https://doi.org/10.1166/jbn.2011.1338

Riaz MU, Ayub MA, Khalid H, et al (2020) Fate of micronutrients in alkaline soils. In: Kumar S, Meena RS, Jhariya MK (eds) Resources use efficiency in agriculture. Springer, Singapore, pp 577–613. https://doi.org/10.1007/978-981-15-6953-1_16

Rios JJ, Carrasco-Gil S, Abadía A, Abadía J (2016) Using perls staining to trace the iron uptake pathway in leaves of a prunus rootstock treated with iron foliar fertilizers. Front Plant Sci 7:893. https://doi.org/10.3389/fpls.2016.00893

Rispail N, De Matteis L, Santos R, et al (2014) Quantum dot and superparamagnetic nanoparticle interaction with pathogenic fungi: Internalization and toxicity profile. ACS Appl Mater Interfaces 6:9100–9110. https://doi.org/10.1021/am501029g

Rives V, del Arco M, Martín C (2013) Layered double hydroxides as drug carriers and for controlled release of non-steroidal antiinflammatory drugs (NSAIDs): a review. J Control Release 169:28–39. https://doi.org/10.1016/j.jconrel.2013.03.034

Rodrigues DB, Marques MC, Hacke A, et al (2022) Trust your gut: bioavailability and bioaccessibility of dietary compounds. Curr Res Food Sci 5:228–233. https://doi.org/10.1016/j.crfs.2022.01.002

Romano A, Stevanato P (2020). Germination data analysis by time-to-event approaches. Plants 9: 617. https://doi.org/10.3390/plants9050617

Rose T, Liu L, Wissuwa M (2013) Improving phosphorus efficiency in cereal crops: is breeding for reduced grain phosphorus concentration part of the solution? Front Plant Sci 4:444. https://doi.org/10.3389/fpls.2013.00444

Rosenblueth M, Martínez-Romero E (2004). *Rhizobium etli* maize populations and their competitiveness for root colonization. Arch Microbiol 181:337–344. https://doi.org/10.1007/s00203-004-0661-9

Rostamizadeh E, Iranbakhsh A, Majd A, et al (2021) Physiological and molecular responses of wheat following the foliar application of iron oxide nanoparticles. Int J Nano Dimens 12:128–134

Rui M, Ma C, Hao Y, et al (2016) Iron oxide nanoparticles as a potential iron fertilizer for peanut (*Arachis hypogaea*). Front Plant Sci 7:1–10. https://doi.org/10.3389/fpls.2016.00815

Sabourin V, Ayande A (2015) Commercial opportunities and market demand for nanotechnologies in agribusiness sector. J Technol Manag Innov 10:40–51. https://doi.org/10.4067/S0718-27242015000100004

SADER (2022) Precios de garantía a productos alimentarios básicos, seguridad y certidumbre a productores. In: 5 julio 2022. https://www.gob.mx/agricultura/articulos/precios-de-garantia-a-productos-alimentarios-basicos-seguridad-y-certidumbre-a-productores. Accessed 5 Jul 2022

Saharan V, Mehrotra A, Khatik R, et al (2013) Synthesis of chitosan based nanoparticles and their *in vitro* evaluation against phytopathogenic fungi. Int J Biol Macromol 62:677–683. https://doi.org/10.1016/j.ijbiomac.2013.10.012

Samarajeewa AD, Velicogna JR, Schwertfeger DM, et al (2020) Ecotoxicological effects of copper oxide nanoparticles (nCuO) on the soil microbial community in a biosolids-amended soil. Sci Total Environ 763:143037. https://doi.org/10.1016/j.scitotenv.2020.143037

Sánchez-López AS, González-Chávez M del CA, Solís-Domínguez FA, et al (2018a). Leaf epiphytic bacteria of plants colonizing mine residues: possible exploitation for remediation of air pollutants. Front Microbiol 9:3028. https://doi.org/10.3389/fmicb.2018.03028

Sánchez-López AS, Thijs S, Beckers B, et al (2018b) Community structure and diversity of endophytic bacteria in seeds of three consecutive generations of *Crotalaria pumila* growing on metal mine residues. Plant Soil 422:51–66. https://doi.org/10.1007/s11104-017-3176-2

Santos CSC, Gabriel B, Blanchy M, et al (2015) Industrial applications of nanoparticles – a prospective overview. Mater Today Proc 2:456–465. https://doi.org/10.1016/J.MATPR.2015.04.056

Sarwar G, Hussain N, Schmeisky H, Muhammad S (2007) Use of compost an environment friendly technology for enhancing rice-wheat production in Pakistan. Pakistan J Bot 39:1553–1558

Satti SH, Raja NI, Javed B, et al (2021) Titanium dioxide nanoparticles elicited agro-morphological and physicochemical modifications in wheat plants to control *Bipolaris sorokiniana*. PLoS One 16:e0246880. https://doi.org/10.1371/journal.pone.0246880

Savjani KT, Gajjar AK, Savjani JK (2012) Drug solubility: importance and enhancement techniques. ISRN Pharm 2012:195727. https://doi.org/10.5402/2012/195727

Schlemmer U, Frølich W, Prieto RM, Grases F (2009) Phytate in foods and significance for humans: food sources, intake, processing, bioavailability, protective role and analysis. Mol Nutr Food Res 53:S330–S375. https://doi.org/10.1002/mnfr.200900099

Schloter M, Nannipieri P, Sørensen SJ, van Elsas JD (2018) Microbial indicators for soil quality. Biol Fertil Soils 54:1–10. https://doi.org/10.1007/s00374-017-1248-3

Sekine R, Marzouk ER, Khaksar M, et al (2017) Aging of dissolved copper and copper-based nanoparticles in five different soils: short-term kinetics vs. long-term fate. J. Environ. Qual., 46: 1198-1205. https://doi.org/10.2134/jeq2016.12.0485

Seleiman MF, Almutairi KF, Alotaibi M, et al (2021) Nano-fertilization as an emerging fertilization technique: why can modern agriculture benefit from its use? Plants 10:2. https://doi.org/10.3390/plants10010002

SEMARNAT (2000) Norma Oficial Mexicana NOM-021-RECNAT-2000, que establece las especificaciones de fertilidad, salinidad y clasificación de suelos. Estudios, muestreo y análisis. http://www.ordenjuridico.gob.mx/Documentos/Federal/wo69255.pdf. Accessed 13 Feb 2022

Senthilkumar M, Amaresan N, Sankaranarayanan A (2021) Quantitative estimation of nitrogenase activity: acetylene reduction assay. In: Plant-Microbe Interactions. Springer Protocols Handbooks. New York, NY., pp 37–39

Ševců A, El-Temsah YS, Joner EJ, Černík M (2011) Oxidative Stress Induced in Microorganisms by Zero-valent Iron Nanoparticles. Microbes Environ 26:271–281. https://doi.org/10.1264/jsme2.ME11126

Shaddox TW, Fu H, Gardner DS, et al (2019) Solubility of ten iron fertilizers in eleven north American soils. Agron J 111:1498–1505. https://doi.org/10.2134/agronj2018.12.0770

Shah AA, Aslam S, Akbar M, et al (2021a) Combined effect of *Bacillus fortis* IAGS 223 and zinc oxide nanoparticles to alleviate cadmium phytotoxicity in *Cucumis melo*. Plant Physiol Biochem 158:1–12. https://doi.org/10.1016/j.plaphy.2020.11.011

Shah T, Latif S, Saeed F, et al (2021b) Seed priming with titanium dioxide nanoparticles enhances seed vigor, leaf water status, and antioxidant enzyme activities in maize (*Zea mays* L.) under salinity stress. J King Saud Univ - Sci 33:101207. https://doi.org/10.1016/j.jksus.2020.10.004

Shaheen SM, Rinklebe J (2015) Impact of emerging and low cost alternative amendments on the (im)mobilization and phytoavailability of Cd and Pb in a contaminated floodplain soil. Ecol Eng 74:319–326. https://doi.org/10.1016/j.ecoleng.2014.10.024

Shariatmadari N, Weng C-H, Daryaee H (2009) Enhancement of hexavalent chromium [Cr(VI)] remediation from clayey soils by electrokinetics coupled with a nano-sized zero-valent iron barrier. Environ Eng Sci 26:1071–1079. https://doi.org/10.1089/ees.2008.0257

Sharma P, Sharma A, Sharma M, et al (2017) Nanomaterial fungicides: *in vitro* and *in vivo* antimycotic activity of cobalt and nickel nanoferrites on phytopathogenic fungi. Glob Challenges 1:1700041. https://doi.org/10.1002/gch2.201700041

Sharma S, Rana VS, Pawar R, et al (2020) Nanofertilizers for sustainable fruit production: a review. Environ Chem Lett. 19: 693–1714. https://doi.org/10.1007/s10311-020-01125-3

Shaw AK, Hossain Z (2013) Impact of nano-CuO stress on rice (*Oryza sativa* L.) seedlings. Chemosphere 93:906–915. https://doi.org/10.1016/j.chemosphere.2013.05.044

Shebl A, Hassan AA, Salama DM, et al (2020) Template-free microwave-assisted hydrothermal synthesis of manganese zinc ferrite as a nanofertilizer for squash plant (*Cucurbita pepo* L). Heliyon 6:e03596. https://doi.org/10.1016/j.heliyon.2020.e03596

Shelar A, Singh A V, Maharjan RS, et al (2021) Sustainable agriculture through multidisciplinary seed nanopriming: prospects of opportunities and challenges. Cells 10:2428. https://doi.org/10.3390/cells10092428

Shenashen M, Derbalah A, Hamza A, et al (2017) Antifungal activity of fabricated mesoporous alumina nanoparticles against root rot disease of tomato caused by *Fusarium oxysporium*. Pest Manag Sci 73:1121–1126. https://doi.org/10.1002/ps.4420

Sher A, Sarwar T, Nawaz A, et al (2019) Methods of Seed Priming. In: Hasanuzzaman M, Fotopoulos V (eds). Priming and pretreatment of seeds and seedlings: implication in plant stress tolerance and enhancing productivity in crop plants. Springer, Singapore, pp 1–10. https://doi.org/10.1007/978-981-13-8625-1_1

Shi Y, Xiao Y, Li Z, et al (2020) Microorganism structure variation in urban soil microenvironment upon ZnO nanoparticles contamination. Chemosphere 128565. https://doi.org/10.1016/j.chemosphere.2020.128565

Shrestha S, Wang B, Dutta P (2020) Nanoparticle processing: understanding and controlling aggregation. Adv Colloid Interface Sci 279:102162. https://doi.org/10.1016/j.cis.2020.102162

Shukla P, Chaurasia P, Younis K, et al (2019) Nanotechnology in sustainable agriculture: studies from seed priming to post-harvest management. Nanotechnol Environ Eng 4:11. https://doi.org/10.1007/s41204-019-0058-2

Siani NG, Fallah S, Pokhrel LR, Rostamnejadi A (2017) Natural amelioration of Zinc oxide nanoparticle toxicity in fenugreek (*Trigonella foenum-gracum*) by arbuscular mycorrhizal (*Glomus intraradices*) secretion of glomalin. Plant Physiol Biochem 112:227–238. https://doi.org/10.1016/j.plaphy.2017.01.001

Sidhu A, Barmota H, Bala A (2017) Antifungal evaluation studies of copper sulfide nano-aquaformulations and its impact on seed quality of rice (*Oryzae sativa*). Appl Nanosci 7:681–689. https://doi.org/10.1007/s13204-017-0606-7

Sigma-Aldrich (2022) Cobalt iron oxide nanopowder. https://www.sigmaaldrich.com/US/en/product/aldrich/773352. Accessed 13 Oct 2022

Siimes N, Sharp EL, Lewis N, Kah M (2022) Determining acceptance and rejection of nano-enabled agriculture: a case study of the New Zealand wine industry. NanoImpact 28:100432. https://doi.org/https://doi.org/10.1016/j.impact.2022.100432

Silva-Silva MJ, Mijangos-Ricardez OF, Vázquez-Hipólito V, et al (2016) Single and mixed adsorption of Cd(II) and Cr(VI) onto citrate-coated magnetite nanoparticles. Desalin Water Treat 57:4008–4017. https://doi.org/10.1080/19443994.2014.991756

Silvertech Kimya Sanayi ve Ticaret Ltd. Products - Silvertech Kimya. http://www.silvertechkimya.com.tr/en/products/agriculture-industry/. Accessed 5 Jan 2021

Simonin M, Guyonnet JP, Martins JMF, et al (2015) Influence of soil properties on the toxicity of TiO_2 nanoparticles on carbon mineralization and bacterial abundance. J Hazard Mater 283:529–535. https://doi.org/10.1016/j.jhazmat.2014.10.004

Singh A, Singh NB, Afzal S, et al (2018). Zinc oxide nanoparticles: a review of their biological synthesis, antimicrobial activity, uptake, translocation and biotransformation in plants. J Mater Sci 53:185–201. https://doi.org/10.1007/s10853-017-1544-1

Singh A, Singh NB, Hussain I, et al (2016) Green synthesis of nano zinc oxide and evaluation of its impact on germination and metabolic activity of Solanum lycopersicum. J Biotechnol 233:84–94. https://doi.org/10.1016/j.jbiotec.2016.07.010

Singh D, Kumar A (2020) Understanding the effect of the interaction of nanoparticles with roots on the uptake in plants. In: Dasgupta N., Ranjan S., Lichtfouse E. (eds). Environmental nanotechnology volume 3. environmental chemistry for a sustainable world. Springer, Cham, pp 277–304. https://doi.org/10.1007/978-3-030-26672-1_9

Singh RP, Handa R, Manchanda G (2021) Nanoparticles in sustainable agriculture: an emerging opportunity. J Control Release 329:1234–1248. https://doi.org/10.1016/j.jconrel.2020.10.051

Singla R, Kumari A, Yadav SK (2019) Impact of nanomaterials on plant physiology and functions. In: Husen A, Iqbal M (eds). Nanomaterials and plant potential. Springer International Publishing, Cham, pp 349–377. https://doi.org/10.1007/978-3-030-05569-1_14

Škarpa P, Školníková M, Antošovský J, et al (2021) Response of normal and low-phytate genotypes of pea (*Pisum sativum* L.) on phosphorus foliar fertilization. Plants 10:1608. https://doi.org/10.3390/plants10081608

Skousen J (2014). Overview of acid mine drainage treatment with chemicals. In: Jacobs J.A., Lehr J.H., Testa S.M. (eds.) Acid mine drainage, rock drainage, acid sulfate soils. John Wiley and Sons, pp 325–337. https://doi.org/10.1002/9781118749197.ch29

Solanki P, Bhargava A, Chhipa H, et al (2015) Nano-fertilizers and their smart delivery system. In: Rai M, Ribeiro C, Mattoso L, Duran N (eds). Nanotechnologies in food and agriculture. Springer, Cham, pp 81–101. https://doi.org/10.1007/978-3-319-14024-7_4

Solanki P, Laura JS (2018) Biofortification of crops using nanoparticles to alleviate plant and human zinc deficiency : a review. Res J Life Sci Bioinformatics, Pharm Chem Sci 4:364–385. https://doi.org/10.26479/2018.0405.29

Song U, Jun H, Waldman B, et al (2013) Functional analyses of nanoparticle toxicity: A comparative study of the effects of TiO_2 and Ag on tomatoes (*Lycopersicon esculentum*). Ecotoxicol Environ Saf 93:60–67. https://doi.org/10.1016/j.ecoenv.2013.03.033

Sorkina TA, Polyakov AY, Kulikova NA, et al (2014) Nature-inspired soluble iron-rich humic compounds: new look at the structure and properties. J Soils Sediments 14:261–268. https://doi.org/10.1007/s11368-013-0688-0

Souza LRR, Pomarolli LC, da Veiga MAMS (2020) From classic methodologies to application of nanomaterials for soil remediation: an integrated view of methods for decontamination of toxic metal(oid)s. Environ Sci Pollut Res 27:10205–10227. https://doi.org/10.1007/s11356-020-08032-8

Sparks DL (2003). Kinetics of soil chemical processes. In: Sparks DLBT-ESC Second E (ed). Academic Press, Burlington, pp 207–244

Sparvoli F, Cominelli E (2015) Seed biofortification and phytic acid reduction: a conflict of interest for the plant? Plants 4:728-755. https://doi.org/10.3390/plants4040728

Spinoso-Castillo JL, Chavez-Santoscoy RA, Bogdanchikova N, et al (2017) Antimicrobial and hormetic effects of silver nanoparticles on in vitro regeneration of vanilla (*Vanilla planifolia* Jacks. ex Andrews) using a temporary immersion system. Plant Cell, Tissue Organ Cult 129:195–207. https://doi.org/10.1007/s11240-017-1169-8

Stadler T, Buteler M, Weaver DK (2010) Novel use of nanostructured alumina as an insecticide. Pest Manag Sci 66:577–579. https://doi.org/10.1002/ps.1915

StatNano (2018) Nanotechnology Products Database (NPD). In: Nanotechnol. Prod. Database. https://product.statnano.com/. Accessed 4 Jan 2021

Stegemeier JP, Schwab F, Colman BP, et al (2015) Speciation matters: bioavailability of silver and silver sulfide nanoparticles to alfalfa (*Medicago sativa*). Environ Sci Technol 49:8451–8460. https://doi.org/10.1021/acs.est.5b01147

Stephano-Hornedo JL, Torres-Gutiérrez O, Toledano-Magaña Y, et al (2020) Argovit™ silver nanoparticles to fight Huanglongbing disease in Mexican limes (*Citrus aurantifolia* Swingle). RSC Adv 10:6146–6155. https://doi.org/10.1039/C9RA09018E

Sun W, Dou F, Li C, et al (2020) Impacts of metallic nanoparticles and transformed products on soil health. Crit Rev Environ Sci Technol 51:1–30. https://doi.org/10.1080/10643389.2020.1740546

Sundaria N, Singh M, Upreti P, et al (2019) Seed priming with iron oxide nanoparticles triggers iron acquisition and biofortification in wheat (*Triticum aestivum* L.) grains. J Plant Growth Regul 38:122–131. https://doi.org/10.1007/s00344-018-9818-7

Suzanne N.S. (2010) Food Analysis Laboratory Manual, Springer, West Lafayette, IN, 2010

Swatsitang E, Phokha S, Hunpratub S, et al (2016) Characterization and magnetic properties of cobalt ferrite nanoparticles. J Alloys Compd 664:792–797. https://doi.org/10.1016/j.jallcom.2015.12.230

Taghdisi SM, Danesh NM, Emrani AS, et al (2015) A novel electrochemical aptasensor based on single-walled carbon nanotubes, gold electrode and complimentary strand of aptamer for ultrasensitive detection of cocaine. Biosens Bioelectron 73:245–250. https://doi.org/10.1016/j.bios.2015.05.065

Tarafdar JC, Raliya R, Mahawar H, Rathore I (2014) Development of zinc nanofertilizer to enhance crop production in pearl millet (*Pennisetum americanum*). Agric Res 3:257–262. https://doi.org/10.1007/s40003-014-0113-y

Taskin MB, Gunes A (2022) Iron biofortification of wheat grains by foliar application of nano zero-valent iron (nZVI) and other iron sources with urea. J Soil Sci Plant Nutr 22:4642–4652. https://doi.org/10.1007/s42729-022-00946-1

The World Bank (2021) Agriculture and Food Overview. https://www.worldbank.org/en/topic/agriculture/overview. Accessed 17 May 2021

Thijs S, Sillen W, Rineau F, et al (2016) Towards an enhanced understanding of plant–microbiome interactions to improve phytoremediation: engineering the metaorganism. Front Microbiol 7:341. https://doi.org/10.3389/fmicb.2016.00341

Thijs S, Sillen W, Weyens N, Vangronsveld J (2017) Phytoremediation: state-of-the-art and a key role for the plant microbiome in future trends and research prospects. Int J Phytoremediation 19:23–38. https://doi.org/10.1080/15226514.2016.1216076

Tian L, Shen J, Sun G, et al (2020) Foliar application of SiO_2 nanoparticles alters soil metabolite profiles and microbial community composition in the pakchoi (*Brassica chinensis* L.) rhizosphere grown in contaminated mine soil. Environ Sci Technol 54:13137–13146. https://doi.org/10.1021/acs.est.0c03767

Timilsena YP, Adhikari R, Casey P, et al (2015) Enhanced efficiency fertilisers: a review of formulation and nutrient release patterns. J Sci Food Agric 95:1131–1142. https://doi.org/10.1002/jsfa.6812

Timmusk S, Seisenbaeva G, Behers L (2018) Titania (TiO_2) nanoparticles enhance the performance of growth-promoting rhizobacteria. Sci Rep 8:617. https://doi.org/10.1038/s41598-017-18939-x

Tipu MI, Akhtar M, Sarwar N, Hussain S (2022) Effectiveness of exogenously applied chelated micronutrients for biofortification of wheat. Arab J Geosci 15:417. https://doi.org/10.1007/s12517-022-09685-0

Tombuloglu H, Slimani Y, AlShammari TM, et al (2021) Delivery, fate and physiological effect of engineered cobalt ferrite nanoparticles in barley (*Hordeum vulgare* L.). Chemosphere 265:129138. https://doi.org/10.1016/j.chemosphere.2020.129138

Toumey C (2009) Plenty of room, plenty of history. Nat Nanotechnol 4:783–784. https://doi.org/10.1038/nnano.2009.357

Trenkel (2013) Slow and controlled-release and stabilized fertilizers: an option for enhancing nutrient efficiency. In: Agriculture international fertilizer industry association, Paris. https://www.fertilizer.org/images/Library_Downloads/2010_Trenkel_slow%20release%20book.pdf. Accessed 17 May 2021

Tsykhanovska I, Evlash V, Alexandrov A, Gontar T (2019) Dissolution kinetics of Fe_3O_4 nanoparticles in the acid media. Chem Chem Technol 13:170–184. https://doi.org/10.23939/chcht13.02.170

Umar A, Hussain S (2022) Seed priming and soil application of zinc decrease grain cadmium accumulation in standard and zinc-biofortified wheat cultivars. Crop Pasture Sci. https://doi.org/10.1071/CP22255

USDA (2022) Food and nutrition security. https://www.usda.gov/nutrition-security#:~:text=Nutrition security is consistent access,Tribal communities and Insular areas. Accessed 11 Jan 2023

Usman M, Farooq M, Wakeel A, et al (2020) Nanotechnology in agriculture: Current status, challenges and future opportunities. Sci Total Environ 721:137778. https://doi.org/10.1016/j.scitotenv.2020.137778

Utembe W, Potgieter K, Stefaniak AB, Gulumian M (2015) Dissolution and biodurability: Important parameters needed for risk assessment of nanomaterials. Part Fibre Toxicol 12:11. https://doi.org/10.1186/s12989-015-0088-2

Van Nguyen D, Nguyen HM, Le NT, et al (2021) Copper nanoparticle application enhances plant growth and grain yield in maize under drought stress conditions. J Plant Growth Regul. 41:364–375 https://doi.org/10.1007/s00344-021-10301-w

Vanti GL, Nargund VB, N BK, et al (2019) Synthesis of gossypium hirsutum-derived silver nanoparticles and their antibacterial efficacy against plant pathogens. Appl Organomet Chem 33:e4630. https://doi.org/10.1002/aoc.4630

Velikova V, Yordanov I, Edreva A (2000) Oxidative stress and some antioxidant systems in acid rain-treated bean plants. Plant Sci 151:59–66. https://doi.org/10.1016/S0168-9452(99)00197-1

Velu G, Bhattacharjee R, Rai K, et al (2008) A simple and rapid screening method for grain zinc content in pearl millet. J SAT Agric Res 6:1–4

Velu G, Ortiz-Monasterio I, Cakmak I, et al (2014) Biofortification strategies to increase grain zinc and iron concentrations in wheat. J Cereal Sci 59:365–372. https://doi.org/10.1016/j.jcs.2013.09.001

Vencalek BE, Laughton SN, Spielman-Sun E, et al (2016) *In situ* measurement of CuO and $Cu(OH)_2$ nanoparticle dissolution rates in quiescent freshwater mesocosms. Environ Sci Technol Lett 3:375–380. https://doi.org/10.1021/acs.estlett.6b00252

Viola R, Davies H V (1992) A microplate reader assay for rapid enzymatic quantification of sugars in potato tubers. Potato Res 35:55–58. https://doi.org/10.1007/BF02357723

Vítková M, Komárek M, Tejnecký V, Šillerová H (2015) Interactions of nano-oxides with low-molecular-weight organic acids in a contaminated soil. J Hazard Mater 293:7–14. https://doi.org/10.1016/j.jhazmat.2015.03.033

Vittori Antisari L, Carbone S, Gatti A, et al (2015) Uptake and translocation of metals and nutrients in tomato grown in soil polluted with metal oxide (CeO_2, Fe_3O_4, SnO_2, TiO_2) or metallic (Ag, Co, Ni) engineered nanoparticles. Environ Sci Pollut Res 22:1841–1853. https://doi.org/10.1007/s11356-014-3509-0

Vryzas Z (2016) The plant as metaorganism and research on next-generation systemic pesticides–prospects and challenges. Front Microbiol 7:1968. https://doi.org/10.3389/fmicb.2016.01968

Wang F, Adams CA, Shi Z, Sun Y (2018a) Chemosphere combined effects of ZnO NPs and Cd on sweet sorghum as influenced by an arbuscular mycorrhizal fungus. Chemosphere 209:421–429. https://doi.org/10.1016/j.chemosphere.2018.06.099

Wang F, Jing X, Adams CA, et al (2018b) Decreased ZnO nanoparticle phytotoxicity to maize by arbuscular mycorrhizal fungus and organic phosphorus. Environ Sci Pollut Res 25:23736–23747. https://doi.org/10.1007/s11356-018-2452-x

Wang F, Liu X, Shi Z, et al (2016a) Arbuscular mycorrhizae alleviate negative effects of zinc oxide nanoparticle and zinc accumulation in maize plants–A soil microcosm experiment. Chemosphere 147:88–97. https://doi.org/10.1016/j.chemosphere.2015.12.076

Wang H-W, Wang Y-J, Chen J-H, et al (2009) Application of modified nano-particle black carbon for the remediation of soil heavy metal pollution. J Agro-Environment Sci 29:431–436

Wang J, Cao X, Wang C, et al (2022) Fe-based nanomaterial-induced root nodulation is modulated by flavonoids to improve soybean (*Glycine max*) growth and quality. ACS Nano 16:21047–21062. https://doi.org/10.1021/acsnano.2c08753

Wang J, Hou L, Yao Z, et al (2021) Aminated electrospun nanofiber membrane as permeable reactive barrier material for effective in-situ Cr(VI) contaminated soil remediation. Chem Eng J 406:126822. https://doi.org/10.1016/j.cej.2020.126822

Wang J, Shu K, Zhang L, Si Y (2017) Effects of silver nanoparticles on soil microbial communities and bacterial nitrification in suburban vegetable soils. Pedosphere 27:482–490. https://doi.org/10.1016/S1002-0160(17)60344-8

Wang X, Sun T, Zhu H, et al (2020) Roles of pH, cation valence, and ionic strength in the stability and aggregation behavior of zinc oxide nanoparticles. J Environ Manage 267:110656. https://doi.org/10.1016/j.jenvman.2020.110656

Wang X, Yang X, Chen S, et al (2016b) Zinc oxide nanoparticles affect biomass accumulation and photosynthesis in *Arabidopsis*. Front Plant Sci 6:1243. https://doi.org/10.3389/fpls.2015.01243

Wang Y, Jiang F, Ma C, et al (2019a) Effect of metal oxide nanoparticles on amino acids in wheat grains (*Triticum aestivum*)in a life cycle study. J Environ Manage 241:319–327. https://doi.org/10.1016/j.jenvman.2019.04.041

Wang Y, Lin Y, Xu Y, et al (2019b) Divergence in response of lettuce (*var. ramosa Hort*.) to copper oxide nanoparticles/microparticles as potential agricultural fertilizer. Environ Pollut Bioavailab 31:80–84. https://doi.org/10.1080/26395940.2019.1578187

Wang Y, Peng C, Fang H, et al (2015) Mitigation of Cu(II) phytotoxicity to rice (*Oryza sativa*) in the presence of TiO_2 and CeO_2 nanoparticles combined with humic acid. Environ Toxicol Chem 34:1588–1596. https://doi.org/10.1002/etc.2953

Wani TA, Masoodi FA, Baba WN, et al (2019). Nanoencapsulation of agrochemicals, fertilizers, and pesticides for improved plant production. In: Ghorbanpour M, Wani SHBT-A in P (eds). Advances in phytonanotechnology. Academic Press, pp 279–298. https://doi.org/10.1016/B978-0-12-815322-2.00012-2

Warner MJ, Kamran MT (2021) Iron deficiency Anemia. https://www.ncbi.nlm.nih.gov/books/NBK448065/. Accessed 19 Apr 2022

Wei X, Viadero RC (2007) Synthesis of magnetite nanoparticles with ferric iron recovered from acid mine drainage: Implications for environmental engineering. Colloids Surfaces A Physicochem Eng Asp 294:280–286. https://doi.org/10.1016/j.colsurfa.2006.07.060

Whitesides GM (2005) Nanoscience, nanotechnology, and chemistry. Small 1:172–179. https://doi.org/10.1002/smll.200400130

WHO (2008) Anaemia. https://www.who.int/data/nutrition/nlis/info/anaemia. Accessed 12 Apr 2021

Worthen AJ, Tran V, Cornell KA, et al (2016) Steric stabilization of nanoparticles with grafted low molecular weight ligands in highly concentrated brines including divalent ions. Soft Matter 12:2025–2039. https://doi.org/10.1039/C5SM02787J

Wu B, Andersch F, Weschke W, et al (2013) Diverse accumulation and distribution of nutrient elements in developing wheat grain studied by laser ablation inductively coupled plasma mass spectrometry imaging. Metallomics 5:1276–1284. https://doi.org/10.1039/C3MT00071K

Xue W, Huang D, Zeng G, et al (2018) Nanoscale zero-valent iron coated with rhamnolipid as an effective stabilizer for immobilization of Cd and Pb in river sediments. J Hazard Mater 341:381–389. https://doi.org/10.1016/j.jhazmat.2017.06.028

Yang Q, Liu Y, Qiu Y, et al (2022) Dissolution kinetics and solubility of copper oxide nanoparticles as affected by soil properties and aging time. Environ Sci Pollut Res 29:40674–40685. https://doi.org/10.1007/s11356-022-18813-y

Yang W, Cheng P, Adams CA, et al (2021) Effects of microplastics on plant growth and arbuscular mycorrhizal fungal communities in a soil spiked with ZnO nanoparticles. Soil Biol Biochem 155:108179. https://doi.org/10.1016/j.soilbio.2021.108179

Yang Y, Wang J, Xiu Z, Alvarez PJJ (2013) Impacts of silver nanoparticles on cellular and transcriptional activity of nitrogen-cycling bacteria. Environ Toxicol Chem 32:1488–1494. https://doi.org/https://doi.org/10.1002/etc.2230

Yao KS, Li SJ, Tzeng KC, et al (2009) Fluorescence silica nanoprobe as a biomarker for rapid detection of plant pathogens. Adv Mater Res 79–82:513–516. https://doi.org/10.4028/www.scientific.net/AMR.79-82.513

Younas A, Sadaqat HA, Kashif M, et al (2020) Combining ability and heterosis for grain iron biofortification in bread wheat. J Sci Food Agric 100:1570–1576. https://doi.org/10.1002/jsfa.10165

Young M, Ozcan A, Myers ME, et al (2018) Multimodal generally recognized as safe ZnO/nanocopper composite: a novel antimicrobial material for the management of citrus phytopathogens. J Agric Food Chem 66:6604–6608. https://doi.org/10.1021/acs.jafc.7b02526

Youssef MS, Elamawi RM (2020) Evaluation of phytotoxicity, cytotoxicity, and genotoxicity of ZnO nanoparticles in *Vicia faba*. Environ Sci Pollut Res 27:18972–18984. https://doi.org/10.1007/s11356-018-3250-1

Yue Z, Chen Y, Hao Y, et al (2022) *Bacillus* sp. WR12 alleviates iron deficiency in wheat via enhancing siderophore- and phenol-mediated iron acquisition in roots. Plant Soil 471:247–260. https://doi.org/10.1007/s11104-021-05218-y

Yuvaraj M, Subramanian KS (2015) Controlled-release fertilizer of zinc encapsulated by a manganese hollow core shell. Soil Sci Plant Nutr 61:319–326. https://doi.org/10.1080/00380768.2014.979327

Zahra Z, Habib Z, Hyun H, Shahzad HM (2022) Overview on recent developments in the design, application, and impacts of nanofertilizers in agriculture. Sustainability 14:9397. https://doi.org/10.3390/su14159397

Zehlike L, Peters A, Ellerbrock RH, et al (2019) Aggregation of TiO_2 and Ag nanoparticles in soil solution–Effects of primary nanoparticle size and dissolved organic matter characteristics. Sci Total Environ 688:288–298. https://doi.org/10.1016/j.scitotenv.2019.06.020

Zhang H, Zhang Y (2020) Effects of iron oxide nanoparticles on Fe and heavy metal accumulation in castor (*Ricinus communis* L.) plants and the soil aggregate. Ecotoxicol Environ Saf 200:110728. https://doi.org/10.1016/j.ecoenv.2020.110728

Zhang L, Lu X, Busnaina AA (2022) The role of carboxylic acids on nanoparticle removal in post CMP cleaning process for cobalt interconnects. Mater Chem Phys 275:125199. https://doi.org/10.1016/j.matchemphys.2021.125199

Zhang M, Wang Y, Zhao D, Pan G (2010) Immobilization of arsenic in soils by stabilized nanoscale zero-valent iron, iron sulfide (FeS), and magnetite (Fe_3O_4) particles. Chinese Sci Bull 55:365–372. https://doi.org/10.1007/s11434-009-0703-4

Zhang W, Dan Y, Shi H, Ma X (2017) Elucidating the mechanisms for plant uptake and in-planta speciation of cerium in radish (*Raphanus sativus* L.) treated with cerium oxide nanoparticles. J Environ Chem Eng 5:572–577. https://doi.org/10.1016/j.jece.2016.12.036

Zhang W, Yao Y, Sullivan N, Chen Y (2011) Modeling the primary size effects of citrate-coated silver nanoparticles on their ion release kinetics. Environ Sci Technol 45:4422–4428. https://doi.org/10.1021/es104205a

Zhao L, Peralta-Videa JR, Rico CM, et al (2014) CeO_2 and ZnO nanoparticles change the nutritional qualities of cucumber (*Cucumis sativus*). J Agric Food Chem 62:2752–2759. https://doi.org/10.1021/jf405476u

Zhao X, Liu W, Cai Z, et al (2016) An overview of preparation and applications of stabilized zero-valent iron nanoparticles for soil and groundwater remediation. Water Res 100:245–266. https://doi.org/10.1016/j.watres.2016.05.019

Zhou DM, Jin SY, Wang YJ, et al (2012) Assessing the impact of iron-based nanoparticles on pH, dissolved organic carbon, and nutrient availability in soils. Soil Sediment Contam 21:101–114. https://doi.org/10.1080/15320383.2012.636778

Zhu Y, Xu F, Liu Q, et al (2019) Nanomaterials and plants: positive effects, toxicity and the remediation of metal and metalloid pollution in soil. Sci. Total Environ. 662:414–421. https://doi.org/10.1016/j.scitotenv.2019.01.234

Zia-ur-Rehman M, Naeem A, Khalid H, et al (2018) Responses of plants to iron oxide nanoparticles. In: Tripathi DK, Ahmad P, Sharma S, et al. (eds) Nanomaterials in plants, algae, and microorganisms. Academic Press, Cambridge, MA, USA. pp 221–238. https://doi.org/10.1016/B978-0-12-811487-2.00010-4

Zulfiqar F, Navarro M, Ashraf M, et al (2019) Nanofertilizer use for sustainable agriculture: Advantages and limitations. Plant Sci 289:110270. https://doi.org/10.1016/j.plantsci.2019.110270

Zuo Y, Zhang F (2011) Soil and crop management strategies to prevent iron deficiency in crops. Plant Soil 339:83–95. https://doi.org/10.1007/s11104-010-0566-0

Zuverza-Mena N, Armendariz R, Peralta-Videa JR, Gardea-Torresdey JL (2016) effects of silver nanoparticles on radish sprouts: root growth reduction and modifications in the nutritional value. Front Plant Sci 7:90. https://doi.org/10.3389/fpls.2016.00090

Zuverza-Mena N, Martínez-Fernández D, Du W, et al (2017) Exposure of engineered nanomaterials to plants: Insights into the physiological and biochemical responses-A review. Plant Physiol Biochem 110:236–264. https://doi.org/10.1016/j.plaphy.2016.05.037

APPENDIX

Research offsprings

Published scientific papers

Perea-Velez YS, González Chávez M del CA, Carrillo-González R, Lopez-Luna J (2022) Dissolution kinetics of citrate coated $CoFe_2O_4$ nanoparticles in soil solution. Environ Sci Nano. 9:2954–2965. https://doi.org/10.1039/D2EN00330A

Perea Vélez YS, Carrillo-González R, González-Chávez M del CA (2021) Interaction of metal nanoparticles–plants–microorganisms in agriculture and soil remediation. J Nanoparticle Res 23:206. https://doi.org/10.1007/s11051-021-05269-3

Participation in congress

Can cobalt-ferrite nanoparticles be an alternative fertilizer for the agronomic iron fortification of wheat? Oral presentation in the Global Symposium on Soils for Nutrition, organized by FAO 26-29 July 2022.

Chapter 1. Supplementary material

Table S1. Properties of soil solution extracted from alkaline soil.

Properties	Unit	Value
pH		7.59 ± 0.15
Electrical conductivity	dS m^{-1}	1.89 ± 5.22
Ionic strength	M	0.04
PO_4^{3-}	mM	0.032 ± 0.005
SO_4^{2-}	$mmol_{(-)}$ L^{-1}	2.41 ± 0.08
Cl^-		7.04 ± 0.50
Ca^{2+}	$mmol_{(+)}$ L^{-1}	25.22±0.55
Mg^{2+}		6.31 ± 0.17
Na^+	mM	2.49 ± 0.13
K^+		1.68 ± 0.15

Mean value and standard deviation, n=3

Table S2. Mathematical models of kinetic dissolution rate.

Kinetic model and linear forms of kinetic equations	Linear plot to determine k	k unit	Observation	Reference
Zero-order kinetic $[M]_t = -kt + [M]_0$	$[M]_t$ vs time	$M\ h^{-1}$	The rate of reaction will be independent of the concentration of reactants	Sparks (2003); Utembe et al. (2015)
First-order $In[M]_t = -kt + In[M]_0$	$ln[M]_t$ vs time	h^{-1}	The rate of reaction depends on the concentration of at least one reactant. Thus, the rate of reaction is proportional to the concentration of the reactant	Sparks 2003; Utembe et al. (2015)
Second-order $1/[M]_t = kt + 1/[M]_0$	1/[M] vs time	$M^{-1}\ h^{-1}$	The rate is proportional to the square of the concentration of one reactant (2A➔products). Also, a second-order reaction has a reaction rate that is proportional to the product of the concentrations of two reactants (A+B➔products)	Sparks (2003); Utembe et al. (2015)
Pseudo-first order $In([M]_0-[M]_t) = In[M]_t - k't$	$In([M]_0-[M]_t)$ vs time	h^{-1}	This rate of reaction occurs when one reacting material is present in great excess or is maintained at a constant concentration compared with the other substance	Chang (2005)
Pseudo-second order $t/[M]_t = 1/k_2[M]_s^2 + t/[M]_s$	$t/[M]_t$ vs time	$L\ mol^{-1}\ h$		Moussout et al. (2018)
One-half- order $[M]_t^{1/2} = -1/2kt + [M]_0^{1/2}$	$[M]_t^{1/2}$ vs time	$M^{1/2}\ h$	Fractional order reactions often indicate a chemical chain reaction or other complex reaction mechanisms	Atkins and De Paula (2006)
Three-half-order $1/[M]_t^{1/2} = 1/2kt + 1/[M]_0^{1/2}$	$1/[M]_t^{1/2}$vs time	$M^{-1/2}\ h$		Atkins and De Paula (2006)
Elovich $[M]_t = (1/\beta)\ In\ (\alpha\beta) + (1/\beta)\ Int$	$[M]_t$ vs In(time)	$M\ h^{-1}$	This model was originally developed to describe the kinetics of heterogeneous chemisorption of gases on solid surfaces, but it seems to describe several reaction mechanisms, including bulk and surface diffusion, activation and deactivation of catalytic surfaces	Sparks (2003)

Kinetic model and linear forms of kinetic equations	Linear plot to determine k	k unit	Observation	Reference
Higuchi model $Mt=kt^{1/2}$	The cumulative amount of drug release vs $t^{1/2}$	$M\ h^{1/2}$	Describe the drug dissolution from the matrix system Assumptions: • The matrix contains an initial drug concentration much higher than the solubility of the drug • The diffusion is unidirectional • The thickness of the dosage form is much larger than the size of the drug molecules • The swelling or dissolution of the matrix is negligible • The diffusivity of the drug is constant • The perfect sink conditions are attained in the release environment	Bruschi (2015)
Hixson-Crowell model $W_0^{1/3} – W_t^{1/3}=k\ t$	$[W0-Wt]^{1/3}$ vs time	$M^{1/3}\ h^{-1}$	It assumes that the drug release is limited by dissolution velocity and not by diffusion	Bruschi (2015)
Korsmeyer-Peppas $(Mt/M\infty)=kt^n$	$(Mt/M\infty)$ vs t^n	h^{-n}	Is a semi-empirical model, and it establishes the exponential relationship between the release and the time. The power-law model is useful for the study of drug release from polymeric systems when the release mechanism is not known or when more than one type of phenomenon of drug release is involved. Depending on the value of n that better adjusts to the release profile of an active agent in a matrix system, it is possible to establish a classification, according to the type of observed behavior: Fickian model or Non-Fickian model	Costa and Sousa Lobo (2001); Bruschi (2015)
Baker-Lonsdale $3/2[1-(1-Mt/M\infty)^{2/3}]-(Mt/M\infty)=kt$	$(Mt/M\infty)$ vs time		Describes the drug-controlled release from a spherical matrix	Costa and Sousa Lobo (2001)

Kinetic model and linear forms of kinetic equations	Linear plot to determine k	k unit	Observation	Reference
Weibull Model $Log[-In (M\infty/(M\infty-Mt)]= b log (t-T_i)-log a$	Log [M]t vs Log time		This model is a distribution function with the property to describe the phenomena and processes associated with a finite time. Take into account that there is not any kinetic fundament and could only describe, but does not adequately characterize, the dissolution kinetic properties of the drug. And there is not any single parameter related to the intrinsic dissolution rate of the drug	Costa and Sousa Lobo (2001)

Notes: $[M]_0$, the Concentration of the reactant at the time 0; $[M]_t$, the cumulative concentration of the compound released at the time t; $[M]_s$, the concentration of the compound released at the saturation concentration for the solute in liquid, W_0, the initial amount of reactant; W_t, the remaining amount of reactant at the time t; $(Mt/M\infty)$, the fraction of drug released at time t; n, it is the release exponent; $M\infty$, amount of dissolved reactant as a function of time; Ti, lag time measured as a result of dissolution process parameters, a scale the parameter that describes the time dependence; b, the shape of dissolution curve (b=1 indicates exponential curve, b=2 indicates sigmoid curve, b=3 indicates parabolic curve).

Atkins P, De Paula J (2006) Atkins' Physical Chemistry. Oxford University Press, Oxford, New York.

Bruschi ML (2015) Mathematical models of drug release. In: Bruschi ML (ed) Strategies to modify the drug release from pharmaceutical systems. Elsevier, Cambridge, UK. pp 63–86. https://doi.org/10.1016/B978-0-08-100092-2.00005-9

Chang R (2005) Physical chemistry for the biosciences. University Science Books, Sausalito

Costa P, Sousa Lobo JM (2001) Modeling and comparison of dissolution profiles. Eur J Pharm Sci 13:123–133. https://doi.org/10.1016/S0928-0987(01)00095-1

Moussout H, Ahlafi H, Aazza M, Maghat H (2018) Critical of linear and nonlinear equations of pseudo-first order and pseudo-second-order kinetic models. Karbala Int J Mod Sci 4:244–254. https://doi.org/10.1016/j.kijoms.2018.04.001

Sparks DL (2003). Kinetics of soil chemical processes. In: Sparks DLBT-ESC Second E (ed). Academic Press, Burlington, pp 207–244

Utembe W, Potgieter K, Stefaniak AB, Gulumian M (2015) Dissolution and biodurability: Important parameters needed for risk assessment of nanomaterials. Part Fibre Toxicol 12:11. https://doi.org/10.1186/s12989-015-0088-2

Table S3. Fitting model parameters and the calculated parameters for Co released form the citrate-coated $CoFe_2O_4$ NPs in soil solution at different pH levels according to different dissolution kinetic models.

Fitting parameters	pH 5	pH 7	pH 8
	Zero-order		
R^2	0.638	0.358	0.089
R^2 adjusted	0.625	0.335	0.056
Intercept	0.010*	0.004*	0.008*
Slope	3.307×10^{-5}*	2.038×10^{-5}*	-1.519×10^{-5}
k (mM h^{-1})	-3.307×10^{-5}	-2.038×10^{-5}	1.519×10^{-5}
Ms (mM)	0.010	0.004	0.008
	First-order		
R^2	0.570	0.268	0.110
R^2 adjusted	0.554	0.242	0.079
Intercept	-4.637*	-5.584*	-4.883*
Slope	0.003*	0.004*	-0.002
k (mM h^{-1})	-2.886×10^{-3}	-3.761×10^{-3}	2.638×10^{-3}
Ms (mM)	0.010	0.004	0.008
	Second-order		
R^2	0.491	0.172	0.122
R^2 adjusted	0.472	0.143	0.090
Intercept	104.136*	277.521*	140.148*
Slope	-0.258*	-0.802*	0.517
k (mM^{-1} h^{-1})	-2.583×10^{-1}	-8.019×10^{-1}	5.169×10^{-1}
Ms (mM)	0.010	0.004	0.007
	Pseudo-first-order		
R^2	0.048	0.176	0.195
R^2 adjusted	0.014	0.146	0.167
Intercept	-1.168*	-1.145*	-1.128*
Slope	-3.559×10^{-5}	1.827×10^{-4}*	1.115×10^{-4}*
k (h^{-1})	3.559×10^{-5}	$-1.827\ 10^{-4}$	-1.115×10^{-4}
Ms (mM)	0.311	0.318	0.324
	Pseudo-second-order		
R^2	0.990	0.805	0.865
R^2 adjusted	0.989	0.798	0.861
Intercept	225.889*	1816.980*	-2179.680
Slope	69.793*	138.250*	260.020*
k (L mol^{-1} h)	21.564	10.519	-31.327
Ms (mM)	0.014	0.007	0.004
	One-half-order		
R^2	0.605	0.316	0.101
R^2 adjusted	0.591	0.291	0.069
Intercept	0.099*	0.061*	0.088*
Slope	1.540×10^{-4}	1.363×10^{-4}*	-9.859×10^{-5}
k ($mM^{1/2}$ h)	3.080×10^{-4}	-2.726×10^{-4}	-1.972×10^{-4}
Ms (mM)	0.010	0.004	0.008
	Three-half-order		
R^2	0.531	0.219	0.118
R^2 adjusted	0.515	0.191	0.085
Intercept	10.183*	16.471*	11.655*

Fitting parameters	pH 5	pH 7	pH 8
Slope	-0.014*	-0.027*	0.018
k ($mM^{-1/2}$ h)	-2.721×10^{-2}	-5.380×10^{-2}	3.639×10^{-2}
Ms (mM)	0.010	0.004	0.006
	Evolich		
R^2	0.641	0.188	0.043
R^2 adjusted	0.628	0.159	0.009
Intercept	0.009*	0.004*	0.007*
Slope	7.878×10^{-4}*	3.507×10^{-4}*	2.524×10^{-4}
α (mM h^{-1})	104.192	20.891	2.025×10^{8}
β (L $mmol^{-1}$)	1269.296	2851.499	3961.965
	Higuchi		
R^2	0.746	0.255	0.009
R^2 adjusted	0.737	0.228	-0.027
Intercept	0.009*	0.004*	0.008*
Slope	4.652×10^{-4}*	2.235×10^{-4}*	-6.223×10^{-5}
k (mM $h^{1/2}$)	4.652×10^{-4}	2.235×10^{-4}	-6.223×10^{-5}
Ms (mM)	0.009	0.004	0.008
	Hixon-Crowell		
R^2	0.048	0.185	0.198
R^2 adjusted	0.014	0.156	0.170
Intercept	0.104*	0.106*	0.108*
Slope	-3.703×10^{-6}	1.981×10^{-5}*	1.216×10^{-5}*
k ($mM^{1/3}$ h^{-1})	-3.703×10^{-6}	1.981×10^{-5}	-1.981×10^{-5}
	Korsmeyer-Peppas		
n	0.070	0.075	0.113
R^2	0.664	0.175	0.019
R^2 adjusted	0.652	0.146	-0.016
Intercept	-0.002*	4.032×10^{-4}	0.018*
Slope	0.0306*	0.012*	3.561×10^{-3}
k (h^{-n})	0.0306	0.012	0.004
	Baker-Lonsdale		
R^2	0.626	0.325	0.093
R^2 adjusted	0.613	0.300	0.060
Intercept	0.003*	0.012*	0.023*
Slope	1.001×10^{-4}*	5.738×10^{-5}*	-4.665×10^{-5}
k (h)	1.001×10^{-4}	5.738×10^{-5}	-4.665×10^{-5}
	Weibull		
R^2	0.625	0.213	0.038
R^2 adjusted	0.611	0.185	0.003
Intercept	-2.034*	-2.439*	-2.192*
Slope	0.071*	0.080*	0.037
a	9.247×10^{-3}	3.639×10^{-3}	6.427×10^{-3}
b	0.071	0.080	0.037

[M]s; theoretical saturation concentration, *Symbol indicates significance with an α=0.05

Table S4. Fitting model parameters and the calculated parameters for ions released from the citrate-coated $CoFe_2O_4$ NPs in artificial root exudates according to different dissolution kinetic models.

Fitting parameters	Fe	Co
	Zero-order	
R^2	0.864	0.745
R^2 adjusted	0.859	0.736
Intercept	0.009*	0.022*
Slope	$6.345x10^{-4}$*	$1.607x10^{-4}$*
k (mM h^{-1})	6.345×10^{-4}	$1.607x10^{-4}$
Ms (mM)	0.009	0.022
	First-order	
R^2	0.630	0.685
R^2 adjusted	0.617	0.674
Intercept	-4.942*	-3.844*
Slope	0.029*	$5.985x10^{-3}$*
k (h^{-1})	2.861×10^{-2}	$-5.985x10^{-3}$
Ms (mM)	0.007	0.021
	Second-order	
R^2	0.640	0.596
R^2 adjusted	0.625	0.581
Intercept	-3.744*	47.053*
Slope	0.030*	-0.231*
k (mM^{-1} h^{-1})	2.977×10^{-2}	-0.231
Ms (mM)	-0.267	0.021
	Pseudo-first-order	
R^2	0.845	0.613
R^2 adjusted	0.839	0.599
Intercept	-0.607*	-1.185*
Slope	$-1.182x10^{-3}$*	$-5.000x10^{-4}$*
k (h^{-1})	1.182×10^{-3}	5.000×10^{-4}
Ms (mM)	0.545	0.306
	Pseudo-second-order	
R^2	0.835	0.981
R^2 adjusted	0.829	0.981
Intercept	307.498*	82.462*
Slope	13.996*	28.801*
k (L mol^{-1} h)	0.637	10.059
Ms (mM)	0.071	0.035
	One-half-order	
R^2	0.794	0.719
R^2 adjusted	0.786	0.709
Intercept	0.091*	0.147*
Slope	$1.987x10^{-3}$*	$4.884x10^{-4}$*
k ($mM^{1/2}$ h)	3.974×10^{-3}	$9.768x10^{-4}$
Ms (mM)	0.008	0.021
	Three-half-order	
R^2	0.508	0.666
R^2 adjusted	0.490	0.654

Fitting parameters	Fe	Co
Intercept	3.521*	2.615*
Slope	-0.021*	$3.715x10^{-3}$*
k ($mM^{-1/2}$ h)	-0.041	-7.431×10^{-3}
Ms (mM)	0.081	0.146
	Evolich	
R^2	0.797	0.691
R^2 adjusted	0.790	0.680
Intercept	0.007*	0.021*
Slope	$9.742x10^{-3}$*	$2.474x10^{-3}$*
α ($mM\ h^{-1}$)	0.020	12.007
β ($L\ mmol^{-1}$)	102.652	404.204
	Higuchi	
R^2	0.921	0.783
R^2 adjusted	0.918	0.775
Intercept	$-8.613x10^{-4}$*	0.019*
Slope	$6.605x10^{-3}$*	$1.661x10^{-3}$*
k ($mM\ h^{1/2}$)	0.007	0.002
Ms (mM)	-0.001	0.019
	Hixon-Crowell	
R^2	0.838	0.611
R^2 adjusted	0.832	0.597
Intercept	0.182*	0.102*
Slope	-2.055×10^{-4}*	-5.004×10^{-5}*
k ($mM^{1/3}\ h^{-1}$)	-2.055×10^{-4}	-5.004×10^{-5}
	Korsmeyer-Peppas	
n	0.538	0.097
R^2	0.922	0.726
R^2 adjusted	0.919	0.712
Intercept	0.010*	-0.003
Slope	$9.879x\ 10^{-3}$*	0.067*
k (h^{-n})	0.010	0.067
	Baker-Lonsdale	
R^2	0.865	0.744
R^2 adjusted	0.860	0.735
Intercept	0.016*	0.066*
Slope	$1.141x10^{-3}$*	$4.875x10^{-4}$*
k (h)	1.141×10^{-3}	$4.875x10^{-4}$
	Weibull	
R^2	0.873	0.703
R^2 adjusted	0.868	0.692
Intercept	-2.270*	-1.681*
Slope	0.538*	0.097*
a	0.005	0.020
b	0.538	0.097

[M]s; theoretical saturation concentration, *Symbol indicates significance with an α=0.05

Chapter 2. Supplementary material

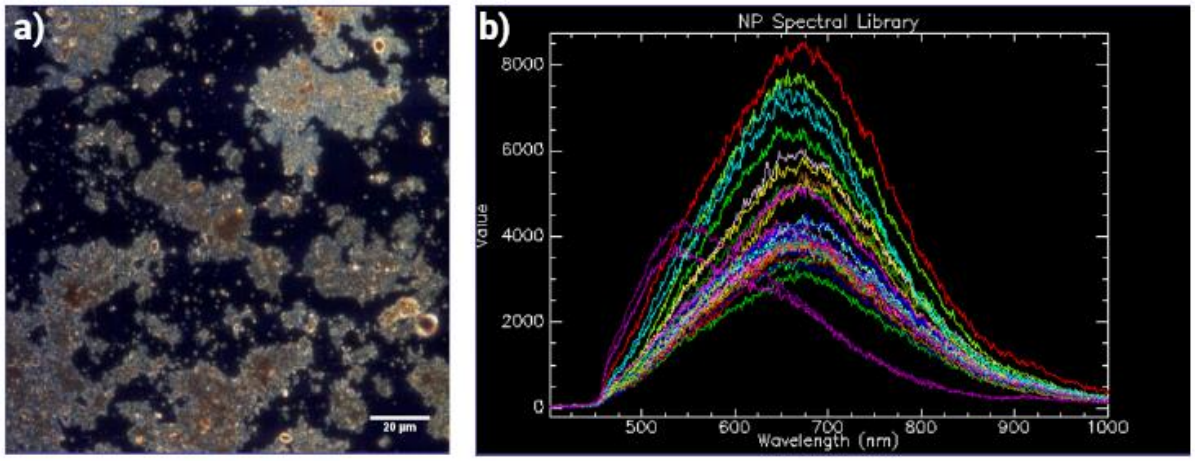

Figure S1. Hyperspectral microscopy imagining analysis of citrate-coated $CoFe_2O_4$ NPs. a) Enhanced darkfield optical image (60x) of NPs, and b) their spectral library.

Table S1 Properties of citrate coated $CoFe_2O_4$ NPs

Feature	Value
pH (supernatant)	6.44
Shape	Semi-spherical
Primary size (nm)	13.41±4.58
Hydrodynamic diameter (nm)	216.06±10.46
Polydispersity (%)	18.53±18.53
Zeta potential (mV, in DI water)	10.5 ±6.6
Point of zero charge (pH)	6.8
Fe composition (% by AAS)	48.48 ± 5.2
Co composition (% by AAS)	29.37 ± 1.8
Maximum repulsive potential (nm)	9

AAS, atomic absorption Spectrophotometry; DI, Deionized water; Data from Perea-Vélez et al. (2022)

Perea-Velez YS, González Chávez M del CA, Carrillo-González R, Lopez-Luna J (2022) Dissolution kinetics of citrate coated $CoFe_2O_4$ nanoparticles in soil solution. Environ Sci Nano. 9:2954–2965. https://doi.org/10.1039/D2EN00330A

Table S2. Chemical properties of the soil used

Feature	Unit	Value	Interpretation
pH		7.71 ± 0.01	Moderately alkaline
Electrical conductivity	dS m^{-1}	2.24 ± 0.01	Very slightly saline
Organic matter	%	5.70 ± 0.40	High
N total		0.82 ± 0.07	
N inorganic	mg kg^{-1}	29.48 ± 5.48	Medium
P (Olsen extraction)		49.59 ± 13.95	High
Exchangeable cations			
Na		1.00 ± 0.01	
K	$cmol_{(+)}$ kg^{-1}	5.39 ± 0.08	High
Ca		88.93 ± 5.04	High
Mg		11.93 ± 0.80	High
Micronutrients (DTPA extraction)			
Cu		0.50 ± 0.02	Adequate
Fe	mg kg^{-1}	3.23 ± 0.31	Marginal
Zn		1.21 ± 0.01	Adequate
Mn		14.87 ± 0.31	Adequate

Mean value and standard deviation, n=3

Interpretation according to the Mexican norm NOM-021-RECNAT-2000

SEMARNAT (2000). Norma Oficial Mexicana NOM-021-RECNAT-2000, que establece las especificaciones de fertilidad, salinidad y clasificación de suelos. Estuidios, mmuestreo y análisis. http://www.ordenjuridico.gob.mx/Documentos/Federal/wo69255.pdf. Accessed 13 Feb 2022

Table S3. Iron fixed in alkaline soil trough fixation assay.

Fe added (mg L^{-1})	Final Fe concentration added (mg L^{-1})	Iron Source					
		$FeSO_4$ 7 H_2O			Citrate-coated $CoFe_2O_4$ NPs		
		Adsorbed Fe (%)	Fe extracted with $CaCl_2$ 0.01M (mg kg^{-1})	Fe extracted with DTPA-TEA-$CaCl_2$ (mg kg^{-1})	Adsorbed Fe (%)	Fe extracted with $CaCl_2$ 0.01M (mg kg^{-1})	Fe extracted with DTPA-TEA-$CaCl_2$ (mg kg^{-1})
0	0		ND	2.77 ± 0.29		ND	2.77 ± 0.29
10	9.09	100	ND	4.24 ± 0.28	100	ND	2.38 ± 0.32
25	22.73	100	ND	5.76 ± 0.46	100	ND	2.05 ± 0.15
50	45.45	100	ND	9.52 ± 0.16	100	ND	2.30 ± 0.20
75	68.18	100	ND	13.05 ± 1.81	100	ND	2.03 ± 0.02
100	90.91	100	ND	17.85 ± 1.84	100	ND	2.33 ± 0.44
200	181.82	100	ND	40.20 ± 6.46	100	ND	2.26 ± 0.32
400	363.64	100	ND	73.50 ± 5.70	100	ND	2.14 ± 0.12
800	727.27	100	ND	144.95 ± 16.21	100	ND	2.75 ± 0.44
1600	1454.55	98.77	ND	170.56 ± 13.98			

ND, No detected

Mean value and standard deviation, n=3

The Fe fixation assay

A sample of 5 g of soil was placed in a Falcon tube. The weight of the tube and soil was recorded. Then 20 mL of Fe solution or suspension of NPs with a known and increasing concentration of Fe (0-1600 mg kg^{-1}) was added. In addition, 2 mL of $CaCl_2$ 0.1 M solution was added to maintain a base ionic strength. The samples were shaken at 120 rpm for 2 h. Afterward, the samples were centrifuged for 10 min at 1200 rpm. The supernatant was recovered, filtered, and stored for further analysis. In parallel, the weight of the tube containing the soil was recorded, and then extraction with 20 mL of $CaCl_2$ 0.1 M solution was carried out. If Fe was detected in the $CaCl_2$ extract, then the extraction was repeated. But if Fe was not detected then extraction with DTPA-TEA-$CaCl_2$ solution was performed.

Table S4 The proportion of electrolytic stock solutions, enzymes, bile salts, and Ca^{2+} that were added in each extraction phase.

Input	5 g of whole wheat grains				
Digestion phase	Oral (SSF)	Gastric (SGF)		Intestinal (SIF)	
Sample of food (g) or digesta (mL)	5	10[b]		20[c]	
mL of electrolyte stock solutions 1.25x[a]	4	8		8	
$CaCl_2(H_2O)_2$ (0.3M, mL)	0.025	0.005		0.04	
Enzyme or Bile salts	-	Pesin	Lipase	Pancreatin	Bile salts
The volume of enzyme/bile to add (mL)	-	0.667	0.48	5	3
H_2O (mL)	0.975	1.228		3.46	
HCl (5M) for pH adjustment (mL)	-	0.1		-	
NaOH (5 M) for pH adjustment (mL)	-	-		0.5	
Final Volume (mL)	10	20		40	

Notes: [a] Pre-warm the electrolyte stock solution at 37°C; [b] Sample from the oral phase; [c] Gastric chyme

Table S5 Estimated production cost (MXN) for the wheat crop of the top three Mexican states producing wheat.

Prices per ha	Sonora (2019)	Baja California (2020)	Sinaloa (2021)	Average
Sowing	$2,381	$2,215	$2,558	$2,385
Labor cost	$168	$186	$667	$340
Irrigation	$2,402	$2,250	$2,385	$2,346
Pest control	$3,708	$2,914	$1,748	$2,790
Harvesting	$1,416	$2,430	$2,357	$2,068
Commercialization	$3,004	$3,259	$2,993	$3,085
Miscellaneous	$1,973	$2,051	$1,865	$1,963

Source: FIRA(FIRA 2022)

FIRA, Agrocostos Interactivo, http://www.fira.gob.mx/agrpcpstpsApp/AgroApp.jps, Accessed 13 October 2022.

Table S6. The estimated cost of NPs production at the laboratory scale and NPs cost in the market.

Reagents	Units	Cost for unit	Cost (MXN)	Cost (USD)
$Fe(NO_3)_3*9H_2O$	4.3 kg	2992.8 (MXN/kg)	12,869	645
$Co(NO_3)_2*6H_2O$	1.5 kg	11089.6 (MXN/kg)	16,634	833
NaOH	3.03 kg	670.48 (MXN/kg)	2,032	102
Sodium citrate	78.42 g	1018.35 (MXN/kg)	80	4
Distilled water	4133.25 L	34.67 (MXN/L)	143,300	7,179
Energy	2000 h	79.81 (MXN/h)	159,620	7,997
Technician	4000 (h)	41.66 (MXN/h)	166,640	8,349
Total			501,175	25,109

Cost in market	Cost (USD/kg)	Source
NanoChemazone	5,750	(Nanochemazone 2022)
Sigma aldrich	19,400	(Sigma-Aldrich 2022)
Sisco Reseach laboratories Pvt.Ltd	17,174	(Laboratories 2022)

Laboratories SR (2022) Cobalt iron oxide nanopowder. https://www.srlchem.com/products/compound/Cobalt-Ferrite-Nanopowder/31570. Accessed 9 Nov 2022

Nanochemazone (2022) Cobalt Ferrite Nanoparticles. https://www.nanochemazone.com/product/cobalt-ferrite-nanoparticles/. Accessed 13 Oct 2022

Sigma-Aldrich (2022) Cobalt iron oxide nanopowder. https://www.sigmaaldrich.com/US/en/product/aldrich/773352. Accessed 13 Oct 2022

Table S7. Degree of biofortification in wheat grains of three different wheat lines fertilized with Fe-EDTA or citrate-coated CoFe2O4 NPs by soil or foliar applications.

Genotype	Type application	Treatment	Degree of biofortification (%)
AF1104	Soil application	Fe-EDTA	6.60±23.39
		NPs 46	3.04±8.46
		NPs 68	-7.40±10.76
	Foliar application	Fe-EDTA	9.59±21.83
		NPs	27.02±33.23
	Mean		**7.77±21.57 B**
AF1116	Soil application	Fe-EDTA	78.28±96.77 b
		NPs 46	6.11±11.41 b
		NPs 68	394.41±121.19 a
	Foliar application	Fe-EDTA	21.35±11.80 b
		NPs	42.00±14.61 b
	Mean		**109.02±161.02 A**
MULTIAF2	Soil application	Fe-EDTA	-10.28±7.27 b
		NPs 46	-25.48±21.50 b
		NPs 68	27.09±5.61 a
	Foliar application	Fe-EDTA	-37.82±4.06 b
		NPs	-31.96±8.75 b
	Mean		**-15.69±25.92 C**
	Soil application	Fe-EDTA	24.86±30.81 b
		NPs 46	-5.44±19.84 b
		NPs 68	138.03±202.25 a
	Foliar application	Fe-EDTA	-1.29±30.81 b
		NPs	12.35±38.67 b

Table S8. The concentration of soluble polysaccharide fractions and free amino acids in wheat grains

Genotype	Type application	Treatment	Glucose (µmol/g)	Fructose (µmol/g)	Saccharose (µmol/g)	Free aminoacids as glicine (mM/kg)
MULTIAF2	Soil application	Control	3.25±1.10	0.05±0.01 b A	13.70±0.59 b	11.75±1.14
		Fe-EDTA	3.22±1.19	0.11±0.02 a	21.54±4.05 a A	14.77±3.26
		NPs 46	3.34±2.29	0.07±0.03 ab B	18.62±2.08 ab	18.75±7.11
		NPs 68	3.74±2.00	0.07±0.03 ab	14.95±0.89 b	12.52±0.45
	Foliar application	Fe-EDTA	3.03±1.19	0.07±0.01 ab	13.90±1.51 b	15.62±6.78
		NPs	2.52±0.58	0.07±0.02 ab	15.68±0.92 b	11.67±1.56
	Mean		3.18 ±1.32	0.07 ±0.03	16.39±3.37	14.18 ±4.45
AF1104	Soil application	Control	0.89±1.15	0.06±0.01	14.72±5.37	12.52±3.81
		Fe-EDTA	3.99±0.72	0.05±0.03	18.13±3.98	13.35±1.18
		NPs 46	2.77±1.16	0.09±0.03	15.00±5.15	9.98±0.84
		NPs 68	1.34±2.13	0.05±0.02	14.10±1.88	15.30±4.80
	Foliar application	Fe-EDTA	2.93±0.84	0.07±0.03	17.14±0.23	12.42±2.71
		NPs	0.81±0.78	0.06±0.01	15.75±1.99	12.21±2.24
	Mean		2.12±1.60	0.06±0.02	15.80±3.37	12.63±2.96
AF1116	Soil application	Control	2.83±1.17	0.05±0.01 A	14.51±0.66	15.85±3.26
		Fe-EDTA	2.77±2.94	0.07±0.04	13.63±2.11	12.93±0.77
		NPs 46	0.41±0.73	0.07±0.02	13.14±1.49 B	11.88±3.30
		NPs 68	3.25±2.59	0.05±0.02	17.57±1.27	12.63±2.79
	Foliar application	Fe-EDTA	1.23±0.98	0.10±0.02	14.50±3.59	19.13±3.51
		NPs	2.17±0.67	0.08±0.02	17.40±0.83	20.54±5.95
	Mean		2.11±1.80	0.07±0.03	15.12±2.40	15.49±2.95

Mean±standar deviation of n=3. Different lowercase letters represent significant differences (Tukey α=0.05) between treatments within the line. Capital letters represent differences due to the treatment*line effect.

Chapter 3. Supplementary material

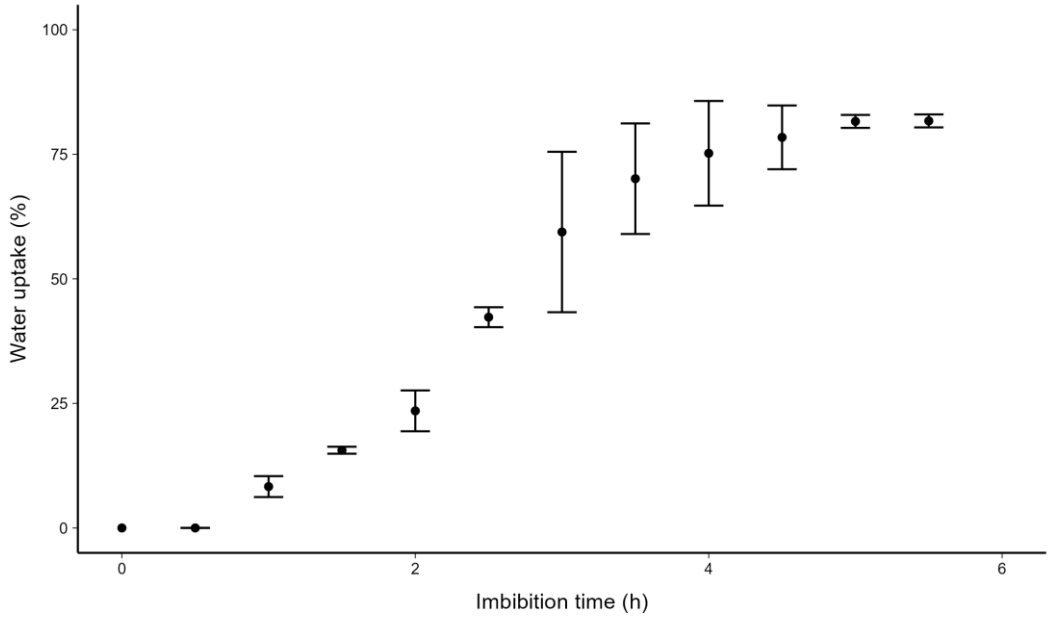

Figure S1. Water uptake curve of OTI bean seeds.

Procedure:

The hydration kinetics of seeds by imbibition was investigated until no changes in the percentage of hydration were observed. Seeds of similar size were chosen, and the initial weight of ten seeds was recorded. The seeds (10) were then placed in a Falcon tube containing 25 mL of distilled water and kept with constant agitation in a rotor shaker (30 turns per minute) at room temperature (20-25°C). Every 30 min, the seeds were taken up from the Falcon tube, and the excess water was removed with a paper tissue. The seeds were then weighted.

Note:

A time of 2 h 30 min was chosen as the imbibition time because seeds with a higher percentage of humidity (80%) fungal emergence was observed during germination trials (despite maintaining sterile conditions).

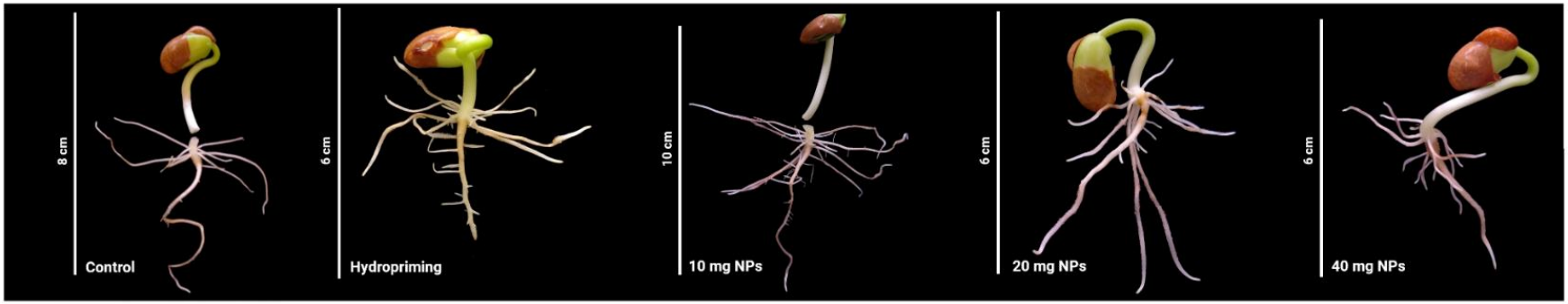

Figure S2. Phenotypic characteristics of seedlings developed from unprimed seeds, hydroprimed and nano-primed seeds.

Table S1. Chemical properties from the soil used to growth nano-primed bean seed.

Property	Value
pH	7.71 ± 0.01
Electrical conductivity (dS m^{-1})	2.24 ± 0.01
Organic matter (%)	5.70 ± 0.40
N total (%)	0.82 ± 0.07
N inorganic (mg kg^{-1})	29.48 ± 5.48
P (Olsen extraction; mg kg^{-1})	49.59 ± 13.95
Exchangeable cations	
Na ($cmol_{(+)}$ kg^{-1})	1.00 ± 0.01
K ($cmol_{(+)}$ kg^{-1})	5.39 ± 0.08
Ca ($cmol_{(+)}$ kg^{-1})	88.93 ± 5.04
Mg ($cmol_{(+)}$ kg^{-1})	11.93 ± 0.80
Micronutrients (DTPA extraction)	
Cu (mg kg^{-1})	0.50 ± 0.02
Fe (mg kg^{-1})	3.23 ± 0.31
Zn (mg kg^{-1})	1.21 ± 0.01
Mn (mg kg^{-1})	14.87 ± 0.31

Mean value and standard deviation, n=3

Table S2. Estimated production cost (MNX) per hectare of bean crop for the top five Mexican states producing beans.

Variable	Zacatecas	Durango	Chihuahua	Sinaloa	Sonora	Average (MNX)
Land preparation	2232	1600	3091	3821	3120	2772.8
Sowing	1125	1450	4657	5191	5874	3659.4
Fertilization	1745	2066	4923	7446	5970	4430.0
Labor cost	1170	450	1527	1343	690	1036.0
Irrigation	0	0	4962	1975	2233	1834.0
Pest control	1487	1860	3062	1835	2760	2200.8
Harvesting, selection, packing	1313	1250	1174	3888	2397	2004.4
Commercialization	250	0	0	0	0	50.00
Miscellaneous	897	1267	2125	3125	3194	2121.6
Seed	575	1205	1632	2683	1617	1542.4
Total	10794	11148	27153	31307	27855	21651.4

Source: FIRA (2023)

FIRA (2023) Agrocostos Interactivo, https://www.fira.gob.mx/agrocostosApp/AgroApp.jsp Accessed 3 Jan 2023.